Identification of Thrombosis Modifier Genes Using ENU Mutagenesis in the Mouse

by

Kärt Tomberg

A dissertation submitted in partial fulfillment
of the requirements for the degree of
Doctor of Philosophy
(Human Genetics)
in the University of Michigan
2016

Doctoral Committee:

Professor David Ginsburg, Chair
Associate Professor Patrick J. Hu
Associate Professor Catherine E. H. Keegan
Associate Professor Jun Li
Assistant Professor Ryan E. Mills

ACKNOWLEDGEMENTS

First and foremost, I would like to thank my thesis mentor David Ginsburg. David has always been there for me throughout this process, either by challenging or encouraging me, pushing or holding me back, all in good proportion. He sets a great example as a scientist, a mentor, and a human being, which I will strive to follow.

Thank you to my dissertation committee (Patrick Hu, Katy Keegan, Jun Li, and Ryan Mills) for your time, great suggestions, intellectual input, encouraging support, and many helpful discussions. I would especially like to thank Ryan for letting me barge into his office, on several occasions, for advice ranging from data analysis to networking. I always left with new ideas!

A special thank you to all the members of the Ginsburg lab. Each and every one of you has helped me at some point along the way. You are such great colleagues, good friends, and have provided me with a kind home away from home. I hope distance and time will not stop us from collaborating and supporting each other. A special shout-out to the amazing undergraduates that trained with me over the years.

My sincere thank you to the faculty and my fellow students at Department of Human Genetics. I have received a lot of encouragement, great ideas, and discussions from so many of you. All the emails, office visits, FAST talk questions, and chats at happy hours have helped me become a better scientist. I would also like to thank all the administrative staff of the Department of Human Genetics, PIBS, and Life Sciences Institute. Somehow I am always the troublemaker and without your kind, timely, and professional support, I would not be here today. In addition, I would like to thank the Fulbright program and the American Heart Association for funding my training. My thanks to the University of Michigan basic science core facilities for excellent support and access to great technologies.

Finally, I would like to thank my friends here in Ann Arbor and around the world, and my family back in Estonia for their constant love and support.

TABLE OF CONTENTS

ACKNOWLEDGEMENTS ii
LIST OF TABLES v
LIST OF FIGURES vi
LIST OF APPENDICES viii
ABSTRACT ix
CHAPTER I: Introduction 1
Venous thromboembolism 1
Mutagenesis screens 4
CHAPTER II: A sensitized mutagenesis screen in Factor V Leiden mice identifies novel thrombosis suppressor loci 20
Abstract 20
Introduction 21
Materials and methods 22
Results 26
Discussion 30
CHAPTER III: Spontaneous 8bp deletion in *Nbeal2* recapitulates the gray platelet syndrome in mice 51
Abstract 51
Introduction 51
Materials and methods 52
Results 58
Discussion 61
CHAPTER IV: ENU mutagenesis and whole exome sequencing to identify thrombosis modifier genes 78
Abstract 78

Introduction 79
Materials and methods 79
Results and discussion 85
CHAPTER V: Conclusions and future perspectives 113
Limitations of traditional mapping strategies 113
Mutation burden approach in a dominant ENU screen 114
Future perspectives for current screen 117
Opportunities beyond the current screen 119
APPENDICES 127
REFERENCES 167

LIST OF TABLES

Table 1-1: Overview of genes used in the specific-locus test 19
Table 2-1: Overview of linkage analysis 39
Table 2-2: Distribution of genotypes from a cross of *F5*$^{L/+}$ *Tfpi*$^{+/-}$ *F8*$^{X+/X-}$ to *F5*$^{L/L}$ 40
Table 2-3: Overview of all identified G1 *F5*$^{L/L}$ *Tfpi*$^{+/-}$ mice 41
Table 2-4: Overview of the ENU pedigrees 44
Table 2-5: Synthetic lethal phenotype on 129 genetic background 45
Table 2-6: Distribution of genotypes from a cross of *F5*$^{L/+}$ *Tfpi*$^{+/-}$ *F3*$^{+/-}$ to *F5*$^{L/L}$ 46
Table 2-7: Candidate ENU-induced mutations 47
Table 2-8: Overview of the WES data 49
Table 3-1: Overview of the exonic variants called from WES in 4 mice from the *MF5L6* pedigree 73
Table 3-2: Expected and observed number of progeny in *Nbeal2*$^{gps/+}$ crosses 74
Table 3-3: CBC mean values and standard deviations by genotype in set 1 mice 75
Table 3-4: Intensity of platelet staining and frequency of emperipolesis events in bone marrow megakaryocytes 76
Table 4-1: CRISPR-Cas9 alleles 103
Table 4-2: Overview of rescue pedigrees 104
Table 4-3: Overview of candidate ENU-induced variants in pedigrees 1, 6, and 13 105
Table 4-4: Overview of WES variants present in 2 or 3 G1 rescues 107

LIST OF FIGURES

Figure 1-1: Prevalence of FVL mutation 13
Figure 1-2: Perinatal lethal thrombosis model 14
Figure 1-3: Mutagenetix database 15
Figure 1-4: Screening strategies 16
Figure 1-5: Sensitized screen for thrombosis modifiers 17
Figure 1-6: ENU gene space saturation 18
Figure 2-1: *F8* deficient thrombosuppression and design of the *Leiden* ENU mutagenesis screen 34
Figure 2-2: Discovery and validation of the chromosome 3 thrombosuppressor locus . 35
Figure 2-3: Allele specific RNA expression of *F3* 36
Figure 2-4: Discovery and validation of *Actr2* as a candidate thrombosuppressor gene by NGS 37
Figure 2-5: Functional analysis of the *Actr2* mutant mice 38
Figure 3-1. Schematic overview of the *Nbeal2* genotyping primers 64
Figure 3-2: Pedigree of the *MF5L6* suppressor line 65
Figure 3-3: *De novo* 8 bp deletion in the *Nbeal2* gene 66
Figure 3-4: Genotyping of 129S1/SvImJ archived samples from the Jackson Laboratory 67
Figure 3-5: Differential allelic expression of *Nbeal2* mRNA in *Nbeal2*$^{gps/+}$ bone marrow, lung, and liver 68
Figure 3-6: Western blot analysis for NBEAL2 and beta Actin 69
Figure 3-7: Comparison of CBCs 70
Figure 3-8: Deficiency in platelet alpha granules 71
Figure 3-9: Emperipolesis of neutrophils in bone marrow and spleen 72
Figure 4-1: *In vitro* cleavage assay for sgRNAs 93
Figure 4-2: A sensitized ENU suppressor screen for thrombosis modifiers 94

Figure 4-3: Distribution of ENU-induced mutations in WES data from 107 G1 rescues 95
Figure 4-4: Genetic mapping of ENU-induced variants in pedigree 1 96
Figure 4-5: Genetic mapping of ENU-induced variants in pedigree 6 97
Figure 4-6: Genetic mapping of ENU-induced variants in pedigree 13 98
Figure 4-7: Segregation of the *Plcb4*^{R335Q} variant 99
Figure 4-8: Mutation enrichment per gene in WES data from 107 G1 rescues 100
Figure 4-9: Validation of *Arl6ip5* as a thrombosis suppressor using CRISPR-Cas9-generated independent null allele 101
Figure 4-10: CRISPR-Cas9-induced INDELs in *F5*$^{L/+}$ *Tfpi*$^{+/-}$ mice used for rescue validation 102
Figure 5-1: Size distribution of ENU pedigrees from performed screens..... 123
Figure 5-2: Distribution of CRISPR-Cas9 induced events by targeted genes 124
Figure 5-3: CRISPR-Cas9 induced alleles 125
Figure 5-4: VTE GWAS results at the *Fabp6* gene locus 126

LIST OF APPENDICES

Appendix 2-1: All used primer sequences 127
Appendix 4-1: Overview of WES mice..... 133
Appendix 4-2: All used primer sequences 136
Appendix 4-3: gRNA sequences, primers, and templates 146
Appendix 4-4: Potentially deleterious ENU-induced variants from WES in genes with >1 mutation 147

ABSTRACT

Abnormal formation of a blood clot in veins, also called venous thromboembolism (VTE), is a major health problem in Western societies that affects 1 in every 1,000 individuals per year. Susceptibility to VTE is governed by both genetic and environmental factors, with approximately 60% of the risk attributed to genetic influences. The most prevalent genetic risk factor among VTE patients is a variant in coagulation factor V, called Factor V Leiden (FVL). While 20-25% of VTE patients carry the FVL variant, only ~10% of FVL carriers develop a VTE in their lifetime, indicating that interactions between FVL and other genetic and/or environmental factors influence the incidence and severity of thrombosis. The goal of this thesis was to identify modifier genes that help understand the differences in VTE phenotype among FVL carriers and more generally the complex genetic factors regulating hemostasis balance.

The work described here took advantage of the synthetic lethal thrombosis phenotype observed in mice carrying two copies of the orthologous FVL ($F5^{L/L}$) mutation together with haploinsufficiency for tissue factor pathway inhibitor ($Tfpi^{+/-}$). *F8* deficiency was found to 'rescue' $F5^{L/L}$ $Tfpi^{+/-}$ lethality, and an initial ENU mutagenesis screen for dominant thrombosis modifier genes additionally identified *F3* and *Actr2* as suppressors for this lethal phenotype (Chapter II).

During the genetic analysis of the ENU-induced mutations, we additionally identified a *de novo* deletion in *Nbeal2* which originated from a non-ENU treated parent, highlighting the potentially confounding effect of spontaneous mutation events in well-characterized mouse strains. Though initially considered a plausible thrombosis modifier, this mutation failed to rescue the synthetic lethal thrombosis (Chapter III).

A complementary burden test that highlights genes enriched for mutations applied to >100 independent $F5^{L/L}$ $Tfpi^{+/-}$ rescues identified 12 novel candidate thrombosis modifiers. Preliminary validation data using independent null alleles suggest successful rescue for mice haploinsufficient for *Sntg1* (Chapter IV).

CHAPTER I: Introduction

Venous thromboembolism

Incidence and acquired risk factors

Venous thromboembolism (VTE) is a condition in which the blood clots inappropriately. It includes deep vein thrombosis (DVT) and its major life threatening complication, pulmonary embolism (PE).

VTE is a major health problem affecting approximately 1 in every 1,000 individuals of European descent [1]. The incidence of VTE is about 30% higher among African-Americans but lower among Asians, Hispanics, and Native-Americans [2, 3]. In the United States alone, the annual number of VTE events (incident and recurrent) is estimated at 600,000, with 10-30% of these events proving fatal within 30 days [4].

VTE is a complex disease determined by various environmental factors, genetic factors, and the interactions of both [5]. The two most prevalent independent risk factors for a first lifetime VTE event are hospitalization or residence in a nursing home (60%) and active cancer (20%) [6]. VTE incidence increases markedly with age in both genders, with incidence rates generally higher in males compared to females after age 45 [1, 7]. Independent risk factors for VTE also include surgery, trauma, smoking, central vein catheterization, and transvenous pacemakers [8, 9]. Additional risk factors among females include oral contraceptive use and hormone replacement therapy (2 to 6 fold increased relative risk for each) [10] as well as pregnancy and the postpartum period [11].

Genetic risk factors for VTE

VTE is highly heritable, with a study of 21 extended Spanish families (398 individuals) resulting in an overall heritability estimate of 61% [12]. A family based approach in the US population of European descent reported a heritability of 52% for

the best fitting inheritance model (unrestricted non-Mendelian) [13]. A high genetic proportion contributing to VTE variance was also seen in males in a Danish twin study (55%). However, no contribution was observed in females, suggesting a possible difference in VTE heritability between sexes [14].

While VTE is a defined clinical manifestation, the acquired or inherited tendency to develop VTE is referred to as thrombophilia. Known causes for inherited thrombophilia can be divided into two main mechanisms: reduced levels of endogenous anticoagulants or increased levels of procoagulant factors. The first report of inherited thrombophilia was published in 1965 by Egeberg and colleagues who described a Norwegian family suffering from VTE due to a deficiency in levels of the anticoagulant antithrombin [15]. Antithrombin III deficiency is inherited in an autosomal-dominant fashion and is caused by ~50% reduction in either protein function and/or level in plasma [16]. More than a decade later, deficiency in other anticoagulants such as protein C [17] and protein S [18] were shown to cause inherited thrombophilia in a similar autosomal-dominant manner. While loss-of-function mutations in these natural anticoagulants are associated with increased risk for VTE, they are rare in the general population (19-77 per 10,000) and their total prevalence in VTE patients is approximately 6% [8].

Thrombophilia has also been associated with elevated plasma levels of several procoagulant proteins. Increased levels of factor I (fibrinogen) [19], II (prothrombin) [20], VIII [21], IX [22], X [23] and XI [24] have been associated with VTE [8]. Differences in factor VIII plasma levels are strongly associated with an individual's ABO blood type. Factor VIII circulates in plasma in a noncovalent complex with its carrier glycoprotein, von Willebrand factor (VWF). Plasma levels of the FVIII-VWF complex are ~25% higher in non-O blood group individuals, likely due to glycosylation differences for the VWF protein driven by the ABO alleles that encode different alleles of a glycosyltransferase [25]. The most prevalent genetic risk factor for VTE [26] is a missense substitution Factor V Leiden (FVL, Arg506Gln) that blocks the inactivation of procoagulant factor V by activated protein C [27, 28]. FVL is present in 4-5% of Europeans [8, 29] and in 20-25% of VTE patients [30, 31]. Another relatively common variant (2% in European population), a substitution in the prothrombin 3' untranslated region (G20210A), is

associated with 30% higher plasma levels of prothrombin [20] and is present in ~4.5% of VTE patients [32]. Recent genome wide association studies (GWAS) confirmed the known common loci contributing to the genetic risk for VTE such as the ABO blood group, FVL, FI, FII and FXI, though few new candidates were identified [26, 33-36].

Most of the above investigations have been limited to subjects of European descent with the identified risk factors of limited relevance to individuals from other parts of the world. For example, two of the common risk variants, FVL and G20210A, arose approximately 20,000-35,000 years ago in European populations after the evolutionary divergence from Africans and Asians and are therefore very rare or absent in most non-European populations [37, 38]. Relatively higher factor VIII levels are found in the African American population that cannot be explained by ABO blood groups alone [39, 40], but the underlying genetic determinants are unknown. In Asian populations, loss-of-function mutations in protein S, protein C, and antithrombin are slightly more prevalent but do not explain the majority of VTE cases [41]. Population-specific GWAS studies could identify common risk variants in these understudied populations while new whole exome/genome sequencing approaches can additionally discover rare variants contributing to VTE risk. At present, <50% of VTE heritability can be explained by currently known genetic risk factors.

FVL

FVL is the most prevalent genetic risk factor for VTE, found in 20-25% of all VTE patients [30, 31] and in 40-60% of patients with familial thrombophilia [42]. While FVL heterozygosity is common among VTE patients, only 10% of individuals heterozygous for the FVL variant experience a VTE in their lifetime (Figure 1-1). The risk is much higher (80% lifetime risk) for people homozygous for FVL [42] but homozygotes are relatively rare in the population (6-7 in 10,000) and thus account for a small proportion of VTE patients. The genetic and environmental modifying factors that determine the clinical expression of FVL are poorly understood. Patients that carry two known thrombotic risk factors such as FVL and deficiency in protein S or protein C have a higher risk of VTE than those with either risk factor alone [43], as do patients with FVL and an acquired risk factor [44]. Though elevated VTE risks are observed in individuals

with FVL mutation (odds ratio, OR=4.9) or the prothrombin G20210A variant (OR=3.8), a notably higher risk for VTE is observed in doubly heterozygous individuals (OR=20) than the sum of the individual estimated risks for these variants [45], a phenomenon referred to as epistasis. In addition to unknown genetic factors that elevate an individual's risk for VTE, there are also likely protective genetic modifiers in the 90% of asymptomatic FVL carriers.

FVL in a mouse model

Our lab previously reported a knock-in mouse with the orthologous FVL mutation introduced into the endogenous murine *F5* gene ($F5^{L}$, Arg504Gln). FVL mice have a very similar phenotype to humans, with occasional sporadic thrombosis in heterozygous mice and more severe manifestations in homozygous animals [46]. Crossbreeding experiments showed that co-inheritance of Factor V Leiden homozygosity ($F5^{L/L}$) together with haploinsufficiency for tissue factor pathway inhibitor ($Tfpi^{+/-}$) results in a nearly uniform perinatal lethal thrombosis (Figure 1-2) [47]. A similar interaction between F5 and TFPI was previously described in a synthetic *in vitro* assay for thrombin generation, where thrombin generation was markedly increased by a combination of 50% reduced TFPI and FVL mutant compared to reduced TFPI and wildtype F5 [48].

These data indicate that reductions in *Tfpi* result in a significant worsening of the FVL thrombotic phenotype in mice and suggest that there may be other gene mutations that will act similarly to modulate thrombosis severity. This synthetic lethality in $F5^{L/L}$ $Tfpi^{+/-}$ mice serves as a baseline phenotype for the genetic screens performed in this thesis.

Mutagenesis screens

De novo mutations

De novo mutations are the source of natural variation in DNA and the drivers of natural selection. The majority of mutations arise due to mistakes made during DNA replication, repair, and recombination processes with different mechanisms involved in different types of mutations [49]. Germline *de novo* mutations in humans are relatively

rare. On average, each individual is expected to harbor approximately 75 single nucleotide variants (SNVs) [50, 51] and an additional 3-5 small insertions/deletions (INDELs) not present in either parent [52]. The frequency of *de novo* medium size structural variants (>20bp) is estimated to be 0.16 per person [53], while *de novo* large copy number variants (>100kb) can be found in one out of 50 individuals [54]. While an important cause of disease in humans, spontaneous mutations in model organisms have long been considered an invaluable source for studying phenotype-genotype correlations.

In model organisms such as *E. coli* or *S. cerevisiae* identifying causative genes can be achieved by selection for spontaneous mutants under appropriate conditions, facilitated by haploid genomes and easy access to millions of individual organisms. For example, resistance to streptomycin can be mapped to a few positions in the *rpsL* gene in *E. coli* by sequencing the rare mutants able to grow in that antibiotic environment [55]. In higher eukaryotes, such as mice, where mutation rates are comparable to humans [56], systematic genetic screening dependent on these rare mutation events would require an unfeasible number of subjects. Nonetheless, large mouse repositories such as the Jackson Laboratory and MRC Harwell have collected such rare mutants, many serving as useful models for phenotypic studies [57-60]. Chapter III addresses one such unexpected variant and its phenotype.

N-ethyl-N-nitrosourea as mutagen

In order to expedite the occurrence of *de novo* mutations in mice, various DNA damaging agents and their effect on germ cells have been investigated in the past. William Russell and colleagues at Oak Ridge National Laboratory demonstrated successful germline mutagenesis using radiation [61] as well as the chemical agents chlorambucil [62] and N-ethyl-N-nitrosourea (ENU) [63]. Additionally, biological agents such as the transposable elements Sleeping Beauty and PiggyBac have been shown to randomly disrupt gene function in the mouse germline [64, 65].

Among these approaches, ENU has become the most commonly used agent for forward genetic screens. ENU is relatively easy to apply by intraperitoneal injection, has a high mutation rate, induces point mutations affecting single loci, and targets

spermatogonial stem cells [66]. ENU acts as a mutagen by transferring the ethyl group of ENU to oxygen in the DNA molecule [67], causing mis-pairing and subsequent base pair substitutions during replication if not corrected by the cell's mismatch repair machinery. The largest publicly available ENU database, Mutagenetix [68], catalogs 298,819 ENU-induced mutations (January 23rd, 2016). The statistics from this database supports the previous reports of ENU preference in base pair modification [69, 70]: 42.4% of induced SNVs are A/T → G/C transition and 26.5% A/T → T/A transversions, while <1% of the mutations are C/G → G/C transitions (Figure 1-3A). Due to the nature of ENU, most protein sequence altering mutations are nonsynonymous SNVs (80.2%), followed by variants at splice acceptor or donor sites (10.4%) and nonsense mutations (4.0%) (Figure 1-3B).

The standard ENU dosage (3 weekly injections at 90 mg/kg) results in approximately 60-65 coding variants per sperm, correlating to about 1.42-1.54 mutations per megabase (Mb) [71, 72]. As expected, not all ENU-induced SNVs are damaging. PolyPhen software [73] predicts no effect on protein function for more than a third of ENU-induced SNVs in the Mutagenetix database; 10% of variants are predicted to be harmful with another 36% predicted to be probably harmful and 17% possibly harmful (Figure 1-3D). As expected, while the majority of phenotype-causing mutations in the Mutagenetix database are still missense variants (66.1%), the proportion of nonsense SNVs is significantly higher (13.6%) than among the total ENU variants (Figure 1-3C).

Russell *et al.* at Oak Ridge estimated the incidence of gene altering ENU mutations using specific-locus tests [74]. The specific-locus test strain T is a mouse strain with seven easily identifiable recessive phenotypic features, including pink eyes and short ears (Table 1-1). ENU treated wildtype males were crossed to homozygous T strain females. All progeny from this cross should be at least heterozygous for all seven loci and would appeared wildtype unless an ENU variant happened to damage the paternal allele for one of the seven loci. After screening 6939 progeny, a total of 64 mutant offspring was identified. Fifty-one of the mutants were independent events, with the rest sharing the ENU parent and therefore the independent occurrence of the mutation could not be tested [75]. While at the time Russell and colleagues did not know

the underlying genes in the specific-locus test and their coding sequence length, we can now calculate the incidence of damaging mutations from their work based on those seven loci. The total number of base pairs (bp) tested for mutants was ~99.57 Mb (14,349 bp (length of the seven genes) * 6939 mice) and the number of independent mutants found was 51. Assuming that all the underlying phenotype-altering SNVs were in coding sequences, we would expect 0.51 damaging mutations per 1 Mb. This suggests that ~35% of all coding ENU variants are phenotype altering. These ENU statistics correlate well with our own data (discussed in Chapters II and IV).

Forward genetic screens

Forward genetics is defined as a strategy that aims to characterize the structural alterations at the genome level that are associated or responsible for a specific phenotype. It is the opposite of reverse genetics approaches which aim to assess the consequences of specific DNA alterations at the phenotypic level [76]. Generation 1 (G1) offspring from an ENU treated male (G0) are heterozygous for a subset of the ENU-induced mutations and can be directly screened for a dominant or semi-dominant phenotype of interest. For most genes, the deleterious effect of a mutation is compensated by the functional wildtype allele. In order to discover the phenotypes caused by such recessive mutations, additional breeding steps are required. The G1 fathers are typically mated with their G2 daughters to homozygose a subset of the mutations in their G3 progeny, which can then be screened for recessive phenotypes (Figure 1-4).

The first genome-wide ENU screens mostly focused on a particular phenotype of interest. Early examples include the Takahashi lab that set out to identify the mouse clock gene. They tested 304 G1 offspring from ENU treated males on a wheel-running activity, a robust behavioral assay for circadian rhythms, and identified one semi-dominant mutant with an abnormal circadian behavior [77]. Bode and colleagues were phenotyping for hyperphenylalaninemia using a Guthrie test that estimates blood levels of phenylalanine by bacterial growth inhibition. Initially, they focused on mapping dominant mutations but failed to find even a single mutant with a positive phenotype in the Guthrie test among >7000 tested G1 offspring. They next screened for recessive

mutants among the G3 generation obtained from intercrossing 105 G1 males to their G2 daughters and successfully identified one recessive mutation [78]. The Dove lab initially followed a circling behavior phenotype of a G1 progeny. While testing for the heritability for the circling phenotype, they noted an adult-onset anemia in some of the mice within the pedigree. This led to discovery of an independently segregating dominant mutation that predisposes mice to multiple intestinal neoplasia due to mutations in the mouse APC gene [79, 80].

In order to maximize discoveries from a genome-wide mutagenesis experiment, a collaborative group of scientists proceeded to screen multiple phenotypes in parallel. The first two large-scale ENU screens were launched in 1997 in Germany [81] and in the UK [82], followed by many others [83]. The first two screens focused on dominant mutations while screening for dozens of different phenotypes including skeletal and coat-color defects, neurological and behavioral abnormalities, atypical results in clinical chemistry tests, and many others. More recent large-scale recessive screens have expanded the list of screened phenotypes to hundreds, turning into “mouse clinics” and have uncovered many interesting induced mutations that would have likely been missed by other laboratories [84]. Still, the “mouse clinics” address only a limited number of assays and a large number of specific phenotypes remain to be explored. In addition to genome-wide approaches, many specialized regional screens including non-complementation, deletion, and balancer screens have proved to be very insightful (reviewed in [66]).

Sensitized suppressor/enhancer screens

Instead of starting the ENU screen with a wildtype animal, a sensitized screen is based on a preexisting phenotype and allows screening for mutations that suppress or enhance that particular phenotype. Such contextual screens have been very successful in yeast and invertebrate model organisms [85-87], and several published examples in mice also proved the feasibility and relevance of sensitized screens in mammalian systems [88-91].

While Matera and colleagues looked for enhancement of pigmentation deficiencies present in *Sox10* haploinsufficient mice in order to identify additional genes

in this pathway [89], other groups searched for genes that suppress the phenotype of interest. For example, Buchovecky *et al.* screened for mutations that suppress symptoms in *Mecp2*-null mice in order to identify potential novel therapeutic targets for patients with Rett syndrome (with mutations in the MECP2 gene) [90]. Sensitized screens could point investigators to novel pathways involved in disease pathology and highlight molecules interacting both directly and indirectly with the sensitizing genetic variant. As many modifier genes do not exhibit a visible phenotype outside of the context of the sensitized background, these genes would be undetected in a typical dominant or recessive screen. For example, mice haploinsufficient for *Tfpi* are phenotypically normal and viable [92] and would not be identified in a dominant screen for thrombosis. Nevertheless, *Tfpi* haploinsufficiency in mice markedly increases thrombosis in the background of $F5^{L/L}$ [47]. Chapters II and IV describe a sensitized screen based on suppression of this $F5^{L/L}$ $Tfpi^{+/-}$ lethal phenotype (Figure 1-5).

Historical mutation mapping strategies

For many years the most challenging part of a mutagenesis screen was mapping the causal mutation. As inbred mice are homozygous throughout the genome, outcrossing to a different strain was necessary to introduce differences into the DNA sequence as markers for genetic mapping. These mixed strain mice were either back-crossed (dominant) or inter-crossed (recessive) and their offspring used to define the markers that co-segregate with the phenotype. During the pre-reference sequence era, the first mapping attempts had only a handful of known polymorphic loci available. As a result, the mapped region was usually very large [77, 78]. After the identification of denser marker maps such as microsatellites and, later, single nucleotide polymorphisms (SNPs), the limitations for mapping were dictated by the recombination events. A candidate region was often 1-3 Mb in length and could contain anywhere from dozens to hundreds of candidate genes, poorly, if at all, annotated before the completion of a comprehensive reference sequence. Even with the correct annotation, some of these gene-rich regions required thousands of meioses to narrow the candidate interval. All candidate genes would have to be individually Sanger sequenced in the search for ENU mutations [93].

While this mapping strategy is straightforward and has proven successful in many cases [94-96], it is also very laborious, with multiple potential pitfalls. First, crossing to a different mouse strain introduces multiple strain-specific modifier effects [97]. Second, generating large pedigrees necessary for mapping from the ENU mutant founders could be complicated due to the biological nature of the phenotype of interest and the effect of all the other random ENU mutations on survival and fertility. Third, while mapping the phenotype to a large chromosomal segment by linkage analysis is straightforward, identifying the underlying mutation within this region can be challenging. Mutation identification is especially complicated if the region harbors many genes with no clear candidate, harbors multiple ENU mutations, or if the causal mutation is non-coding.

Mutation mapping in the next generation sequencing (NGS) era

The emergence of NGS techniques greatly enabled the identification of mutations within the entire genome [98]. In many examples, combining previously identified linkage peaks with whole exome sequencing (WES) data successfully uncovered the underlying ENU mutations [99-101].

Direct identification of ENU variants removes the necessity for outcrossing to another strain and therefore eliminates the potential complication of phenocopies due to strain modifiers. However, the challenge remains of identifying the causal mutation amongst the ~4000 mutations across the mouse genome. Even with the assumption that the underlying mutation has to introduce a change in protein sequence, dozens of mutations typically meet this criterion. Without linkage data, extensive validation is necessary to prove one of the variants responsible for the phenotype [102]. Arnold and colleagues reported that even a coarse linkage to a large chromosomal region may be sufficient to eliminate most of the candidate mutations within the coding region [103]. While they outcrossed their mice into a different strain for mapping, such coarse mapping can also be achieved using the ENU variants themselves as markers for mapping. The latter approach is applied in Chapters II and IV and has also been used by other investigators [104]. While successful in many cases, coupling linkage analysis with NGS still requires production of large pedigrees for the mapping step.

Burden testing in ENU screens

In bacteria where the number of subjects screened can be many orders of magnitude higher than in a mouse experiment, saturating for any nucleotide change at every position of the genome is possible, even without a mutagenizing agent [55]. Extremely rare *de novo* gain-of-function mutations in the human population (such as alpha-1-antitrypsin-Pittsburgh (M358A) [105, 106]) highlight the vast number of individuals needed to find even 2 individuals with the same, specific amino acid change in the human population. In contrast, *de novo* loss-of-function mutations, such as those resulting in Marfan syndrome, are more commonly characterized in a population because loss-of-function of a particular gene can be achieved by many different mutations [107]. WES has proven very successful in finding such loss-of-function variants in patients with diseases caused by *de novo* mutations within a single gene [108, 109] as well as in multiple genes [110, 111]. The causal genes are identified by searching for genes that harbored *de novo* mutations in all or in a subset of unrelated patients. Usually two or three probands with the same disease is enough to highlight the single causal gene, while more patients are required when *de novo* mutations in multiple genes (locus heterogeneity) can result in the same phenotype.

Similar concepts can be applied to map causal variants from an ENU screen. This approach relies on screening enough mice to cover the gene space with multiple disruptive mutations resulting in two or more mice with the same phenotype. The minimum number of mice to be screened will depend on the size of the gene causing the phenotype. Disruption of every average sized gene (~ 1,500 nucleotides of coding sequence) requires screening ~1,000 mice [75], but could range from 100-10,000 mice depending on the size of the gene (Figure 1-6). If there are multiple genes that cause the same phenotype, the proportion of mice identified by the screen is expected to be much higher. Due to differences in gene size and penetrance of each mutation, it is difficult to estimate how many genes underlie the same phenotype without mapping the variants using an NGS approach.

After identifying all of the protein altering ENU-induced SNVs in mice carrying the phenotype of interest, an accumulation of mutations is expected at the causal gene(s). If

only two mice are identified from a screen with the same phenotype and both have a unique mutation within the same gene, it may likely be the causal gene [88]. For phenotypes caused by mutations in multiple genes, examining more mice with the same phenotype is necessary to identify the underlying causal genes [112, 113]. In Chapter II, 8 mice with the same phenotype were whole exome sequenced yet no genes harboring ENU variants were shared between them. In contrast, sequencing 107 mice with the same phenotype in Chapter IV identified 12 genes with more ENU-induced mutations than expected by chance.

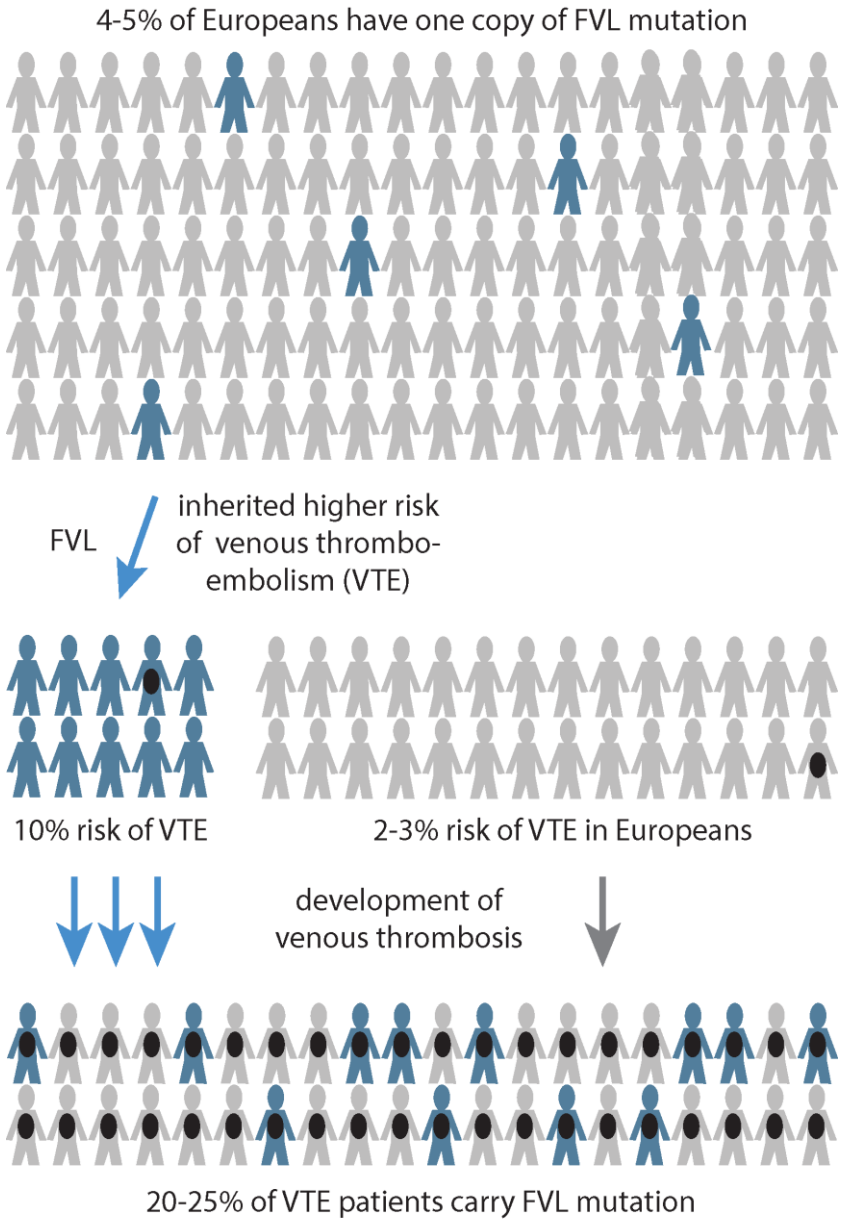

Figure 1-1: Prevalence of FVL mutation
FVL mutation is present in ~5% of people in European populations. While 20-25% of VTE patients carry the FVL mutation, only 10% of FVL carriers experience VTE in their lifetime.

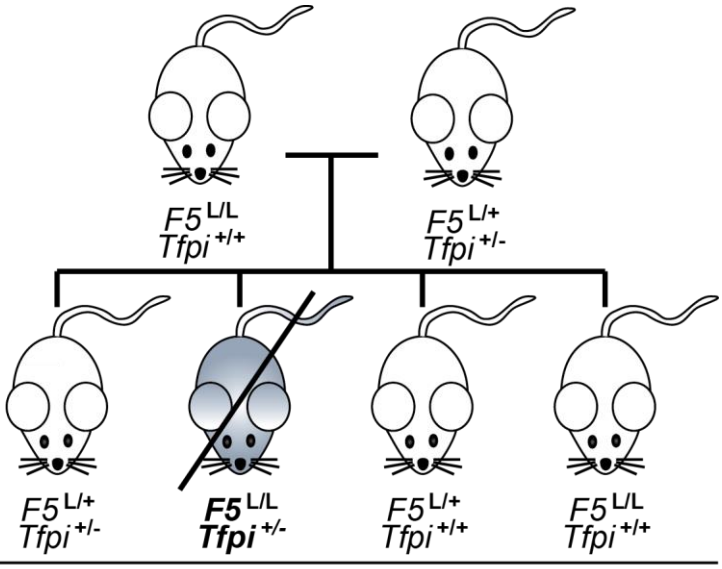

Expected	25%	**25%**	25%	25%
Observed	28%	**2%**	37%	33%
N=94	(26)	**(2)**	(35)	(31)

Figure 1-2: Perinatal lethal thrombosis model
Most mice carrying the genotype *F5$^{L/L}$ Tfpi$^{+/-}$* die by the age of weaning due to severe thrombosis. Figure adopted from Eitzman et al, 2002 [47].

A

Incidental Mutation
DNA Base Changes (assembly)

DNA Base Change	Number*
A ⇒ C	7099
A ⇒ G	63002
A ⇒ T	39310
C ⇒ A	13264
C ⇒ G	1266
C ⇒ T	24853
G ⇒ A	24579
G ⇒ C	1210
G ⇒ T	13047
T ⇒ A	39823
T ⇒ C	63466
T ⇒ G	7334
Total:	298253

B

Incidental Mutation Types

Mutation Type	Number*
makesense	631
missense	239898
nonsense	11934
start codon destroyed	564
start gained	581
synonymous	314
splice acceptor site	15423
splice donor site	15604
critical splice acceptor site	1130
critical splice donor site	4922
splice site	5378
large deletion	0
large insertion	0
rearrangement	0
small deletion	554
small insertion	255
exon	44
frame shift	822
intragenic	5
intron	662
utr 3 prime	39
utr 5 prime	59
Total:	298819

C

Phenotypic Mutation Types

Mutation Type	Number*
makesense	2
missense	528
nonsense	109
start codon destroyed	1
start gained	2
synonymous	1
splice acceptor site	32
splice donor site	33
critical splice acceptor site	17
critical splice donor site	60
splice site	0
large deletion	4
large insertion	0
rearrangement	0
small deletion	2
small insertion	2
exon	0
frame shift	2
intragenic	0
intron	3
utr 3 prime	1
utr 5 prime	0
Total:	799

D

Incidental Mutations

242,898 incidental mutations are currently displayed, and affect 20,951 genes.
41,384 are Possibly Damaging.
86,866 are Probably Damaging.
90,805 are Probably Benign.
23,843 are Probably Null.

Figure 1-3: Mutagenetix database
A) All observed ENU-induced single nucleotide changes B) ENU-induced mutation types within gene coding regions C) ENU-induced mutation types that have been validated to cause a phenotype D) Altered protein function estimated by PolyPhen software. Panels A-D are screenshot from the Mutagenetix website [68] on January 23rd, 2016.

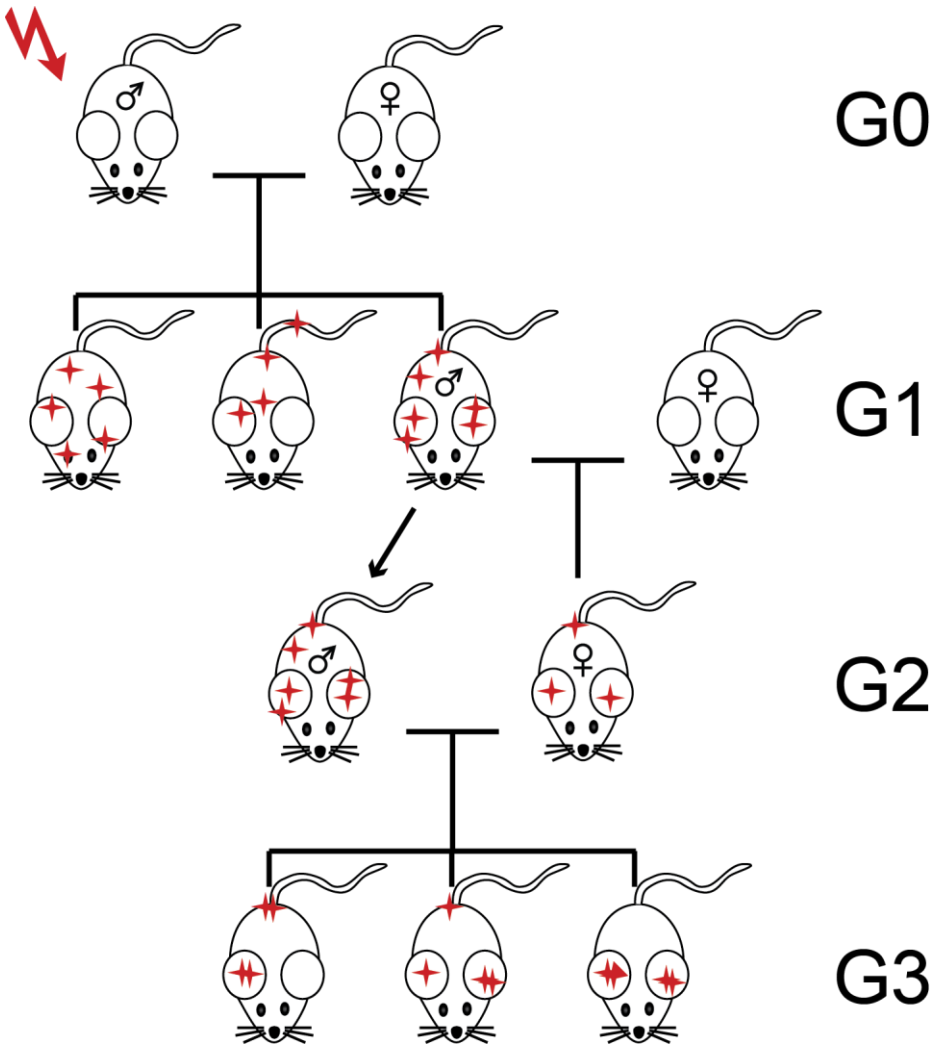

Figure 1-4: Screening strategies
G0 male is treated with mutagen (red arrow). The progeny (G1) of treated males and untreated females will each carry different heterozygous ENU-induced mutations (red stars) that can be screened for dominant phenotypes. To assess recessive mutations, G1 males are mated to their daughters (G2). Each offspring (G3) will be homozygous for a different subset of the original ENU mutations.

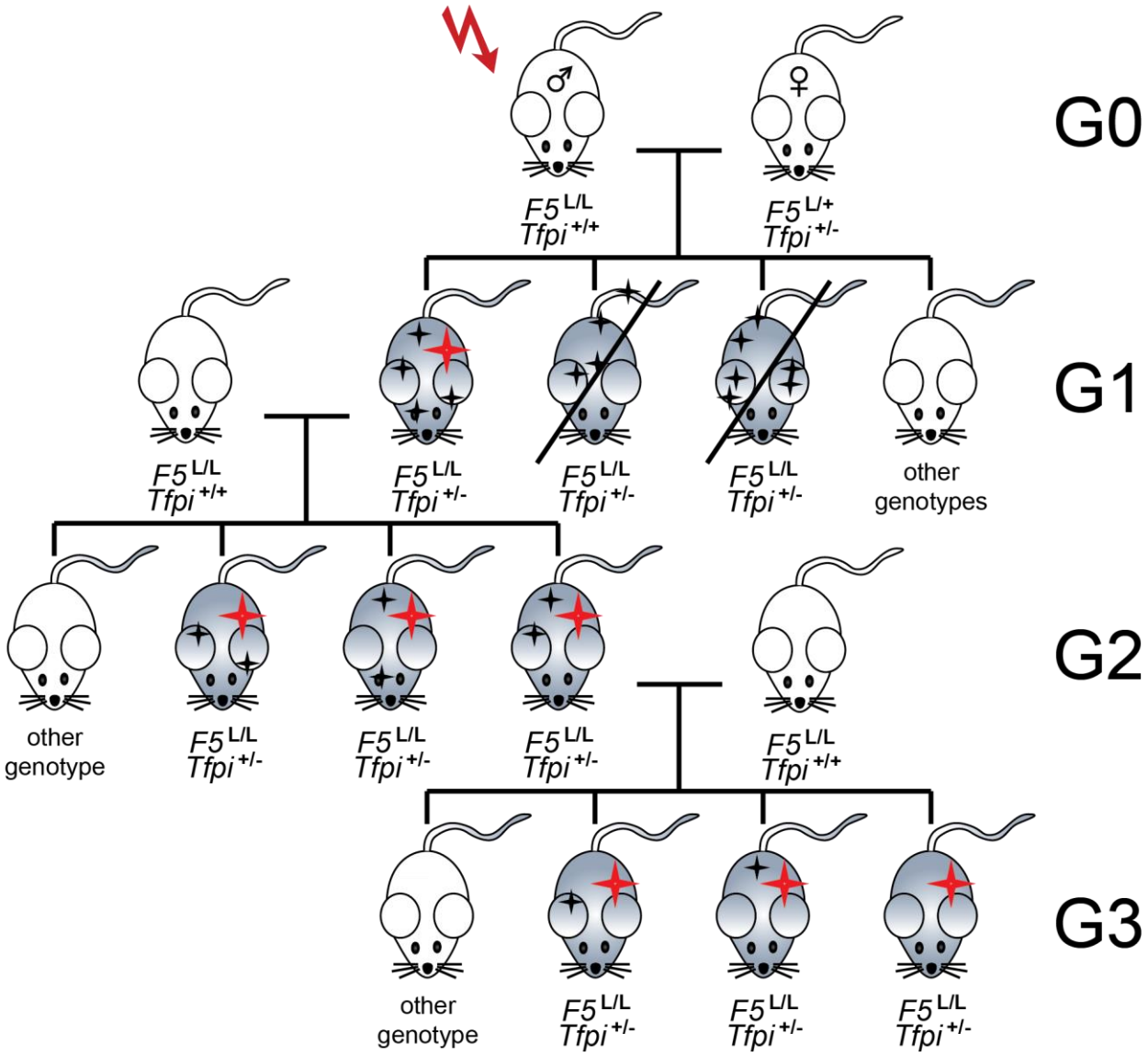

Figure 1-5: Sensitized screen for thrombosis modifiers
ENU treated *F5*$^{L/L}$ males are mated to doubly heterozygous females and the G1 offspring are screened for survivors carrying the lethal *F5*$^{L/L}$ *Tfpi*$^{+/-}$ genotype. The G1 rescue mice are progeny tested by mating to *F5*$^{L/L}$ mice. While ENU-induced mutations are expected to segregate randomly (black stars) to the progeny, the causal 'rescue' mutation (red star) is expected be present in all the rescue mice.

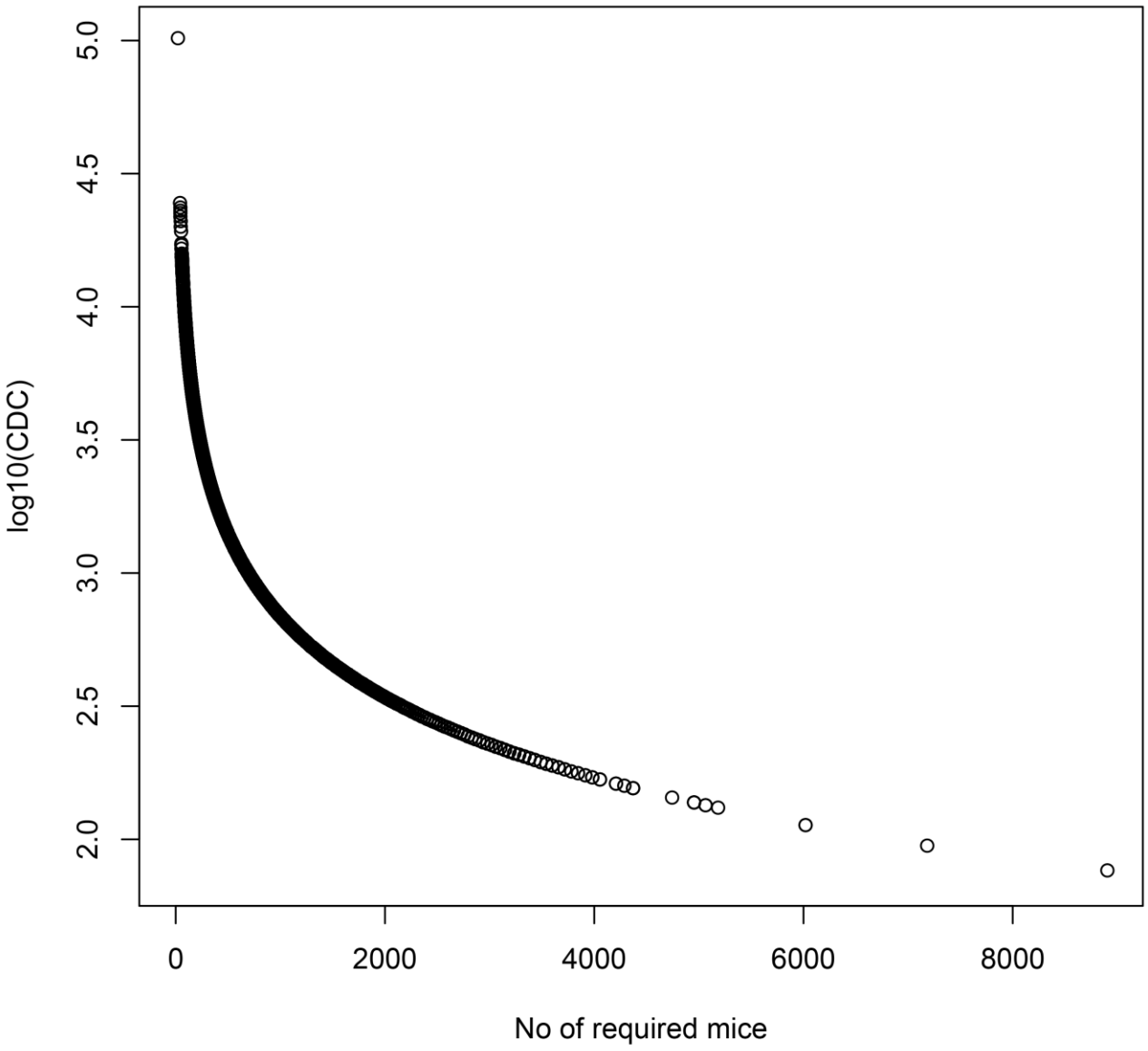

Figure 1-6: ENU gene space saturation
This plot shows on x-axis the expected number of screened progeny of ENU-induced mice necessary to introduce a mutation into every gene with a corresponding coding DNA sequence (CDS) length shown on y-axis in log10 scale assuming published ENU mutation rate of 1.5 mutations per 1,000,000 base pairs. Inducing a mutation to every average sized gene (~1,500 bp) in the genome requires screening ~400 mice, while inducing a disruptive change (~1/3 of all mutations) requires ~1000 mice.

Table 1-1: Overview of genes used in the specific-locus test

Loci	Phenotype	Gene	Location (mm10)	CDS (bp)	Independent mutants	All mutants
a	nonagouti	*a*	chr2:155,013,570-155,051,012	393	0	0
b	brown	*Tyrp1*	chr4:80,846,571-80,850,904	1611	7	8
c	chinchilla at albino	*Tyr*	chr7:87,427,405-87,493,411	1599	10	10
d	dilute	*Myo5a*	chr9:75,071,206-75,223,687	5559	10	14
p	Pink-eyed	*Oca2*	chr7:56,239,771-56,536,517	2499	16	24
s	Piebald-spotting	*Ednrb*	chr14:103814625-103844173	1326	4	4
se	Short-ear	*Bmp5*	chr9:75,775,365-75,899,017	1362	3	3
b/p	intermediate	-	-	-	1	1
			sum:	14349	51	64

Compiled based on data from Russell *et al* [75] and sequence information from UCSC genome browser (genome.ucsc.edu). mm10 = mouse genome alignment number; CDS = coding DNA sequence; bp = base pair

CHAPTER II: A sensitized mutagenesis screen in Factor V Leiden mice identifies novel thrombosis suppressor loci

Abstract

Factor V Leiden (FVL) is a common genetic risk factor for venous thromboembolism (VTE), though only 10% of individuals carrying this variant develop VTE in their lifetime. We conducted a sensitized ENU mutagenesis screen for dominant thrombosis modifier genes based on the previously reported synthetic perinatal lethal thrombosis phenotype in mice homozygous for FVL (*F5*$^{L/L}$) and haploinsufficient for tissue factor pathway inhibitor (*Tfpi*$^{+/-}$). The observation that both hemizygous and heterozygous *F8* deficiency enhanced survival of *F5*$^{L/L}$ *Tfpi*$^{+/-}$ mice demonstrated that genetic mutations in coagulation factor genes, and potentially at other loci, could suppress *F5*$^{L/L}$ *Tfpi*$^{+/-}$ lethality. G1 progeny of crosses between G0 ENU-mutagenized *F5*$^{L/L}$ males and *F5*$^{L/+}$ *Tfpi*$^{+/-}$ females were genotyped at weaning, with 98 surviving *F5*$^{L/L}$ *Tfpi*$^{+/-}$ mice ('rescues') identified. Sixteen of these G1 rescues exhibited transmission of a putative ENU suppressor mutation to subsequent generations. The lines established from each of these G1 founders, and the corresponding modifier genes are referred to as *MF5L* (Modifier of Factor 5 Leiden) 1-16. Linkage analysis in the *MF5L6* pedigree mapped the corresponding modifier locus to a region of chromosome 3 containing the tissue factor gene (*F3*). Though no ENU-induced mutation was identified in the *MF5L6* *F3* gene, a genetic cross with *F3* gene-targeted mice demonstrated that heterozygous tissue factor deficiency (*F3*$^{+/-}$) could modify *F5*$^{L/L}$ *Tfpi*$^{+/-}$ with incomplete penetrance. Thus, like *F8* deficiency, reduced *F3* activity is a major modifier for *F5*$^{L/L}$ *Tfpi*$^{+/-}$ thrombosis. Whole exome sequencing of an *MF5L12* rescue mouse identified a point mutation in a highly conserved domain of the *Actr2* gene (R258G) as the sole candidate. However, when an independent *Actr2* hemizygosity mutation (*Actr2*$^{+/-}$) was tested for its ability to suppress *F5*$^{L/L}$ *Tfpi*$^{+/-}$ lethality, no significant rescue was observed.

These data suggest that either *Actr2*^{R258G} results in gain-of-function or that another, closely linked variant is responsible for the rescue in this line. Taken together, these findings identify *F8* and the *Tfpi*/*F3* axis as key regulators of thrombosis balance in the setting of FVL and demonstrates the utility of this sensitized ENU mutagenesis approach for the identification of dominant thrombosis suppressor loci.

Introduction

Venous thromboembolism (VTE) is a common disease that affects 1 to 3 per 1000 individuals per year [1]. VTE susceptibility exhibits a complex etiology involving contributions of both genes and environment. Genetic risk factors explain approximately 60% of the overall risk for VTE [114]. The Factor V Leiden mutation (FVL) is a common inherited risk factor for VTE with an allele frequency of 2-10% in most European-derived populations [28, 115-117]. FVL is estimated to account for up to 25 percent of the genetically-attributable thrombosis risk in humans [115]. However, penetrance is incomplete, with only ten percent of FVL heterozygotes developing thrombosis in their lifetimes. The severity of thrombosis also varies widely among affected individuals [118]. This incomplete penetrance and variable expressivity limits the clinical utility of FVL genotyping in the management of VTE [119].

The incomplete penetrance and variable expressivity of thrombosis among FVL patients can at least partially be explained by genetic interactions between FVL and other known thrombotic risk factors such as hemizygosity for antithrombin III or proteins C or S, as well as the common prothrombin 20210 polymorphism [119-121]. However, <2 percent of FVL heterozygotes would be expected to co-inherit one or more of these risk factors, suggesting that a large number of additional genetic factors for VTE and/or modifiers of FVL remain to be identified [122]. Although family studies of thrombosis susceptibility display ~60% heritability [114], recent large-scale genome wide association studies (GWAS) have only confirmed *ABO*, *F5*, *FGG* and *F2* as thrombosis susceptibility genes, with few additional novel loci identified [26, 33-36], leaving the major component of VTE genetic risk still unexplained.

Mice carrying the orthologous FVL mutation exhibit a mild to moderate

prothrombotic phenotype [46], closely mimicking the human disorder, with a similarly more severe thrombosis in homozygotes. We previously reported a synthetic lethal interaction between FVL homozygosity (*F5*$^{L/L}$) and hemizygosity for tissue factor pathway inhibitor (*Tfpi*$^{+/-}$). Nearly all mice with this lethal genotype combination (*F5*$^{L/L}$ *Tfpi*$^{+/-}$) succumb to widespread, systemic thrombosis in the immediate perinatal period [47].

ENU mutagenesis in mice has been used effectively to identify novel genes involved in a number of biological processes [123, 124]. The ENU-induced germline mutations transmitted from a mutagenized male mouse (G0) occur at 1.5 mutations per megabase, at least 50 fold higher than the endogenous background mutation rate [93, 125]. Several previous reports have successfully applied an existing phenotype as a sensitizer to identify modifier genes. This method has been used effectively to screen for suppressor mutants of diabetic nephropathy in mice [91], as well as for modifiers of neurochristopathy [89], platelet number [88] and Rett syndrome [90].

We now report the results of a dominant sensitized ENU mutagenesis screen for thrombosis modifier genes based on the synthetic lethal *F5*$^{L/L}$ *Tfpi*$^{+/-}$ interaction, identifying mutations at or near the *F3*, *F8* and *Actr2* loci as suppressors of *F5*$^{L/L}$ *Tfpi*$^{+/-}$ dependent lethal thrombosis.

Materials and methods

Mice

C57BL/6J (B6, stock number 000664), 129S1/SvImJ mice (129, stock number 002448), and DBA/2J (DBA, stock number 000671), A/J (stock number 000646) and BALB/cJ (BALB, stock number 000651) were purchased from the Jackson Laboratory. *F5*$^{L/L}$ (*F5*^{tm2Dgi}/J, stock number 004080) mice were previously generated [46]. *F3* and *Tfpi* deficient mice were a generous gift of Dr. George Broze [92, 126]. *F8* deficient mice were a generous gift of Dr. Haig Kazazian [127]. All mice designated to be on the B6 background were backcrossed greater than 8 generations to B6. *F5*$^{L/L}$ breeding stock for genetic mapping were generated from *F5*^{L} mice serially backcrossed greater than 12 generations to the 129 strain to create *F5*^{L} congenic mice. B6 *F5*$^{L/+}$ *Tfpi*$^{+/-}$ mice were

crossed to the BALB strain to create *F5*$^{L/+}$ *Tfpi*$^{+/-}$ and *F5*$^{L/+}$ *Tfpi*$^{+/+}$ G1 (generation 1) mice. These mice were intercrossed to create B6BALB mixed background G2 mice. B6 *F5*$^{L/+}$ *Tfpi*$^{+/-}$ mice were crossed to *F5*$^{L/+}$ mice on the A/J or DBA strain background (for 6 generations) to generate G1 *F5*$^{L/+}$ *Tfpi*$^{+/-}$ mice, which were backgrossed to B6 *F5*$^{L/+}$ to generate mixed background G2 mice. All mice were maintained on normal chow in a specific pathogen-free facility. All animal care and experimental procedures complied with the principles of Laboratory and Animal Care established by the National Society for Medical Research and were approved by the University of Michigan Committee on Use and Care of Animals.

Genotyping

DNA was isolated from tail biopsies and mice genotyped for *Tfpi*$^{+/-}$ and *F5*^{L} as previously described [47]. Mice were genotyped for *F3* deficiency using custom primers listed in Appendix 2-1. All primers were purchased from IDT, Coralville, IA.

ENU mutagenesis and breeding

ENU was purchased (Sigma Aldrich, St. Louis MO) in ISOPAC vials, and prepared according to the following protocol: http://pga.jax.org/enu_protocol.html. A single ENU dose of 150 mg/kg was administered intraperitoneally into 159 *F5*$^{L/L}$ B6 male mice (referred to as generation 0 or G0 mice). For a second cohort of 900 male *F5*$^{L/L}$ G0 mice, the protocol was changed to three weekly intraperitoneal injections of ENU (90 mg/kg). After a 10-week recovery period, each G0 mouse was bred to *F5*$^{L/+}$ *Tfpi*$^{+/-}$ mice (Figure 2-1B) on the B6 genetic background to produce G1 offspring, which were genotyped at two weeks of age. G1 mice of the *F5*$^{L/L}$ *Tfpi*$^{+/-}$ genotype surviving to greater than three weeks of age (referred to as ‘rescues’) were considered to carry a ‘rescue’ mutation.

Modifier gene transmission

G1 rescue founders were crossed to *F5*$^{L/L}$ mice on the B6 genetic background to produce G2 offspring. G2 mice were outcrossed to *F5*$^{L/L}$ mice on the 129 genetic background. Progeny testing was considered positive with the identification of one or

more rescue offspring, regardless of the total number of progeny.

Genetic mapping

Genetic markers distinguishing the B6 and 129 strains distributed across the genome were genotyped using the Illumina GoldenGate Genotyping Universal-32 platform (Illumina, San Diego CA) at the University of Michigan DNA Sequencing Core. Linkage Analysis was performed on the Mendel platform version 14.0 [128] using 806 informative markers from the total of 1449 genotyped markers. LOD scores ≥3.3 were considered significant [129]. The number of mice, the number of SNP markers, and the LOD scores for each of the mapped pedigrees are listed in Table 2-1.

Sanger sequencing of the *F3* gene

Genomic DNA was extracted from mouse tail biopsies using the Gentra Puregene Tissue Kit (Qiagen, Germantown, MD). A total of 48 overlapping amplicons (primers: F3gene_1-F3gene_35; upstreamF3_1-upstreamF3_13, Appendix 2-1) were used to Sanger sequence the entire *F3* gene (~11kb) and an additional ~5kb of upstream sequence on both strands. Sanger sequencing was performed at the University of Michigan Sequencing Core.

Estimation of *F3* allelic expression

F5$^{L/L}$ *Tfpi*$^{+/-}$ mice with one B6 allele (in *cis* with ENU induced variants) and one 129 allele at the Chr3 candidate region were outcrossed to DBA wildtype females introducing exonic B6-129/DBA SNPs. Five progeny from this cross (2 B6/DBA and 3 129/DBA allele carriers, identified by DNA genotyping) were tested for differential *F3* allelic expression. From each mouse three tissue samples (lung, liver, whole brain) were obtained as previously described [46]. Total RNA was extracted from the tissue samples using RNeasy Plus Mini Kit (Qiagen) according to manufacturer's recommendations and reverse transcribed using SuperScript II (Invitrogen, Carlsbad, CA). cDNA corresponding to exon3-exon5 of *F3* was amplified with primers F3-exon-F (5'TGCTTCTCGACCACAGACAC) and F3-exon-R (5'CTGCTTCCTGGGCTATTTTG), using Gotaq Green Master Mix (Promega, Madison, WI). Primers F3-exon-F and F3-

exon-R were also used to Sanger sequence the *F3* exonic region. The *F3* exonic region harbors 3 known B6-129/DBA SNPs (rs30268372, rs30269285, rs30269288, http://www.ncbi.nlm.nih.gov/SNP/). Relative expression was estimated at SNP sites by dividing the area under the Sanger sequencing peak of one allele to another [130]. Next, the relative expression of each SNP was compared between the B6 and 129 allele carrying progeny.

Whole exome sequencing

Libraries were prepared using Agilent (Agilent Technologies, Santa Clara, CA) or NimbleGen (Roche NimbleGen, Madison, WI) mouse whole exome capture kits. 100 bp paired-end sequencing was performed on the Illumina Hiseq 2000 platform at the University of Michigan DNA Sequencing Core. A detailed overview of the whole exome sequencing (WES) pipeline is available at GitHub (github.com/tombergk/FVL_SUP). Briefly, sequence reads were aligned using Burrows-Wheeler Alignment software [131] to the mouse reference genome (genome assembly GRCm38, Ensembl release 73). Reads were sorted and duplications removed using Picard tools (http://picard.sourceforge.net). Coverage statistics were estimated using QualiMap software [132]. Variants were called across 8 samples using GATK HaplotypeCaller software [133]. Standard hard filters recommended by the Broad Institute were applied using GATK VariantFiltration [133] followed by an in-house developed pipeline to remove variants between the B6 and 129 strains, shared variants within our mouse cohort and variants in closer proximity than 200 base pairs from each other. Variants were annotated using Annovar software [134] with Refseq annotation (release 61). Heterozygous variants within exonic regions with ≥6X coverage unique for only one mouse in the cohort were regarded as potential ENU-induced variants. The candidate ENU-induced variants were validated by Sanger sequencing.

Generation of an independent *Actr2* null allele

Embryonic stem (ES) cells containing the targeted *Actr2*$^{tm1a(KOMP)Wtsi}$ "Knockout First" allele (ES cell clone EPD0727_2_H12, generated by the Wellcome Trust Sanger Institute, Hinxton, UK) were karyotyped by the UC Davis KOMP Repository, Davis, CA

and found to contain 71-80% euploid cells. This ES cell line was then injection into B6 blastocysts by the University of Michigan Transgenic Animal Model Core. Analysis of founders identified 6 chimeras, which were mated yielding germline transmission by a single 20% chimera.

Statistical data analysis

Statistical differences among the potential progeny of mouse crosses were determined using the X^2 test. A paired t-test was used for estimating statistical differences between the weights of rescue mice and their littermates. Relative expression differences for *F3* alleles were estimated using the Wilcoxon rank-sum test. Kaplan Meier analysis was used to assess significance for putative suppressors identified by exome sequencing.

Results

F8 deficiency suppresses *F5*$^{L/L}$ *Tfpi*$^{+/-}$ lethality

To test whether the *F5*$^{L/L}$ *Tfpi*$^{+/-}$ lethal phenotype is genetically suppressible by *F8* deficiency (classic hemophilia A), triple heterozygous *F5*$^{L/+}$ *Tfpi*$^{+/-}$ *F8* X^+X^- female mice were generated and crossed to *F5*$^{L/L}$ male mice (Figure 2-1A). One quarter of conceptuses were expected to carry the *F5*$^{L/L}$ *Tfpi*$^{+/-}$ genotype, with half of all female offspring expected to be also *F8* X^+X^- and half of the male mice completely *F8* deficient (hemizygous). A total of 167 progeny from this cross were genotyped at weaning, with 8 *F5*$^{L/L}$ *Tfpi*$^{+/-}$ *F8* X^-Y male and 2 *F5*$^{L/L}$ *Tfpi*$^{+/-}$ *F8* X^+X^- female mice observed (67% of expected for males and 16.7% for females; Table 2-2).

The *F5*$^{L/L}$ *Tfpi*$^{+/-}$ phenotype is suppressed by dominant ENU induced mutations

A sensitized whole genome ENU mutagenesis screen for dominant thrombosis suppressor genes was implemented as depicted in Figure 2-1B. ENU mutagenized G0 *F5*$^{L/L}$ males were crossed to *F5*$^{L/+}$ *Tfpi*$^{+/-}$ females to generate G1 mice, which were screened by genotyping at weaning for *F5*^{L} and *Tfpi*$^{+/-}$. A number of previously described visible dominant mutants [82] were observed among the G1 offspring, ranging from

belly spotting to skeletal abnormalities in approximately 5.9% of G1 mice, similar to the ~4.2% rate of observable mutants in previous studies [82], and consistent with the estimated ~20-30 functionally significant mutations per G1 mouse expected with this ENU mutagenesis protocol [135]. One quarter of G1 embryos would be expected to carry the synthetic lethal *F5*$^{L/L}$ *Tfpi*$^{+/-}$ genotype. A total of 6,739 G1 mice were screened at weaning, identifying 98 live mice (45 females, 53 males) with the *F5*$^{L/L}$ *Tfpi*$^{+/-}$ genotype, representing 4.43% of the expected 2,214 mice predicted by Mendelian genetics (Table 2-3).

The heritability of each of the 98 G1 putative rescue mutants was evaluated by progeny testing through backcrosses to B6 *F5*$^{L/L}$ mice. The observation of one or more rescue mice among the progeny provided evidence that a particular *MF5L* line carries a transmissible rescue mutation. 72 of the 98 G1 rescues produced no offspring, either due to early lethality or infertility, with ~50 percent of these mice (34/72) exhibiting a grossly runted appearance. Approximately ~45% (44/98) of rescues died by 10 weeks of age, with slightly poorer survival for females (Figure 2-1C).

Twelve male and 4 female G1 rescues produced one or more *F5*$^{L/L}$ *Tfpi*$^{+/-}$ progeny when bred to B6 *F5*$^{L/L}$ mice (Table 2-3). These putative mutant mice were subjected to further breeding to create lines of genetically informative progeny. The distribution and penetrance for each ENU line are listed in Table 2-4. Within the ENU lines, mice with the *F5*$^{L/L}$ *Tfpi*$^{+/-}$ genotype were ~30% smaller than their *F5*$^{L/L}$ littermates at the time of weaning ($p<2.2x10^{-16}$; Figure 2-1D), and the size difference was maintained after outcrossing to the 129 strain (Figure 2-1E).

Identification of a mapping strain preserving the *F5*$^{L/L}$ *Tfpi*$^{+/-}$ lethal phenotype

Four inbred mouse strains were tested by crosses introducing the *F5*^{L} and *Tfpi*$^{-}$ alleles, with only 129 retaining the *F5*$^{L/L}$ *Tfpi*$^{+/-}$ synthetic lethal phenotype (Table 2-5). Analysis of the crosses of *F5*$^{L/L}$ x *F5*$^{L/+}$ *Tfpi*$^{+/-}$ and *F5*$^{L/+}$ x *F5*$^{L/+}$ *Tfpi*$^{+/-}$ on the 129 strain background revealed not only an absence of *F5*$^{L/+}$ *Tfpi*$^{+/-}$ mice, but also a 50% reduction of *F5*$^{L/L}$ *Tfpi*$^{+/+}$ mice at weaning (Table 2-5).

The *MF5L6* suppressor mutation maps to a chromosome 3 interval containing *F3*

The *MF5L1, 6, 8* and *16* lines were crossed to the 129 genetic background and generated significant numbers of $F5^{L/L}$ $Tfpi^{+/-}$ on the mixed 129-B6 genetic background suggesting potentially mappable mutants. *MF5L6* was maintained for 12 generations and had 214 genetically informative $F5^{L/L}$ $Tfpi^{+/-}$ mice out of 336 total progeny. Genome-wide SNP genotyping of the 214 *MF5L6* rescues followed by multipoint linkage analysis identified 2 loci with maximum LOD scores >3.3 (Figure 2-2A). The signal on Chr 2 (maximum LOD score=9.81), spanning the *Tfpi* gene, was expected, since after backcrossing to 129 $F5^{L/L}$ mice, the $Tfpi^{+/-}$ allele is always of B6 origin as it is derived from the B6 $F5^{L/+}$ $Tfpi^{+/-}$ female crossed to the original G0 $F5^{L/L}$ male. This region was therefore excluded from further analysis. The Chr 3 peak exhibited the next highest LOD score (maximum LOD=4.49), with the 1 LOD interval (117.3-124.8 Mb) containing 38 refseq annotated genes (Figure 2-2C). Additional linkage analysis for the *MF5L1*, *MF5L8,* and *MF5L16* ENU lines failed to identify any peaks with LOD >2.5, other than the Chr 2 *Tfpi* locus (Table 2-1).

The *F3* gene located at Chr3:121.7 Mb within the *MF5L6* Chr 3 candidate interval (Figure 2-2C) encodes tissue factor (TF), a procoagulant component of the hemostatic pathway that is regulated in part by *Tfpi*, and thus a highly plausible candidate for a loss-of-function mutation suppressing the $F5^{L/L}$ $Tfpi^{+/-}$ phenotype. However, sequence analysis of the full set of *F3* exons and introns as well as 5 kilobase upstream of exon 1 failed to identify an ENU-induced mutation. Analysis of *F3* mRNA levels in liver, lung, and brain tissues of adult mice failed to identify any differences in the level of expression from the ENU-mutant and wildtype alleles (Figure 2-3). However, this analysis cannot exclude the possibility of a regulatory mutation affecting expression in another tissue or other developmental stage.

***F3* haploinsufficiency suppresses the $F5^{L/L}$ $Tfpi^{+/-}$ lethal phenotype**

To test *F3* as a candidate suppressor of the $F5^{L/L}$ $Tfpi^{+/-}$ phenotype, an independent *F3* null allele was introduced and triply heterozygous $F5^{L/+}$ $Tfpi^{+/-}$ $F3^{+/-}$ mice were crossed to $F5^{L/L}$ B6 mice (Figure 2-2B). Of 272 progeny genotypes at weaning (Table 2-6), 13 $F5^{L/L}$ $Tfpi^{+/-}$ $F3^{+/-}$ were observed, compared to 1 $F5^{L/L}$ $Tfpi^{+/-}$ $F3^{+/+}$ ($p <$

0.0001), though with significantly fewer male than female *F5$^{L/L}$ Tfpi$^{+/-}$ F3$^{+/-}$* mice (2 vs. 11 $p<0.05$). Thus, haploinsufficiency for *F3$^{+/-}$* rescues the synthetic lethality of *F5$^{L/L}$ Tfpi$^{+/-}$*, though with incomplete penetrance that also differs by gender. These data strongly support the idea of a *F3* regulatory mutation responsible for thrombosuppression in *MF5L6*. Further analysis of WES in mice from this line identified two validated ENU variants for *MF5L6* (Table 2-7) neither of which were located on Chr 3. This likely excludes an ENU-induced coding variant responsible for the rescue phenotype in that line and is consistent with the hypothesis of a *F3* regulatory mutation outside of the gene and 5kb upstream region.

WES identifies candidate ENU-induced variants for 8 *MF5L* lines

WES was performed on genomic DNA from one rescue mouse from each of 8 *MF5L* lines with the largest pedigrees (*MF5L1, MF5L5, MF5L6, MF5L8, MF5L9, MF5L11, MF5L12, MF5L16*). The mean coverage of sequenced exomes was more than 90X, with >97% of the captured region covered with at least 6 independent reads (Table 2-8). A total of 125 heterozygous variants were identified as candidate suppressor mutations using an in-house filtering pipeline. 79 variants affected the protein sequence (Table 2-7). 54.5% were nonsynonymous single nucleotide variants (SNVs), followed by UTR (17.6%), synonymous (14.4%) and stopgain SNVs (7.2%). The most common mutation events were A/T→G/C transition (35.2%), while C/G→G/C transitions were the least represented (2.5%). This spectrum of mutations is consistent with previously published ENU reports [70]. Validation was performed on 52 variants using Sanger sequencing. These variants were then checked for parent of origin (either the G1 mutagenized progeny or its nonmutagenized mate). 42 of the variants were identified in the G1 rescue and neither parent, suggesting that they were ENU-induced mutations.

***Actr2$^{+/G}$*, but not *Actr2$^{+/-}$* is associated with rescue of the *F5$^{L/L}$ Tfpi$^{+/-}$* phenotype**

Of the 7 ENU-induced nonsynonymous SNVs identified from WES analysis for the *MF5L12* line, 6 were validated by Sanger sequencing to have arisen in the G1 rescue (Table 2-7). For each of these 6 SNVs, co-segregation with the survival phenotype was tested by Kaplan-Meier analysis of 31 total rescue mice from the

MF5L12 line. Only one variant, a nonsynonymous SNV in the *Actr2* gene (*Actr2*$^{+/G}$) demonstrated a significant survival advantage when co-inherited with the *F5*$^{L/L}$ *Tfpi*$^{+/-}$ genotype ($p=1.7x10^{-6}$; Figure 2-4A). The *Actr2*$^{+/G}$ mutation results in an R258G substitution in exon 7 of *Actr2* at a highly conserved amino acid position, with arginine present at this position for all 60 available vertebrate sequences (https://genome.ucsc.edu) as well as in plants and fungi (Figure 2-4B). In addition, no variants at this position have been identified to date in over 120,000 human alleles (ExAC, http://exac.broadinstitute.org accessed 01/2016).

To test *Actr2* haploinsufficiency as a suppressor of the *F5*$^{L/+}$*Tfpi*$^{+/-}$ phenotype, an independent *Actr2* null allele was generated and *F5*$^{L/+}$*Tfpi*$^{+/-}$ *Actr2*$^{+/-}$ triple heterozygote mice crossed to *F5*$^{L/L}$ mice. Out of 154 progeny from this cross, only one *F5*$^{L/L}$ *Tfpi*$^{+/-}$ *Actr2*$^{+/-}$ mouse survived to weaning (Figure 2-4C), consistent with the expected background survival rate. These data suggest that the thrombosis suppression observed in *MF5L12* is either due to a unique gain-of-function resulting from the *Actr2*$^{+/G}$ mutation or due to another ENU mutation tightly linked to *Actr2*.

Semi-quantitative western blots (Figure 2-5A) demonstrate a significant decrease in total ARP2 protein in *Actr2*$^{+/G}$ platelets compared to *Actr2*$^{+/-}$ and wildtype. Mouse embryonic fibroblasts (MEFs) derived from *Actr2*$^{+/G}$ mice grow poorly in culture compared to control MEFs, are less efficient at forming cell-to-cell contacts and display F-actin aggregates at the root of cellular protrusions on phalloidin staining (Figure 2-5B). *Actr2*$^{+/G}$ MEFs also exhibit a spreading defect on a fibronectin matrix, decreased cell-cell contacts, an abnormal F-actin aggregates, and latency in cell spreading on fibronectin-coated coverslips (Figure 2-5C). Analysis of peripheral blood from *Actr2*$^{+/G}$ mice demonstrates subtle but significant reductions in mean platelet volume and mean platelet mass, compared to littermate controls ($p<0.0001$; Figure 2-5E), as well as reduced platelet aggregation ($P < 0.05$; Figure 2-5D).

Discussion

We conducted a sensitized ENU mutagenesis screen for dominant suppressors of the *F5*$^{L/L}$ *Tfpi*$^{+/-}$ lethal genotype. *F8* deficiency suppressed *F5*$^{L/L}$ *Tfpi*$^{+/-}$, indicating that

the *F5*$^{L/L}$ *Tfpi*$^{+/-}$ lethality is suppressible. This is also consistent with human studies demonstrating elevated *F8* levels as a VTE risk factor. Analysis of offspring from the *Leiden* screen identified 98 *F5*$^{L/L}$ *Tfpi*$^{+/-}$ mice that survived to weaning, with 16 of these rescues exhibiting the transmission of an ENU suppressor mutation. Genetic mapping studies proved to be very difficult due to the presence of mouse strain specific genes capable of interacting with the *F5*$^{L/L}$ *Tfpi*$^{+/-}$ phenotype. Nonetheless, mapping of *MF5L6* localized it to a region of chromosome 3 containing the tissue factor gene. Using an independent *F3* knockout allele, *F3* haploinsufficiency was demonstrated to rescue with incomplete penetrance. WES for *MF5L12* revealed a point mutation in a highly conserved domain in the *Actr2* gene (R258G) as the sole candidate. However, when *Actr2* hemizygosity (*Actr2*$^{+/-}$) was tested for its ability to suppress *F5*$^{L/L}$ *Tfpi*$^{+/-}$ lethality, only a background level of *F5*$^{L/L}$ *Tfpi*$^{+/-}$ survivors was observed. This suggests that either the *Actr2*^{R258G} mutation functions by a mechanism other than haploinsufficiency or a closely linked variant is responsible for the rescue in this ENU line.

A fundamental aspect of our screening strategy is that only dominant and not recessive mutations will be identified. However, it is assumed that most common human modifier genes are dominant in inheritance rather than recessive, as a recessive mutation would be much less likely to reach high population prevalence. The validity of this assumption is supported by the observation that all of the common human thrombophilia mutations already known, including FVL and the prothrombin G20210A mutation, are autosomal dominant.

Our screening strategy will only detect mutations that alter the hemostatic balance in an antithrombotic direction by compensating for *F5*$^{L/L}$ *Tfpi*$^{+/-}$ lethality. ENU-induced mutations are most likely to result in partial or complete loss of function. Thus, most of the mutations identified by our dominant screen can be expected to be due to haploinsufficiency. All or most of these mutations are likely to be silent on a wild-type background and would thus be missed in a conventional, unsensitized mutagenesis screen. Similarly, the corresponding human mutations may also be completely silent by themselves, but may function as important modifier genes when co-inherited with another thrombophilia mutation such as FVL.

At first glance, the 98 independent *F5*$^{L/L}$ *Tfpi*$^{+/-}$ putative suppressor mice

comprised an abundant source of candidates for novel thrombosis suppressor gene identification. However, in our initial report of the *F5*$^{L/L}$ *Tfpi*$^{+/-}$ phenotype, we observed a low level of survival for *F5*$^{L/L}$ *Tfpi*$^{+/-}$ mice (3.75% of expected conceptuses) [47]. The overall observed number of rescues in this screen was 4.43% of expected conceptuses, which is a little higher than the background survival rate. Of note, the survival is close to three fold higher in the mice that received three weekly doses of ENU (5.7%) compared to mice with one dose of ENU (2%) suggesting that at least a subset of the rescues reflect the effect of authentic ENU-induced suppressor mutations. In addition, considering that the increased mutation burden could contribute to overall poorer health in G1 mice produced from a mutagenized parent, this could actually reduce the background survival rate within the screen.

As our initial strategy for suppressor mutant identification was based on traditional genetic mapping/candidate gene analysis, it was necessary to outcross surviving *F5*$^{L/L}$ *Tfpi*$^{+/-}$ to *F5*$^{L/L}$ mice on another genetic background and then perform an incross to generate genetically informative data. To avoid deleterious modifier genes from the 129 genetic background [46], we first chose to test the DBA, A/J and BALB. In each instance, a mixed background cross of *F5*$^{L/+}$ *Tfpi*$^{+/-}$ x *F5*$^{L/+}$ *Tfpi*$^{+/+}$ resulted in completely penetrant non-lethality of the *F5*$^{L/L}$ *Tfpi*$^{+/-}$, demonstrating the existence of powerful thrombosis suppressor genes associated with these strains. Thus, we were forced to resort to the prothrombotic 129 strain as an outcross strain for genetic mapping. As a result, 4 of our lines contained significant numbers of *F5*$^{L/L}$ *Tfpi*$^{+/-}$ on the mixed 129-B6 genetic background. We attempted to genetically map the suppressor mutants in these lines and were successful in mapping *MF5L6* to a region containing the *F3* gene. Although we failed to identify an ENU-induced mutation in or near *F3* gene in *MF5L6*, *F3* represented such a compelling candidate suppressor that we tested the ability of *F3* haploinsufficiency to suppress *F5*$^{L/L}$ *Tfpi*$^{+/-}$. Initiation of coagulation by *F3* is directly opposed by *Tfpi*. Our data demonstrate that reduction of *F3* levels by ~50% restored viability to *F5*$^{L/L}$ *Tfpi*$^{+/-}$ mice, presumably by compensating for the similar reduction in *Tfpi*. Since the surviving *F5*$^{L/L}$ *Tfpi*$^{+/-}$ *F3*$^{+/-}$ mice had a grossly normal appearance and lifespan, the reason for the reduced penetrance is unknown, but could be largely explained by the significant reduction of male *F5*$^{L/L}$ *Tfpi*$^{+/-}$ *F3*$^{+/-}$ compared to

females among surviving progeny. Gender-specific differences in venous thrombosis recurrence have been previously documented [136, 137]. These data are consistent with a critical role of extrinsic pathway control through *F3*/*Tfpi* balance, particularly in the setting of FVL. Thus, modest variations in expression of either *F3* or *Tfpi* could be important for modifying VTE in humans. Indeed, *Tfpi* variants have been associated with both venous thromboembolism and myocardial infarction in human studies [138, 139].

The failure to identify significant linkage in the remaining mappable lines could be due to complex strain modifier gene interactions between the 129 and B6 mouse strains [140]. Since we failed to identify significant linkage peaks in lines other than *MF5L6*, we used a WES approach to identify suppressors in the other lines. This work resulted in the identification of a single heterozygous $Actr2^{+/G}$ mutation that co-segregated with the $F5^{L/L}$ $Tfpi^{+/-}$ survival phenotype in the *MF5L12* line. The *Actr2* gene encodes the ARP2 protein, which is an essential component of the ARP2/3 complex. This mutation occurs at an amino acid position in the ARP2 protein that is conserved from humans to plants and fungi. The ARP2/3 complex is essential for actin branching and polymerization and complete ARP3 deficiency is incompatible with life [141]. The other members of the complex include ARPC 1-5. Disruption of any one of the members of the ARP2/3 complex has been demonstrated to reduce the activity of the complex [141].

Relative to blood coagulation and thrombosis, ARP2 deficiency was demonstrated to influence platelet shape change, a process that is critical for normal platelet function and thus for hemostasis [142]. Given the $Actr2^{+/G}$ mutation changed such a highly conserved amino acid, we surmised that this change would result in loss of function. However, *Actr2* haploinsufficiency via an independent *Actr2* knockout allele ($Actr2^{+/-}$) failed to suppress the $F5^{L/L}$ $Tfpi^{+/-}$ lethal genotype.

In conclusion, through the design and execution of the *Leiden* sensitized ENU mutagenesis screen, we have identified *F3*, *F8*, and *Actr2* as potential suppressor genes for $F5^{L/L}$ $Tfpi^{+/-}$ lethality. Given the observation of potent strain specific modifiers in the *Leiden* screen as well as the utility of NGS in mouse genetic studies [71], performing the entire *Leiden* mutagenesis screen in a single mouse genetic background may enable the rapid identification of additional suppressor genes.

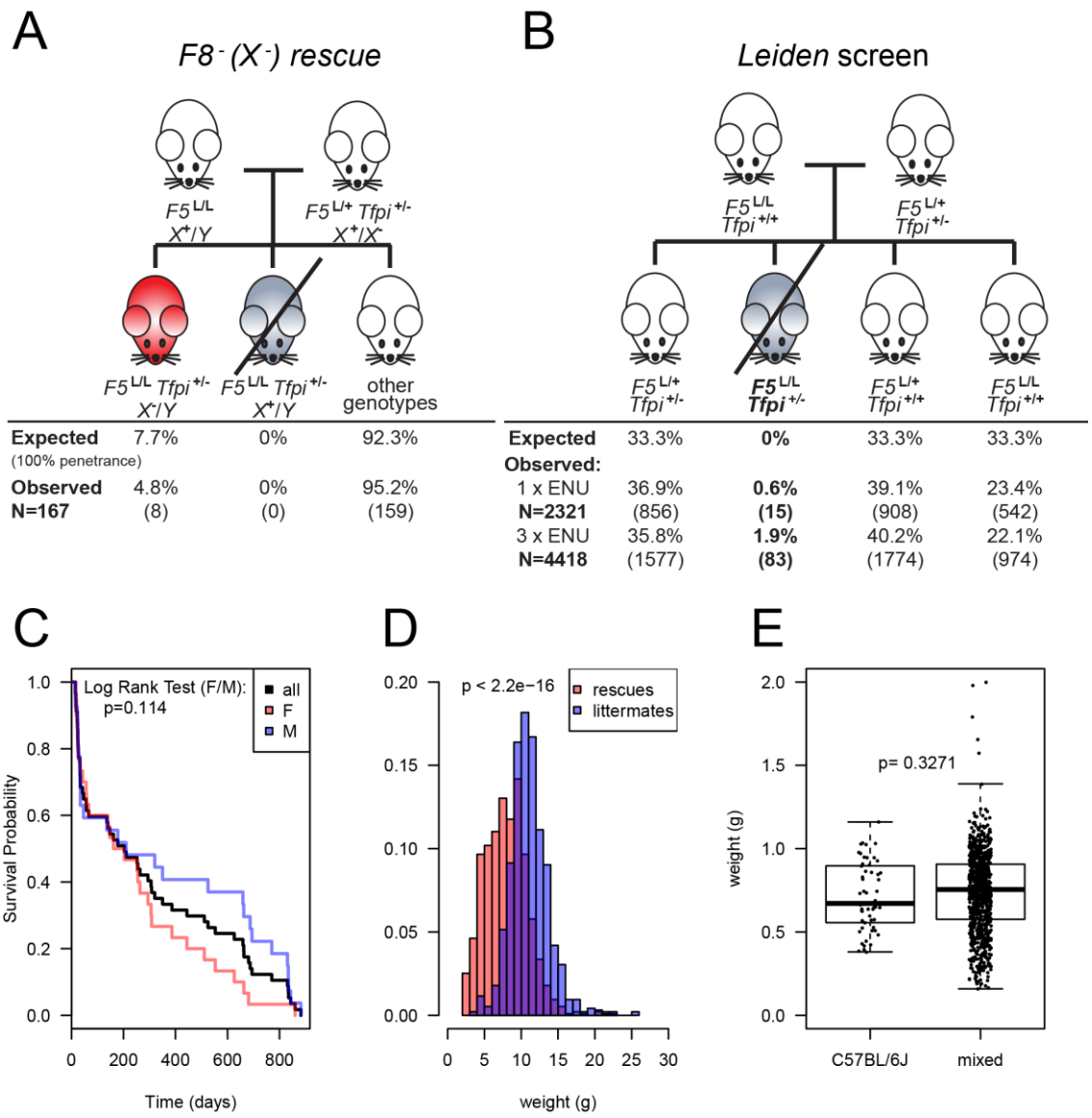

Figure 2-1: *F8* deficient thrombosuppression and design of the *Leiden* ENU mutagenesis screen

A. The mating scheme and observed distributions of the $F5^{L/+}$ $Tfpi^{+/-}$ *F8* deficiency rescue experiments. *F8* X^{-} results in incompletely penetrant suppression of the $F5^{L/+}$ $Tfpi^{+/-}$ phenotype. B. The mating scheme and observed distribution of the *Leiden* screen. $F5^{L/+}$ $Tfpi^{+/-}$ male mice were mutagenized with either 1 x 150mg/kg or 3 x 90 mg/kg ENU and bred with non-mutagenized $F5^{L/L}$ females. Sixteen and 83 $F5^{L/L}$ $Tfpi^{+/-}$ progeny, respectively were observed in each of the dosing regimens, with over twice the rate of $F5^{L/L}$ $Tfpi^{+/-}$ survivors in the progeny of the 3 x 90 mg/kg treated mice. C. On the whole, there were insignificant survival differences among the different genders of $F5^{L/L}$ $Tfpi^{+/-}$ putative suppressor mice. D and E. $F5^{L/L}$ $Tfpi^{+/-}$ putative suppressor mice were distinctly smaller than their non-$F5^{L/L}$ $Tfpi^{+/-}$ littermates in both the pure B6 and mixed B6-129 genetic backgrounds.

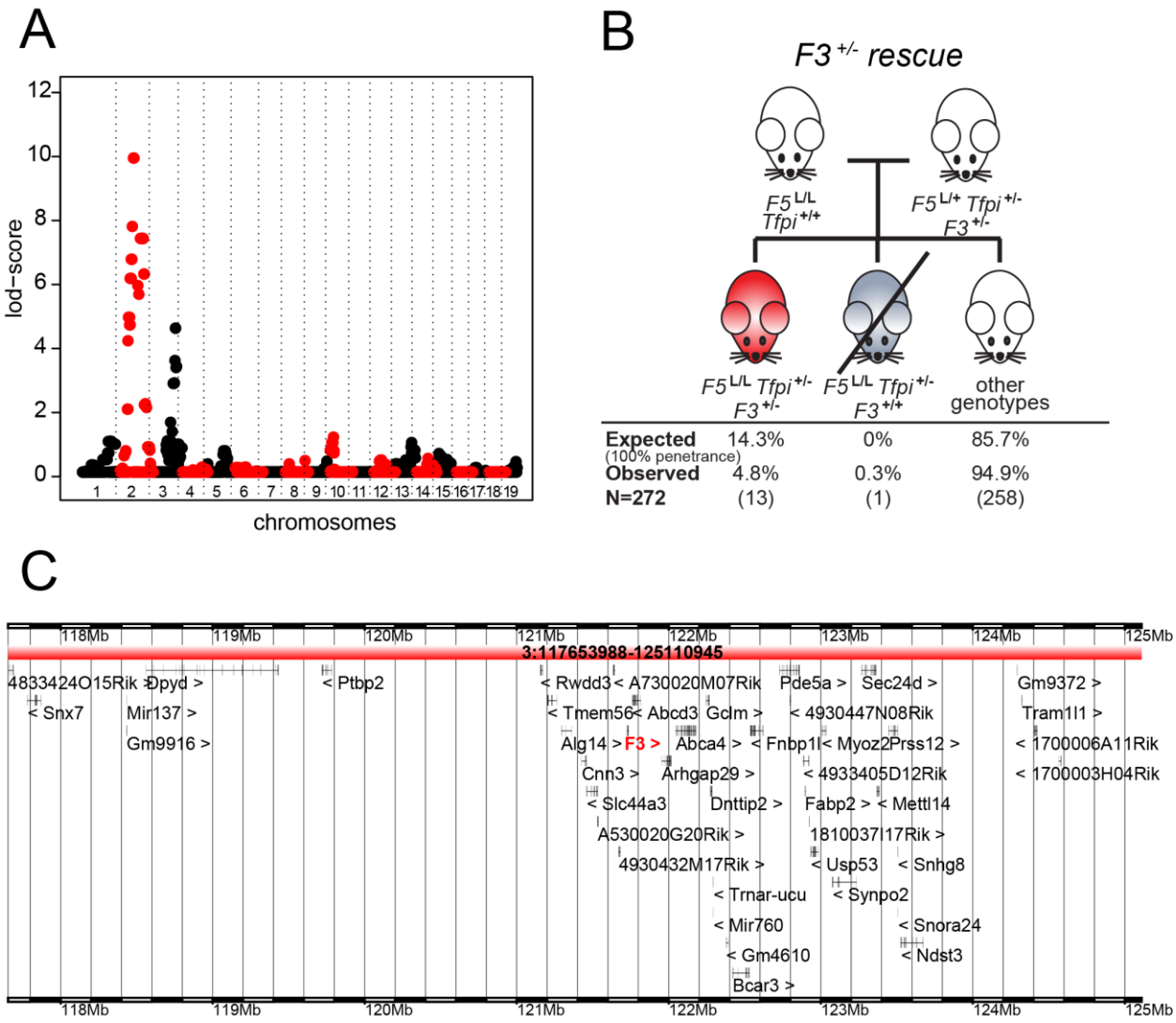

Figure 2-2: Discovery and validation of the chromosome 3 thrombosuppressor locus

A. Linkage analysis for the *MF5L6* line. The Chr 2 locus (LOD score=9.81) includes the *Tfpi* gene. The Chr 3 peak had the highest LOD score in the Chr3 subregion:117.3-124.8Mb (LOD score=4.49, 1 LOD interval). B. The mating scheme and observed distribution of the $F5^{L/+}$ $Tfpi^{+/-}$ *F3* deficiency rescue experiment. $F3^{+/-}$ results in incompletely penetrant suppression of the $F5^{L/+}$ $Tfpi^{+/-}$ phenotype. **C.** The Chr 3 candidate interval (chr3:117.3-124.8 Mb) contains 38 refseq annotated genes, including *F3*.

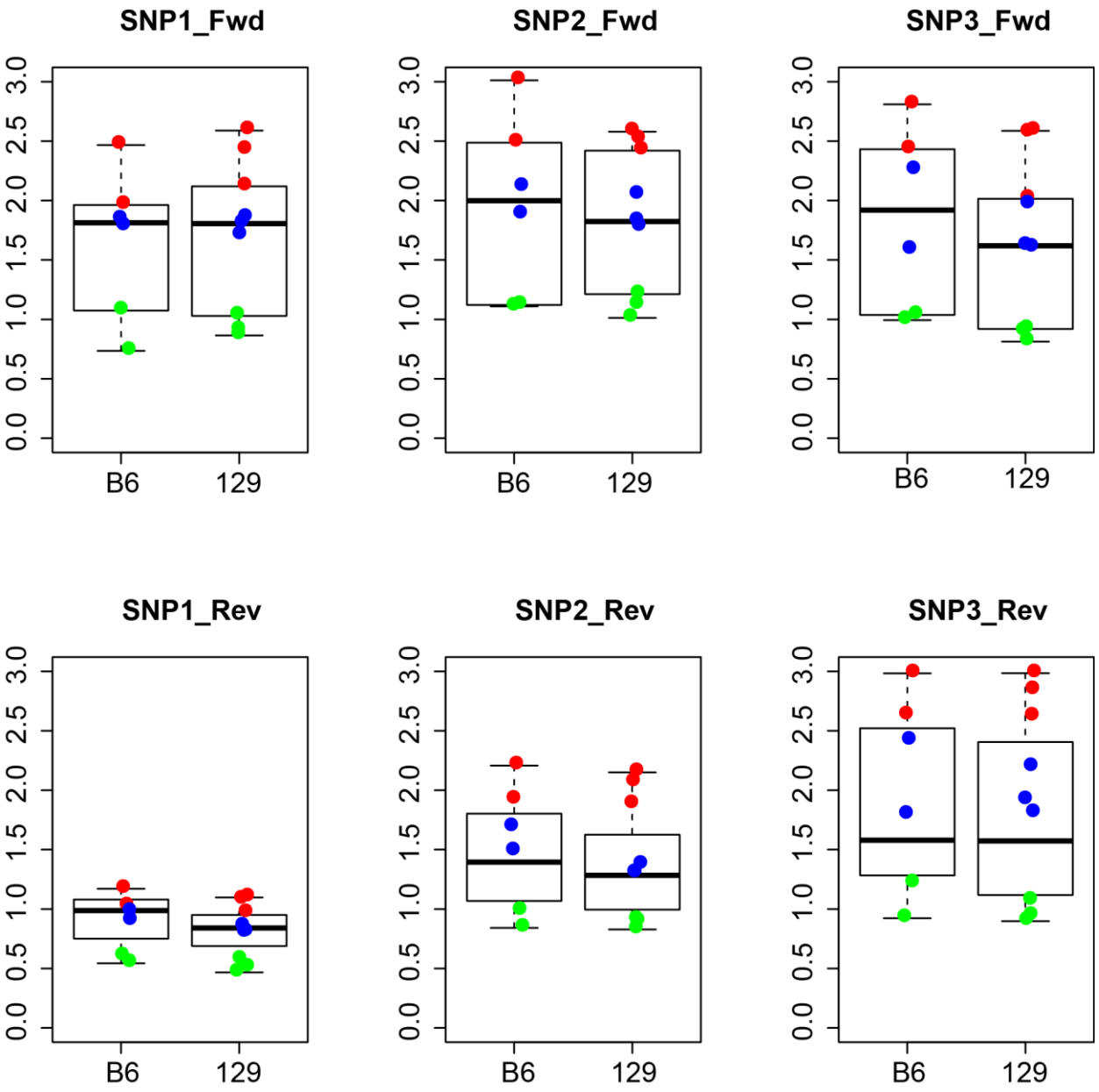

Figure 2-3: Allele specific RNA expression of *F3*
Relative RNA expression of B6 (ENU mutagenized) and 129 alleles from *F3* measured at three DBA-B6/129 SNP sites (SNP1=rs30268372, SNP2=rs30269285, SNP3=rs30269288) in adult lung (red), liver (blue) and whole brain (green) tissues.

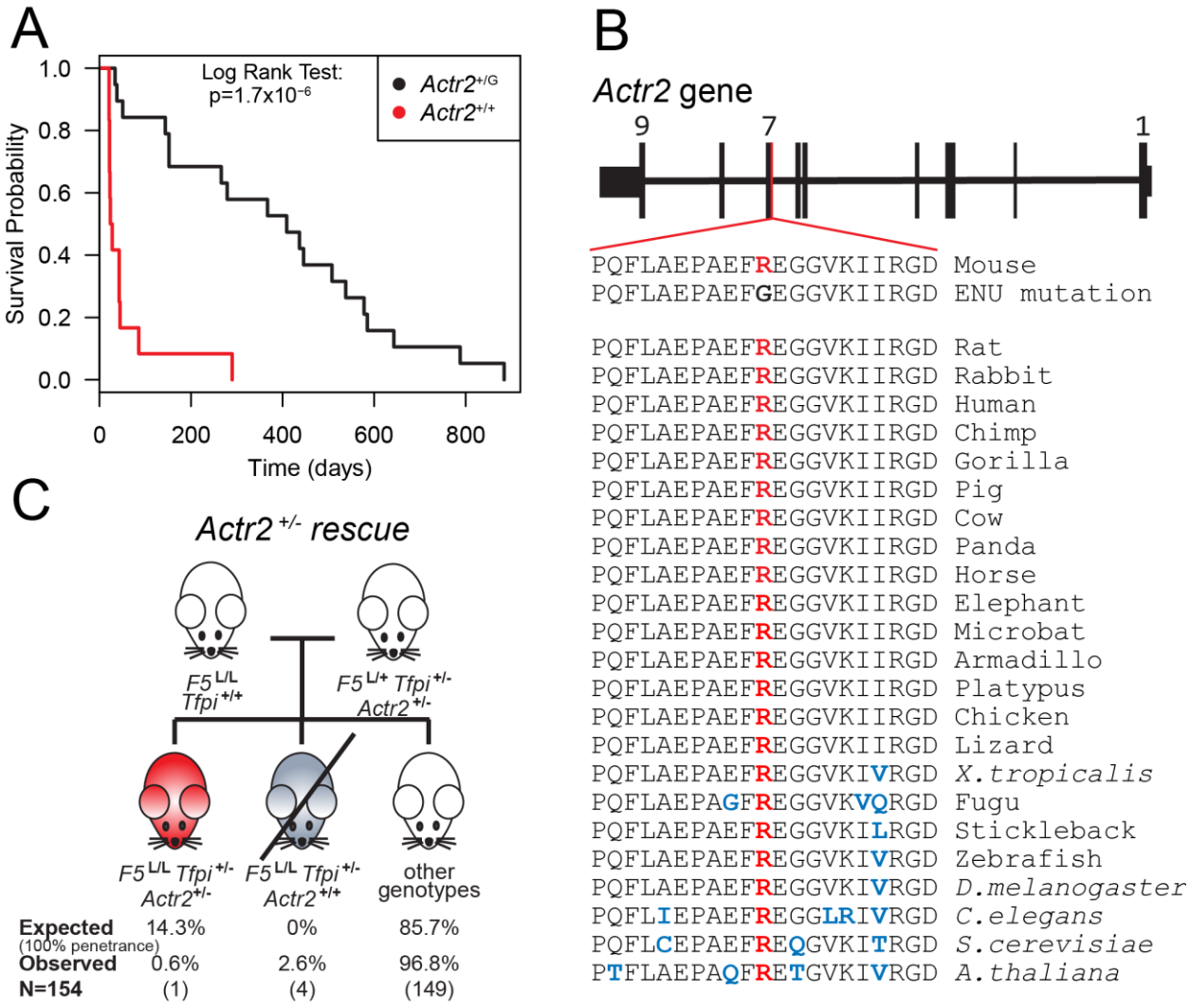

Figure 2-4: Discovery and validation of *Actr2* as a candidate thrombosuppressor gene by NGS

A. Kaplan-Meier survival plot for $F5^{L/L}$ $Tfpi^{+/-}$ mice with and without the $Actr2^{+/G}$ mutation. $F5^{L/L}$ $Tfpi^{+/-}$ $Actr2^{+/G}$ have significantly better survival than $F5^{L/L}$ $Tfpi^{+/-}$ $Actr2^{+/+}$ (n = 35 mice). Probability of survival was calculated and plotted using Medcalc. B. ARP2 amino acid R258 is highly conserved in animals, plants and fungi. C. The mating scheme and observed distribution of the $F5^{L/+}$ $Tfpi^{+/-}$ $Actr2^{+/-}$ rescue experiments. *Actr2* haploinsufficiency failed to suppress the $F5^{L/+}$ $Tfpi^{+/-}$ phenotype.

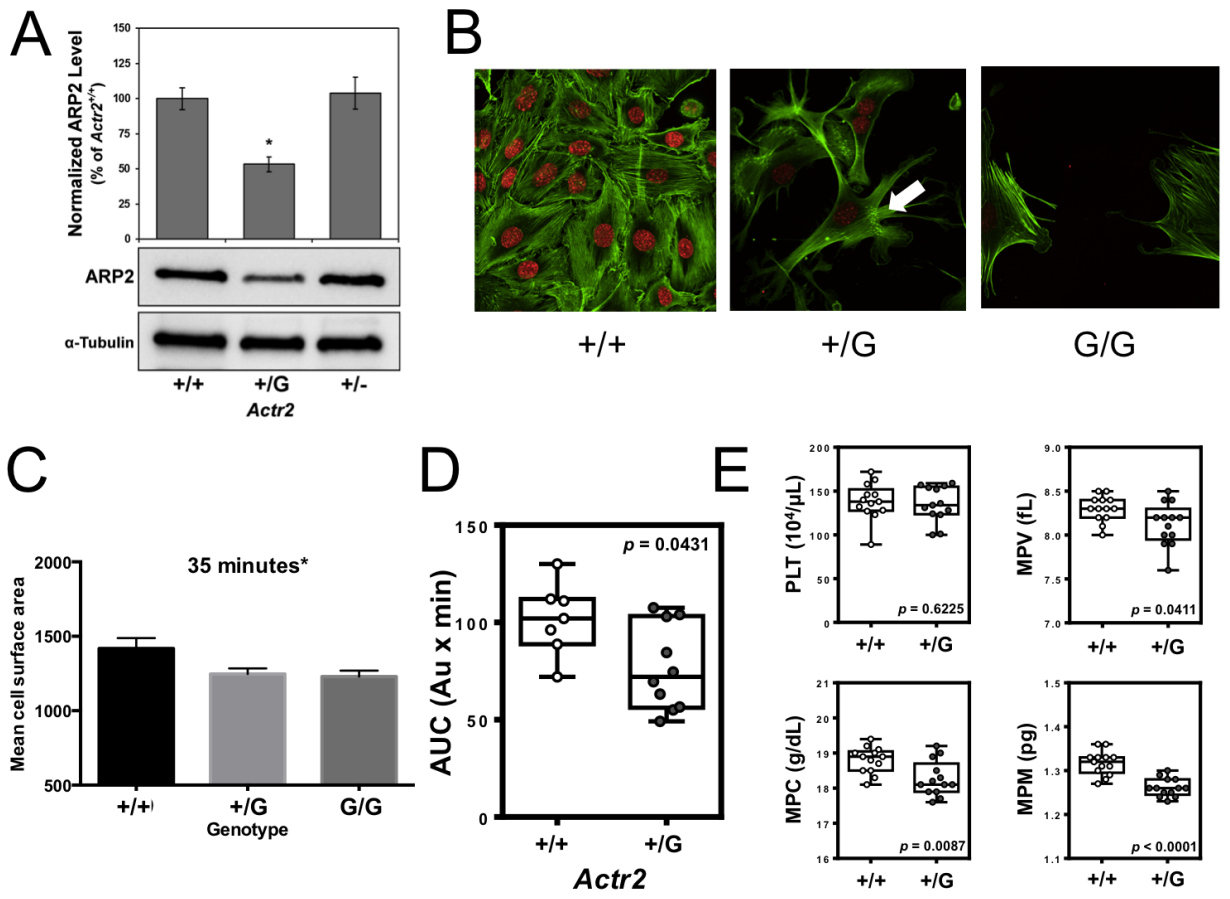

Figure 2-5: Functional analysis of the *Actr2* mutant mice
A. Platelets were analyzed for ARP2 protein in *Actr2*$^{+/G}$, *Actr2*$^{+/-}$ and *Actr2*$^{+/+}$ mice. For the statistical analysis, platelet protein extracts from three independent experiments were analyzed by Western blotting as described in Materials and Methods. The relative intensities of ARP2 as compared to control are displayed as the mean ± SEM (n = 3). The asterisk indicates significant difference when compared to control at $q < 0.05$ (Mann-Whitney, FDR). Platelet alpha tubulin serves as a loading control. B. Mouse embryonic fibroblasts derived from *Actr2*$^{+/G}$, *Actr2*$^{G/G}$, and wildtype mice and stained with phalloidin revealed a tendency to display F-actin aggregates at the root of cellular protrusions. C. A significant spreading defect of *Actr2*$^{+/G}$ murine embryonic fibroblasts on a fibronectin matrix was observed ($p<0.05$). D and E. Whole blood platelet aggregation in *Actr2*$^{+/G}$ heterozygous mice was significantly reduced compared to wildtype littermate control mice ($p<0.05$). Complete blood counts revealed defects in Mean Platelet Volume and Mean Platelet Mass in the *Actr2*$^{+/G}$ mice compared to their littermates ($n=45$, $p<0.0001$).

Table 2-1: Overview of linkage analysis

ENU Lines	Number of mice	Number of markers	Best LOD score	*Tfpi* LOD score	Overlapping SNVs
MF5L1	27	862	1.15	3.47234	no
MF5L6	98	806	4.49	9.80518	no
MF5L9	84	721	2.5	12.81776	no
MF5L16	14	822	1.61	1.61088	no

LOD stands for logarithm of the odds (to the base 10)

Table 2-2: Distribution of genotypes from a cross of *F5*$^{L/+}$ *Tfpi*$^{+/-}$ *F8*$^{X+/X-}$ to *F5*$^{L/L}$

F5 genotype	*Tfpi* genotype	*F8* genotype	Expected	%	Observed	%
L/+	+/-	*X*+/*Y*	13.9	8.3%	12	7.2%
L/+	+/-	*X*-/*Y*	13.9	8.3%	15	9.0%
L/+	+/-	*X*+/*X*+	13.9	8.3%	15	9.0%
L/+	+/-	*X*+/*X*-	13.9	8.3%	17	10.2%
L/+	+/+	*X*+/*Y*	13.9	8.3%	12	7.2%
L/+	+/+	*X*-/*Y*	13.9	8.3%	17	10.2%
L/+	+/+	*X*+/*X*+	13.9	8.3%	11	6.6%
L/+	+/+	*X*+/*X*-	13.9	8.3%	9	5.4%
L/*L*	+/-	*X*+/*Y*	0	0.0%	0	0.0%
L/*L*	+/-	*X*-/*Y*	0	0.0%	8	4.8%
L/*L*	+/-	*X*+/*X*+	0	0.0%	1	0.6%
L/*L*	+/-	*X*+/*X*-	0	0.0%	2	1.2%
L/*L*	+/+	*X*+/*Y*	13.9	8.3%	9	5.4%
L/*L*	+/+	*X*-/*Y*	13.9	8.3%	16	9.6%
L/*L*	+/+	*X*+/*X*+	13.9	8.3%	10	6.0%
L/*L*	+/+	*X*+/*X*-	13.9	8.3%	9	5.4%
			167	100.0%	167	100.0%

Parental genotypes: *F5*$^{L/L}$ *Tfpi*$^{+/+}$ *F8*$^{X+/Y}$ and *F5*$^{L/+}$ *Tfpi*$^{+/-}$ *F8*$^{X+/X-}$

Table 2-3: Overview of all identified G1 *F5$^{L/L}$ Tfpi$^{+/-}$* mice

ENU lines	MouseID	Sex	Age (days)	# Litters	# Progeny	# Rescues	ENU dosage
MF5L1	45201	M	NA	8	30	2	1x150 mg/kg
MF5L2	53882	F	626	4	14	1	1x150 mg/kg
MF5L3	57372	F	263	3	6	1	1x150 mg/kg
MF5L4	57258	M	NA	1	3	1	1x150 mg/kg
MF5L5	80689	M	694	9	36	7	3x90 mg/kg
MF5L6	96560	M	882	3	11	3	3x90 mg/kg
MF5L7	98420	F	681	12	42	1	3x90 mg/kg
MF5L8	14268	M	210	4	19	5	3x90 mg/kg
MF5L9	14411	M	687	17	55	8	3x90 mg/kg
MF5L10	14414	M	835	21	67	6	3x90 mg/kg
MF5L11	24813	M	834	17	40	10	3x90 mg/kg
MF5L12	24582	M	525	5	10	4	3x90 mg/kg
MF5L13	25356	M	843	19	35	4	3x90 mg/kg
MF5L14	25609	M	662	5	22	2	3x90 mg/kg
MF5L15	25605	F	511	3	13	2	3x90 mg/kg
MF5L16	33193	M	178	4	15	6	3x90 mg/kg
NA	2105	M	NA	0	0	0	3x90 mg/kg
NA	2164	M	770	0	0	0	3x90 mg/kg
NA	2216	F	NA	0	0	0	3x90 mg/kg
NA	2383	M	NA	0	0	0	3x90 mg/kg
NA	2730	M	NA	0	0	0	3x90 mg/kg
NA	3000	M	NA	0	0	0	3x90 mg/kg
NA	5260	F	308	0	0	0	3x90 mg/kg
NA	5396	M	NA	0	0	0	3x90 mg/kg
NA	5401	F	NA	0	0	0	3x90 mg/kg
NA	6654	M	NA	0	0	0	3x90 mg/kg
NA	6927	M	24	0	0	0	3x90 mg/kg
NA	7372	M	25	0	0	0	3x90 mg/kg
NA	13019	F	66	0	0	0	3x90 mg/kg
NA	13785	F	58	0	0	0	3x90 mg/kg
NA	13901	F	17	0	0	0	3x90 mg/kg
NA	14126	M	22	0	0	0	3x90 mg/kg
NA	14418	F	42	0	0	0	3x90 mg/kg
NA	14805	F	252	0	0	0	3x90 mg/kg
NA	18589	F	27	0	0	0	3x90 mg/kg
NA	18591	F	663	0	0	0	3x90 mg/kg
NA	22721	M	NA	0	0	0	3x90 mg/kg
NA	23617	F	553	1	0	0	3x90 mg/kg
NA	23899	M	33	0	0	0	3x90 mg/kg
NA	24259	F	33	0	0	0	3x90 mg/kg
NA	24355	F	18	0	0	0	3x90 mg/kg
NA	24511	F	18	0	0	0	3x90 mg/kg
NA	24744	F	294	0	0	0	3x90 mg/kg
NA	24914	F	22	0	0	0	3x90 mg/kg
NA	25293	F	444	2	0	0	3x90 mg/kg

NA	25681	F	255	1	0	0	3x90 mg/kg
NA	25876	F	23	0	0	0	3x90 mg/kg
NA	25948	M	32	0	0	0	3x90 mg/kg
NA	29035	F	56	0	0	0	3x90 mg/kg
NA	31710	F	140	0	0	0	3x90 mg/kg
NA	31881	F	161	1	0	0	3x90 mg/kg
NA	33095	M	46	0	0	0	3x90 mg/kg
NA	33434	M	34	0	0	0	3x90 mg/kg
NA	42058	F	306	0	0	0	1x150 mg/kg
NA	42127	M	320	5	14	0	1x150 mg/kg
NA	42885	F	NA	0	0	0	1x150 mg/kg
NA	45755	M	136	0	0	0	1x150 mg/kg
NA	51255	F	NA	3	8	0	1x150 mg/kg
NA	51283	F	NA	0	0	0	1x150 mg/kg
NA	51665	F	203	1	1	0	1x150 mg/kg
NA	51735	F	NA	5	11	0	1x150 mg/kg
NA	53087	M	NA	0	0	0	1x150 mg/kg
NA	57931	M	34	0	0	0	1x150 mg/kg
NA	60776	F	NA	3	11	0	1x150 mg/kg
NA	74064	F	NA	0	0	0	3x90 mg/kg
NA	74637	M	26	0	0	0	3x90 mg/kg
NA	76278	F	147	1	3	0	3x90 mg/kg
NA	76387	F	NA	0	0	0	3x90 mg/kg
NA	76526	F	24	0	0	0	3x90 mg/kg
NA	76582	F	NA	0	0	0	3x90 mg/kg
NA	76824	M	NA	0	0	0	3x90 mg/kg
NA	76947	M	NA	0	0	0	3x90 mg/kg
NA	76989	M	NA	0	0	0	3x90 mg/kg
NA	80493	M	NA	0	0	0	3x90 mg/kg
NA	80821	F	NA	0	0	0	3x90 mg/kg
NA	80840	F	NA	0	0	0	3x90 mg/kg
NA	89215	M	831	0	0	0	3x90 mg/kg
NA	89285	F	NA	0	0	0	3x90 mg/kg
NA	89957	M	NA	0	0	0	3x90 mg/kg
NA	89965	M	NA	0	0	0	3x90 mg/kg
NA	90152	M	NA	0	0	0	3x90 mg/kg
NA	90488	M	NA	0	0	0	3x90 mg/kg
NA	90832	M	NA	0	0	0	3x90 mg/kg
NA	91310	M	NA	0	0	0	3x90 mg/kg
NA	91570	M	NA	0	0	0	3x90 mg/kg
NA	96245	F	386	0	0	0	3x90 mg/kg
NA	96247	F	NA	0	0	0	3x90 mg/kg
NA	96440	M	NA	0	0	0	3x90 mg/kg
NA	96684	M	15	0	0	0	3x90 mg/kg
NA	96685	M	15	0	0	0	3x90 mg/kg
NA	96839	F	NA	0	0	0	3x90 mg/kg
NA	96868	M	659	3	6	0	3x90 mg/kg
NA	98148	M	NA	0	0	0	3x90 mg/kg
NA	98172	F	860	0	0	0	3x90 mg/kg

NA	98313	M	NA	0	0	0	3x90 mg/kg
NA	98441	M	NA	0	0	0	3x90 mg/kg
NA	98491	M	NA	0	0	0	3x90 mg/kg
NA	98759	M	350	0	0	0	3x90 mg/kg

Table 2-4: Overview of the ENU pedigrees

ENU Lines	Total Mice	Littermates	Total *F5$^{L/L}$ Tfpi$^{+/-}$* mice	Penetrance
MF5L1	654	470	184	78.3%
MF5L2	14	13	1	15.4%
MF5L3	50	47	3	12.8%
MF5L4	3	2	1	100%
MF5L5	255	205	50	48.8%
MF5L6	1393	1057	336	63.6%
MF5L7	42	41	1	4.9%
MF5L8	543	411	132	64.2%
MF5L9	1127	863	264	61.2%
MF5L10	111	96	15	31.3%
MF5L11	459	338	121	71.6%
MF5L12	200	154	46	59.7%
MF5L13	115	102	13	25.5%
MF5L14	47	44	3	13.6%
MF5L15	40	37	3	16.2%
MF5L16	442	323	119	73.7%

Penetrance is calculated as follows: Total # *F5$^{L/L}$ Tfpi$^{+/-}$* mice / (Littermates / 2)

Table 2-5: Synthetic lethal phenotype on 129 genetic background

F5 genotype	*Tfpi* genotype	Expected	%	Observed	%
L/+	+/+	44.25	25.0%	76	42.9%
L/+	+/-	44.25	25.0%	74	41.8%
L/*L*	+/+	44.25	25.0%	27	15.3%
L/*L*	+/-	44.25	25.0%	0	0.0%
		177	100.0%	177	100.0%

Parental genotypes: $F5^{L/L}$ and $F5^{L/+}$ $Tfpi^{+/-}$

Table 2-6: Distribution of genotypes from a cross of *F5*$^{L/+}$ *Tfpi*$^{+/-}$ *F3*$^{+/-}$ to *F5*$^{L/L}$

F5 genotype	*Tfpi* genotype	*F3* genotype	Expected	%	Observed	%
L/+	+/-	+/-	38.9	14.3%	39	14.3%
L/+	+/-	+/+	38.9	14.3%	58	21.3%
L/+	+/+	+/-	38.9	14.3%	38	14.0%
L/+	+/+	+/+	38.9	14.3%	53	19.5%
L/*L*	+/-	+/-	38.9	14.3%	13	4.8%
L/*L*	+/+	+/-	38.9	14.3%	27	9.9%
L/*L*	+/+	+/+	38.9	14.3%	44	16.2%
L/*L*	+/-	+/+	0	0.0%	1	0.4%
			272	100.0%	273	100.0%

Parental genotypes: *F5*$^{L/L}$ *Tfpi*$^{+/+}$ *F3*$^{+/+}$ and *F5*$^{L/+}$ *Tfpi*$^{+/-}$ *F3*$^{+/-}$

Table 2-7: Candidate ENU-induced mutations

Chr	Pos	R	A	Type	ENU lines	Gene	Exon	AA change	Validation
17	25722876	T	A	NS	*MF5L1*	*Chtf18*	13	N541Y	ENU
7	79822260	A	C	NS	*MF5L6*	*Anpep*	20	D955E	ENU
7	101990583	A	T	SG	*MF5L6*	*Numa1*	4	K47X	ENU
1	33746762	T	G	NS	*MF5L8*	*Bag2*	3	I160L	ENU
1	36163249	T	C	NS	*MF5L8*	*Uggt1*	29	Y1089C	ENU
1	40125203	A	G	NS	*MF5L8*	*Il1r2*	9	N410S	ENU
9	123712602	T	G	NS	*MF5L8*	*Lztfl1*	3	I51L	ENU
10	128290865	C	T	SG	*MF5L8*	*Stat2*	23	Q820X	ENU
14	8169757	A	G	NS	*MF5L8*	*Pdhb*	7	S218P	ENU
15	89456795	G	T	SG	*MF5L8*	*Mapk8ip2*	3	G148X	ENU
17	12271353	T	A	NS	*MF5L8*	*Map3k4*	3	N397I	ENU
17	45416968	T	A	SG	*MF5L8*	*Cdc5l*	7	K294X	ENU
19	39563826	C	T	NS	*MF5L8*	*Cyp2c39*	7	A321V	ENU
19	46065668	C	G	NS	*MF5L8*	*Pprc1*	6	I1150M	ENU
7	82868974	G	A	NS	*MF5L9*	*Mex3b*	2	G166R	ENU
9	21634876	T	C	NS	*MF5L9*	*Smarca4*	3	S117P	ENU
10	67538372	T	C	NS	*MF5L9*	*Egr2*	1	M51T	ENU
19	56810315	G	T	SG	*MF5L9*	*A630007B06Rik*	2	S247X	ENU
4	141581029	A	G	NS	*MF5L11*	*Fblim1*	8	I323T	ENU
5	123760656	T	A	SG	*MF5L11*	*Kntc1*	8	C204X	ENU
5	136373331	T	C	NS	*MF5L11*	*Cux1*	5	K144E	ENU
9	123963447	G	T	NS	*MF5L11*	*Ccr1*	2	H349N	ENU
10	84958016	A	G	NS	*MF5L11*	*Ric8b*	4	S248G	ENU
11	57221033	A	T	NS	*MF5L11*	*Gria1*	7	T224S	ENU
11	101740781	T	G	NS	*MF5L11*	*Dhx8*	8	V400G	ENU
13	112368238	G	A	SG	*MF5L11*	*Ankrd55*	9	W506X	ENU
14	32966414	A	G	NS	*MF5L11*	*Wdfy4*	56	W2921R	ENU
16	92605854	T	C	NS	*MF5L11*	*Runx1*	8	Y400C	ENU
5	86719746	T	A	NS	*MF5L12*	*Tmprss11e*	5	D155V	ENU
6	129517379	A	G	NS	*MF5L12*	*Tmem52b*	5	E182G	ENU
6	148237808	G	A	NS	*MF5L12*	*Tmtc1*	20	R939W	ENU
7	141620530	G	A	NS	*MF5L12*	*Ap2a2*	12	G504E	ENU
11	20077297	G	C	NS	*MF5L12*	*Actr2*	7	R258G	ENU
11	67921730	C	T	NS	*MF5L12*	*Usp43*	1	G107S	ENU
6	36523684	A	G	NS	*MF5L16*	*Chrm2*	3	I159V	ENU
8	70259804	G	A	NS	*MF5L16*	*Sugp2*	9	R1023Q	ENU
10	77260815	T	C	NS	*MF5L16*	*Pofut2*	2	F125L	ENU
10	114800967	T	C	NS	*MF5L16*	*Trhde*	1	S112G	ENU
13	61568333	A	T	NS	*MF5L16*	*Cts3*	3	H71Q	ENU
13	90898831	G	A	NS	*MF5L16*	*Atp6ap1l*	4	P76S	ENU
13	94443934	G	A	NS	*MF5L16*	*Ap3b1*	9	A321T	ENU
15	6786636	C	T	SG	*MF5L16*	*Rictor*	31	R1130X	ENU
2	70509665	G	C	NS	*MF5L1*	*Erich2*	2	C158S	chr2
7	14225894	T	C	NS	*MF5L1*	*Sult2a6*	5	Q238R	NA

7	15940142	T	C	NS	*MF5L1*	*Gltscr2*	6	H254R	NA
7	85754889	A	T	NS	*MF5L1*	*Vmn2r72*	1	D31E	NA
8	108949251	A	G	NS	*MF5L1*	*Zfhx3*	9	Q2311R	NA
12	110977486	G	A	NS	*MF5L1*	*Ankrd9*	3	T5I	seq error
3	99352190	A	G	NS	*MF5L5*	*Tbx15*	8	N459S	NA
3	135228816	T	A	NS	*MF5L5*	*Cenpe*	13	D381E	NA
6	35080128	G	A	NS	*MF5L5*	*Cnot4*	2	R3C	NA
8	70913530	A	T	NS	*MF5L5*	*Map1s*	5	I360F	NA
17	70657633	T	G	SP	*MF5L5*	*Dlgap1*	4	c.1368+2 T	NA
1	82741945	C	A	NS	*MF5L6*	*Mff*	6	Q190K	*de novo*
2	67516594	A	G	NS	*MF5L6*	*Xirp2*	7	R3060G	chr2
2	76724952	G	A	NS	*MF5L6*	*Ttn*	167	R22243C	chr2
2	76939280	T	A	NS	*MF5L6*	*Ttn*	34	N2675I	chr2
2	88423385	A	T	NS	*MF5L6*	*Olfr1181*	1	F213L	chr2
2	111537791	A	T	NS	*MF5L6*	*Olfr1294*	1	L166Q	chr2
2	140120707	T	C	NS	*MF5L6*	*Esf1*	14	K815E	chr2
5	108650355	C	T	NS	*MF5L6*	*Dgkq*	18	R679H	not ENU
2	76549471	A	C	NS	*MF5L8*	*Osbpl6*	7	D135A	chr2
2	112407616	G	A	NS	*MF5L8*	*Katnbl1*	5	V152I	chr2
2	112630022	A	G	NS	*MF5L8*	*Aven*	4	T162A	chr2
2	153136757	G	A	NS	*MF5L8*	*Hck*	9	V276M	chr2
2	153225070	T	A	NS	*MF5L8*	*Tspyl3*	1	T83S	chr2
11	52145503	T	C	NS	*MF5L8*	*Olfr1373*	1	E9G	not ENU
11	69129597	A	G	NS	*MF5L8*	*Aloxe3*	4	M156V	not ENU
16	59554543	C	T	NS	*MF5L8*	*Crybg3*	1	R402H	not ENU
2	101696795	C	T	NS	*MF5L9*	*Traf6*	8	R297C	chr2
18	71327504	C	T	NS	*MF5L9*	*Dcc*	24	D1172N	*de novo*
2	30086662	A	G	NS	*MF5L11*	*Pkn3*	15	K572E	chr2
2	40874986	G	T	NS	*MF5L11*	*Lrp1b*	55	Q2943K	chr2
2	61804747	T	C	NS	*MF5L11*	*Tbr1*	1	S14P	chr2
2	144572561	G	A	NS	*MF5L11*	*Sec23b*	10	G398R	chr2
13	100285719	C	T	NS	*MF5L12*	*Naip7*	14	A1269T	seq error
10	117278121	T	C	SL	*MF5L16*	*Lyz2*	4	X149W	NA
11	60710357	G	A	NS	*MF5L16*	*Llgl1*	16	R707H	not ENU
13	34896062	T	A	SG	*MF5L16*	*Prpf4b*	11	L803X	Not ENU

Chr=chromosome; Pos=nucleotide position; R=reference allele; A=alternate allele; NS=nonsynonymous; SP=splicing; SG=stopgain; SL=stoploss; AA change= amino acid change;

Table 2-8: Overview of the WES data

	WHOLE GENOME		AGILENT CAPTURE REGION				
ENU Lines	**# Reads**	**Mapped %**	**# Reads**	**Mapped %**	**Mean coverage**	**% bp covered at ≥6X**	**Mapping quality (max 60)**
*MF5L*1	97388058	91.06%	43177469	44.34%	73.88	>97%	34.42
*MF5L*5	110246719	93.07%	52837528	47.93%	89.9	>97%	34.36
*MF5L*6	133205717	86.03%	56688221	42.56%	93.93	>97%	33.89
MF5L8	128521513	96.48%	61950221	48.20%	105.88	>98%	34.69
MF5L9	109882856	94.18%	55469742	50.48%	95.56	>97%	34.67
*MF5L*11	110448223	96.38%	54907249	49.71%	93.22	>97%	35.08
*MF5L*12	105612822	94.27%	50684794	47.99%	87.28	>97%	34.68
MF5L16	115987369	90.33%	63608463	49.54%	110.83	>98%	34.26
Average	113911660	92.73%	54915461	47.59%	93.81	>97%	34.51

Notes

This chapter is in preparation for submission to the journal PNAS under the title “A sensitized mutagenesis screen in Factor V Leiden mice identifies novel thrombosis suppressor loci” by Randal J. Westrick*, Kärt Tomberg*, Guojing Zhu, Amy E. Siebert, Mary E. Winn, Sarah L. Dobies, Sara L. Manning, Marisa A. Brake, Audrey Cleuren, David R. Siemieniak, Jishu Xu, Jun Z. Li, and David Ginsburg. (* contributed equally)

CHAPTER III: Spontaneous 8bp deletion in *Nbeal2* recapitulates the gray platelet syndrome in mice

Abstract

During the analysis of a whole genome ENU mutagenesis screen for thrombosis modifiers, a spontaneous 8 base pair (bp) deletion causing a frameshift in exon 27 of the *Nbeal2* gene was identified. Though initially considered as a plausible thrombosis modifier, this *Nbeal2* mutation failed to suppress the synthetic lethal thrombosis on which the original ENU screen was based. Mutations in *NBEAL2* cause Gray Platelet Syndrome (GPS), an autosomal recessive bleeding disorder characterized by macrothrombocytopenia and gray-appearing platelets due to lack of platelet alpha granules. Mice homozygous for the *Nbeal2* 8 bp deletion (*Nbeal2*$^{gps/gps}$) exhibit a phenotype similar to human GPS, with significantly reduced platelet counts compared to littermate controls ($p=1.63 \times 10^{-7}$). *Nbeal2*$^{gps/gps}$ mice also have markedly reduced numbers of platelet alpha granules and an increased level of emperipolesis, consistent with previously characterized mice carrying targeted *Nbeal2* null alleles. These findings confirm previous reports, provide an additional mouse model for GPS, and highlight the potentially confounding effect of background spontaneous mutation events in well-characterized mouse strains.

Introduction

The laboratory mouse has been used extensively as a model organism, with multiple inbred mouse strains routinely available from a number of suppliers. These inbred strains have been extensively characterized and the genome of more than 20 have been sequenced [143, 144]. Whole genome sequencing in humans has demonstrated that in addition to approximately 75 *de novo* single nucleotide variants

(SNVs) [145], each human genome carries on average 6-12 new insertions and deletions or 'INDELs' (1-50 bp) and occasional copy number and complex structural variants [52, 146]. Mice have been shown to exhibit comparable mutation rates [56] and therefore elaborate breeding schemes are necessary in large mouse facilities to maintain genetically stable mouse strains [147]. However, identification of the occasional *de novo* deleterious variants in mice has resulted in useful models for phenotypic studies [57-60]. Forward genetic screens can be performed taking advantage of such spontaneous mutations, but given the low *de novo* mutation rate, N-ethyl-N-nitrosourea (ENU) is typically applied to markedly increase the density of random mutations [63, 74]. ENU induces on average 1 mutation per every 700,000 bp, which results in >50 fold increase compared to spontaneous mutation rates seen in mice [93, 125].

NBEAL2 encodes neurobeachin-like-2, a BEACH domain containing protein, with a proposed role in vesicular trafficking and granule development [148]. Mutations in *NBEAL2* were recently shown to be the cause of the autosomal recessive form of Gray Platelet Syndrome (GPS) [149-151]. GPS is a rare bleeding disorder characterized by macrothrombocytopenia and gray-appearing platelets due to lack of platelet alpha granules [152]. Mice with targeted deletion of *Nbeal2* [153-155] exhibit thrombocytopenia, deficiency in platelet alpha granules, a higher than normal mean platelet volume, splenomegaly, impaired platelet aggregation and adhesion, and a mild bleeding tendency, all consistent with the human phenotype [152, 156].

During the analysis of a whole genome ENU mutagenesis screen for thrombosis modifiers, we identified a spontaneous 8 bp deletion causing a frameshift in exon 27 of the *Nbeal2* gene. Analysis of the associated mouse pedigree demonstrated that this mutation arose within the Jackson Laboratory 129S1/SvImJ mouse colony and not from the ENU screen.

Materials and methods

Animal procedures

Animal husbandry in this study was carried out according to the Principles of

Laboratory and Animal Care established by the National Society for Medical Research. The University of Michigan's University Committee on Use and Care of Animals (UCUCA) has approved the protocol number 05191 and the University of Colorado Institutional Animal Care and Use Committee approved the protocol 96114. The care and maintenance of animals was closely supervised by University of Michigan ULAM personnel or University of Colorado Institutional Animal Care and Use Committee (IACUC) and animals were housed in their facilities. ULAM/IACUC also provided expert veterinary advice and assistance when necessary and cages were monitored closely by our laboratory personnel as well as university veterinary staff. To minimize discomfort and unnecessary suffering of experimental mice, analgesics were administered for all procedures involving significant discomfort. Blood samples were obtained from the retro-orbital plexus of anesthetized animals achieved with isoflurane inhalation. Mice were euthanized for collection of tissues for histologic, biochemical, and genetic analysis. The UCUCA Endstage Illness and Humane Endpoint Guidelines were also closely followed and animals euthanized accordingly by carbon dioxide overdose or exsanguination under anesthesia.

F5$^{L/L}$ (*F5*^{tm2Dgi}/J, Jackson Laboratory stock number 004080) mice were previously generated [46], *Tfpi* deficient mice (*Tfpi*^{tm1Gjb}) were a generous gift of Dr. George Broze [92], and *Nbeal2*$^{tm1Lex/tm1Lex}$ mice with targeted deletion of the *Nbeal2* gene were previously generated from cryopreserved spermatozoa obtained from the Mutant Mouse Regional Resource Center at the University of California, Davis [154]. *Nbeal2* allele carrying the spontaneous 8bp deletion described in Results will be referred throughout the text as *Nbeal2*^{gps}. Two cohorts of *Nbeal2*^{gps} mice were analyzed. Set 1 refers to *Nbeal2*^{gps} mice intercrossed after 2 backcrosses to C57BL/6J mice (stock number 000664), while set 2 mice were intercrossed after 7 backcrosses to C57BL/6J.

Whole exome sequencing of thrombosis suppressor line

Genomic DNA (gDNA) was extracted from mouse tail biopsies using the Gentra Puregene Tissue Kit (Qiagen) according to manufacturer's instructions. Exonic DNA was captured with either SureSelect Mouse All Exon (Agilent) or SeqCap EZ Mouse Exome Design (NimbleGen) kits and 100 bp paired-end sequencing was performed on

the Illumina HiSeq 2000 platform at the University of Michigan's DNA Sequencing Core. All generated fastq files have been deposited to the NCBI Sequence Read Archive (Project accession number #SRP063933). Detailed overview of the variant calling pipeline and filtration is available online as a GitHub repository [157]. In short, reads were aligned with the Burrows-Wheeler Aligner [131] to the *Mus Musculus* GRCm38 reference genome, duplicates were removed using Picard [158], and variants across all samples were simultaneously called and filtered with GATK [133]. Variants were annotated using Annovar software [134] with Refseq annotation. Variants between C57BL/6J and 129S1/SvImJ, as well as unannotated variants within our mouse cohort present in more than one independent line, were removed from the ENU candidate list. All unique heterozygous variants present in multiple mice within the suppressor line *MF5L6* (Chapter II) with a minimum of 6X coverage were considered as potential candidates and further validated using Sanger sequencing.

129S1/SvImJ *de novo* mutation analysis

Exome analysis was performed for the parents (F63pF64) and a female sibling (F63pF65) of the 129S1/SvImJ individual sequenced for the Sanger Mouse Genomes Sequencing project [143]. Exome sequencing and variant calling was performed as previously described [159]. Approximately 95% of all variants (SNV and INDELs) in each of the 3 samples were also found in dbSNP, and an additional ~5600 variants that were common between the three exomes were also found in whole genome variant data from the Sanger Mouse Genomes project. There were 92 variants unique to the 129S1/SvImJ female sibling sample, in that they were not found in variant calls from either parental exome. Out of the 92 “unique” called variants, manual analysis of the alignment files in all samples and Sanger sequencing of PCR products revealed that 91 were true variants with false negative calls in one of the parent samples and one variant was a false positive call.

Genotyping *Nbeal2*^{gps} allele

The *Nbeal2*^{gps} allele was detected using two three-primer PCR assays (Figure 3-1) with common forward (5'AAGGCAGGAAGACGTCAGAA, primer F) and reverse

(5'GACCTCAGTGTCCGCCTAGA, primer R) primers. In the first PCR based genotyping design, the third primer (5'AC**|GTCTGGCT|**GTCCGTAGAT, primer WT) is located over the undeleted 8 bp to detect the presence of the wildtype allele. This PCR reaction results in two products (413 bp, 235 bp). In the second PCR design the third primer (5'AACGAC|GTCCGTAGATGAGG, primer DEL) spans the 8 bp deletion to detect the presence of the deletion allele. This reaction also produces two products (405 bp, 227 bp). PCR was performed using GoTaq Green Master Mix (Promega) and the products visualized on a 2% agarose gel. Selected genotyping results were further confirmed by Sanger sequencing.

Estimation of differential allelic expression

Liver, lung, and bone marrow tissue samples were collected in RNAlater (Ambion) from a *Nbeal2*$^{gps/+}$ mouse. Total RNA was extracted using an RNeasy Mini Kit (Qiagen) and converted to coding DNA (cDNA) using SuperScript III One-Step RT-PCR (Invitrogen) following the manufacturer's instructions. gDNA was prepared from a tail biopsy. Forward and reverse genotyping primers (primer F and primer R) were used to amplify the *Nbeal2* deletion region from gDNA and the cDNAs from liver and lung. PCR products were extracted from agarose gels using a QIAquick Gel Purification Kit (Qiagen) and submitted for Sanger sequencing. The differential allelic expression was estimated from the ratio between the wildtype and *Nbeal2*^{gps} sequence peak areas in cDNA samples compared to gDNA using Phred software [160]. This ratio was calculated for multiple positions within the PCR product where the wildtype and *Nbeal2*^{gps} alleles contain a different nucleotide.

Western blot

Murine whole blood was collected via the inferior vena cava into acid/citrate/dextrose. Platelet-rich plasma (PRP) was obtained by centrifugation at 200 g for 5 min. Washed platelets were pelleted from PRP by centrifugation at 1,000 g for 2 min in the presence of prostacyclin PGI1 (0.1 μM) and resuspended in modified Tyrode's buffer (137 mM NaCl, 0.3 mM Na_2HPO_4, 2 mM KCl, 12 mM $NaHCO_3$, 5 mM HEPES, 5 mM glucose) [161]. Total protein was harvested from washed platelets using

cell lysis buffer containing 1% Triton X-100 and protease inhibitors (mini complete tablets, Roche). Protein concentration was measured with Protein Dye Reagent (BioRad), and 30 µg of total protein was separated in duplicate lanes of a 4-15% Mini-Protean TGX gel (BioRad). Protein was transferred to nitrocellulose and probed with a rabbit monoclonal antibody against NBEAL2 (ab187162, Abcam) or a rabbit polyclonal antibody against beta actin (ab8227, Abcam), followed by an HRP-linked goat anti-rabbit secondary antibody (Pierce). Detection was performed with ECL Lightning Plus (Perkin Elmer).

Complete blood counts

Twenty-five microliters of blood were collected from the retro-orbital sinus of 5-6 week old mice from set 1. Blood was anticoagulated with 4% sodium citrate (*Sigma-Aldrich*) and diluted 10x in PBS (phosphate-buffered saline, Gibco) supplemented with 5% bovine serum albumin (Sigma-Aldrich). Complete blood counts (CBC) were performed on the ADVIA 2120 Hematology System (Siemens) according to manufacturer's instructions while being blinded to the genotype of the mouse from which the sample was obtained. Additional blood was collected from >20 week old females from set 2 using heparinized capillary tubes and anticoagulated using EDTA containing tubes (BD microtainer). CBC were performed on the Hemavet 950FS system. All data were analyzed and visualized using the 'stats' and 'beeswarm' packages in R software [162].

Flow cytometry

Absolute neutrophil counts (ANC) were measured by flow cytometry as previously described [163]. Briefly, 50 µl of anticoagulated whole blood was added to Trucount tubes (BD Biosciences) and processed according to the manufacturer's protocol. Samples were incubated at room temperature in the dark for 15 minutes with rat anti-mouse FITC-conjugated Ly-6G clone 1A8 (Molecular Probes) and rat anti-mouse CD45 PE/Cy7 antibodies. This incubation was followed by the addition of 450 µl of red blood cell lysis buffer (eBioscience). Samples were incubated for 30 minutes in the dark at room temperature prior to data acquision using a Gallios 561 flow cytometer

(Beckman Coulter). Data were acquired at medium flow rate for 2 minutes. The neutrophil population was defined as CD45/Ly-6G positive events. The bead population was clearly visualized as different from the neutrophil population. The ANC was calculated according to the formula provided by the manufacturer: ANC (cells/ µl)= (CD45 and Ly-6G positive events/ Trucount beads)x(# beads per test/test volume).

Peripheral blood and bone marrow analysis

Peripheral blood smears were prepared from 9 mice of each genotype and Wright-Giemsa stained using the HealthCare PROTOCOL Hema 3 kit according to the manufacturer's instructions (Fisher Scientific). For each sample, the intensity of platelet staining and platelet granularity were categorized into three levels (light, intermediate or dark) by one of the authors (RK) blinded to the genotype of the mouse from which the sample was obtained. Representative images from the blood smears were taken using a Leica DMLB microscope at 1000x magnification. Bone marrow sections as well as bone marrow cytology slides were prepared by the Unit for Laboratory Animal Medicine histology core. Histopathologic evaluation was performed by an investigator blinded to the genotypes of the evaluated mice.

Transmission electron microscopy

Blood from one *Nbeal2*$^{+/+}$ and one *Nbeal2*$^{gps/gps}$ mouse from set 1 was collected by retro-orbital puncture and fixed in 4% glutaraldehyde as previously described [164]. Fixed samples were further prepared by the University of Michigan's Microscopy and Image Analysis Core for platelet transmission electron microscopy. Platelet sections were examined on a JEOL JEM-1400Plus transmission electron microscope at two different magnifications (5000x, 40000x). Platelet area was measured from images at 5000x magnification using ImageJ software [165] for 100 platelets from 5 different fields for each genotype. The latter analysis was performed with the observer blinded to the genotypes of the platelets.

Statistical analysis

A non-parametric Wilcoxon test was used to estimate significance in the CBC

measured values, platelet area, the assigned platelet staining intensity values of the Wright-Giemsa stained blood smears, and the difference in the level of emperipolesis in bone marrow slides between *Nbeal2*$^{gps/gps}$ and wildtype mice. A chi-square test was applied to estimate deviations from expected Mendelian proportions in *Nbeal2* mouse crosses. All statistical analyses were performed using the 'stats' package in R software [162].

Results

De novo frameshift mutation in *Nbeal2* identified by whole exome sequencing

We performed a sensitized dominant ENU screen designed to identify suppressor mutations for a synthetic lethal thrombosis phenotype (*F5*$^{L/L}$ *Tfpi*$^{+/-}$) [47] in C57BL/6J mice (Chapter II). In order to map the ENU induced mutations, outcrosses were performed between the mutagenized mice and *F5*$^{L/L}$ mice [46] bred >12 generations to the 129S1/SvImJ genetic background. Within a suppressor line, all ENU induced mutations should segregate randomly to the next generation except the suppressor mutation, which is expected to be present in all *F5*$^{L/L}$ *Tfpi*$^{+/-}$ mice. Whole exome sequencing was applied to 4 mice from one of the suppressor lines (*MF5L6*; Figure 3-2) and variants shared between the 4 mice were investigated as candidate suppressor mutations. A total of 215 unique exonic heterozygous SNVs and 8 heterozygous INDELs were identified in the 4 exomes from a total of 76,950 initially called variants. Twelve of the SNVs and one of the INDELs were present in more than one sequenced mouse (Table 3-1), while no variant was present in all 4 mice with the exception of variants closely linked to the *Tfpi*$^{-}$ locus. The only shared INDEL (between G6-ENU and G9-ENU; Figure 3-3A) was an 8 bp deletion (AGCCAGAC) in the 27th exon of *Nbeal2*, confirmed by Sanger sequencing (Figure 3-3B). This allele will be denoted *Nbeal2*^{gps}. Genotyping additional members of the pedigree demonstrated absence of this deletion allele in generation 5 (G5) ENU mutagenized progeny exhibiting the suppressor phenotype (Figure 3-3A). Instead, the G6-ENU mouse inherited the deletion from its non-ENU parent and would have been missed in our mouse cohort if it had not been coincidentally shared by the whole exome sequenced G9-ENU mouse. Absence of the

Nbeal2^{gps} allele in the first five generations of ENU pedigree excludes *Nbeal2*^{gps} as the original suppressor mutation. Additionally, *Nbeal2*^{gps} failed to segregate with the suppressor phenotype in later generations (Figure 3-2). Further genotyping identified a cohort of 129S1/SvImJ mice purchased from the Jackson Laboratory as the likely source of the deletion variant (Figure 3-4A).

The *Nbeal2*^{gps} allele is not segregating in 129S1/SvImJ stock

To minimize cumulative genetic drift, the 129S1/SvImJ colony at the Jackson Laboratory is maintained under a Genetic Stability Program (GSP) [147]. In this scheme, foundation breeding colonies are maintained with cryopreserved embryos that are descendants of a single, founder breeder pair. To trace the origin of the *Nbeal2*^{gps} allele, six archived samples from the 129S1/SvImJ (# 002448) colony at the Jackson Laboratory were genotyped, including the 129S1/SvImJ founder pair, “Adam and Eve” (F60) as well as archived samples from before (F56, F59) and after (F61, F63) implementation of the GSP program. The *Nbeal2* deletion was not found in any of these samples (Figure 3-4B). Exome sequencing data from two additional 129S1/SvImJ samples (F63pF67) [159], whole genome sequencing data from the Sanger Mouse Genomes Project, F63pF65 [143], and exome sequencing data from a female sibling, as well as the dam and sire (F63pF64) of the 129S1/SvImJ individual sequenced by the Sanger Mouse Genomes project identified only wildtype *Nbeal2* (Figure 3-4C). Mice with the *Nbeal2*^{gps} allele were purchased after the implementation of GSP. Since neither Adam nor Eve were carriers, the deletion must have arisen later in the colony but is no longer segregating in the 129S1/SvImJ stock at the Jackson Laboratory.

An 8 bp deletion results in a frameshift mutation in *Nbeal2*

The identified 8bp deletion in *Nbeal2* is expected to cause a frameshift that introduces an early stop codon 28 amino acids downstream of the deletion site (Figure 3-3D). The expression level of *Nbeal2*^{gps} mRNA from bone marrow, liver, and lung tissues was assessed by RT-PCR and Sanger sequencing. Although *Nbeal2*^{gps} mRNA could be detected by RT-PCR, the level was ~64% lower in bone marrow, ~73% lower in liver, and ~59% lower in lung compared to the wildtype allele (Figure 3-5). These

results are consistent with nonsense-mediated decay [166]. In addition, no band was detected at the expected size (~305kDa) by western blot analysis of washed platelets obtained from *Nbeal2*$^{gps/gps}$ mice (Figure 3-3C) and no truncated protein was observed with an N-terminal antibody (Figure 3-6).

Nbeal2$^{gps/gps}$ mice are viable and fertile

A mouse carrying the *Nbeal2* deletion allele (Figure 3-2) was outbred from the ENU suppressor line for two generations to remove the *F5*^{L} and *Tfpi* mutant alleles, as well as the majority of residual, unlinked ENU induced variants. Mice carrying one (*Nbeal2*$^{gps/+}$) or two deletion alleles (*Nbeal2*$^{gps/gps}$) were viable, fertile and had no apparent phenotype by visual inspection. No significant deviation from the expected Mendelian distribution was observed in the progeny when crossing the *Nbeal2*$^{gps/+}$ mice to C57BL/6J wildtype mice or in the progeny from the *Nbeal2*$^{gps/+}$ intercross (Table 3-2).

Nbeal2$^{gps/gps}$ mice exhibit thrombocytopenia and neutropenia

Complete blood counts (CBC) were performed on 24 *Nbeal2*$^{gps/+}$, 26 *Nbeal2*$^{gps/gps}$ mice, and 14 wildtype littermate controls from set 1. No significant differences were observed between *Nbeal2*$^{gps/+}$ and *Nbeal2*$^{+/+}$ mice in any of the measured parameters (Table 3-3) and those genotypes were subsequently grouped together as controls for comparison to *Nbeal2*$^{gps/gps}$ mice. Platelet counts of *Nbeal2*$^{gps/gps}$ mice were significantly reduced compared to control mice (623 vs 968 x 10^3 cells/µl, p=1.63 x 10^{-7}) as was the absolute neutrophil count (0.27 vs 0.77 x 10^3 cells/µl, p=2.44 x 10^{-9}) (Figure 3-7; Table 3-3). All other CBC parameters, including mean platelet volume, were indistinguishable between *Nbeal2*$^{gps/gps}$ and control mice (Table 3-3). In addition, no difference was observed in mean platelet area quantitated in electron microscopy images. However, in CBCs obtained from a second cohort of 6 *Nbeal2*$^{gps/+}$ and 8 *Nbeal2*$^{gps/gps}$ females, both neutrophil counts (p=0.0047) and mean platelet volume (p=0.016) were higher in the *Nbeal2*$^{gps/gps}$ mice compared to littermate controls (Figure 3-7). Additional analysis of neutrophil counts for the set 2 mice by flow cytometry showed no significant differences.

Nbeal2$^{gps/gps}$ platelets are deficient in alpha granules

The intensity of platelet staining with Wright-Giemsa dye was indistinguishable between *Nbeal2*$^{gps/+}$ and wildtype mice (p-value=0.298), but significantly reduced in *Nbeal2*$^{gps/gps}$ mice (p-value=1.9x10^{-4}; Figure 3-8A; Table 3-4) consistent with a reduction in platelet alpha granules [152, 156]. Transmission electron microscopy also displayed a marked reduction of alpha granules in *Nbeal2*$^{gps/gps}$ mouse compared to wildtype control (Figure 3-8B), consistent with the human GPS phenotype [152, 156].

Emperipolesis of neutrophils in bone marrow and spleen of *Nbeal2*$^{gps/gps}$ mice

Nbeal2$^{gps/gps}$ mice exhibit higher levels of megakaryocytic emperipolesis (the presence of an intact cell within the cytoplasm of another cell) in the bone marrow compared to wildtype mice, consistent with previously reported human and mouse GPS phenotypes [152, 153, 167-169]. Though emperipolesis is occasionally observed in megakaryocytes of wildtype mice (~11%), approximately half of the bone marrow megakaryocytes in *Nbeal2*$^{gps/gps}$ mice exhibited some degree of emperipolesis (p=1.9 x 10^{-8}; Figure 3-9A,B; Table 3-4). Megakaryocytes containing more than one neutrophil were observed exclusively in the bone marrow of *Nbeal2*$^{gps/gps}$ mice. Similarly, increased emperipolesis was observed in spleens of *Nbeal2*$^{gps/gps}$ mice (Figure 3-9C,D). *Nbeal2*$^{gps/gps}$ bone marrows demonstrated no defect in myeloid maturation though there appeared to be a mild increase in myeloid and megakaryocytic extramedullary hematopoiesis.

Discussion

We report the identification and characterization of a spontaneous *Nbeal2* mutation in 129S1/SvImJ. Homozygosity for this 8 bp frameshift results in loss of NBEAL2 expression and phenotypic features characteristic of GPS in humans [152, 156]. These findings are also consistent with three other previous reports of *Nbeal2* deficient mice generated by gene targeting [153-155].

Though an initial cohort of *Nbeal2*$^{gps/gps}$ mice (set 1) demonstrated differences in neutrophil counts and mean platelet volumes (Table 3-3) compared to previously

reported mouse and human phenotypes, these features were not confirmed in the second cohort (mice backcrossed 5 additional generations into C57BL/6J). These data suggest that the differences observed in set 1 mice are due to either strain background effects [97] or loosely linked passenger mutations [170] that were removed by consecutive backcrossing. Additional confounding factors could include the difference in age between the two mouse cohorts. Comparison of the absolute neutrophil count (ANC) from the Hemavet analyzer to the ANC obtained by flow cytometry demonstrates consistent overestimates on the Hemavet. This discrepancy could be secondary to limitations of the Hemavet system in discerning between neutrophils and monocytes. Similar results have been previously reported [171]. The quantification of ANC by flow cytometry should identify the population corresponding exclusively to neutrophils. In addition, the use of Trucount counting tubes has been well validated and offers an internal control with respect to sample preparation. The estimated coefficient of variation for our flow cytometry ANC assay using the Trucount beads is 3.48%. Thus, we consider the results obtained by FACS to more accurately represent the ANC.

Our data establish that the *Nbeal2*^{gps} allele is a spontaneous mutation that arose in the 129S1/SvImJ stock at the Jackson Laboratory in 2007 at F63. Though, we were unable to confirm the presence of the mutation in archival samples, this is likely due to the small number of archived samples available. Published rates of spontaneous mutations in mice range from 10^{-5} to 10^{-6} per locus per gamete on the basis of specific locus testing with visible phenotypes [172]. More recently, whole genome sequencing and pedigree analyses have estimated a mutation rate of 5.4×10^{-9} per base/ per generation in wildtype laboratory mice [125], which is roughly 28 mutations, genome wide per generation / diploid genome. New mutations have a 25% chance of becoming fixed in an inbred population, assuming random segregation in the absence of selection [147]. We performed exome sequencing on a single 129S1/SvImJ trio (F63pF64 and F63pF65) and did not find a *de novo*, coding SNV or small INDEL (see Materials and Methods). This is consistent with previously published mutation rates (given a ~50 Mb exome, at 10X minimum coverage where the likelihood of detecting a germ line *de novo*, exonic mutation is ~5% in any individual).

The *Nbeal2*^{gps} allele was identified via whole exome sequencing of the progeny

of an ENU treated mouse. While next generation sequencing approaches have high utility for mapping both spontaneous [49] as well as chemically induced *de novo* variants [71], the origin of a single nucleotide variant cannot be established from sequencing data alone. While ENU-induced mutations are certainly the most common in an ENU colony, spontaneous mutations are also present at predictable frequencies and unlike ENU mutations, spontaneous mutations are not limited to SNVs and can include structural alterations (copy number variants and rearrangements). Therefore, while infrequent, it is not surprising that spontaneous mutations with relevant phenotypes have been recovered in ENU screens [173].

Ultimately, the origin of causative mutations (ENU or spontaneous) can be established through additional genotyping of the ENU pedigree, assuming breeding records and samples have been carefully maintained and archived. Generally, strong dominant phenotypes due to *de novo* variants are easily detected in mouse colonies; however, mild dominant phenotypes or recessive phenotypes may go unnoticed depending on the breeding paradigm. For these reasons, it is important to adhere to published guidelines on mouse colony management and genetic quality control monitoring [174]. In the case of the *Nbeal2*^{gps} allele, the platelet defect had no impact on survival of *F5*$^{L/L}$ *Tfpi*$^{+/-}$ mice and we were able to identify the variant only due to next generation sequencing.

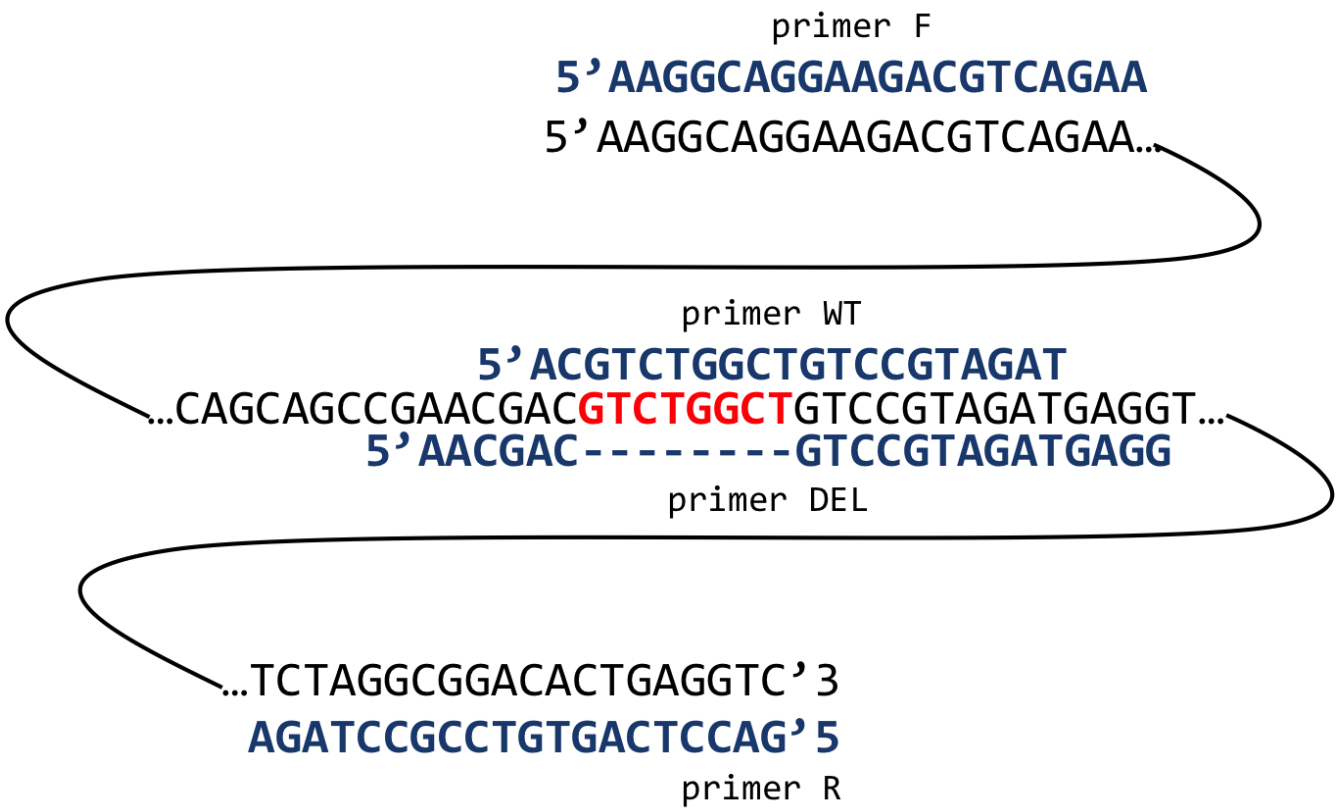

Figure 3-1. Schematic overview of the *Nbeal2* genotyping primers
Common forward (primer F) and reverse (primer R) primers are used in two three-primer PCR assays. In the first PCR based genotyping design, the third primer (primer WT) is located over the undeleted 8 bp to detect the presence of the wildtype allele. This PCR reaction results in two products (413 bp, 235 bp). In the second PCR design the third primer (primer DEL) spans the 8 bp deletion (depicted in red) to detect the presence of the deletion allele. This reaction also produces two products (405 bp, 227 bp).

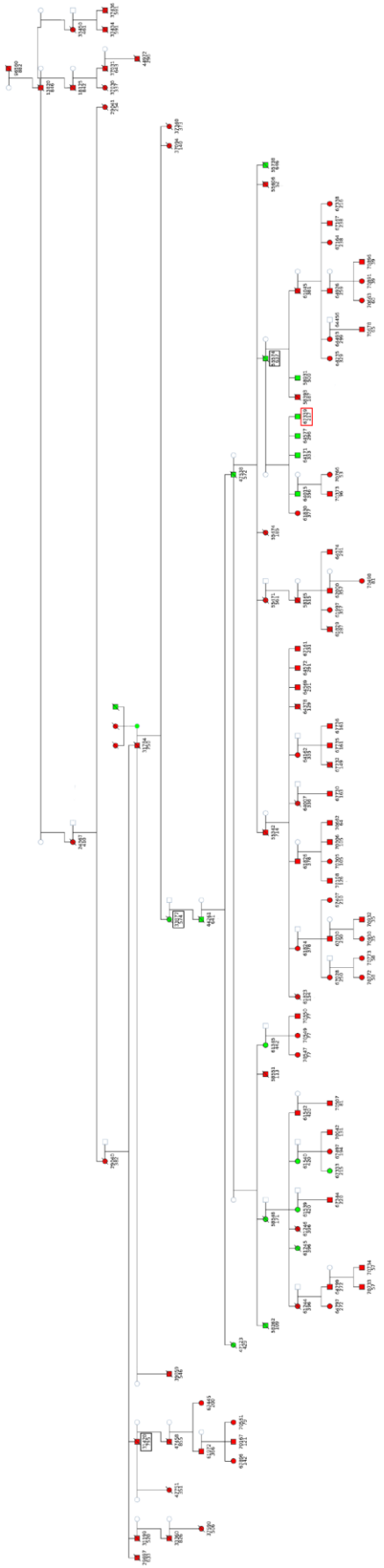

Figure 3-2: Pedigree of the *MF5L6* suppressor line
Only progeny mice with the *F5*$^{L/L}$ *Tfpi*$^{+/-}$ genotype and unaffected parents are shown in the pedigree. Black boxes highlight the mice subjected to whole exome sequencing. The red box highlights mouse 67339 that was used for *Nbeal2*^{gps} allele outcrossing and line establishment.

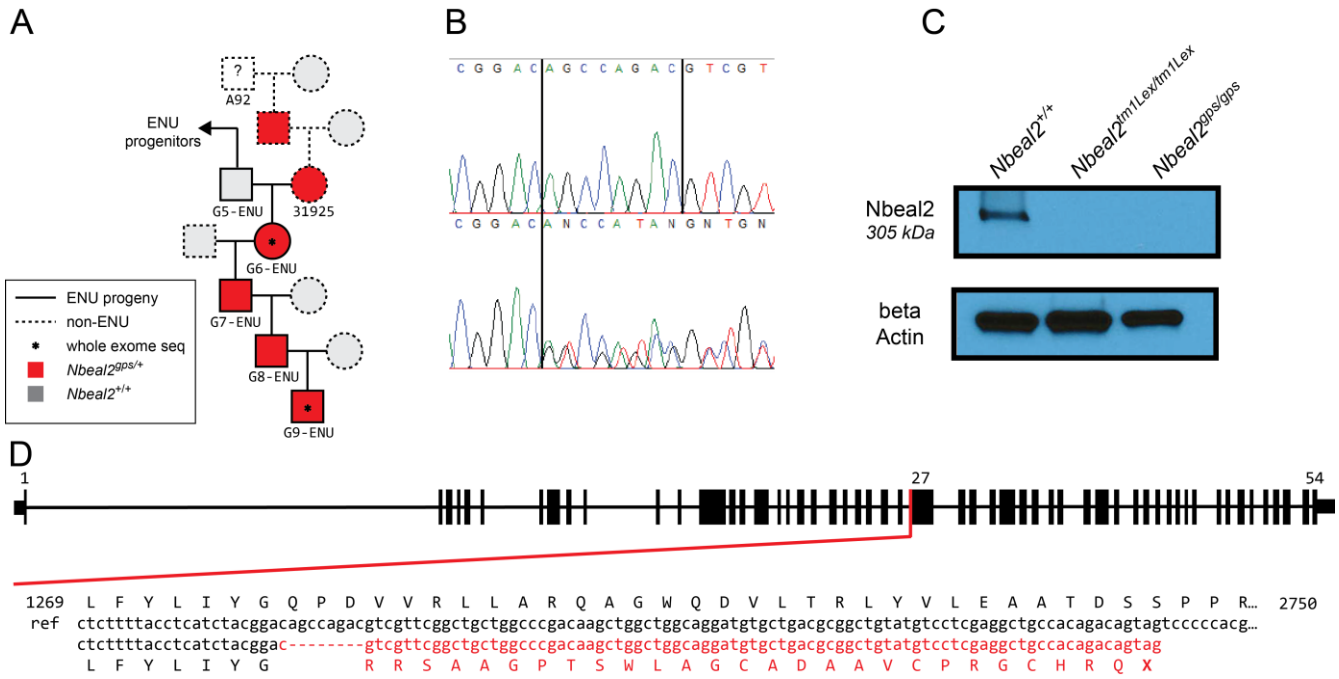

Figure 3-3: *De novo* 8 bp deletion in the *Nbeal2* gene
The whole exome sequenced G6-ENU mouse inherited the *Nbeal2* deletion from a non-ENU parent 31925 (A). Sanger sequencing validates the heterozygous frameshift mutation in the suppressor pedigree (B). Western blot analysis of washed mouse platelets show a band at the expected size for NBEAL2 (~305kDa) in wildtype mice. This band is missing in *Nbeal2*$^{tm1Lex/tm1Lex}$ mice as well as mice homozygous for the *Nbeal2*^{gps} allele (C). Schematic overview of the *Nbeal2* gene, the location of the deletion and the expected frameshift (D).

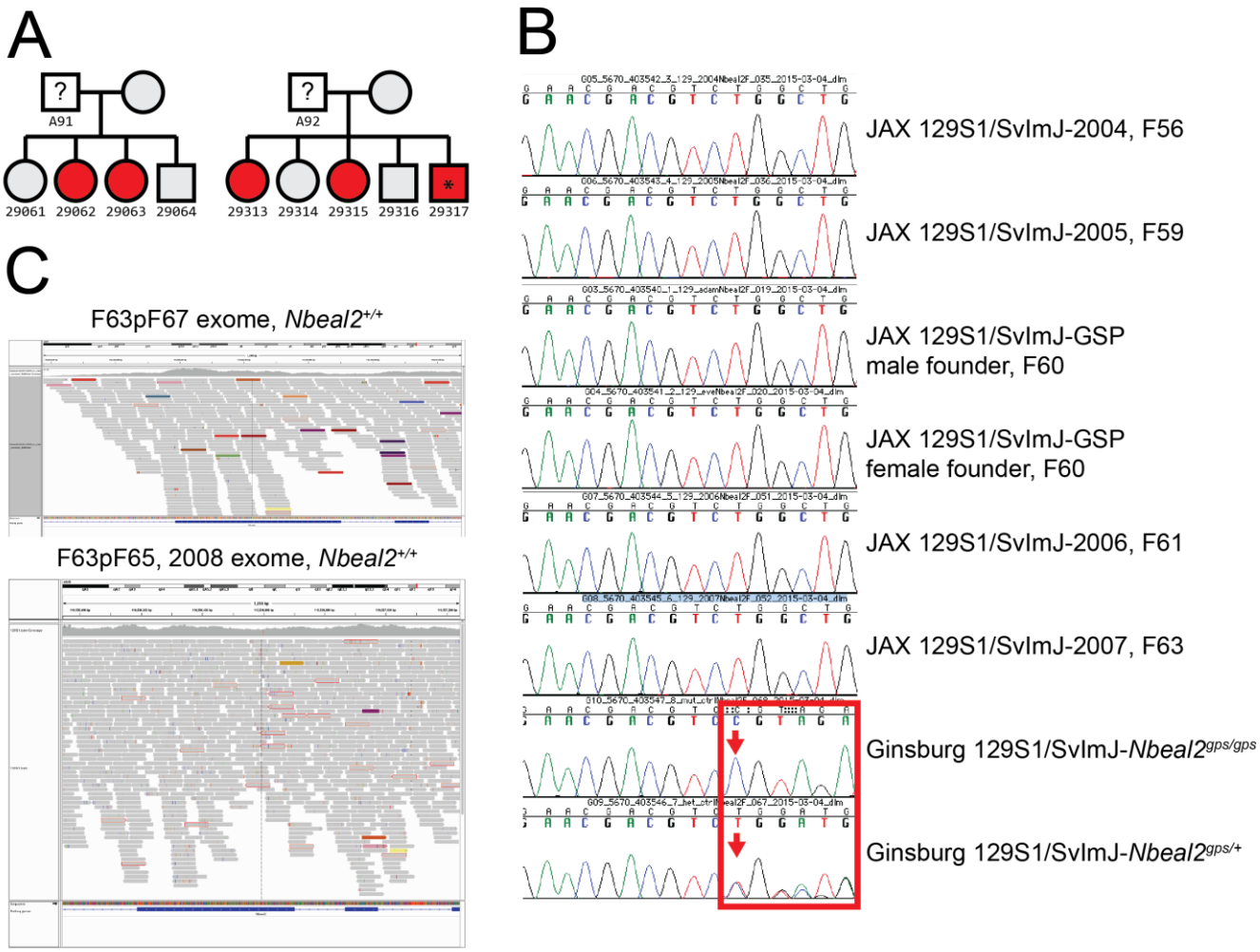

Figure 3-4: Genotyping of 129S1/SvImJ archived samples from the Jackson Laboratory

Two different mice (A91, A92) purchased from the Jackson Laboratory (JAX) had *Nbeal2*$^{gps/+}$ progeny (red). One of these progeny (asterisk) was the sire of the female used to build the ENU suppressor line (A). All genotyped 129S1/SvImJ (# 002448) mice were wildtype at the *Nbeal2* locus, including the "Adam and Eve" founders of the Jackson Laboratory GSP 129S1/SvImJ stock (F60) [147] and two subsequent generations of cryopreserved embryo stock (F61, F63) (B). The *Nbeal2* deletion was also absent in two post-GSP 129S1/SvImJ animals: whole exome sequencing data (F63pF67) from the Mouse Mutant Resource [159] and whole genome sequencing data (F63pF65) from the Sanger Mouse Genomes Project (C) [143].

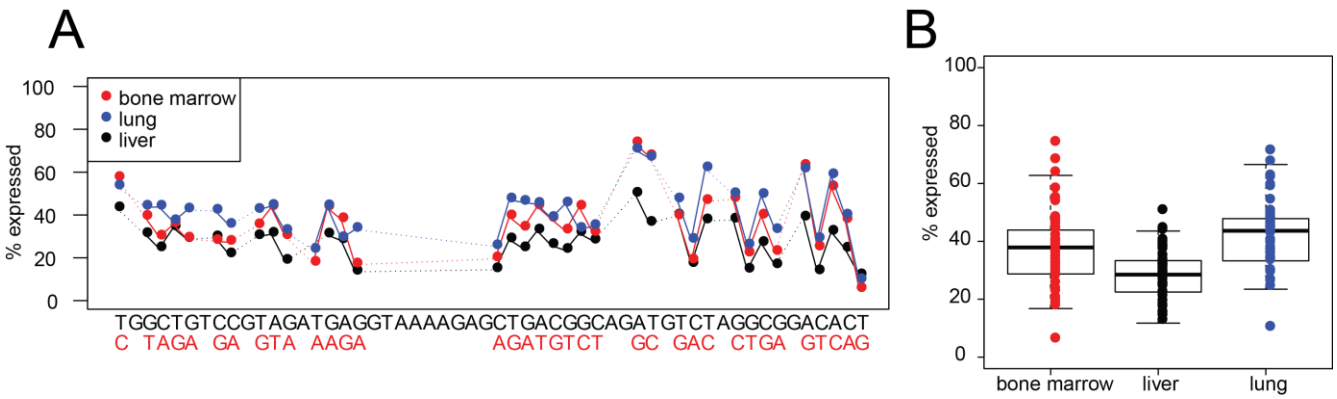

Figure 3-5: Differential allelic expression of *Nbeal2* mRNA in *Nbeal2*$^{gps/+}$ bone marrow, lung, and liver

Allelic expression was measured at every position in the Sanger sequenced RT-PCR product where the reference and deletion alleles had a different nucleotide. Dotted lines fill the gaps. In all tested tissues, the relative expression of *Nbeal2*^{gps} allele is lower than wildtype, set as 100% (A). Boxplot of all data points show on average ~65% reduction in expression of the deletion allele (B).

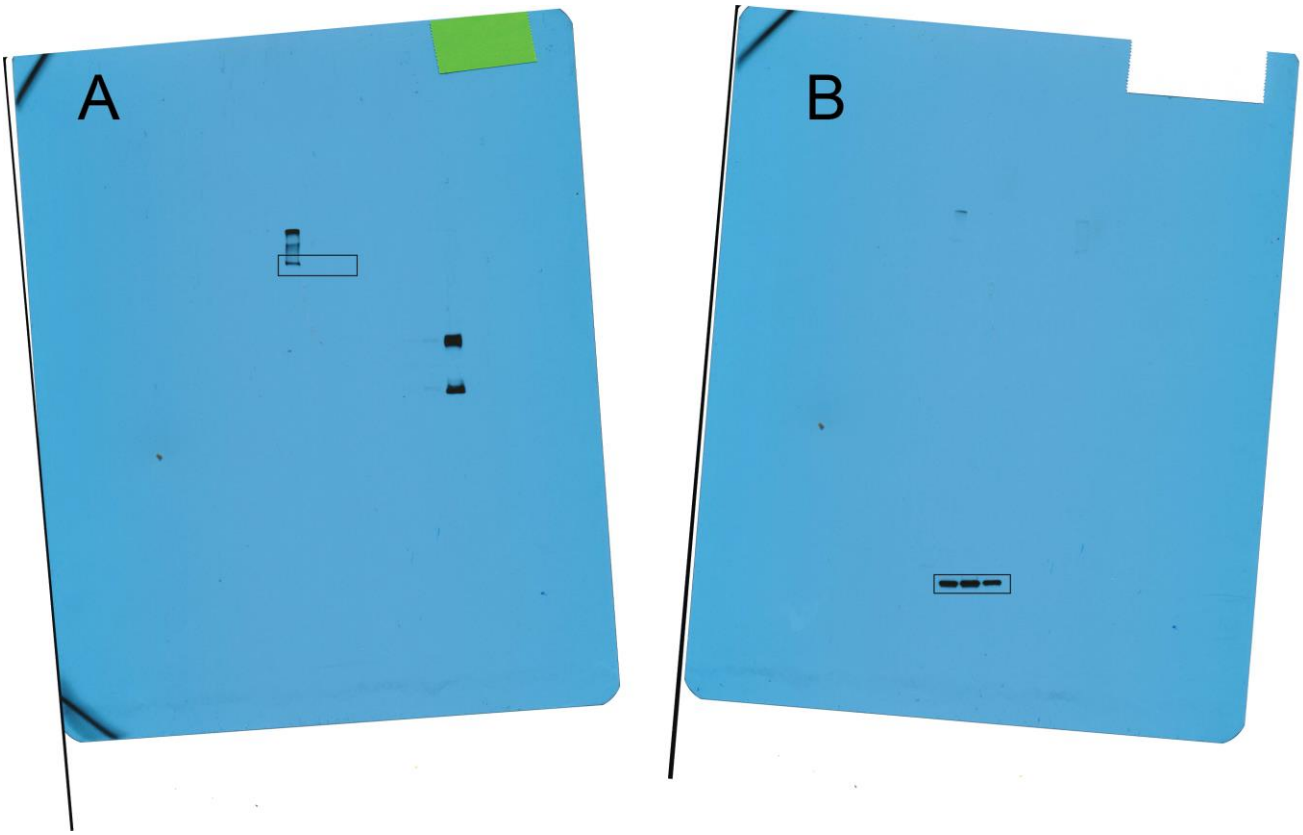

Figure 3-6: Western blot analysis for NBEAL2 and beta Actin
Here we show full blots for the Western blot analysis. Areas surrounded by black boxes were displayed in Figure 3-3C.

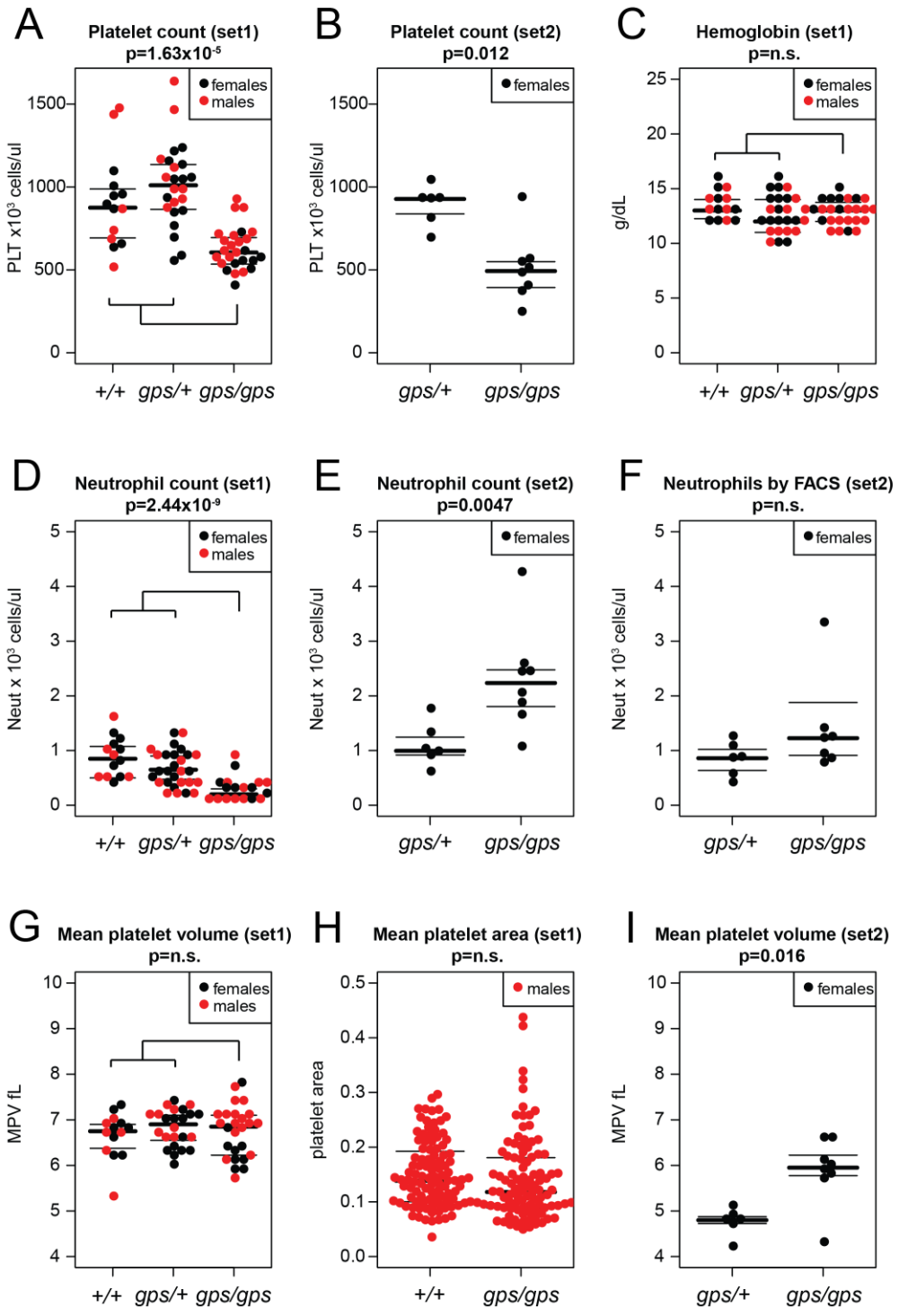

Figure 3-7: Comparison of CBCs
Platelet counts are lower in *Nbeal2*$^{gps/gps}$ mice compared to control mice in both set 1 (A) and set 2 (B) mice while hemoglobin levels are similar between the two groups (C). *Nbeal2*$^{gps/gps}$ mice from set 1 exhibit significant neutropenia (D), which is not observed in set 2 by CBC (E) or flow cytometry (F). Mean platelet volume (G) and area (H) do not differ in set 1 mice, but show an increase in size for *Nbeal2*$^{gps/gps}$ mice in set 2 (I).

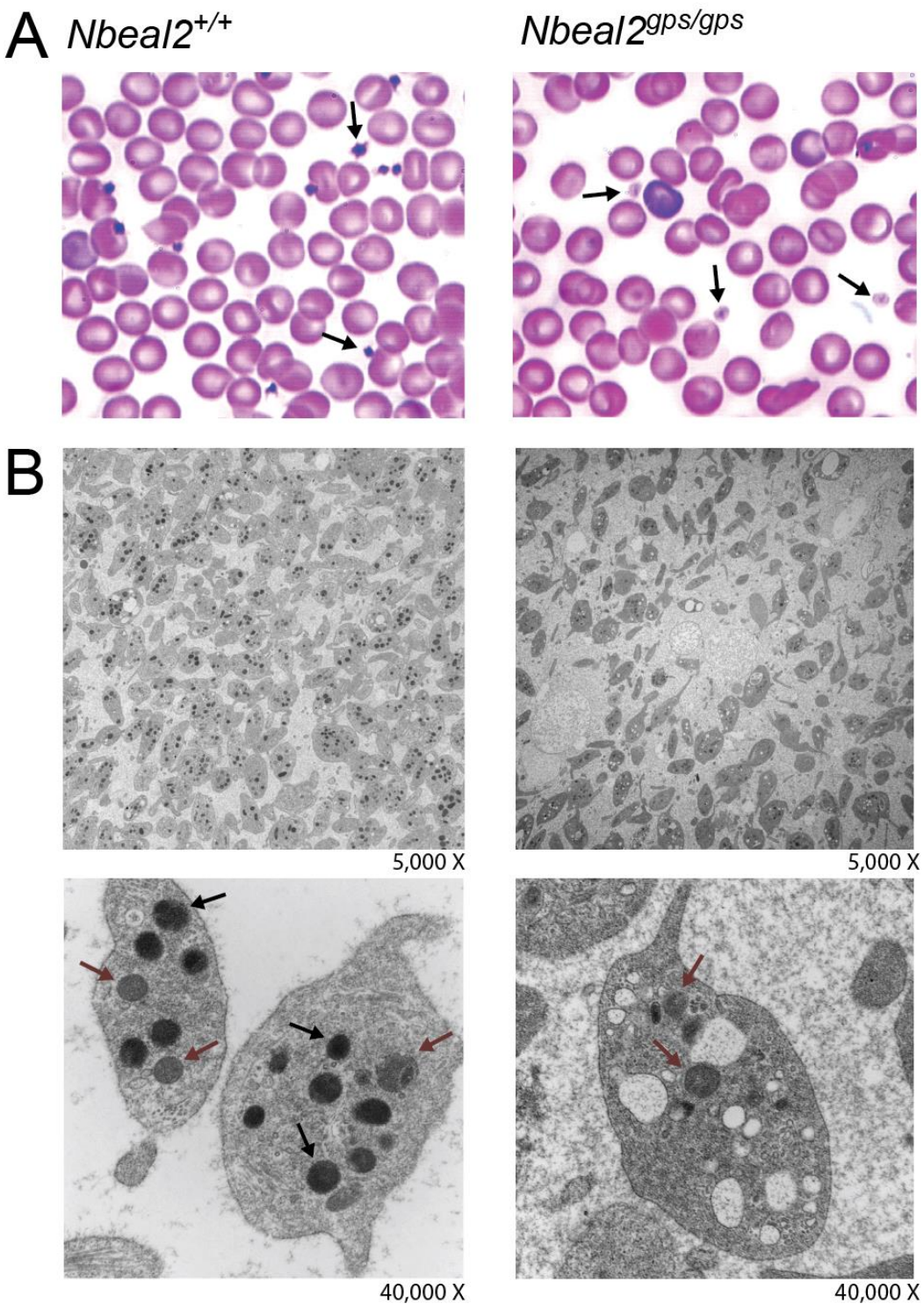

Figure 3-8: Deficiency in platelet alpha granules
Nbeal2$^{gps/gps}$ platelets appear pale compared to wildtype (black arrows, A). Transmission electron microscopy (TEM) images show dark alpha granules in wildtype platelets (black arrows), which are missing in *Nbeal2*$^{gps/gps}$ platelets. Red arrows indicate mitochondria (B).

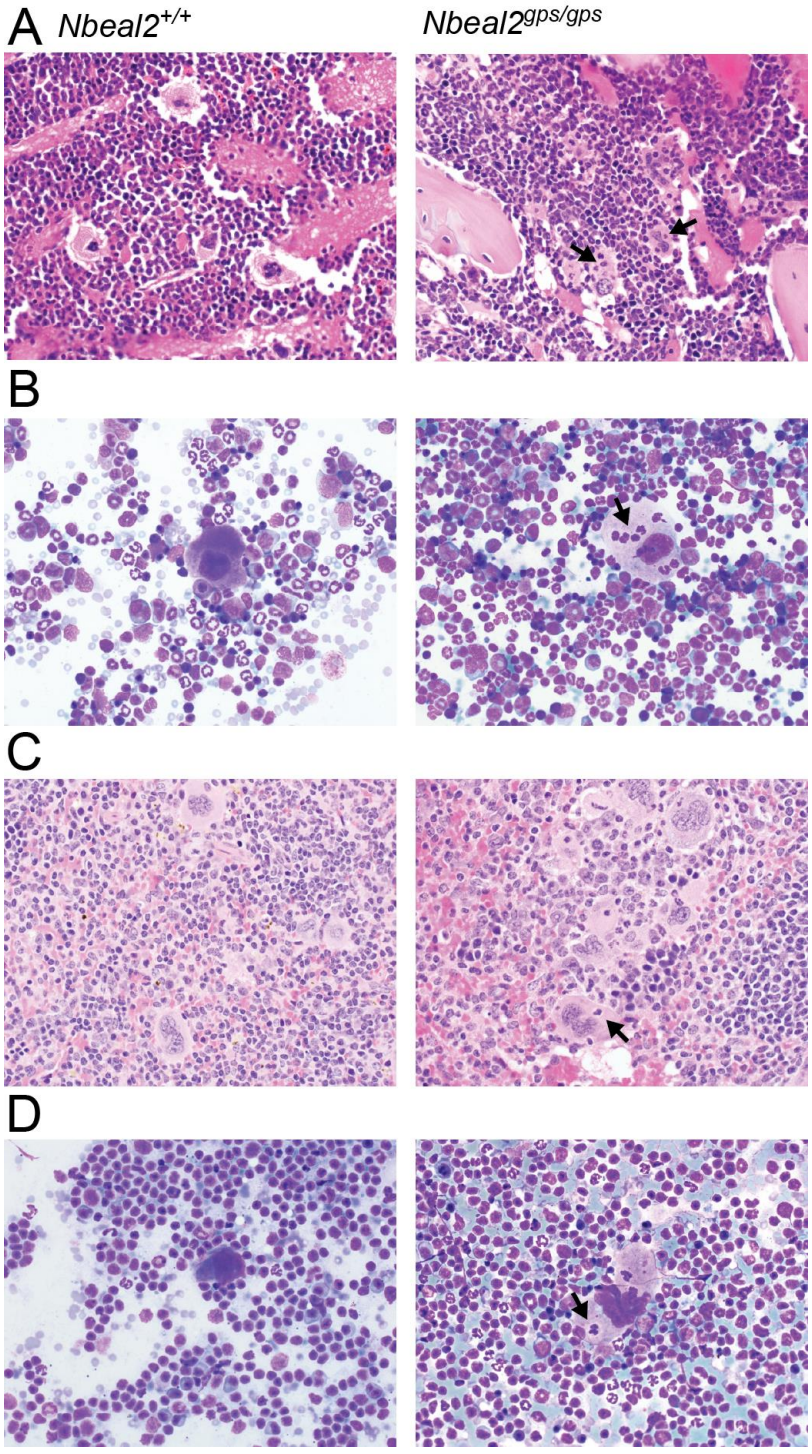

Figure 3-9: Emperipolesis of neutrophils in bone marrow and spleen
Increased emperipolesis of neutrophils (black arrows) in *Nbeal2*$^{gps/gps}$ mice compared to wildtype was observed in both histologic (A) and cytologic (B) preparations of bone marrow as well as spleen (C and D, respectively).

Table 3-1: Overview of the exonic variants called from WES in 4 mice from the *MF5L6* pedigree

Type	**All SNVs**	**Unique SNVs**	**In > 1 mouse**
nonsense	87	3	1
nonsynonymous	11,854	66	6
synonymous	21,130	27	2
splice	90	2	0
exonic	34,288	117	3
Total:	67,449	215	12
Type	**All INDELs**	**Unique INDELs**	**In > 1 mouse**
frameshift	344	3	1 (*Nbeal2*)
nonframeshift	460	0	0
splice	71	1	0
exonic	8626	4	0
Total:	9501	8	1

WES=whole exomose sequencing; Details available at github.com/tombergk/NBEAL2

Table 3-2: Expected and observed number of progeny in *Nbeal2*$^{gps/+}$ crosses

Cross	*Nbeal2*$^{+/+}$	*Nbeal2*$^{gps/+}$	*Nbeal2*$^{gps/gps}$	P-value*
Nbeal2$^{gps/+}$ **x *Nbeal2***$^{+/+}$	46% (37)	54% (44)	-	0.4367
Expected	50%	50%	-	
Nbeal2$^{gps/+}$ **x *Nbeal2***$^{gps/+}$	24% (23)	47% (44)	29% (27)	0.6965
Expected	25%	50%	25%	

**A* chi-square test was applied to estimate deviations from expected Mendelian proportions. Number of mice genotyped available in parentheses.

Table 3-3: CBC mean values and standard deviations by genotype in set 1 mice

Abbr.	*Nbeal2*$^{+/+}$ mean ± sd	*Nbeal2*$^{gps/+}$ mean ± sd	P-value	*Nbeal2*$^{+/+,\ gps/+}$ mean ± sd	*Nbeal2*$^{gps/gps}$ mean ± sd	P-value*
WBC	6.80 ± 1.46	7.23 ± 2.08	0.75	7.07 ± 1.86	7.04 ± 2.34	0.56
RBC	9.45 ± 0.85	8.96 ± 1.08	0.17	9.14 ± 1.02	8.91 ± 0.68	0.46
HGB	13.43 ± 1.28	12.58 ± 1.74	0.12	12.89 ± 1.62	12.77 ± 1.11	0.79
HCT	4.89 ± 0.39	4.66 ± 0.59	0.23	4.74 ± 0.53	4.68 ± 0.34	0.65
MCV	51.88 ± 2.05	52.06 ± 1.72	0.81	51.99 ± 1.82	52.66 ± 1.63	0.13
MCH	14.19 ± 0.48	14.16 ± 0.70	0.84	14.17 ± 0.62	14.47 ± 0.72	0.18
MCHC	27.41 ± 0.95	27.19 ± 1.00	0.62	27.27 ± 0.97	27.48 ± 1.04	0.48
CHCM	28.28 ± 2.02	28.20 ± 2.08	0.95	28.23 ± 2.03	27.10 ± 1.91	0.11
CH	14.67 ± 0.88	14.68 ± 0.83	0.84	14.67 ± 0.84	14.27 ± 1.02	0.09
RDW	15.94 ± 1.93	16.25 ± 1.85	0.40	16.13 ± 1.86	16.16 ± 1.32	0.50
HDW	1.66 ± 0.21	1.61 ± 0.14	0.73	1.63 ± 0.17	1.52 ± 0.09	4.44×10^{-3}
PLT	906.4 ± 280.6	1004.6 ± 247.6	0.15	968.4 ± 260.9	622.7 ± 128.6	**1.63×10^{-7}**
MPV	6.64 ± 0.51	6.80 ± 0.40	0.36	6.74 ± 0.45	6.72 ± 0.57	0.78
Neut	0.86 ± 0.36	0.73 ± 0.29	0.27	0.77 ± 0.32	0.27 ± 0.19	**2.44×10^{-9}**
Lymph	5.05 ± 1.17	5.57 ± 2.10	0.35	5.38 ± 1.81	5.97 ± 2.46	0.56

WBC (White Blood Cell count), RBC (Red Blood Cell count), HGB (Hemoglobin concentration), HCT (Hematocrit), MCV (Mean Corpuscular Volume), MCH (Mean Corpuscular Hemoglobin), MCHC (Mean Corpuscular Hemoglobin Concentration), CHCM (Corpuscular Hemoglobin Concentration Mean), CH (Cellular Hemoglobin Content), RDW (Red Cell Volume Distribution Width), HDW (Hemoglobin Concentration Distribution Width), PLT (Platelet count), MPV (Mean Platelet Volume), Neut (Neutrophil cell count), Lymph (Lymphocyte cell count). * Significant p-values after Bonferroni correction (p-value ≤ 0.0033) for multiple testing are highlighted in bold font

Table 3-4: Intensity of platelet staining and frequency of emperipolesis events in bone marrow megakaryocytes

Intensity of platelet staining (n=9)					
Genotypes	**Light (1)**	**Medium (2)**	**Dark (3)**	**Average**	**P-value**
Nbeal2$^{+/+}$	0	1	8	2.89	
Nbeal2$^{gps/+}$	0	3	6	2.67	0.298
Nbeal2$^{gps/gps}$	7	2	0	1.22	0.0001898
Number of emperipolesis events (n=3)*					
Genotypes	**0**	**1**	**≥2**	**Average**	**P-value**
Nbeal2$^{+/+}$	81 (89%)	10 (11%)	0	0.11	
Nbeal2$^{gps/gps}$	35 (51%)	19 (27%)	15 (22%)	0.71	1.898×10^{-8}

* 3 slides per genotype, >20 megakaryocytes per slide

Notes

This chapter is being revised for publication in the journal PLoS ONE under the title “Spontaneous 8bp Deletion in *Nbeal2* Recapitulates the Gray Platelet Syndrome in Mice” by Kärt Tomberg, Rami Khoriaty, Randal J. Westrick, Heather E. Fairfield, Laura G. Reinholdt, Gary L. Brodsky, Pavel Davizon-Castillo, David Ginsburg, and Jorge Di Paola

CHAPTER IV: ENU mutagenesis and whole exome sequencing to identify thrombosis modifier genes

Abstract

Only ~10% of individuals carrying the common venous thrombosis risk factor, Factor V Leiden (FVL) will develop venous thrombosis in their lifetime. In order to identify potential FVL modifier genes, we performed a sensitized dominant ENU mutagenesis screen, based on the perinatal synthetic lethal thrombosis previously observed in mice homozygous for FVL (*F5*$^{L/L}$) and haploinsufficient for tissue factor pathway inhibitor (*Tfpi*$^{+/-}$). Out of 2595 G1 (generation 1) offspring of mutagenized *F5*$^{L/L}$ males (G0) and unmutagenized *F5*$^{L/+}$ *Tfpi*$^{+/-}$ females, a total of 70 viable *F5*$^{L/L}$ *Tfpi*$^{+/-}$ progeny ('rescues') were identified, with 13 producing ≥1 G2 rescues. Linkage analysis conducted in 3 largest pedigrees using ENU-induced coding variants as genetic markers failed to map the corresponding suppressor loci. However, in one of the pedigrees, a maternally inherited (not ENU-induced) *de novo* mutation (*Plcb4*^{R335Q}) exhibited significant co-segregation with the rescue phenotype (p=0.02). Whole exome sequencing was next applied to DNA from 107 rescue progeny to identify candidate genes that are enriched for ENU mutations. A total of 3481 potentially deleterious candidate ENU variants were identified in 2984 genes. After adjusting for coding region size, the ENU-induced mutation burden was significantly greater than expected by chance for *Arl6ip5*, *C6* and *Itgb6* genes (false discovery rate<0.1, based on 10^6 permutations) and suggestive for 9 additional genes. Simultaneous introduction of CRISPR-Cas9 reagents for the top 6 genes were used to produce >100 null alleles. Preliminary validation data shows significant increase in rescue progeny from mice carrying a subset of CRISPR-Cas9 induced alleles in 5 of the genes ($p=6.7x10^{-5}$, compared to expected background survival).

Introduction

Venous thromboembolism (VTE) affects 1:1000 individuals in the US each year and is highly heritable [12, 13]. The most common known genetic risk factor for VTE is a single nucleotide variant (SNV) in the *F5* gene, referred to as Factor V Leiden (FVL, Arg506Gln) [26]. While the FVL variant is present in ~25% of VTE patients [31], only 10% of individuals heterozygous for FVL develop thrombosis in their lifetime.

To identify genetic variants potentially modifying FVL, we recently employed a dominant ENU screen (Chapter II) in mice sensitized for thrombosis. Mice homozygous for the FVL mutation ($F5^{L/L}$) and haploinsufficient for tissue factor pathway inhibitor ($Tfpi^{+/-}$) die of perinatal thrombosis [47]. After ENU mutagenesis, 98 G1 $F5^{L/L}$ $Tfpi^{+/-}$ progeny survived to weaning ('rescues') and 16 of them exhibited successful transmission of the ENU-induced suppressor mutation. However, subsequent efforts to genetically map the corresponding suppressor loci were largely unsuccessful due to the confounding effects of complex strain-specific differences introduced by the required genetic outcross (Chapter II). Similar genetic background effects have complicated previous mapping efforts [175] and have been noted to significantly alter other phenotypes of interest [97, 176]. Additional challenges of traditional mapping approaches include the requirement for large pedigrees and limited mapping resolution, with candidate intervals typically harboring tens to hundreds of genes and multiple closely linked mutations.

The emergence of high throughput sequencing methods has greatly enabled the direct identification of ENU-induced mutations and removed the necessity for outcrossing to introduce genetic markers for mapping [72, 104]. Here, we initially employed the previously successful approach [113] of mapping causal variants in rescue pedigrees using coding ENU-induced mutations as genetic markers. Application of a novel mutation burden test facilitated the identification of 12 candidate thrombosis modifier genes from bulk sequencing of 107 $F5^{L/L}$ $Tfpi^{+/-}$ rescue mice without the requirement of genetic crosses for mapping.

Materials and methods

Mice

Mice carrying the murine homolog of the FVL mutation (*F5*^{L}; B6.129S2-*F5*^{tm2Dgi}/J, Jackson Laboratory stock #004080) [46] or the TFPI Kunitz domain deletion (*Tfpi*$^{-}$) [92] were generated as previously described. Mice were genotyped using PCR assays with primers and conditions as previously described [46, 92], and maintained on the C57BL/6J background (Jackson Laboratory stock #000664). All animal care and procedures were performed in accordance with the Principles of Laboratory and Animal Care established by the National Society for Medical Research. University Committee on Use and Care of Animals at University of Michigan has approved the protocol number 05191 used for current study. The University of Michigan is fully accredited by the Association for Assessment and Accreditation of Laboratory Animal Care, International (AAALAC, Intl) and the animal care and use program conforms to the standards of "The Guide for the Care and Use of Laboratory Animals," Revised 2011. All animal procedures were approved by the University of Michigan IACUC.

ENU screen

ENU mutagenesis was performed as previously described (Chapter II), with all mice on the C57BL/6J genetic background. Briefly, 189 *F5*$^{L/L}$ male mice (6-8 weeks old) were administrated three weekly intraperitoneal injections of 90 mg/kg of ENU (N-ethyl-N-nitrosourea, Sigma-Aldrich). Eight weeks later, 177 surviving males were mated to *F5*$^{L/+}$ *Tfpi*$^{+/-}$ females and their G1 progeny were genotyped at age 2-3 weeks to identify viable *F5*$^{L/L}$ *Tfpi*$^{+/-}$ offspring. *F5*$^{L/L}$ *Tfpi*$^{+/-}$ G1 rescues were crossed to *F5*$^{L/L}$ mice on the C57BL/6J genetic background and transmission was considered positive with the presence of one or more rescue progeny. Theoretical mapping power in rescue pedigrees was estimated by 10,000 simulations using SIMLINK software [177].

Whole exome sequencing

Gender, age, whole exome sequencing (WES) details, and other characteristics for 108 rescue mice are provided in Appendix 4-1. Genomic DNA (gDNA) extracted from tail biopsies of 56 G1 offspring from the current ENU screen and from an additional 50 *F5*$^{L/L}$ *Tfpi*$^{+/-}$ mice on the C57BL/6J background from the previous screen (Chapter II)

were subjected to WES at the Northwest Genomics Center, University of Washington. Sequencing libraries were prepared using the Roche NimbleGen exome capture system. DNA from an additional two rescue offspring were subjected to WES at Beijing Genomics Institute or Centrillion Genomics Technologies, respectively (Appendix 4-1). These two libraries were prepared using the Agilent SureSelect capture system. 100 bp paired-end sequencing was performed for all 108 exome libraries using Illumina HiSeq 2000 or 4000 sequencing instruments. Two WES mice represented rescue pedigree 1: the G1 founder and a G2 rescue offspring. The latter was used for linkage analysis, but excluded from the burden analysis (Appendix 4-1).

WES data analysis

Average sequencing coverage, estimated by QualiMap software [132], was 77X, and >96% of the captured area was covered by at least 6 independent reads (Appendix 4-1). A detailed description of variant calling as well as in-house developed scripts for variant filtration are online as a GitHub repository (github.com/tombergk/FVL_mod). In short, Burrows-Wheeler Aligner [131] was used to align reads to the *Mus Musculus* GRCm38 reference genome, Picard [158] to remove duplicates, and GATK [133] to call and filter the variants. Annovar software [134] was applied to annotate the variants using the Refseq database. All variants within our mouse cohort present in more than one rescue were declared non-ENU induced and therefore removed. Unique heterozygous variants with a minimum of 6X coverage were considered as potential ENU-induced mutations.

Mutation frequency estimations

All ENU-induced variants predicted to be potentially harmful within protein coding sequences including missense, nonsense, splice site altering SNVs, and out-of-frame insertions-deletions (INDELs), were totaled for every gene. The number of potentially damaging variants per gene was compared to a probability distribution of each gene being targeted by chance. Probability distributions were obtained by running 10 million random permutations using probabilities adjusted to the length of the protein coding region. A detailed pipeline for the permutation analysis is available online

(github.com/tombergk/FVL_mod). Genes that harbored more potentially damaging ENU-induced variants than expected by chance were considered as candidate modifier genes (at false discovery rate (FDR) ≤0.1 and ≤0.25). Statistical correction for multiple testing was applied as previously described [178].

Variant validation by Sanger sequencing

All primers were designed using Primer3 software [179] and purchased from Integrated DNA Technologies. PCR was performed using GoTaq Green PCR Master Mix (Promega), visualized on 2% agarose gel, and purified using QIAquick Gel Extraction Kit (Qiagen). Sanger sequencing of purified PCR products was performed by the University of Michigan Sequencing Core. All PCR primers (named: gene name+'_OF/OR') and internal sequencing primers (named: gene name+'_IF/IR') are listed in Appendix 4-2.

gRNA design and *in vitro* transcription

gRNA target sequences were designed with computational tools [180, 181] (http://www.broadinstitute.org/rnai/public/analysis-tools/sgrna-design or http://genome-engineering.org) and top predictions per each candidate gene were selected for functional testing (Appendix 4-3). sgRNA for *C6*, *Ces3b*, *Itgb6*, and *Sntg1* were *in vitro* synthesized (MAXIscript T7 Kit, Thermo Fisher) from double stranded DNA templates by GeneArt gene synthesis service (Thermo Fisher) while sgRNA for *Arl6ip5* was *in vitro* synthesized using Guide-it sgRNA In Vitro Transcription Kit (Clontech) (Appendix 4-3). The *Cpn1* sgRNA target was cloned into plasmid pX330-U6-Chimeric_BB-CBh-hSpCas9 (Addgene.org Plasmid #42230) [182]. The sgRNAs were purified prior to activity testing (MEGAclear Transcription Clean-Up Kit, Thermo Fisher). Both the Wash and Elution Solutions of the MEGAclear Kit were pre-filtered with 0.02 µm size exclusion membrane filters (Anotop syringe filters, Whatman) to remove particulates from zygote microinjection solutions, thus preventing microinjection needle blockages.

in vitro Cas9 DNA cleavage assay

Target DNA for the *in vitro* cleavage assay was PCR amplified from genomic DNA isolated from JM8.A3 C57BL/6N mouse embryonic stem (ES) cells [183] with candidate gene specific primers (Appendix 4-3). *In vitro* digestion of target DNA was carried out by complexes of synthetic sgRNA and S. pyogenes Cas9 Nuclease (New England BioLabs) according to manufacturer's recommendations. Agarose gel electrophoresis of the reaction products was used to identify sgRNA molecules that mediated template cleavage by Cas9 protein (Figure 4-1A). *Arl6ip5* was assayed separately, with one out of four tested sgRNAs successfully cleaving the PCR template (data not shown).

Cell culture DNA cleavage assay

Synthetic sgRNAs that targeted *Cpn1* were not identified by the *in vitro* Cas9 DNA cleavage assay (Figure 4-1B). As an alternative assay, sgRNA target sequences were subcloned into pX330-U6-Chimeric_BB-CBh-hSpCas9 and co-electroporated into JM8.A3 ES cells as previously described [184]. Briefly, 15 µg of a Cas9 plasmid and 5 µg of a PGK1-puro expression plasmid [185] were co-electroporated into 0.8 X10E7 ES cells. On days two and three after electroporation media containing 2 µg/ml puromycin were applied to the cells; then selection free media was applied for four days. Surviving ES cells were collected and genomic DNA was purified. The *Cpn1* region targeted by the sgRNA was PCR amplified and tested for the presence of indel formation with a T7 endonuclease I assay according to the manufacturer's directions (New England Biolabs).

Generation of CRISPR-Cas9 gene edited mice

CRISPR-Cas9 gene edited mice were generated in collaboration with the University of Michigan Transgenic Animal Model Core. *Arl6ip5* mutant mice: sgRNA targeting *Arl6ip5* was combined with Cas9 protein and microinjected into the male pronucleus of fertilized mouse eggs obtained by the mating of stud males carrying the $F5^{L/+}$ $Tfpi^{+/-}$ genotype on the C57BL/6J background with superovulated (C57BL/6 X SJL) F1 female mice (B6SJLF1/J, Jackson Laboratory stock #100012). Multigenic mutant mice: a premixed solution containing 2.5 ng/µl of each sgRNA for *Arl6ip5*, *C6*, *Ces3b*, *Itgb6*, *Sntg1*,

and 5 ng/µl of Cas9 mRNA (GeneArt CRISPR Nuclease mRNA, Thermo Fisher) was prepared in RNAse free microinjection buffer (10 mM Tris-Hcl, pH 7.4, 0.25 mM EDTA). The mixture also include 2.5 ng/µl of pX330-U6-Chimeric_BB-CBh-hSpCas9 plasmid containing guide C37G1 targeting *Cpn1* and a 2.5 ng/ul of pX330-U6-Chimeric_BB-CBh-hSpCas9 plasmid containing guide C37G2 targeting *Cpn1* (Appendix 4-3). The mixture of sgRNAs, Cas9 mRNA, and plasmids was microinjected into the male pronucleus of fertilized mouse eggs obtained from the mating of stud males carrying the $F5^{L/+}$ $Tfpi^{+/-}$ genotype on the C57BL/6J background with superovulated C57BL/6J female mice. Microinjected eggs were transferred to pseudopregnant B6DF1 female mice (Jackson Laboratory stock #100006). DNA extracted from tail biopsies was genotyped for the presence of gene editing.

Genotyping CRISPR alleles

Initially, gRNA targeted loci were tested using PCR and Sanger sequencing (primer sequences provided in Appendix 4-3). Small INDELs were deconvoluted from Sanger sequencing reads using TIDE software [186]. PCR products carrying small INDELs in 4 $F5^{L/+}$ $Tfpi^{+/-}$ mice were cloned using the Zero Blunt TOPO PCR Cloning Kit (Invitrogen) following the manufacturer's instructions. A minimum of 10 clones from each reaction were selected, expanded in 5 ml of LB broth (Invitrogen), purified using the QIAprep Spin Miniprep Kit (Qiagen), and submitted to Sanger sequencing. Large (>50 bp) deletions were genotyped using PCR reactions that resulted in two visibly distinct product sizes for the deletion and wildtype alleles. One large inversion event (134 bp) was genotyped using inversion specific forward primer. Expected product sizes and genotyping primers for each deletion and the inversion are listed in Table 4-1. All genotyping strategies were initially validated using Sanger sequencing.

RT-PCR

Liver tissue samples were collected in RNAlater (Ambion) from $Arl6ip5^{+/+}$ and $Arl6ip5^{+/-}$ mice. Total RNA was extracted using the RNeasy Mini Kit (Qiagen). Complementary DNA (cDNA) synthesis was performed using the SuperScript III One-Step RT-PCR (Invitrogen). An intron 1 spanning cDNA specific PCR product (RT-PCR primers

5'-3': CAGAGGAACATGGACGTGA, CACCAGCACCACAATGACTC) amplified from the liver mRNA of *Arl6ip5*$^{+/-}$ mice resulted in two expected product sizes (237 bp for the wildtype and 214 bp for the deletion allele). The intensities of the wildtype and deletion allele PCR bands from three *Arl6ip5*$^{+/-}$ mice were quantified and compared to each other using ImageJ software [165].

Statistical analysis

Kaplan-Meier survival curves and log-rank test to estimate significant differences in mouse survival were performed using the 'survival' package in R [187]. A paired two-tailed Student's t-test was applied to estimate differences in weights between rescue mice and their littermates. Chi-square tests were applied to estimate deviations from expected proportions in mouse crosses as well as recombination rates between the *Tfpi* and *Plcb4* loci. Benjamini and Hochberg FDR for ENU burden analysis, Student's t-tests, and chi-square tests were performed using the 'stats' package in R software [162]. Linkage Analysis was performed on the Mendel platform version 14.0 [128] and LOD scores ≥3.3 were considered genome-wide significant [129].

Results and discussion

F5$^{L/L}$ *Tfpi*$^{+/-}$ mice exhibit reduced survival and smaller size

A previously described (Chapter II) sensitized ENU mutagenesis was extended to screen for dominant suppressors of the perinatal lethal *F5*$^{L/L}$ *Tfpi*$^{+/-}$ genotype (Figure 4-2A). 2595 G1 offspring were generated from mutagenized C57BL/6J *F5*$^{L/L}$ males crossed to unmutagenized C57BL/6J *F5*$^{L/+}$ *Tfpi*$^{+/-}$ females, with a total of 70 viable *F5*$^{L/L}$ *Tfpi*$^{+/-}$ rescue progeny identified at weaning. Approximately 50% of the rescue mice died by 6 weeks of age, with slightly worse survival observed in females (p=0.033; Figure 4-2B). Females were also underrepresented compared to males during the initial genotyping (26 females compared to 44 males, p=0.031). In addition, *F5*$^{L/L}$ *Tfpi*$^{+/-}$ rescues were on average 25-30% smaller than their littermates at 2-3 weeks of age ($p=7x10^{-12}$; Figure 4-2C,D). The proportion of identified rescues among G1 offspring, their smaller weight

compared to littermates, and slightly worse survival for female vs male rescues, were all consistent with our previous report (Chapter II).

Rescue pedigrees exhibit reduced fertility and incomplete penetrance

The 35 G1 *F5*$^{L/L}$ *Tfpi*$^{+/-}$ mice alive at 6 weeks of age were mated to *F5*$^{L/L}$ mice to test the heritability of the survival phenotype. Fifteen of these 35 mice generated at least one litter and 13 (1 female, 12 males) produced ≥1 offspring with the *F5*$^{L/L}$ *Tfpi*$^{+/-}$ genotype (Table 4-2). Across all pedigrees, mice beyond G1 (≥G2) continued to exhibit reduced survival with more pronounced underrepresentation of females ($p=0.001$; Figure 4-2E), and an average ~27% lower body weight compared to littermates at the time of genotyping ($p=2x10^{-16}$; Figure 4-2F). In the previous screen (Chapter II), rescues were outcrossed to the 129S1/SvImJ strain to introduce genetic diversity required for subsequent mapping experiments. However, complex strain modifier gene interactions confounded this analysis and resulted in a large number of "phenocopies" (defined as viable rescues despite lacking the original rescue mutation). To minimize this problem in the current screen, rescue pedigrees were maintained exclusively on the C57BL/6J background. While half of the pedigrees (8/16) previously generated on the mixed 129S1/SvImJ-C57BL/6J background generated >45 rescue progeny per pedigree (Table 2-4 in Chapter II) all pedigrees on the pure C57BL/6J background in the current study yielded <30 rescue mice, with the majority of pedigrees generating ≤3 rescues (Table 4-2). Such poor breeding performance in comparison to the previous screen is likely explained by a general positive effect of mixing 129S1/SvImJ-C57BL/6J strain background either directly on rescue fertility (hybrid vigor) or indirectly by reducing the severity of the *F5*$^{L/L}$ phenotype. C57BL/6J and 129S1/SvImJ strains have been shown to exhibit significant differences in a number of hemostasis-related parameters including platelet count, TFPI and TF expression levels [188]. Variation in genes underlying such strain specific differences may have contributed as modifiers to the rescue pedigrees in Chapter II.

WES identifies 6771 ENU-induced variants in 107 rescues

In order to identify all/most exonic ENU mutations, a total of 107 G1 rescues (57 from the current ENU screen and an additional 50 rescues from the previous screen (Chapter II)) were subjected to WES (Appendix 4-1). From ~1.5 million initially called variants, 6735 SNVs and 36 INDELs within exonic regions were identified as potential ENU-induced mutations, using an in-house filtering pipeline (see Materials and methods). The most common exonic variants were nonsynonymous SNVs (47%), followed by mutations in 3' and 5' untranslated regions (31%) and synonymous SNVs (15%). The remaining variants (7%) were classified as splice site altering, stoploss, stopgain, or INDELs (Figure 4-3A). T/A -> C/G (47%), and T/A -> A/T (24%) SNVs were overrepresented, while C/G -> G/C (0.8%) changes were greatly underrepresented (Figure 4-3B), consistent with previously reported ENU studies [70, 84]. Since ENU is administered to the G0 father of G1 rescues, only female progeny are expected to carry induced mutations on the X chromosome, while males inherit their only X chromosome from the unmutagenized mother. Among the called variants, all chromosomes harbored a similar number of mutations in both sexes, with the exception of the X chromosome where females had a >35 fold increase in SNVs per mouse (Figure 4-3C). The average number of exonic ENU mutations for G1 rescues from the current and previous screens was ~65 SNV per mouse (Figure 4-3D), consistent with expected ENU mutation rates [72, 84]. These data suggest that most called variants are likely to be of ENU origin.

Linkage analysis with coding ENU variants fails to map suppressor loci

The three largest pedigrees (1, 6, and 13) were still poorly powered (29.6%, 21.7% and 39.4%, respectively) to identify the rescue variants by linkage analysis (Figures 4-4A, 4-5A, 4-6A). A total of 86 candidate ENU variants across the three pedigrees were validated by Sanger sequencing (Table 4-3). Sixty-nine variants present in G1 rescue but not in their parents (G0) were further genotyped in all other rescue progeny in respective pedigrees. As expected from the power estimations, none of the 19 ENU variants tested in pedigree 1 (Figure 4-4B), showed linkage with a LOD-score >1.25 (Figure 4-4C). Similarly, 26 and 24 variants analyzed in pedigrees 6 and 13, respectively (Figures 4-5B, 4-6B) also failed to demonstrate a LOD-score >1.5 (Figures

4-5C, 4-6C). Failure to map the causal loci in any of these pedigrees was likely due to the lack of genetic power for mapping. However, we cannot exclude a contribution from insufficient marker coverage. While WES has been successfully applied to identify causal ENU variants within inbred lines [113] and in mixed background lines [71, 100], ~3000 ENU variants identified by whole genome sequencing (WGS) provide a much denser and more even coverage of the entire genome and expectedly outperforms WES in mapping [104]. On the other hand, WGS requires sequencing multiple pedigree members [72], or pooled samples at high coverage [104] and may present the challenge of interpreting causality from many closely linked non-coding variants.

Six independent G1 rescues derived from the same G0 mating

142 G0 matings (1 ENU-treated G0 male crossed with 2 untreated females) produced a total of 70 rescues (Figure 4-2A) from a subset of 42 G0 matings, with a single rescue from 27 G0 matings, and 2-3 rescues from 14 G0 matings (Figure 4-7A). However, one G0 mating produced 6 rescues out of a total of 39 offspring ($p=2x10^{-5}$ compared to all G0 matings; p=0.02 compared to G0 matings with rescue offspring, Figure 4-7A). This observation suggests a potential shared 'rescue' variant rather than 6 independent rescue mutations in the same G0 founder. A similar observation was previously reported by Wansleeben and colleagues where 7 independent ENU pedigrees with an identical cardiac edema phenotype were mapped to the same genetic locus and hypothesized to share the underlying causal variant [175].

A *Plcb4* mutation co-segregates with the rescue phenotype in 3 G1 siblings and their rescue offspring

Our in-house pipeline for ENU-induced variant analysis (see Methods) filters out all variants shared between 2 or more G1 rescue mice based on the assumption that ENU-induced variants should be unique in each individual G1. However, rescue siblings could theoretically originate from the same mutagenized spermatogonial stem cell and share ~50% of their induced mutations [63]. Among 107 whole exome sequenced G1 mice, 38 were siblings (13 sib-pairs and 4 trios, Appendix 4-1). 190 heterozygous variants present in 2-3 mice (representing sibpairs or trios) out of 107 rescues were exam-

ined, with 15 found to be shared by siblings (Table 4-4). Of the 7 sibs/trios sharing an otherwise novel variant, none shared >10% of their identified variants – inconsistent with the expected 50% for progeny originating from the same ENU-treated stem cell.

However, three shared protein-altering variants (*Plcb4*^{R335Q}, *Pyhin1*^{G157T}, and *Fignl2*^{G82S}) were identified for the unusual G0 mating with 6 G1 rescues (Table 4-4). *Plcb4*^{R335Q} was detected as a *de novo* mutation in one of the G0 females (Figure 4-7B) and was present in 3 out of 6 G1 rescue siblings. *Plcb4* is located approximately 50 megabases upstream of the *Tfpi* locus on chromosome 2, with predicted recombination rate of ~14.1% (Figure 4-7C) [189, 190]. While non-rescue littermates exhibited the expected rate of recombination (14.9%) between the *Plcb4*^{R335} and *Tfpi* loci, all 32 rescue mice (3 G1s and their ≥G2 progeny) were non-recombinant and carried the *Plcb4*^{R335} variant. This co-segregation between the *Plcb4*^{R335} variant and the rescue phenotype is statistically significant (p=0.02; Figure 4-7C). *Plcb4*^{R335Q} lies within a highly conserved region of *Plcb4* (Figure 4-7D) and is predicted to be deleterious by Polyphen-2 [191]. The other identified non-ENU variants (*Pyhin1*^{G157T} and *Fignl2*^{G82S}) did not segregate with the rescue phenotype.

Although the estimated *de novo* mutation rate for inbred mice (~5.4 x 10^{-9} bp/generation) is ~100X lower than the ENU mutation rate [125], other *de novo* variants have coincidentally been identified in ENU screens (Chapter III) [173]. Mutations identified by DNA sequencing of offspring from ENU screen will not distinguish between an ENU-induced and *de novo* origin, though the former is generally assumed, given its much higher prevalence in the setting of a mutagenesis screen. *De novo* mutations originating in the G0 paternal or maternal lineages will be identified by analysis of parental genotypes, as was the case for the *Plcb4*^{R355Q} variant. However, this variant was originally removed from the candidate list by a filtering step based on the assumption that each ENU-induced mutation should be unique to a single G1 offspring. This filtering algorithm has been very efficient for removing false positive variants in our and previous screens [71]. However, our findings illustrate the risk for potential false negative results that this approach confers.

Mutation burden analysis identifies additional candidate thrombosis suppressor genes

WES data for 107 independent rescue mice were jointly analyzed to identify candidate genes that are enriched for potentially deleterious ENU-induced variants including missense, nonsense, frameshift, and splice site altering mutations (3481 variants in 2984 genes, Appendix 4-4). The majority of genes harbored only a single ENU-induced variant while in *Ttn*, the largest gene in the mouse genome, 15 SNVs were identified, with the rest of the genes harboring ≤5 ENU variants (Figure 4-3E). After adjusting for coding region size, the ENU-induced mutation burden was significantly greater than expected by chance for 3 genes (FDR<0.1, *Arl6ip5*, *Itgb6*, *C6*) and suggestive for 9 additional genes (FDR<0.25) (Figure 4-8). Sanger sequencing validated 36 of the 37 variants within these 12 candidate genes. Two additional, independent ENU-induced mutations were identified in *Plcb4.* After including the two $Plcb4^{R335Q}$ mutations removed by the original variant filtering (see above), this gene was also enriched for mutations (FDR<0.25). Similar concepts to the mutation burden analysis have been applied to identify genes underlying rare diseases caused by *de novo* loss-of-function variants in humans [108-111]. This approach enables the identification of multiple candidate genes in parallel and does not require the maintenance or survival of rescue mice for pedigree generation.

Testing candidate thrombosis modifiers by independent CRISPR-Cas9-generated alleles

In order to validate the top candidate thrombosis suppressor genes identified above, independent null alleles were generated with CRISPR-Cas9. First, $F5^{L/+}$ $Tfpi^{+/-}$ males and B6SJLF1/J females were mated to generate zygotes for microinjection with complexed *Arl6ip5* sgRNA and Cas9 protein. Out of 354 injected zygotes, 155 offspring were generated, with genotyping identifying one mouse mosaic for a 23 base pair deletion in exon 1 of *Arl6ip5* ($F5^{L/+}$ $Tfpi^{+/+}$ $Arl6ip5^{-}$, Figure 4-9). This frameshift mutation is expected to result in an early stop codon. RT-PCR from heterozygous mice showed decreased levels of mRNA from the deletion allele compared to the wildtype allele, consistent with nonsense-mediated decay (Figure 4-9D). Mice triply heterozygous for the

F5^{L}, *Tfpi*$^{-}$ and *Arl6ip5*$^{-}$ alleles were generated and crossed to *F5*$^{L/L}$ mice. Out of 123 progeny, 5 *F5*$^{L/L}$ *Tfpi*$^{+/-}$ mice were identified, 2 of which carried the *Arl6ip5* null allele (Figure 4-9E). The additional three *F5*$^{L/L}$ *Tfpi*$^{+/-}$ *Arl6ip5*$^{+/+}$ mice were viable, suggesting strain modifiers from the SJL background as the cause of their rescue. Therefore, the influence of the *Arl6ip5* null allele on *F5*$^{L/L}$ *Tfpi*$^{+/-}$ survival phenotype could not be assessed in this system.

To eliminate the potential confounding influence of the SJL strain, the CRISPR-Cas9 experiment was repeated using C57BL/6J egg donors, though these are known to be less efficient for transgenesis than eggs derived from B6SJLF1/J females [192]. In addition to reagents targeting *Arl6ip5*, we pooled guides against five additional candidate genes (*C6, Itgb6, Cpn1, Sntg1 and Ces3b;* Figure 4-8). From 294 microinjected zygotes, we obtained 39 progeny, 70% fewer than on the mixed background (155 with B6SJLF1/J, see above). Nevertheless, approximately 190 independent targeting events were observed across the 6 genes in 36 mice including small INDELs, single nucleotide changes, and several large (>50bp) deletions or inversions. Targeted alleles were either homozygous, heterozygous, or mosaic. While the number of editing events varied greatly for different sgRNAs (2.5-85%) the strategy to simultaneously target multiple genes [182] proved successful and cost-effective.

Preliminary validation data suggest increased number of rescues progeny for combined CRISPR-Cas9 alleles

From the 39 progeny of the CRISPR-Cas9 targeting experiment, 4 males with the *F5*$^{L/+}$ *Tfpi*$^{+/-}$ genotype in addition to multiple targeted alleles in *Itgb6, Cpn1, Sntg1, Ces3b,* and/or *Arl6ip5* (Figure 4-10) were directly crossed to untreated C57BL/6J *F5*$^{L/L}$ females. Out of 15 progeny, 2 viable *F5*$^{L/L}$ *Tfpi*$^{+/-}$ mice were identified at genotyping (46.2% of the expected *F5*$^{L/L}$ *Tfpi*$^{+/-}$ conceptuses), significantly more than the previously observed background survival rate (3.75%, p=0.0002). These 2 rescue mice each carried a different CRISPR-Cas9-induced mutation in the *Sntg1* gene (*Sntg1*-A or *Sntg1*-C; Figure 4-10) but were wildtype at the other 5 targeted loci.

In conclusion, we performed a dominant, sensitized ENU mutagenesis screen for

modifiers of thrombosis, identifying 70 viable rescues with the otherwise synthetic lethal *F5*$^{L/L}$ *Tfpi*$^{+/-}$ genotype. Reduced fertility on a pure C57BL/6J genetic background limited the generation of expanded pedigrees, complicating efforts to map the corresponding putative suppressor loci. However, application of a novel mutation burden test to WES data derived from a total of 107 rescue mice identified 12 novel thrombosis modifier candidate genes. Rescue mice carrying CRISPR-Cas9-induced alleles in *Sntg1* were identified at significantly higher frequency compared to background ($p=0.0002$) serving as preliminary validation for this approach.

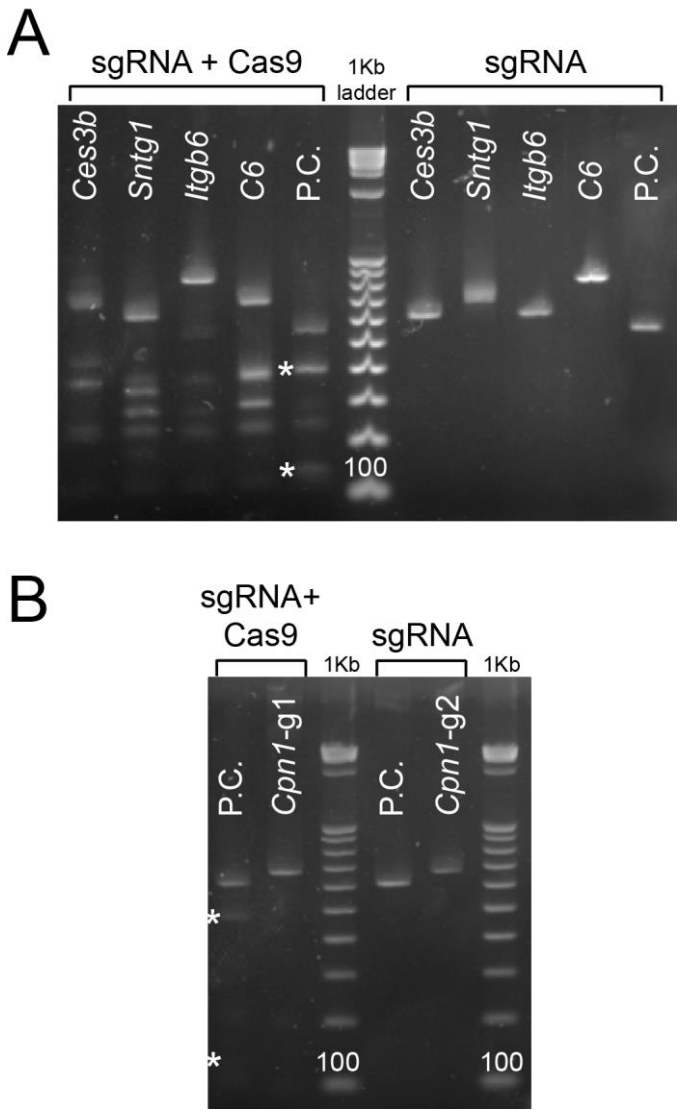

Figure 4-1: *In vitro* cleavage assay for sgRNAs
A) sgRNA+Cas9 targeting created double strand breaks in DNA templates obtained from genomic DNA by PCR. Expected sizes after sgRNA+Cas9 endonuclease activity: 430bp/240bp (*Ces3b*), 334bp/273bp (*Sntg1*), 530bp/275bp (*Itgb6*), and 383bp/296bp (*C6*). B) sgRNA+Cas9 complexes targeting *Cpn1* using two different guides (g1, g2) failed to created double strand breaks. Positive control (P.C.) was added to ensure Cas9 protein activity, with expected sizes after cleavage (390bp/140bp) indicated by white stars.

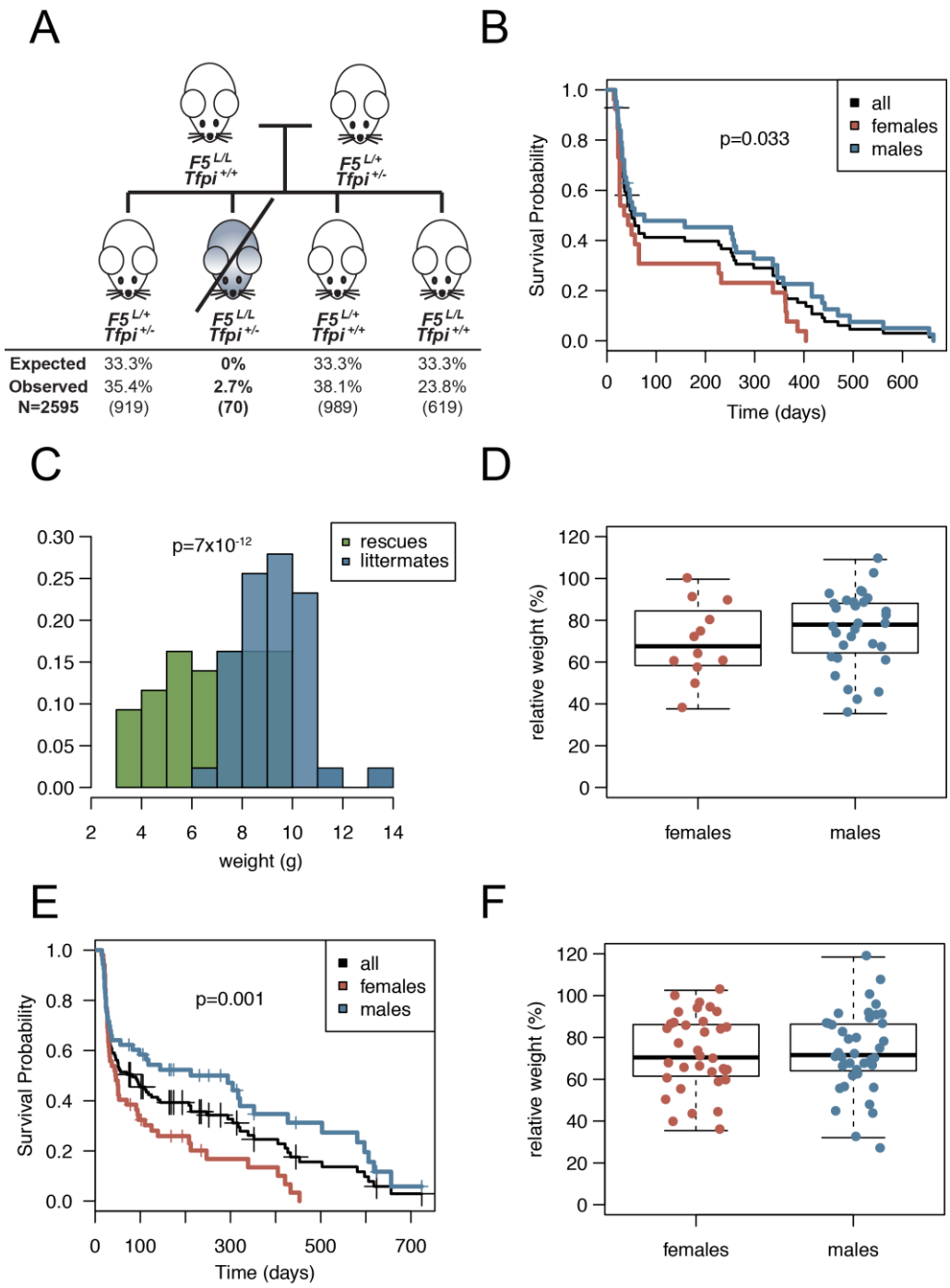

Figure 4-2: A sensitized ENU suppressor screen for thrombosis modifiers
A) The ENU screen strategy is depicted here, along with the total numbers of G1 offspring by genotype. B) Survival curves for G1 rescue mice. Survival for females is slightly reduced compared to males (p=0.033). C-D) Weight at genotyping (at 14-21 days) for G1 rescues compared to control littermates. E) Survival of rescue mice beyond G1 (≥G2) is also reduced, also with worse outcome in females (p=0.001). F) ≥G2 rescue offspring also exhibit reduced weights compared to their littermates at genotyping.

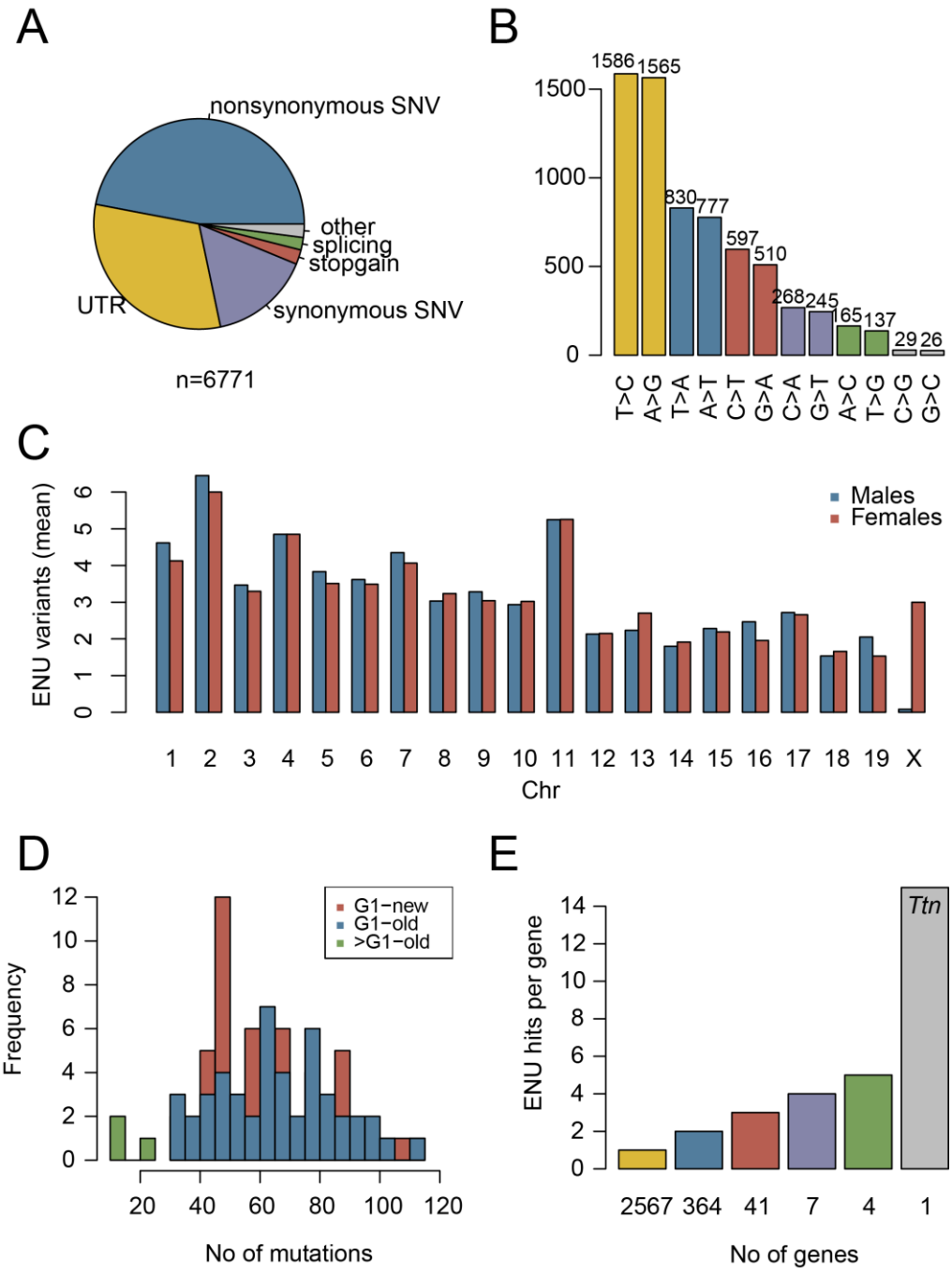

Figure 4-3: Distribution of ENU-induced mutations in WES data from 107 G1 rescues

A) Overview of mutation types for the 6771 observed ENU-induced exonic variants. B) Distribution of missense mutations by nucleotide substitution type. C) Distribution of ENU-variants by chromosome. D) The average number of exonic SNVs is ~65 for both the current (G1-new) and previous (G1-old) screens. E) Number of genes (x-axis) sorted by the number of protein-altering ENU-induced mutations observed per gene (y-axis). Most genes (2567) carry only 1 mutation. In contrast, the ~0.1 megabase coding region of *Ttn* carries a total of 15 independent ENU variants.

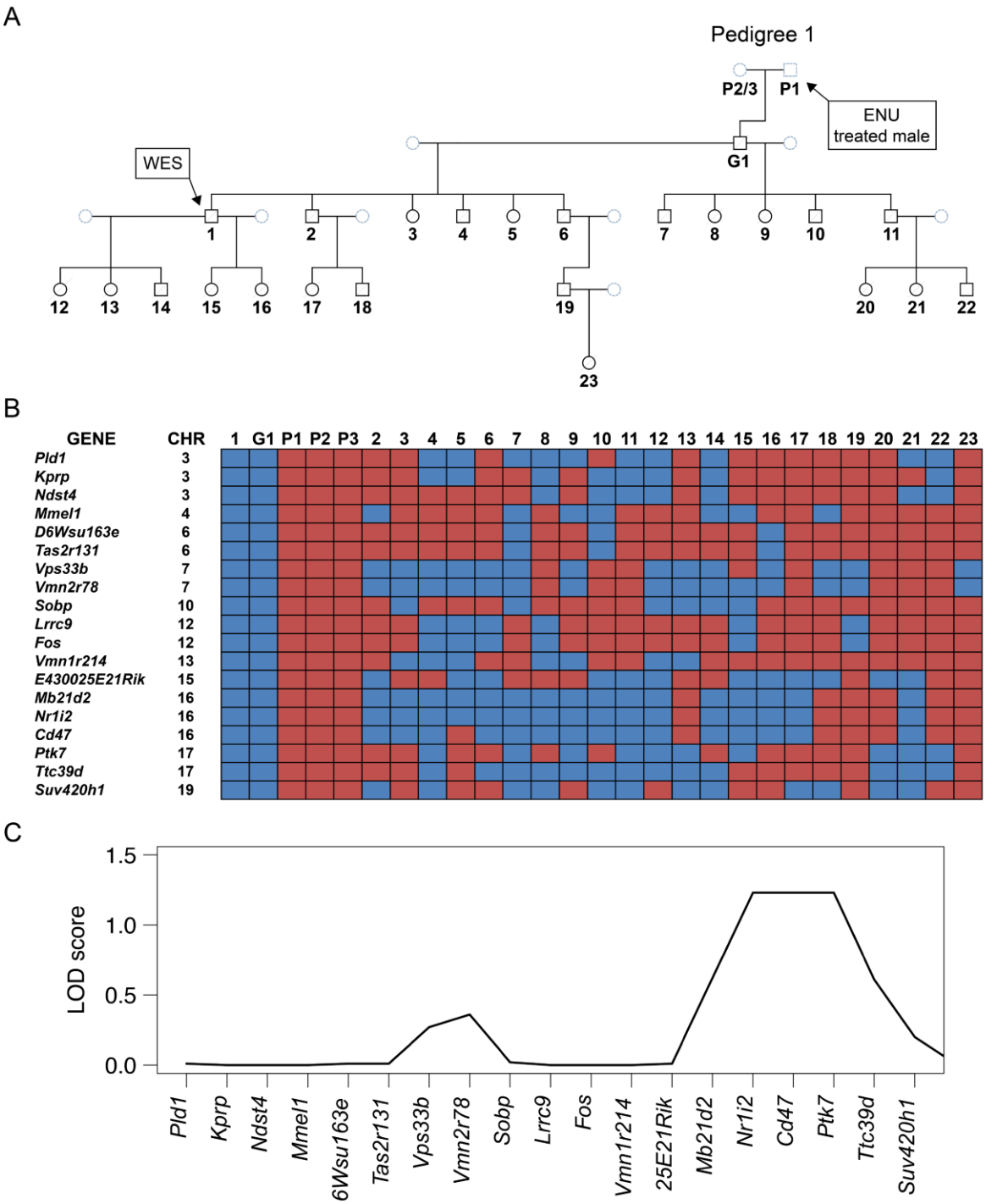

Figure 4-4: Genetic mapping of ENU-induced variants in pedigree 1
A) Overview of pedigree 1 (only rescue mice displayed). B) All coding ENU-induced mutations identified by WES were genotyped in all rescues from the pedigree by Sanger sequencing. Blue boxes indicate presence and red boxes indicate absence of the mutation. P1-P3 refers to 3 parental genotypes (G0 male and 2 untreated females). C) Linkage analysis using the ENU-induced variants from (B) as genetic markers.

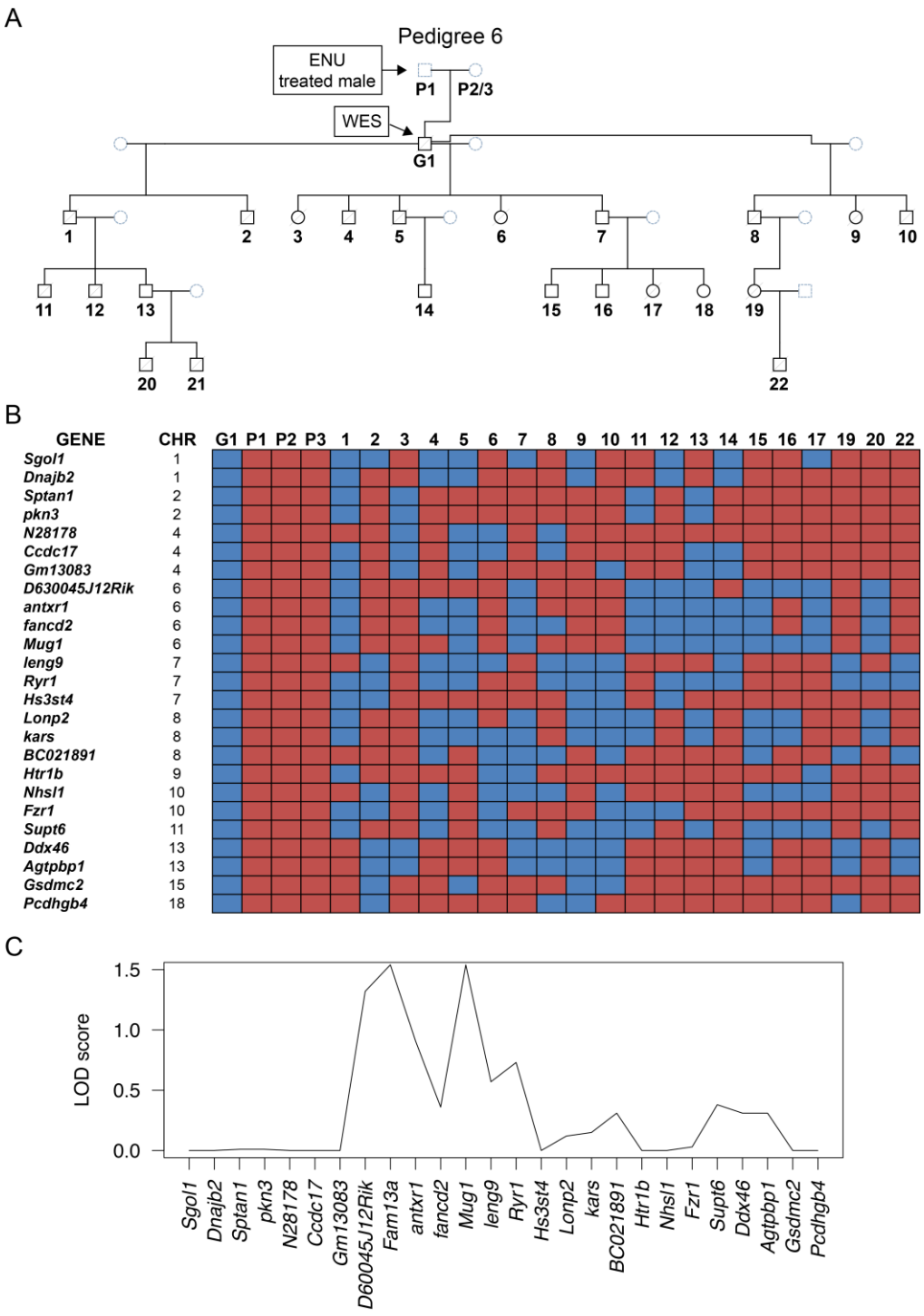

Figure 4-5: Genetic mapping of ENU-induced variants in pedigree 6
A) Overview of pedigree 6 (only rescue mice displayed). B) All coding ENU-induced mutations identified by WES were genotyped in most rescues from the pedigree by Sanger sequencing. Blue boxes indicate presence and red boxes indicate absence of the mutation. P1-P3 refers to 3 parental genotypes (G0 male and 2 untreated females). C) Linkage analysis using the ENU-induced variants from (B) as genetic markers.

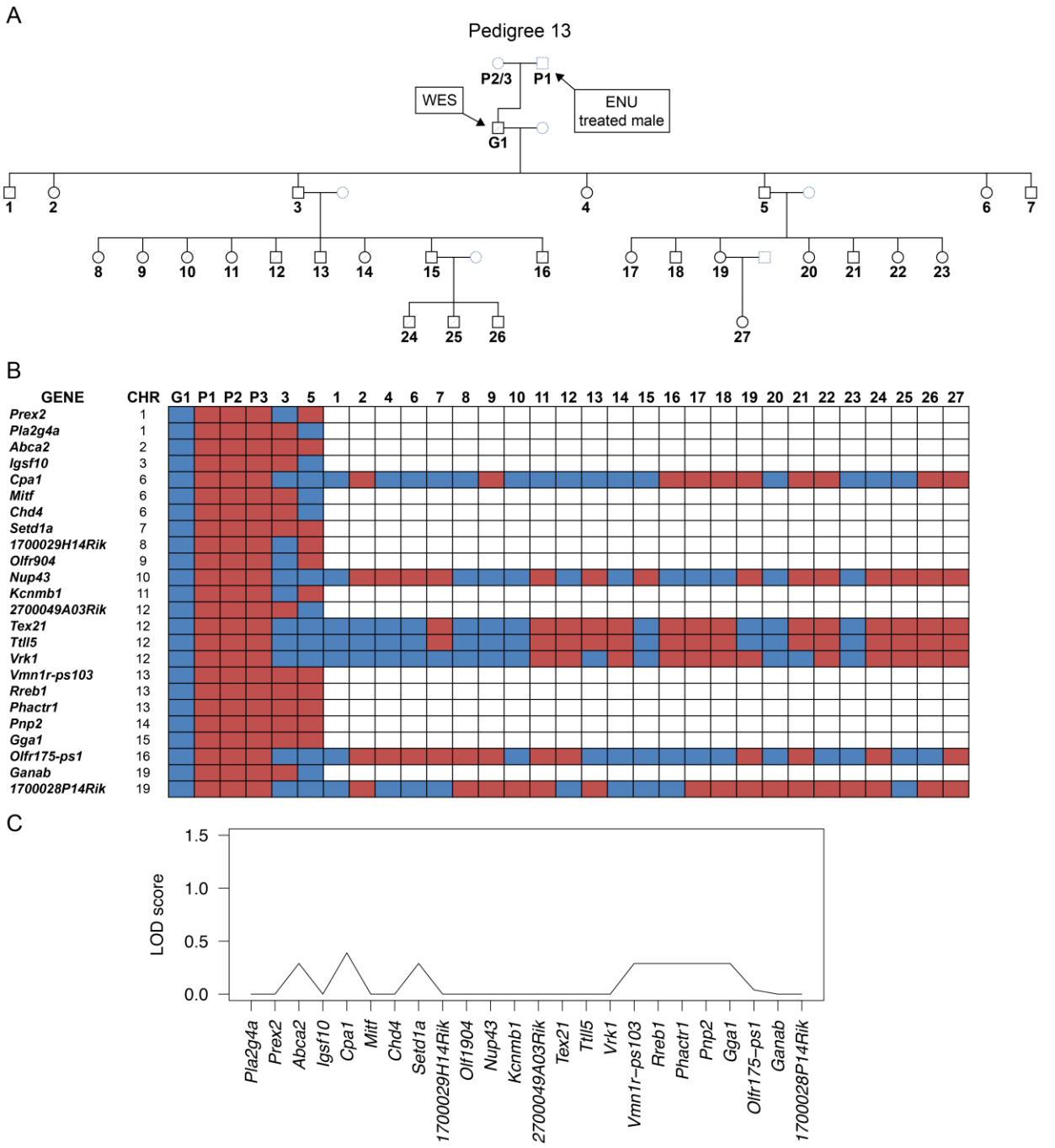

Figure 4-6: Genetic mapping of ENU-induced variants in pedigree 13
A) Overview of pedigree 13 (only rescue mice displayed). B) All coding ENU-induced mutations identified by WES were genotyped in all rescues from the pedigree if present in key mice 3 and 5 by Sanger sequencing. Blue boxes indicate presence and red boxes indicate absence of the mutation. P1-P3 refers to 3 parental genotypes (G0 male and 2 untreated females). C) Linkage analysis using the ENU-induced variants from (B) as genetic markers.

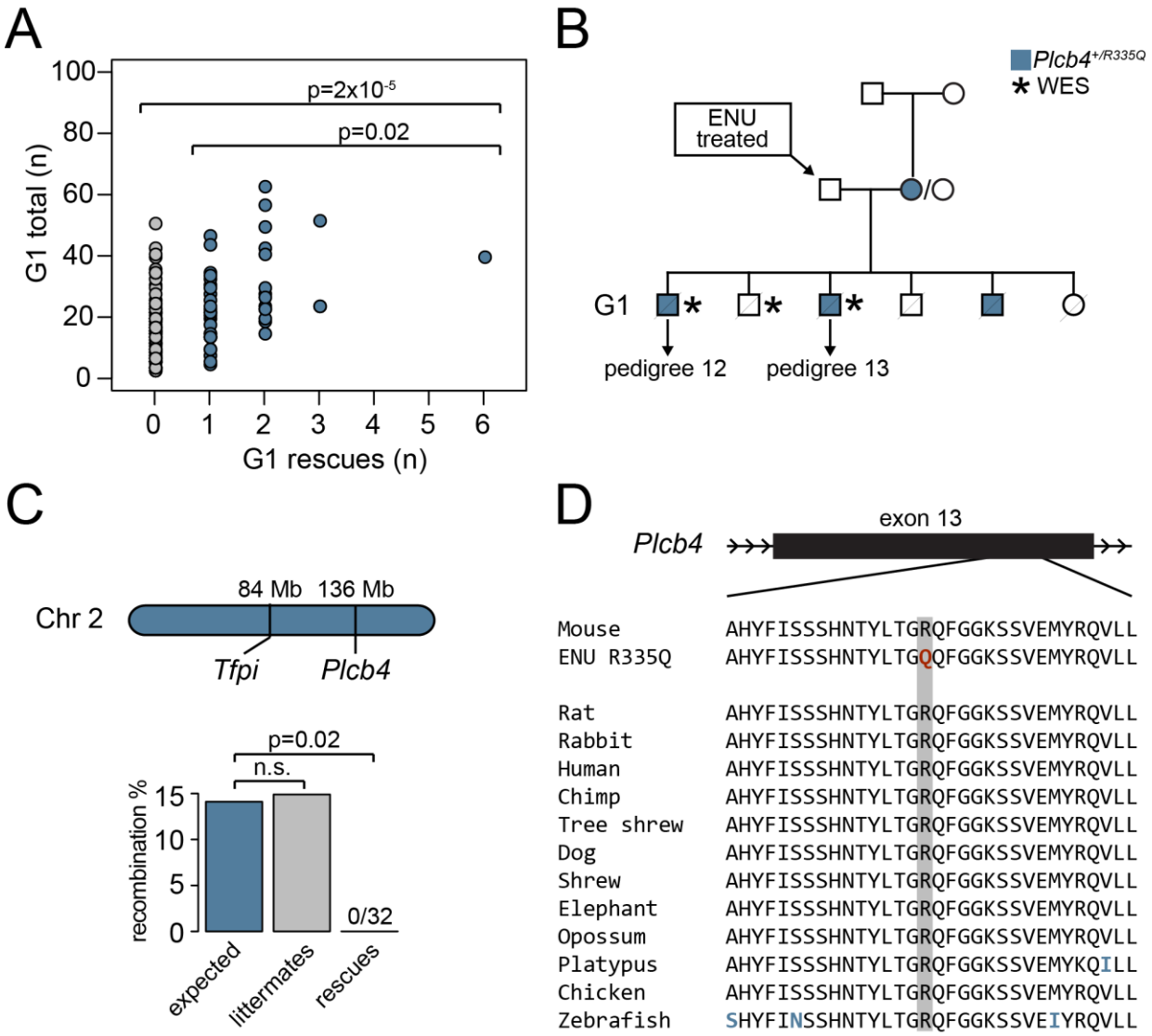

Figure 4-7: Segregation of the *Plcb4*^{R335Q} variant
A) The number of G1 rescues (x-axis) and the number of all progeny (y-axis) produced from each of the 142 G0 ENU matings is depicted here. Nearly all matings generated ≤2 G1 rescues, with 1 mating producing a significantly higher number of G1 rescue progeny (n=6) compared to all other ENU matings ($p=2x10^{-5}$). B) Partial pedigree of the ENU mating with 6 G1 rescues. Three G1 rescues inherited the *de novo* SNV (R335Q) in *Plcb4* gene from the G0 mother. Arrows highlight the founder G1 rescues of pedigrees 12 and 13. C) Top, relative locations of the *Plcb4* and *Tfpi* genes on chromosome 2, with predicted recombination rate is ~14%. Bottom, recombination rates observed among 32 rescues carrying the *Plcb4*^{R335Q} variant and their littermates (n=139). D) The *Plcb4*^{R335Q} mutation lies in a highly conserved region of exon 13.

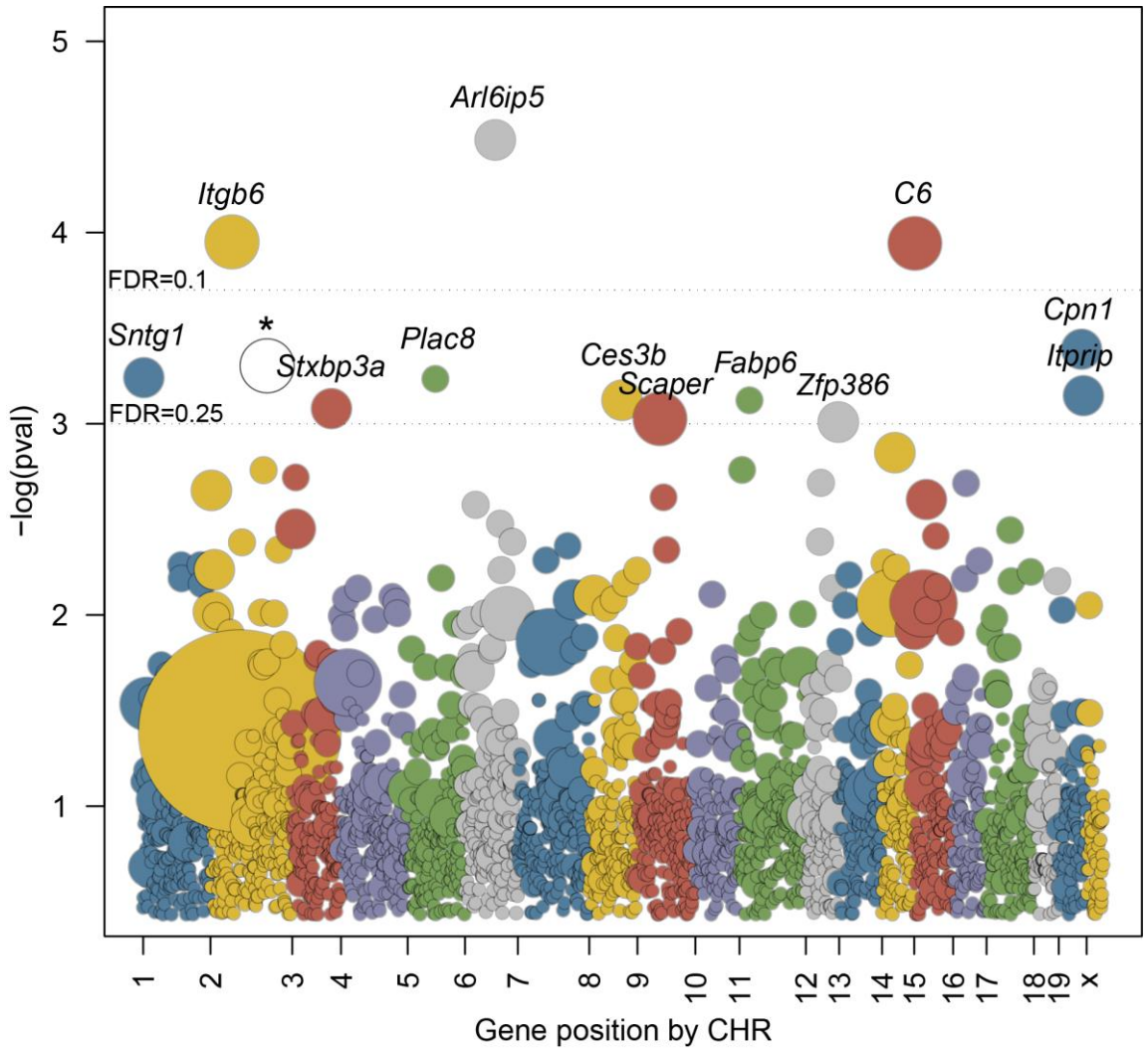

Figure 4-8: Mutation enrichment per gene in WES data from 107 G1 rescues
All genes with potentially deleterious ENU mutations are sorted by their chromosomal position of the x-axis, with the y-axis indicating the statistical significance (negative log of the p-value) of each gene's enrichment based on 10,000,000 permutations and normalized to coding region size. Each dot represents a gene and the diameter is proportional to the number of mutations observed. Dotted lines represent FDR values of 0.1 and 0.25. White dot highlighted with star represents the *Plcb4* gene after including the filtered non-ENU mutations.

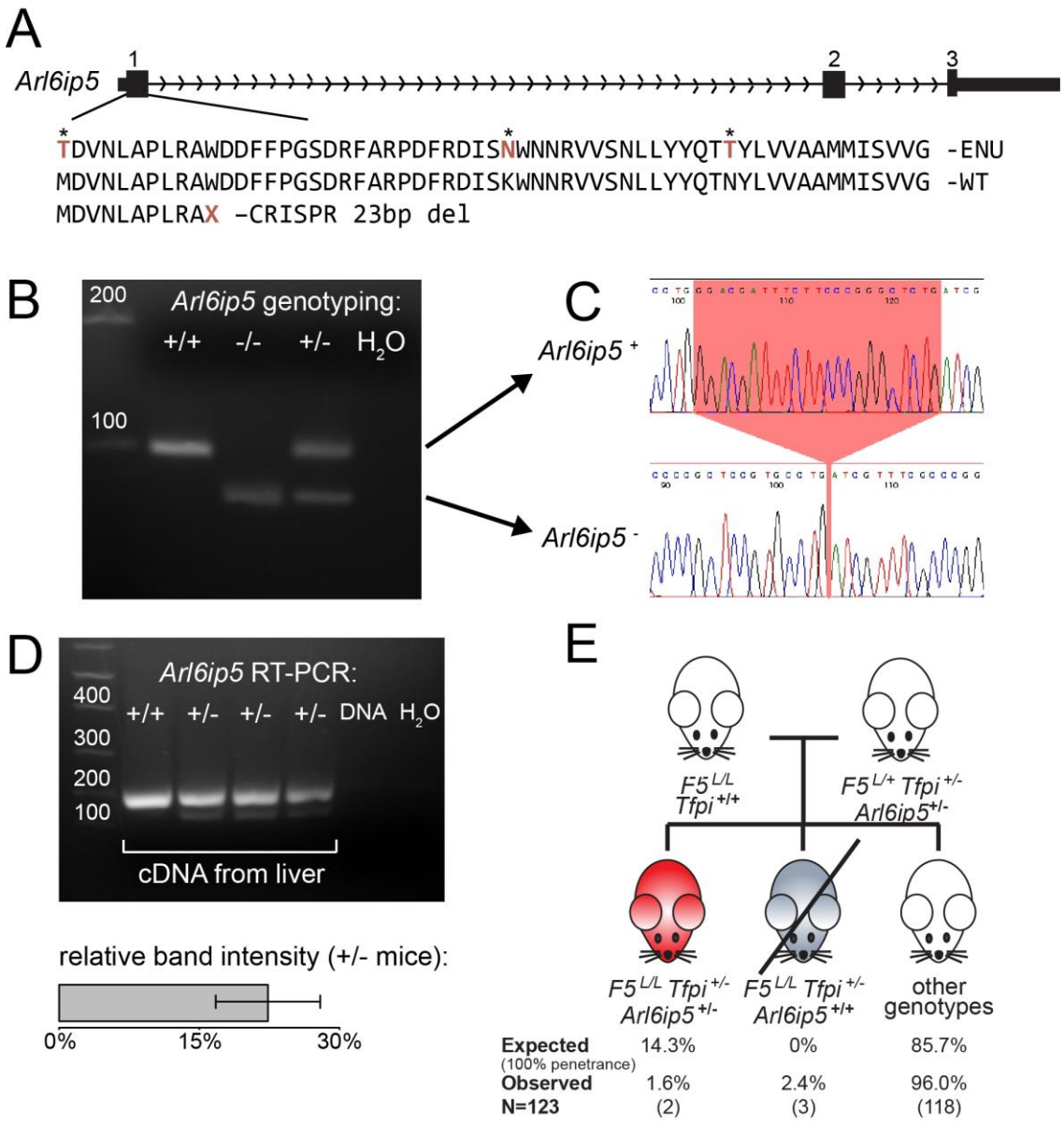

Figure 4-9: Validation of *Arl6ip5* as a thrombosis suppressor using CRISPR-Cas9-generated independent null allele

A) Schematic overview of the *Arl6ip5* protein sequence and the early stop codon introduced by the 23 bp frameshift deletion. Stars highlight the original three ENU-induced mutations. B) *Ar6ip5* genotyping assay and C) the Sanger sequence for the wildtype and deletion allele. D) Top, RT-PCR with intron spanning cDNA specific primers show two bands for the Arl6ip5$^{+/-}$ mice. The upper band represents the wildtype allele and the faint lower band represents the null allele. Bottom, the lower band intensity is ~20% that of the upper band, consistent with nonsense mediated decay. E) Among 123 progeny from the validation mating, 5 *F5$^{L/L}$ Tfpi$^{+/-}$* mice were genotyped, two of which were *Arl6ip5$^{+/-}$* and three of which were *Arl6ip5$^{+/+}$*.

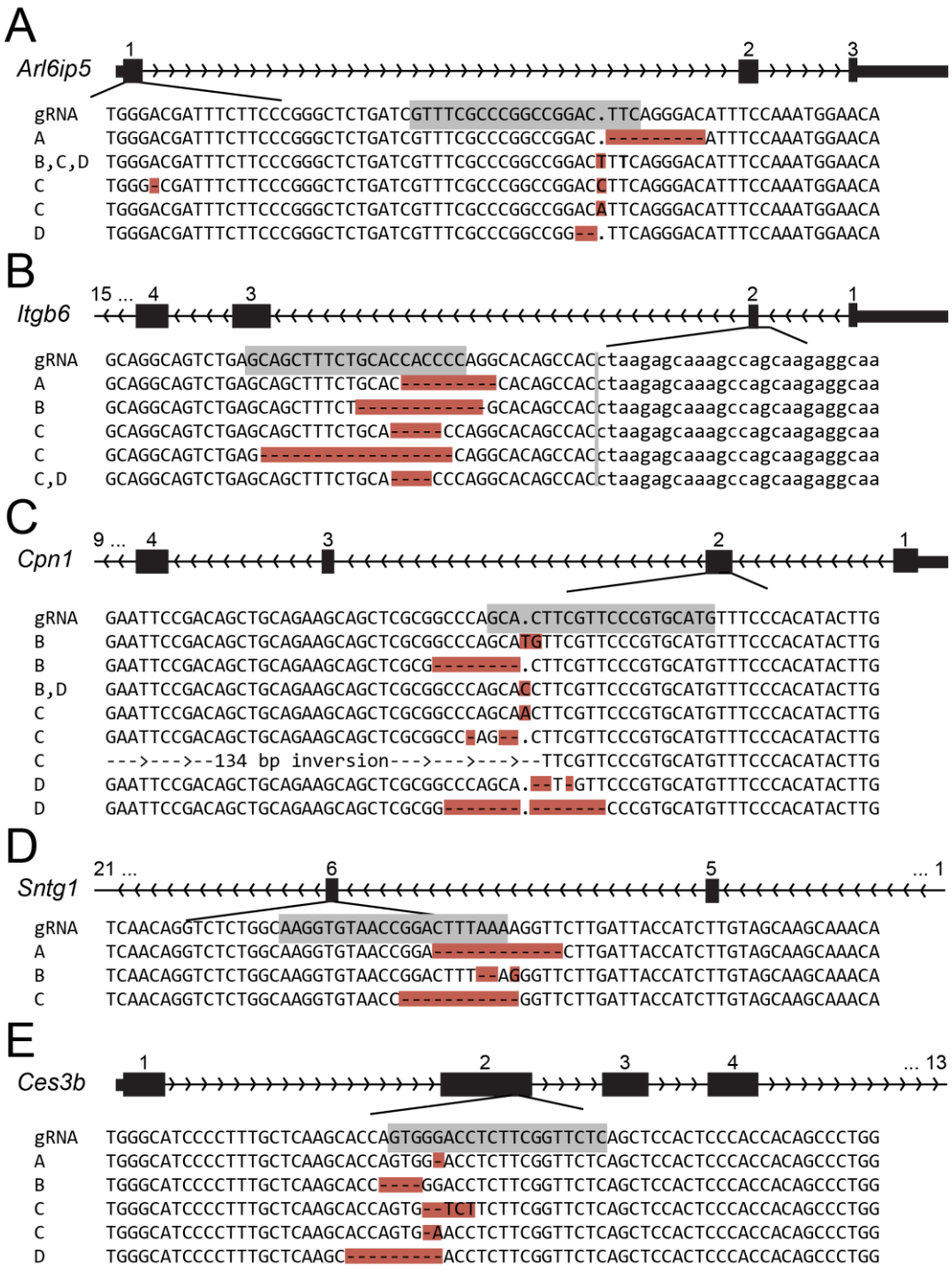

Figure 4-10: CRISPR-Cas9-induced INDELs in *F5*$^{L/+}$ *Tfpi*$^{+/-}$ mice used for rescue validation

The sequence of the gRNAs and the CRISPR-Cas9 induced mutations are shown for A) *Arl6ip5* B) *Itgb6* C) *Cpn1* D) *Sntg1* and E) *Ces3b*. All edited positions are highlighted in red, with dash referring to a deleted position. The letters A-D on the left of each allele refer to the 4 different *F5*$^{L/+}$ *Tfpi*$^{+/-}$ mice. Each mouse carries multiple mutations in different genes.

Table 4-1: CRISPR-Cas9 alleles

Gene	Allele name	Mutation type	Mutation length	Genotyping/Sequencing primers: Forward, Reverse (5'-3')	Expected PCR product sizes
Arl6ip5	del63	in frame deletion	63 bp	CAGAGGAACATGGACGTGAA GAAAGGGGACCTCAGAGAGC	371 bp 308 bp
	del151	frameshift deletion	151 bp	TTTAACCGCAGAACCAATCC GAAAGGGGACCTCAGAGAGC	469 bp 318 bp
Itgb6	del163	splice site deletion	163 bp	CATTCAACCGCACTGAGAGA AAATTAAGCGGCAGGTGTTG	446 bp 283 bp
	del11	frameshift deletion	11 bp	AATCCGACTTTGGTCCACTG GTGTTGTCCGGATAGCCACT	SS
C6	ins1	frameshift insertion	1 bp	GGGTTCTCAAGCTCCCTTCAA GGAGAAGTCAGTGGGGTTCAG	SS
	del3	in frame deletion	3 bp	GGGTTCTCAAGCTCCCTTCAA GGAGAAGTCAGTGGGGTTCAG	SS
Cpn1	del81	splice site deletion	81 bp	GTTCATGGAAGGCAGGATGT GTGGAATGGGGTGAGACAAG	296 bp 215 bp
	inv134	frameshift inversion	144 bp -12 bp (5') +2 bp (3')	GTTCATGGAAGGCAGGATGT ACATCCTGCCTTCCATGAAC GTGGAATGGGGTGAGACAAG	296 bp 226 bp
Sntg1	del11	frameshift deletion	11 bp	TACGACAGCCAGGACTCAGTA GGCGTGGAGACCAGATTTTC	SS
	del2	Frameshift deletion	2 bp	TACGACAGCCAGGACTCAGTA GGCGTGGAGACCAGATTTTC	SS
Ces3b	del14A	frameshift deletion	14 bp	ACAAATAGACGCTGGAGGAGC CCCTTGTAGCCCAGGGTATT	SS
	del14B	frameshift deletion	14 bp	ACAAATAGACGCTGGAGGAGC CCCTTGTAGCCCAGGGTATT	SS

SS=Sample is subjected to Sanger sequencing and analyzed using TIDE software [186]

Table 4-2: Overview of rescue pedigrees

Rescue pedigree	G1 rescue ID	Sex	Total # progeny	# Rescues	Penetrance
PED1	60654	M	208	23	33.2%
PED2	82147	M	34	2	17.7%
PED3	82723	M	91	2	6.6%
PED4	83071	F	50	2	12%
PED5	83217	M	4	1	76.9%
PED6	83457	M	188	22	35.1%
PED7	83737	M	18	3	50%
PED8	83796	M	19	3	47.6%
PED9	83882	M	4	1	76.9%
PED10	83875	M	39	8	61.5%
PED11	10382	M	25	3	36.1%
PED12	11241	M	32	5	46.9%
PED13	11954	M	107	27	75.8%

PED=pedigree; Penetrance is calculated as follows: #Rescues / (Total # of progeny - #Rescues) / 2

Table 4-3: Overview of candidate ENU-induced variants in pedigrees 1, 6, and 13

PED	Chr	Position	Ref	Alt	Type	Gene	Exon	AA change	Validation
PED 1	3	28048031	T	A	SG	*Pld1*	10	C310X	ENU
PED 1	3	92825401	A	G	NS	*Kprp*	2	V114A	ENU
PED 1	3	125561508	C	A	NS	*Ndst4*	3	T355K	ENU
PED 1	4	154887641	C	T	S	*Mmel1*	10	Y264Y	ENU
PED 1	6	126975169	T	C	NS	*D6Wsu163e*	14	V542A	ENU
PED 1	6	132957264	A	T	SG	*Tas2r131*	1	L194X	ENU
PED 1	7	80284342	C	A	NS	*Vps33b*	10	D253E	ENU
PED 1	7	86923065	A	T	NS	*Vmn2r78*	5	T545S	ENU
PED 1	10	43022236	A	C	NS	*Sobp*	6	M451R	ENU
PED 1	12	72481551	T	A	NS	*Lrrc9*	20	W876R	ENU
PED 1	12	85476338	T	A	NS	*Fos*	4	F341L	ENU
PED 1	13	23034506	A	T	NS	*Vmn1r214*	1	M57L	ENU
PED 1	15	59341976	T	C	NS	*E430025E21Rik*	21	D877G	ENU
PED 1	16	28827933	G	T	NS	*Mb21d2*	2	R430S	ENU
PED 1	16	38266025	A	G	NS	*Nr1i2*	2	I26T	ENU
PED 1	16	49896392	T	C	NS	*Cd47*	7	I262T	ENU
PED 1	17	46576613	G	A	NS	*Ptk7*	12	R592C	ENU
PED 1	17	80216552	T	A	S	*Ttc39d*	1	P213P	ENU
PED 1	19	3793072	T	C	S	*Suv420h1*	5	H56H	ENU
PED 1	14	12376664	C	T	NS	*Cadps*	28	D1283N	not ENU
PED 1	16	33885002	C	T	S	*Itgb5*	5	L221L	not ENU
PED 1	2	26439278	A	C	S	*Sec16a*	2	A908A	not in G1
PED 1	3	133084916	G	A	NS	*Gstcd*	2	T30M	not in G1
PED 1	7	39474173	C	T	NS	*Zfp939*	5	T550I	not in G1
PED 1	11	116539241	C	T	NS	*Ube2o*	18	A1224T	not in G1
PED 1	12	4865787	G	T	SG	*Mfsd2b*	12	Y408X	not in G1
PED 1	1	26687400	A	T	NS	*4931408C20Rik*	1	N9K	seq error
PED 1	1	171356715	G	C	NS	*Pfdn2*	3	D59H	seq error
PED 1	5	24326433	C	T	S	*Kcnh2*	6	V493V	seq error
PED 1	6	116042915	C	G	NS	*Tmcc1*	4	R485S	seq error
PED 1	10	79268510	T	A	NS	*Vmn2r81*	3	H322Q	seq error
PED 1	11	50603529	T	G	S	*Adamts2*	2	G143G	seq error
PED 1	14	78513605	G	A	S	*Akap11*	7	F447F	seq error
PED 6	1	58017826	T	C	S	*Sgol2*	7	S1056S	ENU
PED 6	1	75243553	A	G	NS	*Dnajb2*	8	T239A	ENU
PED 6	2	30008245	A	G	NS	*Sptan1*	30	S1326G	ENU
PED 6	2	30090396	T	C	S	*Pkn3*	21	V803V	ENU
PED 6	4	42939543	T	A	NS	*N28178*	10	I345N	ENU
PED 6	4	116599350	T	A	NS	*Ccdc17*	11	W439R	ENU
PED 6	4	143617300	T	C	NS	*Gm13083*	3	L390P	ENU
PED 6	6	38195359	A	G	NS	*D630045J12Rik*	2	S625P	ENU
PED 6	6	58935706	A	G	NS	*Fam13a*	18	V654A	ENU

PED 6	6	87282723	G	A	S	*Antxr1*	8	N200N	ENU
PED 6	6	113591215	A	G	S	*Fancd2*	42	E1363E	ENU
PED 6	6	121849860	A	G	NS	*Mug1*	6	K214R	ENU
PED 6	7	4149610	A	G	S	*Leng9*	1	C22C	ENU
PED 6	7	29109255	T	C	NS	*Ryr1*	13	E464G	ENU
PED 6	7	123983815	T	C	NS	*Hs3st4*	1	V212A	ENU
PED 6	8	86713501	A	G	NS	*Lonp2*	13	K710E	ENU
PED 6	8	112002558	A	G	S	*Kars*	5	Y172Y	ENU
PED 6	8	125941760	C	A	NS	*BC021891*	9	T695K	ENU
PED 6	9	81631894	A	G	NS	*Htr1b*	1	L220P	ENU
PED 6	10	18516089	T	A	NS	*Nhsl1*	5	V197E	ENU
PED 6	10	81370704	A	G	NS	*Fzr1*	5	L127P	ENU
PED 6	11	78212187	C	T	NS	*Supt6*	31	D1407N	ENU
PED 6	13	55652099	T	A	NS	*Ddx46*	7	V274E	ENU
PED 6	13	59536282	T	C	NS	*Agtpbp1*	3	T42A	ENU
PED 6	15	63825049	A	T	SG	*Gsdmc2*	14	Y424X	ENU
PED 6	18	37720736	A	T	NS	*Pcdhgb4*	1	L61F	ENU
PED 13	1	11140236	A	T	NS	*Prex2*	17	I588F	ENU
PED 13	1	149840641	A	G	NS	*Pla2g4a*	17	F698L	ENU
PED 13	2	25443328	T	C	NS	*Abca2*	30	V1655A	ENU
PED 13	3	59325883	T	A	NS	*Igsf10*	6	T1810S	ENU
PED 13	6	30641588	A	G	NS	*Cpa1*	5	K194E	ENU
PED 13	6	97993317	T	A	NS	*Mitf*	3	M166K	ENU
PED 13	6	125101969	T	A	NS	*Chd4*	7	I289N	ENU
PED 13	7	127788499	T	G	NS	*Setd1a*	12	D997E	ENU
PED 13	8	13562168	T	G	NS	*1700029H14Rik*	1	K61Q	ENU
PED 13	9	38464760	A	T	NS	*Olfr904*	1	T240S	ENU
PED 13	10	7678676	A	G	NS	*Nup43*	8	E341G	ENU
PED 13	11	33964797	G	A	NS	*Kcnmb1*	2	V33I	ENU
PED 13	12	71154824	C	T	NS	*2700049A03Rik*	8	R341C	ENU
PED 13	12	76204304	T	C	NS	*Tex21*	9	T453A	ENU
PED 13	12	85926893	T	C	NS	*Ttll5*	24	I805T	ENU
PED 13	12	106042885	T	G	NS	*Vrk1*	3	V70G	ENU
PED 13	13	22441416	T	C	NS	*Vmn1r-ps103*	1	Y49H	ENU
PED 13	13	37931499	A	C	NS	*Rreb1*	10	K945Q	ENU
PED 13	13	43057177	A	T	SP	*Phactr1*	6	NA	ENU
PED 13	14	50964318	T	C	NS	*Pnp2*	6	S254P	ENU
PED 13	15	78888476	C	A	NS	*Gga1*	9	T269K	ENU
PED 13	16	58824697	T	A	NS	*Olfr175-ps1*	2	D4V	ENU
PED 13	19	8912851	T	C	NS	*Ganab*	18	Y715H	ENU
PED 13	19	23616626	T	C	SP	*1700028P14Rik*	3	NA	ENU
PED 13	2	86046847	A	T	NS	*Olfr1034*	1	M122L	seq error
PED 13	9	44417150	A	T	NS	*Ccdc84*	3	M115K	seq error
PED 13	14	7549840	G	C	NS	*Gm3558*	6	L187V	seq error

PED=pedigree; NS=nonsynonymous; S=synonymous; SP=splicing; SG=stopgain

Table 4-4: Overview of WES variants present in 2 or 3 G1 rescues

#	G1-1	G1-2	G1-3	Chr	Pos	Ref	Alt	Type	Gene
3	118774	118780	NA	13	60800325	G	A	S	*Ctsll3*
3	118774	118780	NA	15	99624277	T	TTGG	NFSI	*Racgap1*
5	105078	118769	NA	13	67041404	ATCTT T	A	FSD	*Zfp712*
5	105078	118769	NA	13	67041411	G	GCCG AGAAA	FSI	*Zfp712*
5	105078	118769	NA	13	67041413	T	A	NS	*Zfp712*
7	105079	118776	NA	5	108502429	C	T	UTR	*Pcgf3*
7	105079	118777	NA	7	75752211	C	T	UTR	*Akap13*
7	105079	118777	NA	9	44849652	C	T	NS	*Kmt2a*
10	118761	118765	NA	7	62464404	C	T	UTR	*Peg12*
13	118789	118790	NA	1	71030121	A	C	UTR	*Bard1*
16	**118798**	**118802**	**FCH**	**1**	**173637462**	**G**	**T**	**NS**	***Pyhin1***
16	**118798**	**FCH**	**NA**	**2**	**135950362**	**G**	**A**	**NS**	***Plcb4***
16	118798	FCH	NA	9	65075750	C	A	S	*Dpp8*
16	**118798**	**118802**	**NA**	**15**	**101054156**	**C**	**T**	**NS**	***Fignl2***
17	118831	118832	NA	5	142173682	CA	C	FSD	*Sdk1*
	118789	118790	105081	1	173874425	C	CT	FSI	*Mndal*
	118761	118821	118766	3	152235750	TTG	T	UTR	*Fubp1*
	105079	118833	NA	4	148001086	T	A	NS	*Nppa*
	118789	105080	NA	5	33640643	TA	T	UTR	*Slbp*
	118831	118832	118836	6	18853853	T	G	UTR	*Naa38*
	105078	118782	NA	7	3717638	A	T	NS	*Pirb*
	118789	118808	NA	9	64708711	A	T	UTR	*Megf11*
	105079	105082	105085	11	93885765	C	G	UTR	*Utp18*
	118789	105079	NA	17	55799717	A	T	NS	*Emr4*
	118831	FCH	NA	19	8707650	C	T	UTR	*Slc3a2*
	105079	118806	NA	19	8736205	G	T	S	*Wdr74*
	118773	118774	118780	1	36424939	G	A	NS	*Lman2l*
	105076	118816	118771	1	42698791	TCGC	T	UTR	*Pou3f3*
	105076	105077	118782	1	66175367	C	T	UTR	*Map2*
	119158	105087	NA	1	74160515	GACAA	G	UTR	*Cxcr2*
	118792	118793	118832	1	89892184	GCGC A	G	UTR	*Agap1*
	118872	118819	NA	1	105813719	T	C	NS	*Tnfrsf11a*
	118792	105086	118774	1	106172068	TGGC	T	NFSD	*Phlpp1*
	105077	118786	NA	1	134994010	C	T	NS	*Lgr6*
	118766	118779	NA	1	139458389	G	A	S	*Aspm*
	105069	105073	118836	1	151344527	CGCG	C	UTR	*Ivns1abp*
	118805	118804	NA	1	171286664	G	GGGG C	FSI	*Usp21*
	105083	105088	NA	1	194815569	T	C	UTR	*Plxna2*
	118801	118831	NA	2	11690278	A	C	UTR	*Il2ra*
	118868	118826	NA	2	22971229	G	A	SG	*Abi1*
	119157	FCH	NA	2	25271399	C	A	UTR	*Ssna1*

	118858	118779	NA	2	28549061	G	A	NS	*Ralgds*
	105069	105072	NA	2	29991921	G	T	NS	*Sptan1*
	118792	118771	NA	2	59858718	T	C	NS	*Wdsub1*
	118803	118804	118807	2	62517699	G	A	S	*Fap*
	105070	105071	118803	2	65238415	G	C	NS	*Cobll1*
	118799	118800	118801	2	70574141	A	G	NS	*Gad1*
	118794	118796	NA	2	91555431	C	A	NS	*Ckap5*
	118794	118796	NA	2	91991212	C	T	NS	*Creb3l1*
	118858	118845	118851	2	118697652	G	A	UTR	*Pak6*
	105070	118805	118807	2	119321322	G	C	NC	*Gm14207*
	105070	118805	118807	2	119321324	G	C	NC	*Gm14207*
	118872	118816	118823	2	127080607	C	CCT	UTR	*Blvra*
	118805	118851	118781	2	130103303	TATTATA	T	UTR	*AU015228*
	105066	118875	NA	2	130397415	G	C	NS	*Cpxm1*
	105068	118875	118829	2	131083323	T	C	NS	*Siglec1*
	118805	118821	NA	2	132306308	C	T	UTR	*Cds2*
	105088	118812	118831	2	160906675	G	A	UTR	*Emilin3*
	118836	118838	NA	2	180058100	A	G	NS	*Ss18l1*
	118815	118830	NA	3	96155661	C	T	NS	*Otud7b*
	118847	118852	118853	4	41395315	T	A	NS	*Kif24*
	118791	118799	NA	4	88722309	T	C	UTR	*Klhl9*
	105065	105080	NA	4	109982772	TTGGG	T	UTR	*Dmrta2*
	119160	118847	NA	4	118160162	C	T	NS	*Kdm4a*
	105075	118825	NA	4	133338995	C	T	SP	*Wdtc1*
	118765	118826	NA	4	141003992	T	C	S	*Atp13a2*
	105084	105087	118776	4	146195792	C	T	S	*Zfp600*
	118826	118838	NA	4	154281898	C	T	NS	*Arhgef16*
	118781	118787	NA	5	5508078	G	A	S	*Cldn12*
	118771	118787	NA	5	27851909	C	T	UTR	*Htr5a*
	105086	118785	NA	5	36486732	T	C	UTR	*Ccdc96*
	118868	118851	NA	5	37336642	C	T	NS	*Evc*
	105085	118761	NA	5	53200293	T	C	NS	*Sel1l3*
	105082	118812	118826	5	90366149	GGCC	G	UTR	*Ankrd17*
	105082	118848	NA	5	93043898	A	G	NS	*Sowahb*
	119158	118798	FCH	5	97087608	G	A	S	*Bmp2k*
	119157	118831	NA	5	107830346	G	A	UTR	*Ube2d2b*
	118808	118813	118774	5	111387757	TTCC	T	UTR	*Pitpnb*
	105069	118765	118772	5	111387787	TTCC	T	UTR	*Pitpnb*
	105066	118819	NA	5	121853037	A	G	NS	*Fam109a*
	118815	118825	NA	5	123961301	C	T	NS	*Ccdc62*
	105070	105071	118804	5	135377864	C	T	UTR	*Pom121*
	105070	105071	118804	5	135377865	A	G	UTR	*Pom121*
	118855	118829	NA	5	138141436	C	CTTTCT	UTR	*Zfp113*
	118855	118845	NA	5	149624997	T	C	NS	*Hsph1*
	105066	118765	118832	6	24664944	AGCG	A	UTR	*Wasl*
	118820	118830	118831	6	24800820	G	A	UTR	*Spam1*

	105074	118762	119157	6	30129559	AT	A	UTR	*Nrf1*
	119158	118836	NA	6	78428475	G	GA	UTR	*Reg1*
	105084	118771	NA	6	82738394	A	G	S	*Hk2*
	105072	118765	NA	6	91950692	C	T	UTR	*4930590J08Rik*
	118790	105065	NA	6	116634875	GAAC	G	UTR	*Rassf4*
	118805	118807	NA	6	124845055	G	A	S	*Leprel2*
	118790	105072	NA	6	125339139	A	G	NS	*Scnn1a*
	105088	118812	NA	6	136708398	G	A	S	*Gucy2c*
	105068	118804	NA	7	5059580	C	T	NS	*Ccdc106*
	118875	118836	NA	7	16945553	G	A	NS	*Pnmal2*
	105083	FCH	NA	7	22691836	G	C	NS	*Gm8693*
	118764	118829	NA	7	25439439	C	T	NC	*4732471J01Rik*
	118845	118847	NA	7	27529549	A	T	NS	*Hipk4*
	118799	118761	NA	7	29705126	A	T	NS	*Catsperg2*
	118787	FCH	NA	7	30447942	C	T	UTR	*Kirrel2*
	118851	118775	118785	7	34133101	CCCG	C	UTR	*Wtip*
	118858	118845	NA	7	46245375	G	A	S	*Otog*
	105074	FCH	NA	7	47112788	T	C	UTR	*Ptpn5*
	118791	118825	NA	7	102268218	T	C	UTR	*Stim1*
	105076	105079	118780	7	114043054	G	GTA	UTR	*Spon1*
	118806	118829	NA	7	128252809	G	A	S	*Tgfb1i1*
	105073	118847	NA	8	13396751	C	T	NS	*Atp4b*
	118803	119157	NA	8	24950714	AC	A	UTR	*Adam9*
	118853	118765	NA	8	70072934	C	T	UTR	*Tm6sf2*
	105072	105078	118779	8	70596077	ATGTGTT	A	NFSD	*Isyna1*
	105068	118821	118824	8	70783517	C	T	NS	*Mast3*
	118791	118800	NA	8	119446196	T	G	UTR	*Osgin1*
	118858	118868	118872	9	22208225	A	AAAACC	NC	*1810064F22Rik*
	118847	118852	NA	9	27323340	C	T	S	*Igsf9b*
	118769	118833	NA	9	39258290	A	G	S	*Olfr945*
	118858	118830	NA	9	54734546	C	A	UTR	*Wdr61*
	105075	119157	NA	9	54764815	T	A	UTR	*Crabp1*
	105075	118832	NA	9	87221292	T	C	NS	*4922501C03Rik*
	118813	118814	118816	9	106880189	C	CG	UTR	*Vprbp*
	118813	118814	118816	9	106880191	CA	C	UTR	*Vprbp*
	118792	118831	NA	9	108489283	C	A	S	*Lamb2*
	118846	118872	NA	9	108961099	G	A	SP	*Col7a1*
	118858	118848	118851	10	34152583	ATCT	A	NFSD	*Dse*
	105087	118855	NA	10	40251193	C	T	S	*Gtf3c6*
	118821	118779	NA	10	76436466	G	A	S	*Pcnt*
	118851	118852	NA	10	78612011	G	T	NS	*Olfr1357*
	118847	118775	NA	10	80786000	C	T	S	*Dot1l*
	118792	118793	118802	10	81400280	C	T	UTR	*Nfic*
	118801	118824	NA	10	84725951	GAGC	G	UTR	*Polr3b*

	118792	118803	NA	10	89806205	G	A	S	*Uhrf1bp1l*
	105066	105088	118803	10	93527671	G	A	S	*Amdhd1*
	105087	118821	NA	10	111473269	CCCG	C	UTR	*Nap1l1*
	105088	118786	NA	10	128670959	T	C	NS	*Suox*
	118803	118808	NA	10	129754805	TA	T	FSD	*Olfr807*
	118803	118808	NA	10	129754808	G	T	NS	*Olfr807*
	118872	119157	118779	11	4094482	C	A	S	*Mtfp1*
	118847	118852	NA	11	50853988	A	G	NS	*Grm6*
	118796	118805	NA	11	59780560	A	G	UTR	*Mprip*
	118793	119159	NA	11	77719484	A	T	NS	*Cryba1*
	105080	118779	NA	11	78034535	C	T	NS	*Dhrs13*
	118796	118855	NA	11	82942399	A	G	NC	*Slfn5os*
	118824	118829	NA	11	83188993	C	T	NS	*Slfn4*
	118792	119160	NA	11	97700261	T	C	UTR	*Pcgf2*
	118790	118832	NA	11	102403687	A	T	NS	*Slc25a39*
	118813	118820	NA	11	119144127	TG	T	UTR	*Tbc1d16*
	105073	118762	NA	12	57364197	G	A	NS	*Mipol1*
	105084	118818	NA	12	84943390	C	A	UTR	*Arel1*
	105071	105088	NA	12	87773716	T	C	S	*Gm21319*
	105075	105077	118771	13	21722322	A	G	S	*Hist1h2bm*
	105077	118771	NA	13	21722331	T	G	S	*Hist1h2bm*
	105070	118776	NA	13	25209451	TAAAAC	T	UTR	*Dcdc2a*
	105071	118805	118808	13	30382122	C	CCCCCCCG	UTR	*Agtr1a*
	118799	118803	NA	13	48967821	A	G	NS	*Fam120a*
	105075	118821	NA	13	67365318	A	T	UTR	*Zfp456*
	105080	118777	118779	13	72630732	A	C	S	*Irx2*
	118847	118775	NA	13	74050127	G	T	NS	*Cep72*
	105087	118841	NA	13	100223394	T	C	NS	*Naip5*
	105087	118841	NA	13	100223424	T	C	NS	*Naip5*
	105087	118841	NA	13	100223443	A	G	S	*Naip5*
	105076	118825	NA	14	8225665	G	T	UTR	*Acox2*
	118778	118784	NA	14	18204378	G	T	UTR	*Nr1d2*
	105075	105083	118766	14	27403249	TCAAA	T	UTR	*Arhgef3*
	118799	118764	119157	14	50425002	CCAT	C	NFSD	*Olfr739*
	118790	118794	118766	14	55519400	C	A	UTR	*Nrl*
	118868	118825	NA	14	117978631	T	A	UTR	*Gpc6*
	118810	118762	118779	15	8444175	A	AAG	UTR	*Nipbl*
	105085	118780	NA	15	76173066	C	T	NS	*Plec*
	105070	118800	NA	15	76304239	G	A	SG	*Oplah*
	118805	118804	118820	15	92341925	G	A	UTR	*Cntn1*
	118845	118848	NA	16	32142967	A	T	UTR	*Nrros*
	118818	118784	NA	17	19811890	A	T	NS	*Vmn2r103*
	105071	118771	NA	17	21733940	C	T	UTR	*Zfp229*
	118851	FCH	NA	17	23359573	G	A	S	*Vmn2r115*
	118851	FCH	NA	17	23359602	T	C	NS	*Vmn2r115*
	119158	118791	119160	17	35172151	G	A	NS	*Aif1*
	105080	118764	NA	17	46752154	C	A	UTR	*Cnpy3*

	105077	119157	NA	17	74395668	G	A	NS	*Slc30a6*
	118791	118815	118830	18	15063301	TTCC	T	NFSD	*Kctd1*
	105072	118769	NA	18	45685164	A	G	NC	*A330093E 20Rik*
	118846	118833	NA	18	67289316	C	T	UTR	*Impa2*
	118819	118766	NA	18	84012957	C	A	UTR	*Tshz1*
	105070	118807	NA	19	32820156	T	TA	UTR	*Pten*
	118846	118847	NA	19	44550268	T	C	UTR	*Ndufb8*
	105072	105078	118762	19	55279482	GCCT GTTAC A	G	NFSD	*Acsl5*
	119157	118829	NA	X	73353972	C	A	SG	*Zfp275*
	118794	118816	NA	X	73458848	A	G	NS	*Haus7*
	118805	118806	NA	X	139236314	C	T	NS	*Mum1l1*
	119158	118791	NA	X	143861625	A	AG	UTR	*Dcx*

#=sibpair number (Appendix 4-1); NS=nonsynonymous; S=synonymous,;SP=splicing; SG=stopgain; UTR=untraslated region; NC=non-coding RNA exonic; FSD=frameshift deletion; FSI=frameshift insertion; NFSD=nonframeshift deletion; NFSI=nonframeshift insertion

Notes

This chapter is in preparation for submission under the title “ENU mutagenesis and whole exome sequencing to identify thrombosis modifier genes” by Kärt Tomberg, Randal J. Westrick, Emilee N. Kotnik, David Siemieniak, Guojing Zhu, Thomas L. Saunders, and David Ginsburg.

CHAPTER V: Conclusions and future perspectives

Limitations of traditional mapping strategies

Suppression of the perinatal lethality of the *F5*$^{L/L}$ *Tfpi*$^{+/-}$ genotype with haploinsufficiency or complete loss of *F8* (Chapter II) demonstrated the feasibility of our proposed sensitized ENU screen, and indeed a total of 168 viable *F5*$^{L/L}$ *Tfpi*$^{+/-}$ mice (henceforth 'rescues') were obtained from the ENU screens described in Chapter II and Chapter IV. A subset of these rescues could represent the previously described low background survival rate (3.75% of the expected *F5*$^{L/L}$ *Tfpi*$^{+/-}$ conceptuses) [47]. However, the observed number of rescues was higher in both screens (4.43% and 8.32% of the expected *F5*$^{L/L}$ *Tfpi*$^{+/-}$ conceptuses, p=0.22 and p=4x10^{-10}), suggesting that at least a subset of the rescues reflect the effect of authentic ENU-induced suppressor mutations.

Before the introduction of NGS, traditional mapping of the loci responsible for specific phenotype(s) relied on genetic markers based on differences between two inbred mouse strains. Our initial ENU mutagenesis was performed on the C57BL/6J genetic background, with the surviving G1 rescues outcrossed to 129S1/SvImJ strain to introduce genetic markers for mapping (Chapter II). 16 of the 98 rescues produced progeny with the *F5*$^{L/L}$ *Tfpi*$^{+/-}$ genotype, with 8/16 generating large pedigrees with >45 rescue progeny (Table 2-4). The size of these pedigrees should have provided sufficient power to map an ENU-induced variant co-segregating with the rescue phenotype to a specific genetic locus. With the exception of the *F3* locus for pedigree *MF5L6* (Chapter II), no significant linkage peaks were identified for any of the remaining pedigrees by this approach. We suspect that complex strain modifiers introduced by outcrossing to 129S1/SvImJ resulted in a high number of phenocopies obscuring mapping of the original ENU-induced suppressor mutations within these pedigrees. Consistent with this hypothesis, we observed suppression of the *F5*$^{L/L}$ *Tfpi*$^{+/-}$ phenotype by outcrossing to other strains (DBA/2J, A/J, BALB/cJ) in the absence of ENU. Our failure to identify one or

more significant linkage peaks within our mixed C57BL/6Jx129S1/SvImJ pedigrees (analyzed individually and jointly) suggests complex interactions among multiple strain-specific modifiers rather than a single modifier locus. Genetic background is known to influence multiple traits in mice, including engineered phenotypes such as ENU mutants [193, 194]. Such heterogeneous genetic background has previously confounded efforts to both map [175] and phenotype ENU-induced mutations [195]. However, the mixed strain background likely increased the mating efficiency in the ENU rescue pedigrees as pedigrees maintained on the pure C57BL/6J background exhibited significantly reduced fertility in comparison ($p=0.02$; Figure 5-1). This latter effect markedly limited our power to map the causal loci using ENU-induced variants in crosses maintained in C57BL/6J.

To exclude possible effects from linked variants and demonstrate causality for a mapped ENU-induced mutation that co-segregates with the lethal phenotype, a validation using an independent allele is desirable. In Chapter II we identified an ENU-induced variant in the *Actr2* gene (*Actr2*^{R258G}) that co-segregated with the rescue phenotype in one of the pedigrees. However, an independent loss-of-function allele failed to validate the rescue phenotype. Possible explanations include a linked unidentified variant (ENU, *de novo* or mixed strain variant) as the causal mutation or a unique gain-of-function resulting from the ENU-induced R258G variant in *Actr2*. We are currently exploring the latter possibility by generating an independent knock-in allele of *Actr2*^{R258G} using the CRISPR-Cas9 system [196]. A similar validation approach is also being applied to the *Plcb4*^{R335Q} variant identified in pedigree 13 (Chapter IV) with independent knock-in and knock-out alleles for the *Plcb4* gene.

Mutation burden approach in a dominant ENU screen

Recent advances in high throughput sequencing and genome editing, in addition to the limitations of pedigree-based mapping strategies discussed above, led us to test the mutation burden in 107 rescue mice by WES, as described in Chapter IV. The strengths of this approach include the potential to uncover all or most genes for which haploinsufficiency will rescue the sensitized phenotype. This approach does not require the phenotyped mice to survive past genotyping, be fertile, or produce pedigrees and

therefore can expand dominant ENU screening strategies to multiple phenotypes such as developmental abnormalities and sterility that could not be addressed with the traditional approach. Also, it substantially reduces the number of required mouse cages and experimental time.

However, the mutation burden analysis introduces certain limitations. Currently, this approach is restricted to protein coding variants, as our knowledge of the functional significance of non-coding/regulator variants is still limited. It is particularly difficult to assess the “harmfulness” of a non-coding variant as well as to assign that effect to a specific target gene or genes. Also, the majority of phenotype causing ENU variants have been mapped to coding regions [197]. In addition, only genes acting through a loss-of-function mechanism will be readily detected, as gain-of-function mutations are generally restricted to a single or small number of specific substitutions. To increase screening resolution from gene level to a single amino acid/nucleotide level would require much higher and currently unrealistic numbers of mice.

The power of the mutation burden analysis is directly associated with the number of mice screened. The more mice screened, the better the distinction between mutations accumulating within functionally important genes and the background mutations in all other genes. The estimated number of screened mice required for obtaining an ENU mutation in a particular gene is approximately proportional to the size of the coding region of that gene. Assuming the published ENU mutation rate of ~1.5 mutations per megabase (Mb, see Introduction for details), the largest gene in the mouse genome (*Ttn*, ~0.1 Mb coding region) should require screening of less than 10 mice on average to obtain one ENU-induced mutation. A medium size gene (~1200 bp coding region) requires screening ~500 mice, whereas *Sln* (93 bp coding region) would require analysis of more than 7,000 mice on average to be hit once by ENU. With analysis of approximately 20,000 mice, the entire coding genome should be saturated by multiple mutations, with an average of ~3 independent mutations in the smallest genes, and ~3000 mutations in *Ttn*.

Here, we screened approximately ~2,500 conceptuses carrying the lethal $F5^{L/L}$ $Tfpi^{+/-}$ genotype (total from screens in Chapter II and Chapter IV) and identified 3481 potentially harmful variants in 107 WES mice (~32.5 variants per mouse), which

corresponds to a mutation rate of 0.96 per Mb. Assuming this mutation rate, we on average targeted genes with a coding region of 1250 bp or larger (~10,000 genes) with at least three independent potentially harmful mutations, giving us power to theoretically test enrichment in ~48% of the genes in the mouse genome. However, this estimate is further limited by the fact that we did not have access to WES data from all 186 identified rescues. In addition, even if the mutation had suppressor potential in the screen, it could only act if the context of other mutations would facilitate it. For example, if the suppressor variant was co-induced with another harmful variant in an essential developmental gene, the latter would define the phenotypic outcome. The lack of coverage for smaller genes might explain why we did not achieve significant enrichment for mutations in the *F3* gene (882 bp coding region) identified as a modifier gene in Chapter II. The enrichment for mutations in *F8*, shown in Chapter II to suppress the lethality of $F5^{L/L}$ $Tfpi^{+/-}$, was further limited by its location on the X chromosome, and thus only female offspring will inherit ENU-induced mutations from the mutagenized G0 male. Of note, the number of exomes examined in the current screen does not provide sufficient power to exclude any genes as modifiers based on significant underrepresentation within the data set.

Identification of 12 potential candidate genes from a screen with ~25% genome coverage (rough estimation taking into account the above mentioned limitations), suggest the presence of ~30-40 additional modifier genes that could be captured with genome wide coverage. The number of modifier genes could be much larger when also considering genes with moderate penetrance, requiring even higher coverage for identification. While still preliminary, the CRISPR-Cas9 validation experiments suggests that this sensitized forward screen coupled with the burden analysis approach has enabled us to identify previously unknown modifiers of thrombosis.

Variation in these genes in humans could explain a significant portion of the incomplete penetrance and variable expressivity among patients with FVL, offer new insights into the overall regulation of hemostasis, and facilitate the development of future novel therapeutic interventions.

Future perspectives for current screen

Independent alleles for 6 candidate genes

Out of 39 progeny from the CRISPR-Cas9 targeting experiment (Chapter IV), 36 mice carried one or more targeted alleles in *Itgb6, Cpn1, Sntg1, Ces3b, C6,* and *Arl6ip5* (Figure 5-2). Two different alleles per each gene were maintained for further analysis (Figure 5-3; Table 4-1). Currently, most of these alleles co-exist with other CRISPR-Cas9 induced mutations in these mice and one or more outcrosses will be required to isolate each of the alleles. Once isolated, each allele will be tested for rescue of $F5^{L/L}$ $Tfpi^{+/-}$ lethality to validate the corresponding gene as an authentic suppressor.

All validated genes will be further subjected to functional studies. While the particular experiments will vary depending on existing information about each candidate protein's function and expression pattern, initial characterization of these CRISPR-Cas9-edited alleles will be similar to experiments described for the *Nbeal2* allele in Chapter III. We will assess the predicted effect of the deletion at both mRNA and protein levels in relevant tissues for mice heterozygous and homozygous for the deletion. Additionally, mice will be observed for deviations from Mendelian segregation and gross phenotype changes. Complete blood counts and other assays (e.g. blood clotting times) will be applied to evaluate the thrombotic state of these mice. The ultimate goal will be to understand how the candidate gene interacts with the coagulation system and affects thrombosis.

Investigating overlap with human VTE studies

The coagulation cascade is well conserved between humans and mice and the latter have served as a useful model to study VTE [198]. None of the candidate genes identified in Chapter IV have been previously reported to associate with significant signals in previous human VTE GWAS. Similar to other complex traits, the underlying genetic variants contributing to VTE range from rare alleles with large effects such as loss-of-function alleles in antithrombin III [15] to common variants with only moderate associated risk like non-O bloodtype (OR≈1.5) [199]. Common risk alleles for VTE have been identified by multiple GWAS efforts combined in a recent meta-analysis [26]. While

overlap in genes harboring rare and common variants is theoretically possible, no common risk alleles have been identified for a number of known genes that segregate with familial VTE such as *SERPINC1*, *PROS* and *PROC* (encoding antithrombin III, protein S, and protein C, respectively; see Introduction for details). Although ENU-induced rescue variants in our screen have a large effect on the sensitized mouse phenotype, we explored potential overlap between the candidate genes and common risk alleles identified by GWAS. We obtained the p-values for all available variants within the candidate genes' human orthologous loci ±1Mb from the INVENT consortium that published the largest VTE meta-analysis [26]. As expected none of the single nucleotide polymorphisms (SNP) in those regions reached genome-wide significance. However, the lead SNP (rs72812220) at the *Fabp6* gene locus had a suggestive p-value of 1.28×10^{-6} (Figure 5-4).

Overlap of the identified candidates and rare alleles with large effects in VTE patient populations would be theoretically more interesting and relevant given the lack of an obvious signal in GWAS. Unfortunately, WES/WGS has not been applied to a large VTE patient cohort to date but targeted sequencing of a few candidate genes has shown an enrichment of rare alleles in VTE patients [200]. Our lab is currently analyzing WES from ~400 VTE patients and ~7,000 controls, which should provide a powerful data set to compare with our mouse data.

The six candidate genes identified in Chapter IV (*Arl6ip5, Itgb6, C6, Cpn1, Sntg1,* and *Ces3b*) have been reported to exhibit a wide range of functions in diverse tissues and may identify multiple biological pathways that influence overall hemostatic balance. C6 is a component of the complement system and has been linked to endothelial cell activation and thrombosis. Mice deficient in C3, C5, or C6 were reported to be resistant to thrombosis induced by antiphospholipid antibodies [201]. *Cpn1* encodes the active subunit of Carboxypeptidase N (CPN), which has been shown to reduce fibrinolysis by decreasing cellular plasminogen binding [202, 203]. Haploinsufficiency for CPN could increase fibrinolysis leading to enhanced dissolution of $F5^{L/L}$ $Tfpi^{+/-}$ associated thrombi. *Itgb6* encodes the beta subunit of integrin αVβ6. While a number of other integrins (e.g. α1β1, α2β6, αIIbβ3) have been shown to play important roles in platelet adhesion and aggregation, αVβ6 has been primarily associated with enhanced fibrosis [204]. *Arl6ip5*

is a negative regulator of intracellular protein trafficking from the endoplasmic reticulum (ER) [205]. Although, not yet associated with known hemostatic proteins, *Arl6ip5* could influence the transport of key coagulation proteins, since the majority are either secreted or cell surface bound. For example, combined deficiencies of coagulation factors V and VIII result from a defect in an ER-Golgi transport system [206]. Less is known about *Ces3b, Sntg1,* and *Plcb4* and their potential role in thrombosis. *Ces3b* is a member of a large family of carboxylesterases but its function has not been investigated while *Sntg1* is only known to encode a brain specific protein [207]. *Plcb4* encodes phospholipase C, beta 4 and has been recently associated with auriculocondylar syndrome [208].

Opportunities beyond the current screen

Alternative thrombosis mutagenesis screening strategies

There are many other possible ways to set up a mutagenesis screen for a thrombotic phenotype in mice. While a non-sensitized dominant ENU mutagenesis screen (reviewed in Introduction) for thrombosis would be more direct, with all G1 progeny being informative, there are two major challenges with this approach. First, an effective screen requires an assay that would serve as a proxy for the phenotype of interest while feasible to be tested in hundreds to thousands of animals. Directly screening of mice for a rare thrombotic event somewhere in their vasculature is unfeasible. An alternative would be measurement of various thrombosis biomarkers in plasma, such as D-dimer. In addition, there is a possibility of not identifying any dominant ENU-induced mutations that cause thrombosis without provocation. An early ENU screen by Bode *et al* for hyperphenylalaninemia [78] failed to identify a causative dominant mutation in 7000 screened mice, illustrating this potential risk (reviewed in Introduction). In line with this concern, mice haploinsufficient for known autosomal dominant VTE risk factors such as antithrombin III and protein C are phenotypically normal without a thrombogenic stimulus [209, 210].

A non-sensitized recessive screen (reviewed in Introduction) is more likely to reveal a phenotype based on the observation that most Mendelian disorders have a re-

cessive rather than a dominant mode of inheritance. Recessive screens require a more elaborate mating scheme and much larger number of animals and have therefore been mainly executed by large centers where mouse mutants are screened for hundreds of phenotypes in parallel [83]. Phenotypes related to thrombosis, including the above-mentioned D-dimer test and others, were measured as part of a recessive screen by the Jackson Laboratory Center for Mouse Heart, Lung, Blood, and Sleep Disorders [211]. However, the MGI database (informatixs.jax.org), lists only one mouse (hlb258) from that screen with a coagulation abnormality (in fibrinogen levels). While there are multiple explanations for why only one mouse was identified, the assay and the age of phenotyping play an important role. For example, complete depletion of antithrombin III [209] results in embryonic or perinatal lethality. Of course, hypomorphic alleles often present with a milder phenotype and therefore might be detected.

A screen sensitized for lethal thrombosis addresses a number of the above challenges. First, survival is a straightforward phenotype that only required genotyping of the G1 mice. Second, a sensitized background may be necessary to unmask the effect of haploinsufficient protein levels that without the background would not display a phenotype. There are many alternative lethal thrombosis models that could be used for a sensitized screen. For example, *Tfpi*$^{-/-}$ mice die around embryonic day 10.5 [92], which theoretically makes the screening for survival already possible at birth and also might screen for genes influencing a different aspect of the coagulation system. Genetic suppression of TFPI lethality has been previously described and demonstrates the feasibility of such a screen. For example, *Tfpi*$^{-/-}$ *Par4*$^{-/-}$ mice survive to adulthood [212], while partial rescue (until birth) is observed for mice additionally haploinsufficient or completely deficient for factor VII [213]. Mice exhibiting very low levels of tissue factor also partially rescue *Tfpi*$^{-/-}$ lethality [214]. In addition, low tissue factor levels also prolong embryonic survival by ~2 days for antithrombin III null mice [209] while factor XI deficiency has been shown to rescue protein C deficiency [215].

Alternative mutagenesis strategies

While ENU has proven to be a valuable mutagen in mouse screens, it has a number of limitations. First, the requirement for three generations of mice to test for

complete deficiency of a screened gene limits the utility of recessive screens. Also, while ENU-induced point mutations may occasionally reveal interesting gain-of-function variants and hypomorphic phenotypes, typically ~30% of coding ENU variants result in loss-of-function alleles and the majority of the coding ENU-variants (>60%) will have no functional consequence (Introduction).

The emergence of CRISPR-Cas9 may enable new screening approaches. CRISPR-Cas9 can efficiently generate null (homozygotes and compound heterozygotes) and heterozygote, as well as mosaic animals. The diversity in events induced by CRISPR-Cas9 is potentially larger. In our CRISPR-Cas9 data, we have observed INDELs, SNVs, large deletions as well as inversions, with a higher proportion of coding mutations predicted to be harmful compared to ENU. CRISPRs could be designed to target the complete genome or just a subregion/subset of genes.

While genome-wide CRISPR screens have already proven successful in cell culture [216, 217], there are a number of technical limitations that need to be addressed before such screens become feasible for mice. First, the delivery of the CRISPR reagents into the mouse is currently limited to either zygote injections or embryonic stem (ES) cells. Zygote injections require highly skilled personnel and are time consuming, while the injection efficiency is usually very high. Targeting ES cells on the other hand produce chimeric animals and requires additional matings. Delivering CRISPR reagents to male spermatogonial stem cells is a potential alternative but has not yet been reported. A knock-in mouse expressing low levels of guide sequences targeting all >20,000 genes (or all random target combinations like hexamers) with a temporally controlled *Cas9* gene (e.g. under a germ cell specific promoter) could serve as another potential strategy.

Simultaneous targeting of multiple genes located on different chromosomes by CRISPR-Cas9 has been successful for us and others [218] but when two targeting sgRNAs are located on the same chromosome and in close proximity, large deletions (>1 Mb) rather than two independent targeting events are typically observed [219]. Such deletions could be used to generate a systematic deletion series to cover the entire genome. 20 gRNA pairs targeting 20 different chromosomes could be co-injected simultaneously. 300 different gRNA cocktails would be enough to cover the entire

genome with overlapping deletions and is a feasible number for zygote injections. This approach might be further complicated by the byproduct of homozygous deletions that will result in lethality if the deletion overlaps an essential gene.

Recent advances in high throughput sequencing and gene editing technologies have tremendously expanded opportunities to apply forward genetic screen approaches for identification of underlying genetic risk factors for VTE and numerous other human diseases. This thesis provides examples of how to utilize these new technical advances for discovering novel genes involved in thrombosis.

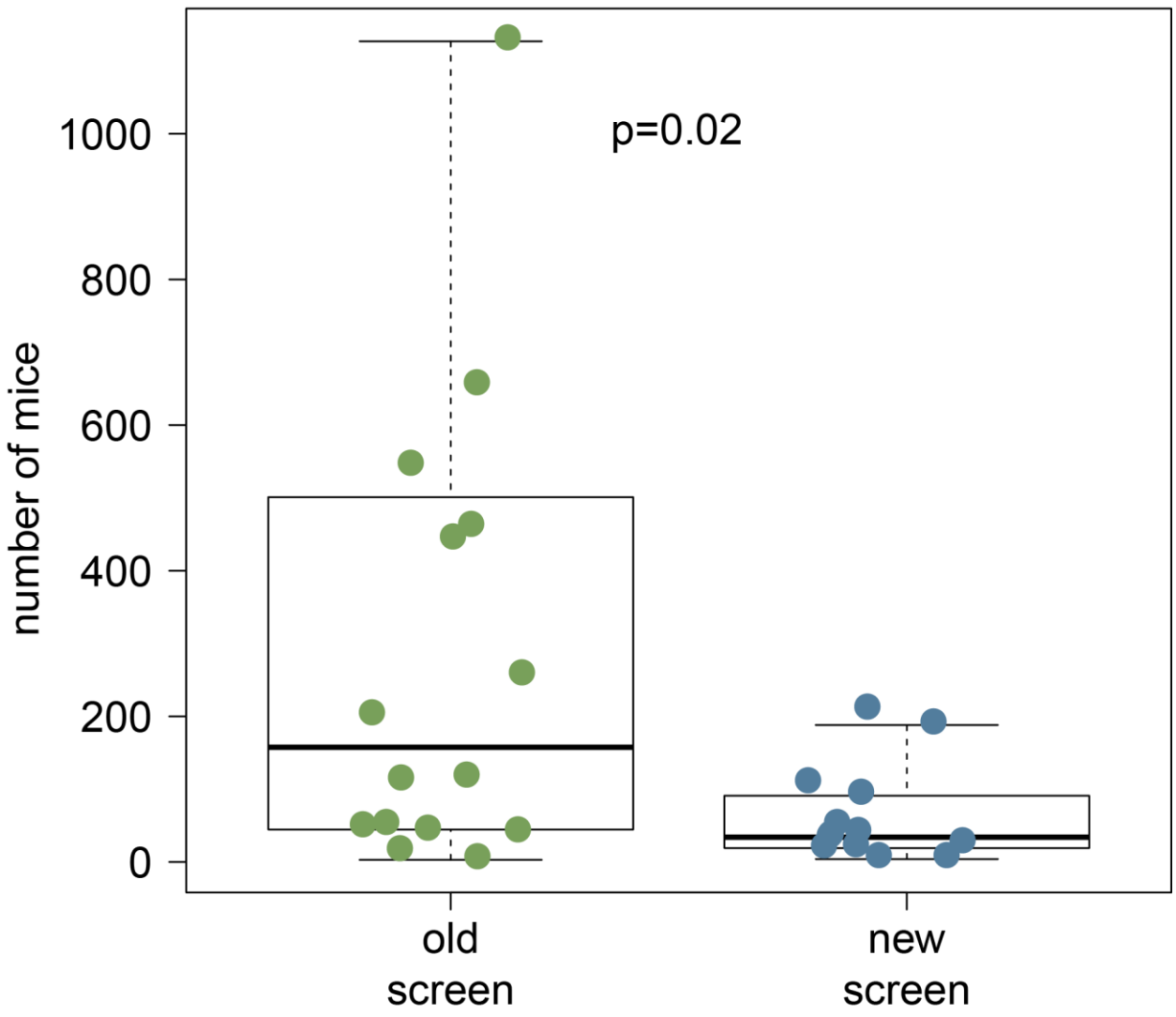

Figure 5-1: Size distribution of ENU pedigrees from performed screens
The ENU rescue pedigrees from the screen in Chapter II (old screen, n=16; Table 2-4) are significantly larger than the ENU rescue pedigrees from the screen in Chapter IV (new screen, n=13; Table 4-2).

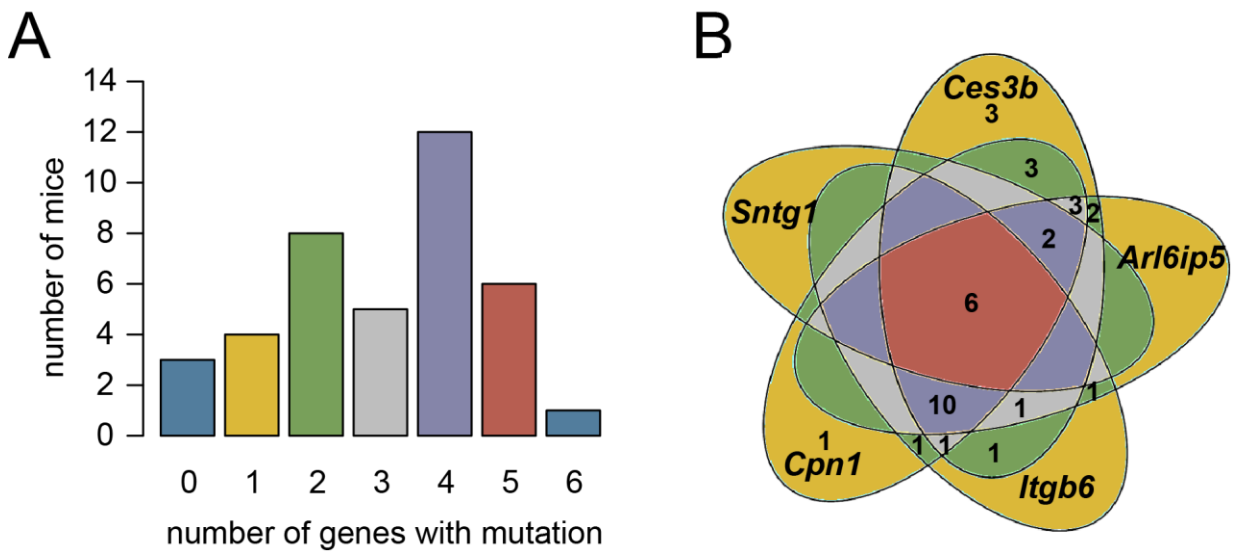

Figure 5-2: Distribution of CRISPR-Cas9 induced events by targeted genes
A) Distribution of CRISPR-Cas9 induced events in total of 39 mice. B) Complementary Venn diagram depicting which combinations of the five targeted genes were present in mice (excluding the one mouse with targeting events in all six genes including *C6*).

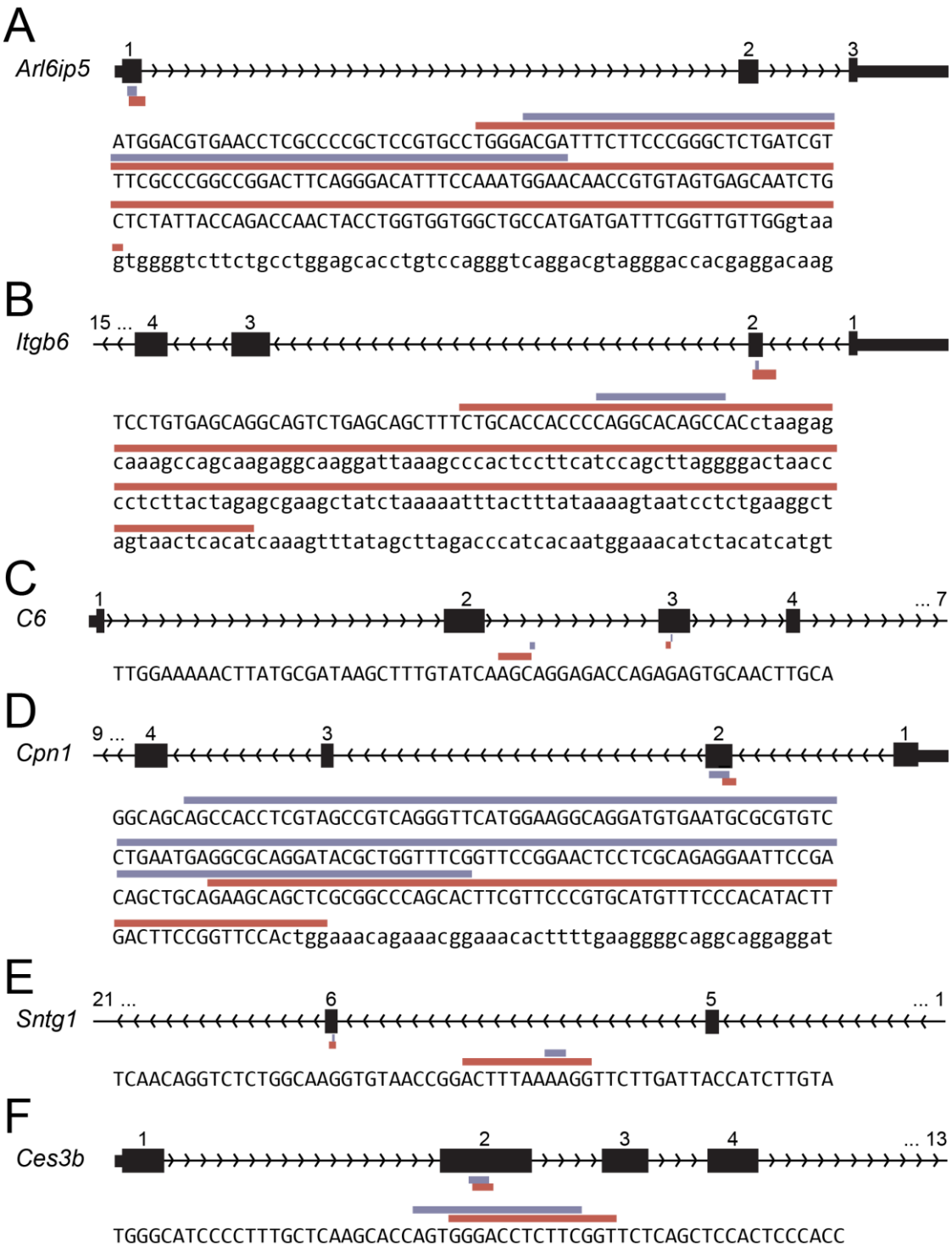

Figure 5-3: CRISPR-Cas9 induced alleles
The overview of CRISPR-Cas9 induced deletion alleles maintained for validation for A) *Arl6ip5* B) *Itgb6* C) *C6* D) *Cpn1* E) *Sntg1* and F) *Ces3*b. Details of the alleles are provided in Table 4-1.

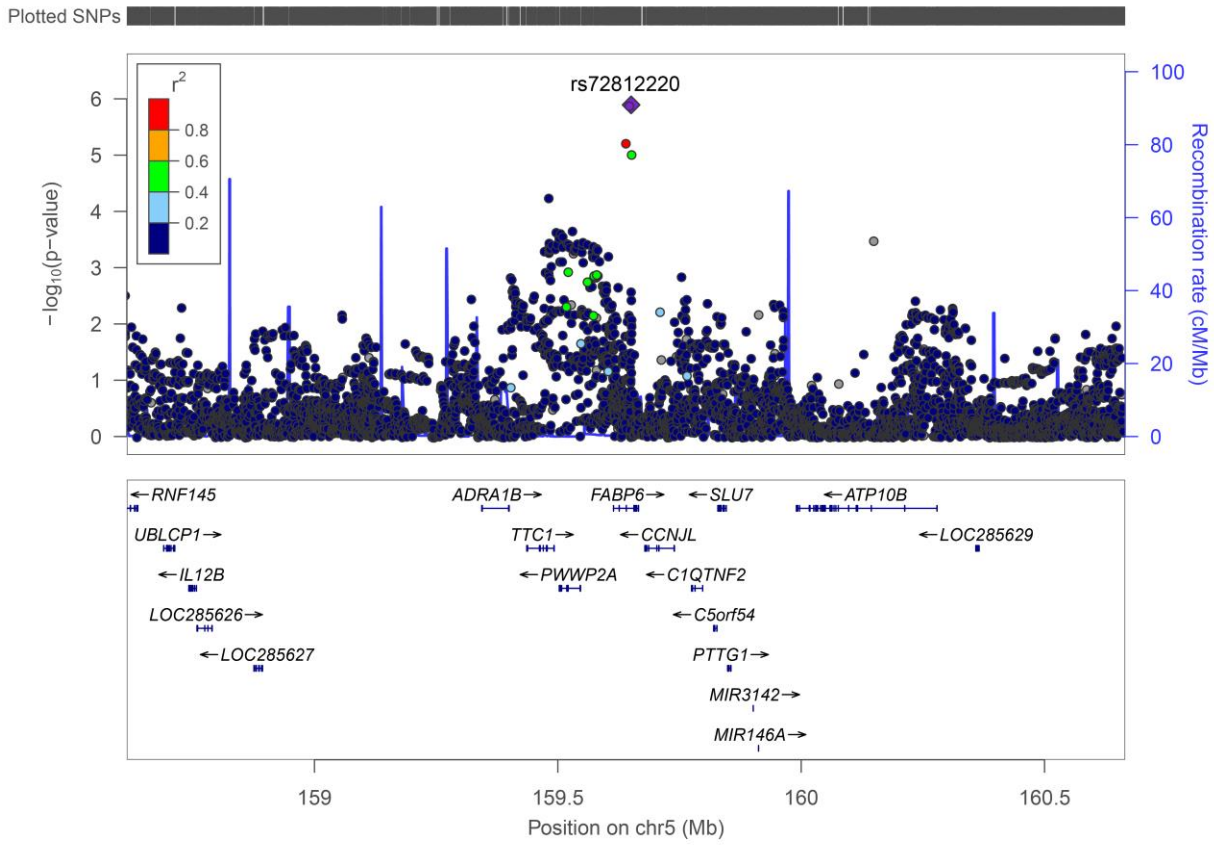

Figure 5-4: VTE GWAS results at the *Fabp6* gene locus
Regional association results were plotted using LocusZoom software [220]. The plot shows all SNPs tested for association with VTE within the *Fabp6* gene ± 1Mb. The lead SNP in this region (rs72812220) is located in the 3rd intron of *Fabp6* gene and has a p-value of 1.28×10^{-6}.

APPENDICES

Appendix 2-1: All used primer sequences

PRIMER NAME	PRIMER SEQ 5'->3'
F3_GENOTYPING_F	CTCCCATTTCTTTTCCTCCTC
F3_GENOTYPING_R	GGGGCGTTTGTAAATGGCGG
F3-NEO	CCTGACTAGGGGAGGAGTAG
UPSTREAMF3_1F	GACACGCCATCTGTCCAGTA
UPSTREAMF3_1R	CAAAAAGGTGGGCAGCTAAG
UPSTREAMF3_2F	AGCAGCTCCTGCAACTCACT
UPSTREAMF3_2R	GCACAGAGGAAGAGCAAAGG
UPSTREAMF3_3F	CACAGGGGCCTTTATTTTGA
UPSTREAMF3_3R	AAAGTAGGGCAGGGGAAAAA
UPSTREAMF3_4F	ACCATCTTTGAAGCCCAGAA
UPSTREAMF3_4R	AGGATGGAGCAGAACTGAGG
UPSTREAMF3_5F	CTGTCCTGGGAAACCTGTGT
UPSTREAMF3_5R	CATGCACCACTGCACCTATC
UPSTREAMF3_6F	CCAGGACAGCCTCGAACTTA
UPSTREAMF3_6R	AGAAAATGGCTGCTGTGCTT
UPSTREAMF3_7F	TGGCCTAGCAACTGTATTTTGA
UPSTREAMF3_7R	CAGAAGCTGCTCAGTCATGG
UPSTREAMF3_8F	GTCCTTTTCCTGGGAAGACA
UPSTREAMF3_8R	CAGTTTACAAGCACCCAGGAG
UPSTREAMF3_9F	GCTTCAGCGACAAGAGTTCA
UPSTREAMF3_9R	ACTCCCAACTGAGCAAAGGA
UPSTREAMF3_10F	TCTTCACGCATGTCTGCTTT
UPSTREAMF3_10R	TGCTTTGTACAATCTTCCTTCC
UPSTREAMF3_11F	TGAGTGGGACGACAGCTTAG
UPSTREAMF3_11R	CACTTGCAAGCTTTGGGTTT
UPSTREAMF3_12F	TGTCGAGCAAATGCTACCAG
UPSTREAMF3_12R	GCAGTGGCTAGCAGATCATTC
UPSTREAMF3_13F	TCTCAGGCTTCATGTTGCAG
UPSTREAMF3_13R	CCCCTCCTGTAGGAAACTCC
F3GENE_1F	GGTCTCCGCAGTACCTGGAT
F3GENE_1R	TTCTCAGGACCAATGCCACT
F3GENE_2F	GCTCCTGTAGCGTAGCCAAC
F3GENE_2R	CTTCAAGGGCCCAACATCTA
F3GENE_3F	GCCCTGAGGATTTGAATGAA
F3GENE_3R	TGTCACATGGTGGGATGCTA

F3GENE_4F	TCAGGCAAGACAGAGTGCAT
F3GENE_4R	CATACTGCAATCCGTGGAAA
F3GENE_5F	ACGTGTGTGGGGGACTAGC
F3GENE_5R	CGCTTTCTCTGGAATGCCTA
F3GENE_6F	CACACCCTCTGCTCTTGACA
F3GENE_6R	TGTAGGATGGCCTGGAACTC
F3GENE_7F	GCCAGGTTAAAACCAAAGCA
F3GENE_7R	CACTGCTTCAGGGCAGTGTA
F3GENE_8F	CACTGTGGTCACTGTGTTGCT
F3GENE_8R	GAAACCAAAAGCTTGCCAAA
F3GENE_9F	CCAATGCCCTTTTCTGGTTA
F3GENE_9R	GCATGCATGAACACACACAC
F3GENE_10F	GACAGCTCTCGGGAACAAGT
F3GENE_10R	CAAGCTGTGCAGGGATTACA
F3GENE_11F	TGGTGATGCAGGTCAGTTGT
F3GENE_11R	TGCCTTGACTAATGGCAATG
F3GENE_12F	AAGGTGGTCACCATTGAGGT
F3GENE_12R	TATGGACTGGATGGACAGCA
F3GENE_13F	TCACACTGACTGCTGGTGGT
F3GENE_13R	GGGCTCTGGGTGAAGTCATA
F3GENE_14F	TGCTGTCCATCCAGTCCATA
F3GENE_14R	ACATTCAGCAGGGGAGTCAC
F3GENE_15F	TGGGTCAAACAAAACACTGC
F3GENE_15R	AAAGAACCCAGCACCTCCTT
F3GENE_16F	TTTGTGCCTCTTCTGTGTGG
F3GENE_16R	TCTGCTTAGCGCTCTTCTCC
F3GENE_17F	ATTCTGCTGGGCTCTTTGAA
F3GENE_17R	GAGCTGGGTTTGTTTGCTTC
F3GENE_18F	GGAGATCTGGAACTCGCTTG
F3GENE_18R	TGTCTGTGGTCGAGAAGCAC
F3GENE_19F	TCGGAGGCTCAGACTTTGTT
F3GENE_19R	TAAAAACTTTGGGGCGTTTG
F3GENE_20F	TCCCGTTTCTTTTCCTCCTT
F3GENE_20R	CCCCTGGTCTGATGAAAGAA
F3GENE_21F	CACACACACCAAGGAGATGC
F3GENE_21R	AGGGGACAGATGGGGATTAC
F3GENE_22F	GTGTGTGAGCCTGCCATCTA
F3GENE_22R	ACACATCCCACACCCAATCT
F3GENE_23F	GGATGAAGGGCAATTGAGAA
F3GENE_23R	ATGCATTAGAGGCTGGGAAG
F3GENE_24F	AGATTGGGTGTGGGATGTGT
F3GENE_24R	TGGTGACGGTCTTGTAGCTG
F3GENE_25F	CCTGGTAGCCATCACTCACA
F3GENE_25R	GCATGCTGTGGAGAATCAAA
F3GENE_26F	CATCTGCAAGGAAGGGTCTC

F3GENE_26R	GGGGTCCCCAATATGAAGAT
F3GENE_27F	CAAGCACGGGAAAGGTAAGA
F3GENE_27R	ATTGACGCACGAGGGATTAG
F3GENE_28F	GTATGTGCTTGCGTGTGTGA
F3GENE_28R	GGAAGTGACCAAGGGAACAA
F3GENE_29F	CAAAATAGCCCAGGAAGCAG
F3GENE_29R	GCTACTGCCCCCTTAGTCGT
F3GENE_30F	TTGTTCCCTTGGTCACTTCC
F3GENE_30R	ATGCCCCTTGGTCTCTTTCT
F3GENE_31F	TAGCTATGGCCTGGCTCTGT
F3GENE_31R	TGATGGTGGAGACGAAGAGA
F3GENE_32F	TTCTGCCTTCTTGCCTCTGT
F3GENE_32R	ACCACTGCTCCCACAATGAT
F3GENE_33F	CCCCAGCCAACTACTGTCTC
F3GENE_33R	ATGTTGCACAGTTCCCATCA
F3GENE_34F	CGAGCCTCCATGTTGACTTT
F3GENE_34R	AATCACAAAGATGCCCCAAG
F3GENE_35F	CCAGCTAACGCTTTGATTCC
F3GENE_35R	TTGTCTCAATTCCCAATCACC
MFF_OF	CACTCATTGCTGGGTCCTTT
MFF_OR	ATTTCCAAGTGCAACCAAGC
MFF_IF	CCCTCTGCTCGGATTGATAC
MFF_IR	TATGCAACAAAGTGGCAAGG
DGKQ_OF	TGTCCAAAACTGTGCCAGAC
DGKQ_OR	CCACACAGGTTCCACCTTTT
DGKQ_IF	CCACAGGCTTCAGTCAACAA
DGKQ_IR	ACAGGTGGGCTTAGTCATCG
ANPEP_OF	TAGCTTCAGAGCTGGGCTTC
ANPEP_OR	GGGCTGTGGTTTCACAACTT
ANPEP_IF	CTCCAGAGGCTGGAGACTTC
ANPEP_IR	GGTGAGCACTTAACCCCAAA
NUMA1_OF	TCCCAAACATTTTGCCATTT
NUMA1_OR	TTTTCTTGCAAGGGAAAGGA
NUMA1_IF	CTTACCCGCCACACATTTTC
NUMA1_IR	CTGGACCTGACACGGACTCT
BAG2_OF	CTGTGTCTGCCAACACTGGA
BAG2_OR	GTTGCTGACGTGGGAAGTTT
BAG2_IF	CCGGTGAATTTGAAGGCTAA
BAG2_IR	GACTGCCAACCGTCTGATG
UGGT1_OF	TCCCTAGCACTGCTTCCTGT
UGGT1_OR	GCAGAAGGCTTGGCTTATTG
UGGT1_IF	CGGGAAGGCATCTGAATAAA
UGGT1_IR	GACGCTGAGACTGCATCAAG
IL1R2_OF	CCACCTAACCCAAGCCTCTA
IL1R2_OR	GGCTGCTATGGCTTGTTCTC

IL1R2_IF	GTCAACCTATGGTGCCCTGT
IL1R2_IR	CCTCCACATTTTCTCCCAGA
LZTFL1_OF	TGAGTGCTCCTCAAGGAAGG
LZTFL1_OR	CAGAAAGTGGGGGAGTTAAGTG
LZTFL1_IF	AGTGACTGTGCCTTGCTGTT
LZTFL1_IR	TGTCATGATGTCGGTCTCTTG
STAT2_OF	TGTCCCATTGTCTGTCCTTG
STAT2_OR	GCCCTTGCATTTCCTATCAA
STAT2_IF	GACCAGGAGTTGCCATTGAT
STAT2_IR	AGGTCCTCAGGCAAATCTGA
OLFR1373_OF	CAGGGTGCATAATGGTTGTG
OLFR1373_OR	ACACCAGGGCCAAGAAGT
OLFR1373_IF	CACCTTCCAAAGCTGATGGT
OLFR1373_IR	GGGGGAGGGTATAGGGAACT
ALOXE3_OF	AATCGGTGCTGGGATCTATG
ALOXE3_OR	AAGTCTCAACCCTGCCCTTT
ALOXE3_IF	TGAGGCTTAGGGATGGCTTA
ALOXE3_IR	CATCTCAACACACGGTGGTC
PDHB_OF	ACTGGTCTTGAATGGGCAAC
PDHB_OR	GGGGCATCTAGTGAGGCTTA
PDHB_IF	GGCAGCTATGGCCTGTCTTA
PDHB_IR	CTGCATACCTGCACATTTGG
MAPK8IP2_OF	GCAGCCACACCCTATTTGTT
MAPK8IP2_OR	TACTTCATGGCGCTCCTCTT
MAPK8IP2_IF	ACAGGCACTTGCTGGAGACT
MAPK8IP2_IR	CAGAGCAGGGAGTTGGGTTA
CRYBG3_OF	TGAGTCCTGGAAGTCTGCAA
CRYBG3_OR	GTCTCTCCTGTTTCCCGACA
CRYBG3_IF	ACTGGAGGTCGTTGGTTCAC
CRYBG3_IR	TGAGGCATTTGATGGAGACA
MAP3K4_OF	CTTCAGTGCTTTGTCCACGA
MAP3K4_OR	CCTCAGGAGACAAACCGTGT
MAP3K4_IF	TCCTCTGACTCGAGCCTCTC
MAP3K4_IR	AGCAGGTGAAGCGGATAATG
CDC5L_OF	CAAGAACTGCCACCACTTGA
CDC5L_OR	GCCTCCATTTATCTTTTTCTGC
CDC5L_IF	ACCGTGTTTAGTGCCCTCAT
CDC5L_IR	TGCCTGTGTGTAATCTTTTTCTG
CYP2C39_OF	GACAACAGGGCAGATGGAGT
CYP2C39_OR	CTGCCCTCTGGACCATAAAG
CYP2C39_IF	AACACTAGTGACCTTAACCAAGGA
CYP2C39_IR	CACGGGGTATGTTGTTAGGG
PPRC1_OF	GACCCAGGAGAACAGACCAA
PPRC1_OR	CCCTGCATCCTCTCTTCATC
PPRC1_IF	TGTTGCAAAGCTACCTGCTG

PPRC1_IR	AAAGGAGGCACAGACGAGAA
MEX3B_OF	CCTGGCTTCCAGGTTGTAAA
MEX3B_OR	GTTGCGATAGCTGGAGAAGG
MEX3B_IF	GGAGGAGCCTGTCTTTGTTG
MEX3B_IR	AGATCAAAGCCCACGTCTGT
SMARCA4_OF	TGGTGAGTGCCTCAGAGCTA
SMARCA4_OR	TGAACCCCAGGACCTAGTGA
SMARCA4_IF	TCTGTGTGGTCCCCTTTCTC
SMARCA4_IR	TTGCTAGCCTCCAGGCTCTA
EGR2_OF	GGAGGGCAAAAGGAGATACC
EGR2_OR	CTAGCCCAGTAGCGCAGAGT
EGR2_IF	AGTTGGGTCTCCAGGTTGTG
EGR2_IR	GCTTCAAGGACCAGGAGATG
DCC_OF	GAAGGAAGGCAACAGGATGA
DCC_OR	CTGGGGATTCATCTCAGCAT
DCC_IF	CTTTTCTCACCCCAAAGCAA
DCC_IR	GGAAAGACAGCCAGGACAAG
A630007B06RIK_OF	AGTGCCAAAGTGTCCCAAAG
A630007B06RIK_OR	TCGTCTGCTTGCTTCTCTTG
A630007B06RIK_IF	TTTGGGCAGAAAATGTGCTA
A630007B06RIK_IR	CAGTCACTCGATGGTGAGGA
FBLIM1_OF	TGGTCCAGTTTGCCACCTAT
FBLIM1_OR	GCACAATGGGTAGCTGGATT
FBLIM1_IF	GGCTCGCCACCTATGTTTT
FBLIM1_IR	ACCCCTGTCGGGAAGAGTAG
KNTC1_OF	GCCATTGAGAACACGGACTT
KNTC1_OR	TGATTTATGGGAGGGTGCAT
KNTC1_IF	TCAGCCAAGAAGGTAAGCAAA
KNTC1_IR	TCATCGAGCCTCTAGCCTTT
CUX1_OF	GACCCTTTGATCAGGAGCTG
CUX1_OR	GGCTTGCCTAGAATTCACCA
CUX1_IF	GGCGACACATCAGTCTTTGA
CUX1_IR	GTGCAGCGTCTACACGACAT
CCR1_OF	GGAATGCCCCATTTTGTTTA
CCR1_OR	TGCTATGCAGGGATCATCAG
CCR1_IF	GACCTTCCTTGGTTGACACC
CCR1_IR	CTGCTCAGAAGACCCAGTGA
RIC8B_OF	GAACAGAAGAACCGGGACTG
RIC8B_OR	GCCTGGGAGCTACTCTCAAA
RIC8B_IF	CCCTGAATGGAATGGAGAGA
RIC8B_IR	ACAAATGCCCAAGTCTGACC
GRIA1_OF	GAAGGCCAACTGATTTTCCA
GRIA1_OR	TGGCATCACATTTTCATGGT
GRIA1_IF	AGCTGATTTGCTGGACTGGT
GRIA1_IR	GTCCCACGTTTGACTTGGAT

DHX8_OF	CAGTGCTCTCGTTGTGCTTT
DHX8_OR	CTTCCCTTGCCACCACAG
DHX8_IF	ACCCAGACAGACCCACTCAC
DHX8_IR	CCATGGAACACTGTCTCTGC
ANKRD55_OF	CCACCTTTGACAGTGTCGTG
ANKRD55_OR	CAGCCCATTCAGGGTAGAAA
ANKRD55_IF	CCACCAATCAGAACCCAGAG
ANKRD55_IR	TGGCTGTAGTTCCCGTTTTT
WDFY4_OF	CACACACACACATGCTTGCT
WDFY4_OR	CCCCACACACACACCTGTTA
WDFY4_IF	GGCTTGCTCACCCAATAACT
WDFY4_IR	GGGCACTTTGGTGTACCACT
RUNX1_OF	AGTTTCCCTCCGGGATTCTT
RUNX1_OR	GGCAGTCTAGGAAGCCTGTG
RUNX1_IF	GATGGCGCTCAGCTCAGTAG
RUNX1_IR	CTACTCTGCCGTCCATCTCC

Appendix 4-1: Overview of WES mice

SeqID	Mouse ID	Sex	Days	Gen	Sibling sets	Sample origin	Seq	Capture	Mean Coverage
82305*	82305	M	300	G2		S2	CGT	A	31.79
105065	33586	M	884	G2		S1	NGC	R	60.54
105066	39748	M	585	G3		S1	NGC	R	67.99
105068	53882	F	626	G1		S1	NGC	R	61.91
105069	55922	M	750	G4		S1	NGC	R	64.52
105070	57258	M	>100	G1		S1	NGC	R	60.54
105071	57372	F	263	G1		S1	NGC	R	61.03
105072	82086	F	227	G1	11	S2	NGC	R	65.52
105073	82458	M	358	G1		S2	NGC	R	62.92
105074	82620	F	337	G1		S2	NGC	R	65.03
105075	82723	M	416	G1	4	S2	NGC	R	59.27
105076	82841	F	404	G1		S2	NGC	R	46.35
105077	83071	F	232	G1		S2	NGC	R	56.26
105078	83188	F	365	G1	5	S2	NGC	R	59.5
105079	83217	M	258	G1	7	S2	NGC	R	61.05
105080	83230	F	362	G1		S2	NGC	R	63.49
105081**	83457	M	437	G1	4	S2	NGC	R	62.24
105082	83737	M	663	G1		S2	NGC	R	60.65
105083	83796	M	561	G1	8	S2	NGC	R	67.12
105084	83875	M	396	G1		S2	NGC	R	60.78
105085	83882	M	255	G1		S2	NGC	R	58.38
105086	88129	M	493	G1		S2	NGC	R	61.07
105087	96868	M	659	G1		S1	NGC	R	57.75
105088	98420	F	681	G1		S1	NGC	R	55.54
118761	60654	M	416	G1	10	S2	NGC	R	81.36
118762	60693	F	22	G1	11	S2	NGC	R	78.75
118763	60712	M	28	G1	10	S2	NGC	R	80.03
118764	60716	F	50	G1		S2	NGC	R	80.04
118765	82147	M	346	G1	10	S2	NGC	R	81.18
118766	82194	M	31	G1	1	S2	NGC	R	78.53
118767	82395	F	17	G1	1	S2	NGC	R	80.62
118769	82744	F	57	G1	5	S2	NGC	R	82.19
118770	83010	F	65	G1	2	S2	NGC	R	79.06
118771	83140	F	22	G1		S2	NGC	R	80.46
118772	83164	M	36	G1	6	S2	NGC	R	141.92
118773	83411	F	23	G1	2	S2	NGC	R	81.77
118774	83520	M	17	G1	3	S2	NGC	R	78.04
118775	83619	M	46	G1	12	S2	NGC	R	79.34
118776	83685	F	35	G1	7	S2	NGC	R	79.45
118777	83689	M	35	G1	7	S2	NGC	R	82.98
118778	83794	F	27	G1	8	S2	NGC	R	80.53
118779	83929	M	35	G1		S2	NGC	R	88.99
118780	83971	F	65	G1	3	S2	NGC	R	102.62
118781	88025	M	56	G1		S2	NGC	R	79.16

118782	88041	F	43	G1	6	S2	NGC	R	78.85
118784	88262	M	252	G1	9	S2	NGC	R	78.14
118785	88503	M	25	G1	9	S2	NGC	R	82.96
118786	88547	F	26	G1	4	S2	NGC	R	83.89
118787	88955	F	26	G1	12	S2	NGC	R	104.35
118789	10177	F	363	G1	13	S2	NGC	R	67.88
118790	10178	M	39	G1	13	S2	NGC	R	70.28
118791	10382	M	469	G1	14	S2	NGC	R	102.03
118792	10451	M	47	G1		S2	NGC	R	82.23
118793	10562	M	22	G1		S2	NGC	R	74.15
118794	10653	M	30	G1	14	S2	NGC	R	93.52
118796	11082	M	76	G1		S2	NGC	R	86.69
118798	11241	M	337	G1	16	S2	NGC	R	76.98
118799	11468	M	20	G1		S2	NGC	R	78.23
118800	11477	F	23	G1	15	S2	NGC	R	74.31
118801	11478	F	23	G1	15	S2	NGC	R	78.35
118802	11600	M	31	G1	16	S2	NGC	R	76.63
118803	42885	F	NA	G1		S1	NGC	R	82.93
118804	45755	M	136	G1		S1	NGC	R	85.15
118805	42058	F	306	G1		S1	NGC	R	78.88
118806	51255	F	>100	G1		S1	NGC	R	72.66
118807	51283	F	NA	G1		S1	NGC	R	85.73
118808	57931	M	34	G1		S1	NGC	R	87.82
118810	22721	M	NA	G1		S1	NGC	R	83.76
118812	76278	F	147	G1		S1	NGC	R	76.84
118813	76387	F	NA	G1		S1	NGC	R	80.86
118814	76526	F	24	G1		S1	NGC	R	95.4
118815	76824	M	NA	G1		S1	NGC	R	79.79
118816	76582	F	NA	G1		S1	NGC	R	78.66
118818	76989	M	>100	G1		S1	NGC	R	88.59
118819	80493	M	>100	G1		S1	NGC	R	71.19
118820	80821	F	>100	G1		S1	NGC	R	77.77
118821	80840	F	>100	G1		S1	NGC	R	82.13
118823	89285	F	NA	G1		S1	NGC	R	83.55
118824	89957	M	NA	G1		S1	NGC	R	87.92
118825	89965	M	NA	G1		S1	NGC	R	79.96
118826	90152	M	NA	G1		S1	NGC	R	75.21
118829	91310	M	<100	G1		S1	NGC	R	96.11
118830	91570	M	NA	G1		S1	NGC	R	95.28
118831	96245	F	539	G1	17	S1	NGC	R	80.34
118832	96247	F	NA	G1	17	S1	NGC	R	77.35
118833	96440	M	NA	G1		S1	NGC	R	87.01
118836	96839	F	NA	G1		S1	NGC	R	95.44
118838	98172	F	860	G1		S1	NGC	R	101.62
118839	98313	M	NA	G1		S1	NGC	R	103.59
118841	98491	M	>100	G1		S1	NGC	R	77.99
118844	2164	M	770	G1		S1	NGC	R	82.43
118845	2216	F	NA	G1		S1	NGC	R	80.36
118846	2383	M	NA	G1		S1	NGC	R	87.26

118847	2730	M	NA	G1		S1	NGC	R	77.88
118848	3000	M	NA	G1		S1	NGC	R	86.7
118851	5401	F	NA	G1		S1	NGC	R	94.12
118852	6654	M	NA	G1		S1	NGC	R	78.29
118853	6927	M	24	G1		S1	NGC	R	82.06
118855	13019	F	66	G1		S1	NGC	R	91.97
118858	14418	F	42	G1		S1	NGC	R	85.67
118868	24744	F	294	G1		S1	NGC	R	78
118872	29035	F	56	G1		S1	NGC	R	82.41
118875	33095	M	46	G1		S1	NGC	R	86.25
119157	82522	M	346	G1		S2	NGC	R	73.89
119158	10020	F	387	G1		S2	NGC	R	85.87
119159	10722	M	442	G1		S2	NGC	R	86.95
119160	11187	M	298	G1		S2	NGC	R	77.46
FCH***	11954	M	158	G1	16	S2	BGI	A	22.25

Gen=Generation; Seq=Sequencing platform; F=Female; M=Male; S1=screen 1; S2=screen 2; CGT=Centrillion Genomics Technologies; NGC=Northwest Genomics Center; BGI=Beijing Genomics Institute; A=Agilent SureSelect Mouse All Exon Kit; R=Roche/NimbleGen SeqCap EZ System

*Used for Pedigree 1 analysis; excluded from burden analysis as G1 mouse (60654) was included instead

**Used for Pedigree 6 analysis

***Used for Pedigree 13 analysis

Appendix 4-2: All used primer sequences

Primer Name	Primer sequence (5'->3')	Experient
4931408C20RIK_OF	AAGGCAAATCATAGGCTGCT	PEDIGREE 1
4931409C20RIK_OR	ATTGTGGGGATCAAGCAGAG	PEDIGREE 1
4931410C20RIK_IF	TTCACACCTGTCCTTCTAGGG	PEDIGREE 1
4931411C20RIK_IR	TATGGAAAGCCAGGAAGTGG	PEDIGREE 1
PFDN2_OF	GCCTTTGTAACTTGCCATCC	PEDIGREE 1
PFDN2_OR	TTCTGACTCAGGGATCCACA	PEDIGREE 1
PFDN2_IF	GCTGGCTTTAATCGCCTTC	PEDIGREE 1
PFDN2_IR	CACAGCCAACAACTCCTCAC	PEDIGREE 1
SEC16A_OF	AAGAGGCTGCTGAGAAGCTG	PEDIGREE 1
SEC16A_OR	CCCTCCCAAGGTAGGAGAAG	PEDIGREE 1
SEC16A_IF	ATTGCCAGCAGGGCTACTAA	PEDIGREE 1
SEC16A_IR	AGTGCAGGCAAGTTCTGGTT	PEDIGREE 1
PLD1_OF	CCCCACACAGTTCAAGGTCT	PEDIGREE 1
PLD1_OR	GGTACGCTCCCCATACAAAA	PEDIGREE 1
PLD1_IF	AGTGAGGAGCCTGCTGAGTC	PEDIGREE 1
PLD1_IR	TTCAAAGCTGATCCCAGGTC	PEDIGREE 1
KPRP_OF	GGCCACAGTTGGTGTAGGAA	PEDIGREE 1
KPRP_OR	GACCATGTGTGACCAGCAAC	PEDIGREE 1
KPRP_IF	ATTGAGGAGTGCAGCTACCG	PEDIGREE 1
KPRP_IR	GGAAGCTCCATGTGAGATGA	PEDIGREE 1
NDST4_OF	GCAGTTGGAGAATTGGCTCT	PEDIGREE 1
NDST4_OR	TTAAAAATGCTGCCCAATGA	PEDIGREE 1
NDST4_IF	TCATGCACACACACTGTGAAA	PEDIGREE 1
NDST4_IR	CCGTGATGATGGTTCCTCTT	PEDIGREE 1
GSTCD_OF	TCTTGAGGGCTCAGCTTCAT	PEDIGREE 1
GSTCD_OR	CAGGAACCGGGTGTAAAAGA	PEDIGREE 1
GSTCD_IF	GCAAACAGCAATTCTGGACA	PEDIGREE 1
GSTCD_IR	CATGCAGAGTGGGGAAAGTT	PEDIGREE 1
MMEL1_OF	TCTGAAAAACCGTCCTCACC	PEDIGREE 1
MMEL1_OR	CCGAGTGCCAGCCATATTAG	PEDIGREE 1
MMEL1_IF	ATGTTCCCTTCTGTGCTGGA	PEDIGREE 1
MMEL1_IR	GGGTCTCACCTTCAGACCAA	PEDIGREE 1
KCNH2_OF	ATGCCGAGAATGAGGAAAGA	PEDIGREE 1
KCNH2_OR	GCAGATGTGCTGCCTGAGTA	PEDIGREE 1
KCNH2_IF	AATGCCTCTTCCAGCTCCTT	PEDIGREE 1
KCNH2_IR	CCTGCTGCTGGTCATCTACA	PEDIGREE 1
TMCC1_OF	AGCTTGAGCTTCGCGTTAAA	PEDIGREE 1
TMCC1_OR	GTCGTCTCCAAACCCAGAGA	PEDIGREE 1
TMCC1_IF	ACTGCTTTGCTGACTGACGA	PEDIGREE 1
TMCC1_IR	GGAAAGGCTTTAGGGGTGAT	PEDIGREE 1
D6WSU163E_OF	CTACCCTCGACAGCTCTGAA	PEDIGREE 1
D6WSU163E_OR	CGGAAGTGCAACGAAATACA	PEDIGREE 1
D6WSU163E_IF	TGAATCCCTCAGGAAAGACAA	PEDIGREE 1
D6WSU163E_IR	CACCATCATTCCCTGATAGGA	PEDIGREE 1
TAS2R131_OF	AATTTGCCAGTGACCTTCCA	PEDIGREE 1
TAS2R131_OR	ACATTTCCCATCCCCTTTTC	PEDIGREE 1

TAS2R131_IF	TTAATTGGCCTGCTCATTGG	PEDIGREE 1
TAS2R131_IR	GGAGATTGAGAGGTGTGCTTG	PEDIGREE 1
ZFP939_OF	GTTCACAGTGCAGGAAAGCA	PEDIGREE 1
ZFP939_OR	GGTATGCGTGAGGGAGAAAA	PEDIGREE 1
ZFP939_IF	AGCAAGTCTGGGCTTACTGC	PEDIGREE 1
ZFP939_IR	CAGGGATTCTCCCTTGTTTG	PEDIGREE 1
VPS33B_OF	GTCGGAAACCAGAGATTGGA	PEDIGREE 1
VPS33B_OR	GCAGCGGTCCTGAGTAAATC	PEDIGREE 1
VPS33B_IF	CTGGTGAAGTTGGGGTCCTA	PEDIGREE 1
VPS33B_IR	AGCACCTTCAGGCTCTTGTC	PEDIGREE 1
VMN2R78_OF	TCACTCATTCACTCACTCATGTTT	PEDIGREE 1
VMN2R78_OR	CAATTGAAAATGAAAACTGTCAAA	PEDIGREE 1
VMN2R78_IF	GAGATCGTTCGGTGGCTTT	PEDIGREE 1
VMN2R78_IR	AAGTTTGAAACATGCAACCAT	PEDIGREE 1
SOBP_OF	GAATCGTTCACATGGGGAAT	PEDIGREE 1
SOBP_OR	TCTGACACTGCCAACTGCTC	PEDIGREE 1
SOBP_IF	GGCACTATCACTGGGTACGG	PEDIGREE 1
SOBP_IR	CATCTTCATGGAGCAGCAAA	PEDIGREE 1
VMN2R81_OF	CCCCCAAAGACACAGCTCTA	PEDIGREE 1
VMN2R81_OR	CTGCCAGGGGAATAACAGAG	PEDIGREE 1
VMN2R81_IF	TCTGGGGGAAACCCTACTTC	PEDIGREE 1
VMN2R81_IR	GCCACTGCATACACAGCATT	PEDIGREE 1
ADAMTS2_OF	TCAGAGTCTCCGAGGTCTCC	PEDIGREE 1
ADAMTS2_OR	AAATCGTCCCCCTTTCTCTG	PEDIGREE 1
ADAMTS2_IF	GTGTCCCACGTGGTGTCTTT	PEDIGREE 1
ADAMTS2_IR	CCCTAAGCACTGTGGAGGAG	PEDIGREE 1
UBE2O_OF	GCAGCAGAAGGCTCCAATTA	PEDIGREE 1
UBE2O_OR	CATTAATCCGTGTGGTGCAG	PEDIGREE 1
UBE2O_IF	GGGCAGCTACTTGTCCTCTG	PEDIGREE 1
UBE2O_IR	GAATTGAGTCCTGGCTGGAA	PEDIGREE 1
MFSD2B_OF	CCAGGTTACCAGGGAGGAGT	PEDIGREE 1
MFSD2B_OR	CTCTCCTGCTGTCCTGTTCC	PEDIGREE 1
MFSD2B_IF	CGGAGGCTCTGACCTTCTCT	PEDIGREE 1
MFSD2B_IR	AGGGCCACCAGTTACTTCCT	PEDIGREE 1
LRRC9_OF	TCATGGGAGCATTAGATGGA	PEDIGREE 1
LRRC9_OR	TGGTAGTTTCTGGGGATGGA	PEDIGREE 1
LRRC9_IF	TGGGGAACAAGCCTTCTTAG	PEDIGREE 1
LRRC9_IR	ATGAGTGCTGAGGGGCTAGA	PEDIGREE 1
FOS_OF	GGATTTGACTGGAGGTCTGC	PEDIGREE 1
FOS_OR	CTGGAAGAGGTGAGGACTGG	PEDIGREE 1
FOS_IF	GAAGGCAGAACCCTTTGATG	PEDIGREE 1
FOS_IR	CACAGCCTGGTGTGTTTCAC	PEDIGREE 1
VMN1R214_OF	TCAACCAGTTACCAAACACCTG	PEDIGREE 1
VMN1R214_OR	GGAAGAATGGAAGGATGTGC	PEDIGREE 1
VMN1R214_IF	CTCATCTGCAACATGCGTCT	PEDIGREE 1
VMN1R214_IR	CCTCCTCCATCCAGATGCT	PEDIGREE 1
CADPS_OF	GCAATTCGAAGGCACAAGAG	PEDIGREE 1
CADPS_OR	GGACAGAGCCTCAAGTCACA	PEDIGREE 1
CADPS_IF	AGGGGTTTGTGTGATCTGGA	PEDIGREE 1

CADPS_IR	AAGAGTCCCAGGTTCCATCC	PEDIGREE 1
AKAP11_OF	CCAAACTTTTCCCCACAAGA	PEDIGREE 1
AKAP11_OR	TTGAGCTGCCTGAAATTCCT	PEDIGREE 1
AKAP11_IF	CGTATGATTTCTTCCCCTTTTAAT	PEDIGREE 1
AKAP11_IR	TGGAGACTTACTTGCTCATGGA	PEDIGREE 1
E430025E21RIK_OF	GGCTCATAACCACCGAGTGT	PEDIGREE 1
E430025E21RIK_OR	CAGTGCTATTCCCCTGCAAT	PEDIGREE 1
E430025E21RIK_IF	CAAAAGCTGGGGTTCAAGAC	PEDIGREE 1
E430025E21RIK_IR	TGCTCTGGGCTCCTAACCTA	PEDIGREE 1
MB21D2_OF	AAACAGCAAAATCAGGCAGAA	PEDIGREE 1
MB21D2_OR	GACTCCCTGCCAGCTACTTG	PEDIGREE 1
MB21D2_IF	CCAAGTCCAATGTTAGCTGGA	PEDIGREE 1
MB21D2_IR	TTTCATCCCTCAGTGCAACA	PEDIGREE 1
ITGB5_OF	GGTAGGGGCTGTAAGGATGG	PEDIGREE 1
ITGB5_OR	GGATTCCCCAGTAAGGCAAT	PEDIGREE 1
ITGB5_IF	CCTGAGTTGAATTCTCTGCACTT	PEDIGREE 1
ITGB5_IR	CACACCCAACACAAGCTCAA	PEDIGREE 1
NR1I2_OF	CAGCAGAAGAAGAGGCCTTG	PEDIGREE 1
NR1I2_OR	AATGCCGTGGTCACATTTTT	PEDIGREE 1
NR1I2_IF	AGTTAGGAGGGGAGGCTTTG	PEDIGREE 1
NR1I2_IR	CCCGAATGAGAGTCTTGCTC	PEDIGREE 1
CD47_OF	GAAAGGCACAGCTCTTGTCC	PEDIGREE 1
CD47_OR	GGGAAGCTATGTGGCTATGG	PEDIGREE 1
CD47_IF	GAGGTTAGGTTTGGGTGCTG	PEDIGREE 1
CD47_IR	GTGTGACTCACCCATGATGC	PEDIGREE 1
PTK7_OF	GTGCATCCTGTCGTGAGAGA	PEDIGREE 1
PTK7_OR	GCTTGTTTGGGGTAGAGACG	PEDIGREE 1
PTK7_IF	CTAGCATCCGAGGAAAGGTG	PEDIGREE 1
PTK7_IR	CGAGATGATGCTGGCAACTA	PEDIGREE 1
TTC39D_OF	CGCCATCAACCTTATTCACC	PEDIGREE 1
TTC39D_OR	TGTTAAAACGTGCACGGAAA	PEDIGREE 1
TTC39D_IF	AGTTCATACCACGCCCTGAT	PEDIGREE 1
TTC39D_IR	TGGCAGCAGTAGAAGCCTTT	PEDIGREE 1
SUV420H1_OF	GTCTGCATCCCCATTGTCTT	PEDIGREE 1
SUV420H1_OR	TTTCCAGATTCTGCCTGCTT	PEDIGREE 1
SUV420H1_IF	GTCAGCTGCCTACGTTCTCC	PEDIGREE 1
SUV420H1_IR	CTCTTGCCTCACAGAAAATTG	PEDIGREE 1
SGOL2_OF	TCGGTTGTTCTCCTGAAACC	PEDIGREE 6
SGOL2_OR	TGTCCAAACACATGAAAAGAGG	PEDIGREE 6
SGOL2_IF	CGGTGGAGATAACACCCAAC	PEDIGREE 6
SGOL2_IR	TGTTTCAACTGAAAACACACCA	PEDIGREE 6
DNAJB2_OF	TTGGAACCTTTGCGTGTGTA	PEDIGREE 6
DNAJB2_OR	GTGGAGGGACAGAGTTTGGA	PEDIGREE 6
DNAJB2_IF	CTCTTGCAGGTGTCCCAGAT	PEDIGREE 6
DNAJB2_IR	GGGCCACACTATTCTGCACT	PEDIGREE 6
SPTAN1_OF	CTTTGAGAGGGACCTTGCAG	PEDIGREE 6
SPTAN1_OR	TCCCCTGCCTTTAACTTGTG	PEDIGREE 6
SPTAN1_IF	AAGCTGAGGCCTGAACTCTG	PEDIGREE 6
SPTAN1_IR	TTCAGTGCTATGCCTGCTGT	PEDIGREE 6

PKN3_OF	CCCACTTTCTGTCAGTGCAA	PEDIGREE 6
PKN3_OR	AGGACTCCAGGAACTGCTCA	PEDIGREE 6
PKN3_IF	TGGGTGTACCCTGCCTCTAC	PEDIGREE 6
PKN3_IR	CTGGTGAACTCTCCCTCGAA	PEDIGREE 6
N28178_OF	CAGGCTCCAGACACATTTGA	PEDIGREE 6
N28178_OR	AAGGAGTTTGAAGGCATGGA	PEDIGREE 6
N28178_IF	TTTAGCAGAGCCGACCCTAA	PEDIGREE 6
N28178_IR	TCTTGGGGCCTCTCACTATG	PEDIGREE 6
CCDC17_OF	AGCATTACCTCCAGCCCTTT	PEDIGREE 6
CCDC17_OR	AGCCTACAGGCTGACCAGAA	PEDIGREE 6
CCDC17_IF	GCCTGTGCCCAGGTTAGTAG	PEDIGREE 6
CCDC17_IR	GGGTTGATCTCTGCCAATGT	PEDIGREE 6
GM13083_OF	AGGAGGTTCTGCAACCTTGA	PEDIGREE 6
GM13083_OR	ACCTGCCTTCCATTTGTCAG	PEDIGREE 6
GM13083_IF	ACCAGCTCAAACACCTGGAT	PEDIGREE 6
GM13083_IR	GCCTAGCAATGACCTCACCT	PEDIGREE 6
D630045J12RIK_OF	GAGAGTCAGAGGGGGAGCTT	PEDIGREE 6
D630045J12RIK_OR	AGGTGGATGTGAGTGGCATT	PEDIGREE 6
D630045J12RIK_IF	CAGCCATGGTGGAAAAAGTT	PEDIGREE 6
D630045J12RIK_IR	TCTCCACACCAAGCTCACTG	PEDIGREE 6
FAM13A_OF	TGGTGTGTCTAATCGCTGCT	PEDIGREE 6
FAM13A_OR	TTTACTGGCCCTCAAGTTGC	PEDIGREE 6
FAM13A_IF	GGATTGCCTGCTTTGTGAGT	PEDIGREE 6
FAM13A_IR	GGAACCTCCAGAAAAGAACCA	PEDIGREE 6
ANTXR1_OF	CTGACTGGGCTTGGCTTACT	PEDIGREE 6
ANTXR1_OR	CCGCAGATATTTGTGCAAGA	PEDIGREE 6
ANTXR1_IF	TGGAGGATAGAGTTGGCACA	PEDIGREE 6
ANTXR1_IR	GGTTGGCTCCTTACTGCTGA	PEDIGREE 6
FANCD2_OF	AGGCACTAGAGGTGTTGATGG	PEDIGREE 6
FANCD2_OR	GAACTGTAGCTCCAGCCTCCT	PEDIGREE 6
FANCD2_IF	TCTCTTCAGATTCGCCAGGA	PEDIGREE 6
FANCD2_IR	CCAATTTTGTGACAGCTTTGC	PEDIGREE 6
MUG1_OF	TGGTGTGTCTAATCGCTGCT	PEDIGREE 6
MUG1_OR	TTTACTGGCCCTCAAGTTGC	PEDIGREE 6
MUG1_IF	GGATTGCCTGCTTTGTGAGT	PEDIGREE 6
MUG1_IR	GGAACCTCCAGAAAAGAACCA	PEDIGREE 6
LENG9_OF	GGAAGCGGAAGTAGCGTATG	PEDIGREE 6
LENG9_OR	AAGACGTGACTCCCTGGATG	PEDIGREE 6
LENG9_IF	GAATGGCTCTTCCTGCACTC	PEDIGREE 6
LENG9_IR	GGTTCCCAGTGGCTTACAAA	PEDIGREE 6
RYR1_OF	AAAAGGCCAGATCCCAGACT	PEDIGREE 6
RYR1_OR	AAACCCTTGCTTGGTCCTCT	PEDIGREE 6
RYR1_IF	AAATGTTCACAGGGCTCCAC	PEDIGREE 6
RYR1_IR	GCCAAGGCCTTTCTATTTCC	PEDIGREE 6
HS3ST4_OF	GAGCGCTTCACGACTCCT	PEDIGREE 6
HS3ST4_OR	TCCTCCGCTTGTTCTCAACT	PEDIGREE 6
HS3ST4_IF	ACCCCTGATTATGGGGAGAA	PEDIGREE 6
HS3ST4_IR	CCCTGTATTGGCCTGGATT	PEDIGREE 6
LONP2_OF	CAGTGTGATTAAAGTGCTCTGGA	PEDIGREE 6

LONP2_OR	AAAGGGGGAAAAAGAAAGGA	PEDIGREE 6
LONP2_IF	AGTCAACCTGGAGTGGCAAT	PEDIGREE 6
LONP2_IR	TGAGTGAGGTCTGGACGGTA	PEDIGREE 6
KARS_OF	CCCAACCATGTCTCACTCCT	PEDIGREE 6
KARS_OR	CCATCGTCCAAGAATCCACT	PEDIGREE 6
KARS_IF	CAACTGCCTGTCTGTTACGC	PEDIGREE 6
KARS_IR	ATTGTTGTGATCCGTGTTGC	PEDIGREE 6
BC021891_OF	CGTTTCAGTGGTGGTGTTTG	PEDIGREE 6
BC021891_OR	GAGCCAGGATCTGGAGTGAG	PEDIGREE 6
BC021891_IF	TGCAAAGACAGCCAGAGAGA	PEDIGREE 6
BC021891_IR	GAGCATTCCCCAAAGATGAC	PEDIGREE 6
HTR1B_OF	GAAACCAGCAGGCATCCTTA	PEDIGREE 6
HTR1B_OR	GCTGTCGTCGGATATCACCT	PEDIGREE 6
HTR1B_IF	TGATCCCTAGGGTCTTGGTG	PEDIGREE 6
HTR1B_IR	CTGGTGTGGGTCTTCTCCAT	PEDIGREE 6
NHSL1_OF	AAGCGCTTTTTGAAGCAGTC	PEDIGREE 6
NHSL1_OR	CTCAAGGTCCCTGGAAATGA	PEDIGREE 6
NHSL1_IF	CCATGTGACCTGGCTAACCT	PEDIGREE 6
NHSL1_IR	TCCACTGCACAGAGCGTAAC	PEDIGREE 6
FZR1_OF	AGCCCTGGCTTACCTTTTGT	PEDIGREE 6
FZR1_OR	AGGGCATAGCCTCATGTGAT	PEDIGREE 6
FZR1_IF	GCTTGCTGCTGAGGGAATAC	PEDIGREE 6
FZR1_IR	GACAATGGCAAAGGTGAGG	PEDIGREE 6
SUPT6_OF	GCTGGTATCCCAGGAGGAAC	PEDIGREE 6
SUPT6_OR	GCTCCCCGGTGTTCATAAAT	PEDIGREE 6
SUPT6_IF	GAAGGTGGGCTTCTCCTTCT	PEDIGREE 6
SUPT6_IR	CTTTGCAGTGGGGTGAGATT	PEDIGREE 6
DDX46_OF	AAACTGGCCTTTGTCCTCCT	PEDIGREE 6
DDX46_OR	GCACTTCTTTTCCCGTGTTC	PEDIGREE 6
DDX46_IF	TTCCCACAAGACAAGTGCAG	PEDIGREE 6
DDX46_IR	GGGCCAATAAAGAGGAGGAG	PEDIGREE 6
AGTPBP1_OF	AGGTGACTGACTTGGCTGCT	PEDIGREE 6
AGTPBP1_OR	GGTGAACGTGTGTTTGTTGC	PEDIGREE 6
AGTPBP1_IF	CCTCCTAAAGGGCCAAAAAC	PEDIGREE 6
AGTPBP1_IR	CGGTCTGTGTGAGCAACATT	PEDIGREE 6
GSDMC2_OF	TTGGAAGGGGTGGATTAAAA	PEDIGREE 6
GSDMC2_OR	CACACACCGGCAGATGATAC	PEDIGREE 6
GSDMC2_IF	ATTCCCACTGGCCTAAAACA	PEDIGREE 6
GSDMC2_IR	TCAGGCCTTGCTCATTAGGT	PEDIGREE 6
PCDHGB4_OF	TCAGCCTTTACACCGCTTCT	PEDIGREE 6
PCDHGB4_OR	TTGTCCCTGGTTTTGAGGAC	PEDIGREE 6
PCDHGB4_IF	ATATCCACACCACGCAGCTT	PEDIGREE 6
PCDHGB4_IR	AATGTCCTCCAGCTCCACAC	PEDIGREE 6
PREX2_OF	GCTGATGAGGAAATGGAAGG	PEDIGREE 13
PREX2_OR	CCCTATGCACCTTCCAAAAA	PEDIGREE 13
PREX2_IF	CTGGGCAGTGATTAGCACAA	PEDIGREE 13
PREX2_IR	TGGGACAATACTGGGGACAC	PEDIGREE 13
PLA2G4A_OF	TCAGGGAAGCTGAGAAGGAA	PEDIGREE 13
PLA2G4A_OR	AGAGGAACGTGACCCATCTG	PEDIGREE 13

PLA2G4A_IF	TAAGGCACCATGTTTTGCAT	PEDIGREE 13
PLA2G4A_IR	GTGGCTGACTAGGGAATGGA	PEDIGREE 13
ABCA2_OF	ATGTGCCTGGAGTCCTTCAC	PEDIGREE 13
ABCA2_OR	AATCTTCCGCACCATAGGAG	PEDIGREE 13
ABCA2_IF	AACATGTCCCTGCCACCTAC	PEDIGREE 13
ABCA2_IR	CCAAAGGATGCTGGGATAGA	PEDIGREE 13
IGSF10_OF	CTGCGAGGCAGTTTCTATCC	PEDIGREE 13
IGSF10_OR	GCGCTGCCTCTAATCCACTA	PEDIGREE 13
IGSF10_IF	AGTGCCCCTGACTGAAGAAA	PEDIGREE 13
IGSF10_IR	TTCCTGGATACTCGCAAACC	PEDIGREE 13
CPA1_OF	TGAGCATCAGAACTGGGTCA	PEDIGREE 13
CPA1_OR	GACCTACTTGCCCCTTCCTC	PEDIGREE 13
CPA1_IF	ACCATTTCCCTGCCTCTTTT	PEDIGREE 13
CPA1_IR	ACTTGTGGGGCTCAAAGGTA	PEDIGREE 13
MITF_OF	ACCTGAAAGCCCCGAATAAC	PEDIGREE 13
MITF_OR	GCTTTCCCTTTCCACTTTCC	PEDIGREE 13
MITF_IF	AGCTCAGAGGCACCAGGTAA	PEDIGREE 13
MITF_IR	GTGATGGGAGTTACGGAAGC	PEDIGREE 13
CHD4_OF	CTGTGGTTGAGAGCATGGTG	PEDIGREE 13
CHD4_OR	CTTACGGCTCCGACTACTGC	PEDIGREE 13
CHD4_IF	GCAAAGGTGCAGTGGAATTT	PEDIGREE 13
CHD4_IR	AATCGTCGTCCTCACTCTGG	PEDIGREE 13
SETD1A_OF	CGAGAGAAGGAAGCTGGAGA	PEDIGREE 13
SETD1A_OR	CCTCTAGGACCTGGGGAGAG	PEDIGREE 13
SETD1A_IF	CAAGGCAAACACCGAAAATC	PEDIGREE 13
SETD1A_IR	GGGCATTGGCTAACACAACT	PEDIGREE 13
1700029H14RIK_OF	TAAGAAAAGCCCCAAGCAAA	PEDIGREE 13
1700029H14RIK_OR	CCTAGAGCCAGCATGACCTC	PEDIGREE 13
1700029H14RIK_IF	AGAAAGGCAGGGTTTCCATT	PEDIGREE 13
1700029H14RIK_IR	GAGATGCCTTTGGTCTGAGG	PEDIGREE 13
OLFR904_OF	TCGCTATGTGGCCATCTGTA	PEDIGREE 13
OLFR904_OR	AGCATGCCTCTAACCACAGG	PEDIGREE 13
OLFR904_IF	TGCCATGTCCCCTAAATTGT	PEDIGREE 13
OLFR904_IR	GGATTCATCATGGGAACCAC	PEDIGREE 13
NUP43_OF	CACAGGTTTCCAAAGCCAAT	PEDIGREE 13
NUP43_OR	GGACCCTCTGATGCTCTCAA	PEDIGREE 13
NUP43_IF	GTCATGCTCCCTCATGGACT	PEDIGREE 13
NUP43_IR	CAAATGCCACTTTCTGGTGA	PEDIGREE 13
KCNMB1_OF	GTTACCAGAGGCCAGAGCAG	PEDIGREE 13
KCNMB1_OR	TCAGAGGCATTTGTGCAGAC	PEDIGREE 13
KCNMB1_IF	GCTCCATGTAAGTTGCAAAGC	PEDIGREE 13
KCNMB1_IR	ATGCCTCGTCTGTCCTGACT	PEDIGREE 13
2700049A03RIK_OF	TGAGCCATCTCTCTAGCCCTAA	PEDIGREE 13
2700049A03RIK_OR	GCCTTGCTGGAAAAAGTGAG	PEDIGREE 13
2700049A03RIK_IF	GTGTGTGTGTGTGGTGCTCA	PEDIGREE 13
2700049A03RIK_IR	CTAAGCAGCCTCCTGCAATC	PEDIGREE 13
TEX21_OF	GCTGTTGCTGGTGTATGAGG	PEDIGREE 13
TEX21_OR	GGTTCCCGTGTTTTGTTTTG	PEDIGREE 13
TEX21_IF	GACCTCTTGCTCTCGTCCTG	PEDIGREE 13

TEX21_IR	CAGAGGGCTGAGGAGCTCTA	PEDIGREE 13
TTLL5_OF	GCATGAAATGGTGACCAAAA	PEDIGREE 13
TTLL5_OR	GAACAAATCTGGCCTCGGTA	PEDIGREE 13
TTLL5_IF	GGTGGTGGAAGTTCAGGAAG	PEDIGREE 13
TTLL5_IR	AACTGGCTGAGAAACGGAGA	PEDIGREE 13
VRK1_OF	CAGTGCGTCCGCATACTAAA	PEDIGREE 13
VRK1_OR	ACACACACACGTCGGCTAAG	PEDIGREE 13
VRK1_IF	AGAGGGTTCAAGGGCCTAAG	PEDIGREE 13
VRK1_IR	ACCACACCTGCCTAAGGTGA	PEDIGREE 13
VMN1R-PS103_OF	CACACGAACACACATGCAAA	PEDIGREE 13
VMN1R-PS103_OR	CCAGATGCTCTGGGACTGAT	PEDIGREE 13
VMN1R-PS103_IF	TCCCACAGACCACAGGATAA	PEDIGREE 13
VMN1R-PS103_IR	CCACTCTCCCCAGGTAAACA	PEDIGREE 13
RREB1_OF	CATCGAGAGCTACGTGCTTG	PEDIGREE 13
RREB1_OR	ATTGCCCAAGAGGGGAGTAT	PEDIGREE 13
RREB1_IF	AGAGGGCAGCTGTGTCACTT	PEDIGREE 13
RREB1_IR	TGAGTGTGGGGCTCTAGCTT	PEDIGREE 13
PHACTR1_OF	CCTAATGGGCACAAAGAGGA	PEDIGREE 13
PHACTR1_OR	GCATCCCGTGAAAATAGCAT	PEDIGREE 13
PHACTR1_IF	CTCATAGGACACACCCATGC	PEDIGREE 13
PHACTR1_IR	AATGAGCATCCCAAGTCCTG	PEDIGREE 13
GM3558_OF	CTCAAGAAGGGCTCCAACAC	PEDIGREE 13
GM3558_OR	TCCTGTGGAATATGGCTGGT	PEDIGREE 13
GM3558_IF	TTGAACCAGGCTACCTCCAC	PEDIGREE 13
GM3558_IR	ATGACCTGCCTCTGTTTGGT	PEDIGREE 13
PNP2_OF	GGCTGCAAGATGGACTCATT	PEDIGREE 13
PNP2_OR	CTCCCGAGTCACACCAAGTT	PEDIGREE 13
PNP2_IF	CAGCGAGTGCTCTGCACTAA	PEDIGREE 13
PNP2_IR	CAGGTGAAGGCAGTGTCAAA	PEDIGREE 13
GGA1_OF	CATCGAGGAGGTCAACAACA	PEDIGREE 13
GGA1_OR	CCAGGCAGGGAGTAGAGACA	PEDIGREE 13
GGA1_IF	CACCCCAACCCACTCATAAC	PEDIGREE 13
GGA1_IR	GATACACTGGGGCTGTGACC	PEDIGREE 13
OLFR175-PS1_OF	GGTACTGCAGAGGGTTGCAT	PEDIGREE 13
OLFR175-PS1_OR	CCTGGGAATTTCAACGATGT	PEDIGREE 13
OLFR175-PS1_IF	AGCAGTCTGCAGTTTCAGCA	PEDIGREE 13
OLFR175-PS1_IR	AGGCAGTGGGTGGTGTTTAC	PEDIGREE 13
GANAB_OF	TGGGGTTTTGATTGGGATAA	PEDIGREE 13
GANAB_OR	CCCATTTCATTTGCCTGTTT	PEDIGREE 13
GANAB_IF	CCTGGGCATGAACAAAGAAT	PEDIGREE 13
GANAB_IR	CTTACAAACAAGGCCCTGGA	PEDIGREE 13
1700028P14RIK_OF	CCTCCAGAACTCTTGCTCCA	PEDIGREE 13
1700028P14RIK_OR	TGGTGTTTCTGCGACAGTCT	PEDIGREE 13
1700028P14RIK_IF	ACAGCATGCTAAGCACTCCA	PEDIGREE 13
1700028P14RIK_IR	TCAGCATTCCTTGAAAAGAGG	PEDIGREE 13
ARL6IP5_OF	AACCACTTCCAGCCAATCAC	BURDEN ANALYSIS TOP HIT
ARL6IP5_OR	TCAGCGTTTTCCTCACCTCT	BURDEN ANALYSIS TOP HIT
ARL6IP5_IF	TTTAACCGCAGAACCAATCC	BURDEN ANALYSIS TOP HIT
ARL6IP5_IR	GAAAGGGGACCTCAGAGAGC	BURDEN ANALYSIS TOP HIT

ITGB6_1_OF	GGAGGTGATACCTGGTCCAA	BURDEN ANALYSIS TOP HIT
ITGB6_1_OR	CAGCCCCCTCATTACCATAA	BURDEN ANALYSIS TOP HIT
ITGB6_1_IF	ACATTGGCAGTGGAACACAA	BURDEN ANALYSIS TOP HIT
ITGB6_1_IR	GGCACCTGCTTTGAGCTACT	BURDEN ANALYSIS TOP HIT
ITGB6_2_OF	GTCGCAGTCACATTCTGCAC	BURDEN ANALYSIS TOP HIT
ITGB6_2_OR	GCAGCACATCATAGGTTGGA	BURDEN ANALYSIS TOP HIT
ITGB6_2_IF	CACATTGAAGGATGCCTGGT	BURDEN ANALYSIS TOP HIT
ITGB6_2_IR	CCTCCTTCCACAGCAAGAGT	BURDEN ANALYSIS TOP HIT
ITGB6_3_OF	AGATCCAATCTCGAGGCAGA	BURDEN ANALYSIS TOP HIT
ITGB6_3_OR	AAAGGGCAGCTTATCATCCA	BURDEN ANALYSIS TOP HIT
ITGB6_3_IF	TACCTGCAAGGGTTGGTGAT	BURDEN ANALYSIS TOP HIT
ITGB6_3_IR	TCCTCACTGCTGAGGGATTT	BURDEN ANALYSIS TOP HIT
ITGB6_4_OF	GGACAGGCAAAGCAGAAAAG	BURDEN ANALYSIS TOP HIT
ITGB6_4_OR	CACCAAATGCTCTCCTTGGT	BURDEN ANALYSIS TOP HIT
ITGB6_4_IF	GGGAAGGTGGGGAGACTTAG	BURDEN ANALYSIS TOP HIT
ITGB6_4_IR	CCGGTGTTTCTATTGTGCTG	BURDEN ANALYSIS TOP HIT
C6_1_OF	ATGGCAGGCTAGGAGAGACA	BURDEN ANALYSIS TOP HIT
C6_1_OR	TCATTGAATTGAACAGCGAAA	BURDEN ANALYSIS TOP HIT
C6_1_IF	CCTATGGGATGCGCTACAGT	BURDEN ANALYSIS TOP HIT
C6_1_IR	TTAAATGACAGGCAGCCTCA	BURDEN ANALYSIS TOP HIT
C6_2_OF	TCACATTTTCCTCCGAGCTT	BURDEN ANALYSIS TOP HIT
C6_2_OR	CTGTTCCGCAGTGAGATGAA	BURDEN ANALYSIS TOP HIT
C6_2_IF	GTTCCTTTTTGCAGGGATCA	BURDEN ANALYSIS TOP HIT
C6_2_IR	CGGCAAGTGTGAACAATTTTA	BURDEN ANALYSIS TOP HIT
C6_3_OF	GCTCCAATTTTATCCCACGTT	BURDEN ANALYSIS TOP HIT
C6_3_OR	TGCTGGGTAAATGACTCATCC	BURDEN ANALYSIS TOP HIT
C6_3_IF	TGAGCCTTCCTCTGGAGTCA	BURDEN ANALYSIS TOP HIT
C6_3_IR	TGACCTCATTGGGTTTTGGT	BURDEN ANALYSIS TOP HIT
C6_4_OF	GGTAGCCCTCGCTGCTTATT	BURDEN ANALYSIS TOP HIT
C6_4_OR	CAACTCCATGCAGCACATCT	BURDEN ANALYSIS TOP HIT
C6_4_IF	CCCATGAGTACTGCATCCAC	BURDEN ANALYSIS TOP HIT
C6_4_IR	GCTTCTTGTTGCTTGATTGC	BURDEN ANALYSIS TOP HIT
CPN1_1_OF	CGGGAGACTTTCTTCACAGC	BURDEN ANALYSIS TOP HIT
CPN1_1_OR	TAGCCTAGGCAGACCTGGAA	BURDEN ANALYSIS TOP HIT
CPN1_1_IF	CCAGAGTCCCCAGCTTACAG	BURDEN ANALYSIS TOP HIT
CPN1_1_IR	CTCAGGAACAGCTCTGTGGA	BURDEN ANALYSIS TOP HIT
CPN1_2_OF	TCATTGAGGACTTGCTGCTG	BURDEN ANALYSIS TOP HIT
CPN1_2_OR	TCAGCTAGCCTCCTGCATCT	BURDEN ANALYSIS TOP HIT
CPN1_2_IF	TGCGTGCTTAATTCTTGACG	BURDEN ANALYSIS TOP HIT
CPN1_2_IR	TGTCCATTTGTCTGTCCTTCC	BURDEN ANALYSIS TOP HIT
SNTG1_1_OF	AATATGGCCCCTTCAGCTTT	BURDEN ANALYSIS TOP HIT
SNTG1_1_OR	AGAAATGTTGGTGGCACCTG	BURDEN ANALYSIS TOP HIT
SNTG1_1_IF	TCTGGAGTAATGCCTTTCAATG	BURDEN ANALYSIS TOP HIT
SNTG1_1_IR	TGGTGTTGGGGCACATTATT	BURDEN ANALYSIS TOP HIT
SNTG1_2_OF	ACGCACACACTCACACACAC	BURDEN ANALYSIS TOP HIT
SNTG1_2_OR	CGAAGGGAAATGTCTGCCTA	BURDEN ANALYSIS TOP HIT
SNTG1_2_IF	TGCATTTCTATTTGCCCCTAA	BURDEN ANALYSIS TOP HIT
SNTG1_2_IR	GGGCTGCTTTTTATTGGAGA	BURDEN ANALYSIS TOP HIT
SNTG1_3_OF	TGTGATCCCAGTCTTTTCCTG	BURDEN ANALYSIS TOP HIT

SNTG1_3_OR	GTGCCTGTGTACATGGGAGT	BURDEN ANALYSIS TOP HIT
SNTG1_3_IF	CATCCCAGATTACAACCCACT	BURDEN ANALYSIS TOP HIT
SNTG1_3_IR	CTTTGTGGTCCAGATTGTGGT	BURDEN ANALYSIS TOP HIT
PLAC8_OF	CAAGCCCAGCTTCAACTTGT	BURDEN ANALYSIS TOP HIT
PLAC8_OR	GAGGGTGGAGGGAGAGAACT	BURDEN ANALYSIS TOP HIT
PLAC8_IF	GAGATGGCACGGGAGACTTA	BURDEN ANALYSIS TOP HIT
PLAC8_IR	CGCACTCGAACACACACAC	BURDEN ANALYSIS TOP HIT
ITPRIP_1_OF	AGGGCCATCTGAAACCACTT	BURDEN ANALYSIS TOP HIT
ITPRIP_1_OR	ACCTCTGGACCACACTCTGC	BURDEN ANALYSIS TOP HIT
ITPRIP_1_IF	ACCAGAACTCTGGGTGGAAG	BURDEN ANALYSIS TOP HIT
ITPRIP_1_IR	GGTCCTCTTCCTGATCATCG	BURDEN ANALYSIS TOP HIT
ITPRIP_2_OF	AGCAGATCATCCACGAAACC	BURDEN ANALYSIS TOP HIT
ITPRIP_2_OR	GGAGACAGCTATCGGCTGAG	BURDEN ANALYSIS TOP HIT
ITPRIP_2_IF	CCTCGATGATCAGGAAGAGG	BURDEN ANALYSIS TOP HIT
ITPRIP_2_IR	AGAGCCAGAACCATCACCAG	BURDEN ANALYSIS TOP HIT
CES3B_1_OF	ACTGCCTGACCCTCAACATC	BURDEN ANALYSIS TOP HIT
CES3B_1_OR	TTTTGCCTCTTGGTTTTTGG	BURDEN ANALYSIS TOP HIT
CES3B_1_IF	GACCCCATCCAACTCGACTA	BURDEN ANALYSIS TOP HIT
CES3B_1_IR	GCCACACCCAGCTTTTACAT	BURDEN ANALYSIS TOP HIT
CES3B_2_OF	AGCTGAGCTGGTCCAGTGTT	BURDEN ANALYSIS TOP HIT
CES3B_2_OR	ATTTCCAGGGGCTTAATGCT	BURDEN ANALYSIS TOP HIT
CES3B_2_IF	TGGTGACAGTGGCTCAGAAC	BURDEN ANALYSIS TOP HIT
CES3B_2_IR	AACCATTCACCACCACGAAT	BURDEN ANALYSIS TOP HIT
CES3B_3_OF	TGCTGCTCTCTGGAATTGTG	BURDEN ANALYSIS TOP HIT
CES3B_3_OR	GTATCCTGCCCGAAGTACCA	BURDEN ANALYSIS TOP HIT
CES3B_3_IF	GGGCTACACTGCACTTCTCC	BURDEN ANALYSIS TOP HIT
CES3B_3_IR	GGGCTTGAAGGTTGCTGTAG	BURDEN ANALYSIS TOP HIT
FABP6_1_OF	TTCAAGATCCTCCTGGCTTG	BURDEN ANALYSIS TOP HIT
FABP6_1_OR	GACCAGCCCCCACTTTTTAT	BURDEN ANALYSIS TOP HIT
FABP6_1_IF	TGTTGAGATTGCAGGCATTT	BURDEN ANALYSIS TOP HIT
FABP6_1_IR	GTCCACCAAGCCAGCTCTAC	BURDEN ANALYSIS TOP HIT
FABP6_2_OF	CCCAAGAGTTTGGGTTCCTA	BURDEN ANALYSIS TOP HIT
FABP6_2_OR	AGGCTGAGGAGAGCTTAGGG	BURDEN ANALYSIS TOP HIT
FABP6_2_IF	CAGGGAAGGGACACAAAGAA	BURDEN ANALYSIS TOP HIT
FABP6_2_IR	GGCTGAGCAGAGAGGTGAAT	BURDEN ANALYSIS TOP HIT
STXBP3A_1_OF	GTGCCAAAGGCAAAACAAAT	BURDEN ANALYSIS TOP HIT
STXBP3A_1_OR	CCTCACCTGCCTCATGTCTT	BURDEN ANALYSIS TOP HIT
STXBP3A_1_IF	CAACACAGGCTTTGGTGCTA	BURDEN ANALYSIS TOP HIT
STXBP3A_1_IR	TGCATGTTGGGATGACTGTT	BURDEN ANALYSIS TOP HIT
STXBP3A_2_OF	CACGCCTGGTGACCTAAGTT	BURDEN ANALYSIS TOP HIT
STXBP3A_2_OR	TGCTAAGCGTTTGCACAGAG	BURDEN ANALYSIS TOP HIT
STXBP3A_2_IF	CGCATGCGTTCTCTCTCTAA	BURDEN ANALYSIS TOP HIT
STXBP3A_2_IR	TGAGAAAGGACTCCCACCAG	BURDEN ANALYSIS TOP HIT
STXBP3A_3_OF	TGAAGCAGAGCTTGTTCATTG	BURDEN ANALYSIS TOP HIT
STXBP3A_3_OR	AGCCATGAGCCAGTTAAGGA	BURDEN ANALYSIS TOP HIT
STXBP3A_3_IF	GAAGCAAGGGACTGCTATGC	BURDEN ANALYSIS TOP HIT
STXBP3A_3_IR	CCTTCCTGAGAATTGTTTGTTTC	BURDEN ANALYSIS TOP HIT
SCAPER_1_OF	GAGTGATCTGAGCCGAGAGG	BURDEN ANALYSIS TOP HIT
SCAPER_1_OR	TTTCCCTAGGCTGGGAGTTT	BURDEN ANALYSIS TOP HIT

SCAPER_1_IF	GGGAAAAGACGATTCTGTGC	BURDEN ANALYSIS TOP HIT
SCAPER_1_IR	GTCTGTTGTAGGGGCAGAGG	BURDEN ANALYSIS TOP HIT
SCAPER_2_OF	ACTATGGGCTCACCCCTTTC	BURDEN ANALYSIS TOP HIT
SCAPER_2_OR	ATAGCCTTTGCCTTCCCTTC	BURDEN ANALYSIS TOP HIT
SCAPER_2_IF	CTTCTTGGTTTGGGAATGGA	BURDEN ANALYSIS TOP HIT
SCAPER_2_IR	TTCCCTGCAGTGAGAGATCA	BURDEN ANALYSIS TOP HIT
SCAPER_3_OF	TGGCCTCAGACTCACAGAGA	BURDEN ANALYSIS TOP HIT
SCAPER_3_OR	AGTGCATGGACAGATTTGGA	BURDEN ANALYSIS TOP HIT
SCAPER_3_IF	CAGCAGGGCCAAGTTTTAAG	BURDEN ANALYSIS TOP HIT
SCAPER_3_IR	TCTTCAGACCTGAGGGGTCTA	BURDEN ANALYSIS TOP HIT
ZFP386_1_OF	TTGTGGATTGCCTGCTACTG	BURDEN ANALYSIS TOP HIT
ZFP386_1_OR	TGGTGCTGACCAAGAATTGA	BURDEN ANALYSIS TOP HIT
ZFP386_1_IF	TCTGGTCAGCGTGACAAAGT	BURDEN ANALYSIS TOP HIT
ZFP386_1_IR	TCTGCCACATTCTTCACACC	BURDEN ANALYSIS TOP HIT
ZFP386_2_OF	CAAGCCTTCAGAAACACCAAG	BURDEN ANALYSIS TOP HIT
ZFP386_2_OR	TGTAGGGTTTCTCCCAAGGA	BURDEN ANALYSIS TOP HIT
ZFP386_2_IF	TGTGCAGAATGTGGCAAATC	BURDEN ANALYSIS TOP HIT
ZFP386_2_IR	CCCCCAGTTTGAATTAGAGGA	BURDEN ANALYSIS TOP HIT
PYHIN1_OF	ATGGCCCATTTCACAATCTC	SHARED VARIANT
PYHIN1_OR	TCAGAATGCCCCCAAAGATA	SHARED VARIANT
PYHIN1_IF	ATGGCATGGGTCTTTCACTC	SHARED VARIANT
PYHIN1_IR	CACCAAAATAGGCCATGTCA	SHARED VARIANT
PLCB4_OF	TCTTGGGAAGGACCATGAAG	SHARED VARIANT
PLCB4_OR	TCATAATAGCAGCCCCAAGG	SHARED VARIANT
PLCB4_IF	TGAAAATGCCCCTGTCTTCT	SHARED VARIANT
PLCB4_IR	GCAGTGAAGCTGCCGATATT	SHARED VARIANT

Appendix 4-3: gRNA sequences, primers, and templates

Gene	Active Guide Sequence	PCR Genotyping Primers	Amplicon Size	Synthetic template
Arl6ip5	GTTTCGCCCGGCCGGACTTC	Primer1: 5' GGATAAAGCCCACTGCTCTG 3' Primer2: 5' TGGGAGGGGGTAGTTCTCAT 3'	663 bp	5' tcgatttcttggctttatatatcttGATCACTAATACGACTCACTATAGGGTTTCGCCCGGCCGGACTTCgttttagagctaGAAAtagcaagttaaaataaggctagtccgttatcaacttgaaaaagtggcaccgagtcggtgctttt 3'
C6	gCGATAAGCTTTGTATCAAGC	Primer1: 5' GAAGGGATTCCTGTGTGGCTT 3' Primer2: 5' TGGTATGACCAGAGGTGGAC 3'	679 bp	5' tcgatttcttggctttatatatcttGATCACTAATACGACTCACTATAGGCGATAAGCTTTGTATCAAGCgttttagagctaGAAAtagcaagttaaaataaggctagtccgttatcaacttgaaaaagtggcaccgagtcggtgctttt 3'
Ces3b	GAGAACCGAAGAGGTCCCAC	Primer1: 5' ACAAATAGACGCTGGAGGAGC 3' Primer2: 5' CCCTTGTAGCCCAGGGTATT 3'	673 bp	5' tcgatttcttggctttatatatcttGATCACTAATACGACTCACTATAGGGAGAACCGAAGAGGTCCCACgttttagagctaGAAAtagcaagttaaaataaggctagtccgttatcaacttgaaaaagtggcaccgagtcggtgctttt 3'
*Cpn1**	g1: gACAGCTGCAGAAGCAGCTCG* g2: GCTGTCGGAATTCCTCTGCG*	Primer1: 5' CAGGGATGGTTGGACACAGG 3' Primer2: 5' TGAGGTTAGCTGGACTGGTG 3'	815 bp	NA
Itgb6	GCAGCTTTCTGCACCACCCC	Primer 1: 5' CAGGTGTTGAACAGGAGGCT 3' Primer2: 5' TGGCCACCAATTATCCAGACA 3'	810 bp	5' tcgatttcttggctttatatatcttGATCACTAATACGACTCACTATAGGGCAGCTTTCTGCACCACCCCgttttagagctaGAAAtagcaagttaaaataaggctagtccgttatcaacttgaaaaagtggcaccgagtcggtgctttt 3'
Sntg1	AGGTGTAACCGGACTTTAAA	Primer 1: 5' CACTGTTATACGACAGCCAGGA 3' Primer2: 5' CAGCCTGAGTCTCACTTTGG 3'	607 bp	5' t tcgatttcttggctttatatatcttGATCACTAATACGACTCACTATAGGAGGTGTAACCGGACTTTAAAgttttagagctaGAAAtagcaagttaaaataaggctagtccgttatcaacttgaaaaagtggcaccgagtcggtgctttt 3'

*Neither sgRNA *Cpn1*-g1 nor *Cpn1*-g2 were active when tested with in vitro assays. Zygote microinjection with the guide sequences in pX330-U6-Chimeric_BB-CBh-hSpCas9 nevertheless resulted in gene-editing in mice.

Appendix 4-4: Potentially deleterious ENU-induced variants from WES in genes with >1 mutation

C	Position	R	A	Type	Mouse ID	Gene	E	AA	#	P-val
2	76708957	T	C	NS	45755	*Ttn*	186	p.T26235A	15	4.0E-02
2	76718079	T	A	NS	83071	*Ttn*	180	p.T23633S	15	4.0E-02
2	76742907	T	TC	FSI	10562	*Ttn*	154	p.K17554fs	15	4.0E-02
2	76742918	T	C	NS	83411	*Ttn*	154	p.N17550S	15	4.0E-02
2	76747394	T	C	NS	96440	*Ttn*	154	p.D16058G	15	4.0E-02
2	76757126	C	T	NS	90152	*Ttn*	145	p.R13214H	15	4.0E-02
2	76758848	T	C	NS	10382	*Ttn*	143	p.T12997A	15	4.0E-02
2	76759160	C	T	NS	11187	*Ttn*	142	p.R12923H	15	4.0E-02
2	76764765	A	G	NS	82147	*Ttn*	133	p.I12020T	15	4.0E-02
2	76768436	C	T	NS	11477	*Ttn*	132	p.A11051T	15	4.0E-02
2	76769813	C	T	NS	2383	*Ttn*	129	p.E10679K	15	4.0E-02
2	76781067	A	G	NS	10653	*Ttn*	110	p.C9047R	15	4.0E-02
2	76856801	A	G	SP	96868	*Ttn*	na	na	15	4.0E-02
2	76877986	T	A	NS	29035	*Ttn*	93	p.D8018V	15	4.0E-02
2	76889411	G	T	NS	3000	*Ttn*	74	p.A6224E	15	4.0E-02
4	32669030	A	G	NS	83520	*Mdn1*	6	p.T363A	5	2.3E-02
4	32686337	T	C	NS	98313	*Mdn1*	19	p.V868A	5	2.3E-02
4	32726897	A	C	NS	11600	*Mdn1*	52	p.K2652T	5	2.3E-02
4	32746482	A	G	NS	83164	*Mdn1*	76	p.S4143G	5	2.3E-02
4	32760731	A	G	NS	11478	*Mdn1*	89	p.E4927G	5	2.3E-02
7	56100169	T	A	NS	51255	*Herc2*	13	p.S564R	5	1.4E-02
7	56138950	A	G	NS	82086	*Herc2*	35	p.Q1816R	5	1.4E-02
7	56157762	T	C	NS	91570	*Herc2*	47	p.V2533A	5	1.4E-02
7	56163760	T	A	NS	10451	*Herc2*	49	p.C2580S	5	1.4E-02
7	56206639	T	C	SP	45755	*Herc2*	na	na	5	1.4E-02
14	31265420	T	C	NS	57931	*Dnah1*	67	p.T3541A	5	8.7E-03
14	31269461	T	C	NS	82458	*Dnah1*	59	p.E3120G	5	8.7E-03
14	31269841	T	C	NS	22721	*Dnah1*	58	p.E3068G	5	8.7E-03
14	31292482	C	T	NS	83071	*Dnah1*	34	p.A1769T	5	8.7E-03
14	31307925	G	T	SG	11187	*Dnah1*	10	p.Y474X	5	8.7E-03
15	44479643	T	C	NS	60716	*Pkhd1l1*	6	p.V172A	5	8.7E-03
15	44491110	A	T	NS	80493	*Pkhd1l1*	11	p.D299V	5	8.7E-03
15	44529638	A	T	NS	98491	*Pkhd1l1*	38	p.I1790L	5	8.7E-03
15	44545499	G	T	SP	98172	*Pkhd1l1*	na	na	5	8.7E-03
15	44564366	A	G	NS	76582	*Pkhd1l1*	59	p.D3273G	5	8.7E-03
1	20310555	T	A	NS	83929	*Pkhd1*	50	p.N2687Y	4	2.9E-02
1	20350445	A	T	NS	13019	*Pkhd1*	47	p.I2479N	4	2.9E-02
1	20350524	C	A	NS	83619	*Pkhd1*	47	p.G2453W	4	2.9E-02
1	20364141	T	C	NS	88503	*Pkhd1*	44	p.N2358D	4	2.9E-02
2	40876669	A	T	SG	88129	*Lrp1b*	54	p.C2845X	4	4.1E-02
2	40882215	C	T	NS	89957	*Lrp1b*	52	p.V2775M	4	4.1E-02
2	41122947	T	A	NS	83875	*Lrp1b*	37	p.D1996V	4	4.1E-02
2	41295549	T	G	NS	83010	*Lrp1b*	27	p.T1499P	4	4.1E-02

2	60611441	T	A	NS	13019	*Itgb6*	13	p.N675I	4	1.1E-04
2	60628375	G	T	NS	10562	*Itgb6*	9	p.P401Q	4	1.1E-04
2	60668525	T	G	NS	45755	*Itgb6*	4	p.Q119P	4	1.1E-04
2	60674011	C	T	SP	11468	*Itgb6*	na	na	4	1.1E-04
6	125566323	T	C	NS	10020	*Vwf*	5	p.F173L	4	9.8E-03
6	125665197	T	A	SG	88129	*Vwf*	41	p.C2360X	4	9.8E-03
6	125666677	T	C	NS	83140	*Vwf*	42	p.C2394R	4	9.8E-03
6	125683632	G	A	NS	6927	*Vwf*	49	p.C2701Y	4	9.8E-03
9	55580247	A	C	NS	83971	*Scaper*	30	p.V1270G	4	9.4E-04
9	55685898	A	T	NS	82522	*Scaper*	25	p.V978D	4	9.4E-04
9	55883916	C	T	NS	29035	*Scaper*	9	p.A233T	4	9.4E-04
9	55883919	A	G	NS	83882	*Scaper*	9	p.S232P	4	9.4E-04
13	81433679	A	G	NS	13019	*Gpr98*	70	p.S4749P	4	8.5E-02
13	81522247	T	C	NS	88547	*Gpr98*	32	p.T2327A	4	8.5E-02
13	81543527	T	C	NS	29035	*Gpr98*	23	p.D1647G	4	8.5E-02
13	81592638	C	A	NS	82522	*Gpr98*	4	p.V124L	4	8.5E-02
15	4755321	C	A	NS	29035	*C6*	6	p.T223N	4	1.1E-04
15	4759850	T	G	NS	83010	*C6*	7	p.I259S	4	1.1E-04
15	4781860	C	T	SG	83737	*C6*	9	p.Q397X	4	1.1E-04
15	4789620	A	T	NS	83796	*C6*	10	p.E478V	4	1.1E-04
1	8414292	A	T	NS	14418	*Sntg1*	20	p.F436I	3	5.7E-04
1	8677834	A	T	NS	13019	*Sntg1*	10	p.N112K	3	5.7E-04
1	8681990	A	G	NS	24744	*Sntg1*	7	p.F68L	3	5.7E-04
1	34192554	T	C	NS	11600	*Dst*	39	p.L3254P	3	2.1E-01
1	34266912	T	A	NS	11187	*Dst*	77	p.I6405N	3	2.1E-01
1	34268807	A	G	NS	83685	*Dst*	79	p.T6503A	3	2.1E-01
1	53413767	C	A	NS	83217	*Dnah7a*	63	p.V3851L	3	9.2E-02
1	53565718	A	T	NS	76824	*Dnah7a*	25	p.Y1294N	3	9.2E-02
1	53605839	C	A	NS	80821	*Dnah7a*	20	p.V1013L	3	9.2E-02
1	150573553	C	T	NS	80821	*Hmcn1*	105	p.C5445Y	3	1.5E-01
1	150619087	G	A	SG	98491	*Hmcn1*	81	p.Q4084X	3	1.5E-01
1	150723332	T	A	NS	89965	*Hmcn1*	31	p.D1611V	3	1.5E-01
2	6427781	A	G	NS	80840	*Usp6nl*	13	p.M299V	3	2.2E-03
2	6440935	C	A	NS	89957	*Usp6nl*	15	p.N551K	3	2.2E-03
2	6441137	C	A	NS	88129	*Usp6nl*	15	p.P619T	3	2.2E-03
2	14271327	C	T	SG	13019	*Mrc1*	9	p.Q491X	3	9.6E-03
2	14315239	G	A	NS	83929	*Mrc1*	22	p.V995I	3	9.6E-03
2	14325245	C	T	NS	83882	*Mrc1*	26	p.P1222S	3	9.6E-03
2	21399337	G	A	NS	11082	*Gpr158*	2	p.D307N	3	5.8E-03
2	21810680	A	T	NS	6927	*Gpr158*	8	p.H628L	3	5.8E-03
2	21826776	A	C	NS	10653	*Gpr158*	11	p.T896P	3	5.8E-03
2	59900770	A	G	NS	29035	*Baz2b*	36	p.V2084A	3	2.4E-02
2	59962147	T	C	NS	80840	*Baz2b*	9	p.R546G	3	2.4E-02
2	59978601	G	T	NS	82147	*Baz2b*	5	p.H101Q	3	2.4E-02
2	112728922	T	C	NS	91570	*Ryr3*	64	p.D3039G	3	1.3E-01
2	112756284	A	C	NS	33095	*Ryr3*	55	p.D2740E	3	1.3E-01
2	112756516	T	A	NS	89285	*Ryr3*	54	p.T2728S	3	1.3E-01
3	30936887	A	G	NS	91570	*Phc3*	8	p.S394P	3	3.5E-03
3	30958021	C	T	NS	83875	*Phc3*	4	p.M133I	3	3.5E-03

3	30965808	A	G	NS	60712	*Phc3*	2	p.S48P	3	3.5E-03
3	97699199	A	G	NS	82744	*Pde4dip*	37	p.C1983R	3	3.4E-02
3	97754545	C	T	NS	51255	*Pde4dip*	11	p.E452K	3	3.4E-02
3	97793564	C	A	NS	11187	*Pde4dip*	3	p.R88L	3	3.4E-02
3	108821795	T	C	NS	88547	*Stxbp3a*	6	p.E144G	3	8.3E-04
3	108827107	T	A	NS	83737	*Stxbp3a*	3	p.I34L	3	8.3E-04
3	108827586	T	A	NS	10177	*Stxbp3a*	2	p.E29V	3	8.3E-04
4	128395066	A	C	NS	80821	*Csmd2*	21	p.S1133R	3	7.6E-02
4	128483386	A	T	NS	82086	*Csmd2*	40	p.M2020L	3	7.6E-02
4	128546684	T	C	NS	60716	*Csmd2*	60	p.S3181P	3	7.6E-02
5	3960225	A	T	NS	11468	*Akap9*	7	p.L309F	3	8.2E-02
5	4029850	T	A	NS	76387	*Akap9*	23	p.D1867E	3	8.2E-02
5	4044016	A	T	NS	83929	*Akap9*	28	p.R2179S	3	8.2E-02
5	96657145	G	A	SP	98491	*Fras1*	na	na	3	9.1E-02
5	96691359	C	T	NS	82086	*Fras1*	36	p.T1579M	3	9.1E-02
5	96700523	A	G	NS	96245	*Fras1*	40	p.D1799G	3	9.1E-02
5	124750855	C	T	NS	98313	*Dnah10*	14	p.P755L	3	1.2E-01
5	124754254	T	C	NS	22721	*Dnah10*	16	p.I839T	3	1.2E-01
5	124803391	A	G	NS	88025	*Dnah10*	49	p.D2821G	3	1.2E-01
6	38158085	A	C	NS	96868	*D630045J12 Rik*	11	p.S1387A	3	2.0E-02
6	38195359	A	G	NS	83457	*D630045J12 Rik*	2	p.S625P	3	2.0E-02
6	38196361	C	T	NS	96440	*D630045J12 Rik*	2	p.V291I	3	2.0E-02
6	97210822	T	C	NS	53882	*Arl6ip5*	1	p.M1T	3	3.3E-05
6	97210913	A	T	NS	83217	*Arl6ip5*	1	p.K31N	3	3.3E-05
6	97210957	A	C	NS	83071	*Arl6ip5*	1	p.N46T	3	3.3E-05
6	108381201	A	T	NS	83875	*Itpr1*	18	p.K576M	3	4.3E-02
6	108386813	A	G	NS	6927	*Itpr1*	21	p.T799A	3	4.3E-02
6	108405515	A	G	NS	82194	*Itpr1*	34	p.D1456G	3	4.3E-02
7	75611077	A	T	NS	80821	*Akap13*	7	p.T1150S	3	4.5E-02
7	75723901	T	C	NS	10562	*Akap13*	20	p.S1869P	3	4.5E-02
7	75735725	T	A	NS	11241	*Akap13*	27	p.V2216D	3	4.5E-02
7	105758172	G	A	NS	10722	*Dchs1*	15	p.P2112S	3	6.3E-02
7	105762230	C	A	NS	76278	*Dchs1*	10	p.V1560L	3	6.3E-02
7	105772940	T	C	NS	88955	*Dchs1*	2	p.H91R	3	6.3E-02
7	112059064	T	C	NS	33095	*Usp47*	6	p.Y217H	3	8.3E-03
7	112082440	T	C	NS	76582	*Usp47*	13	p.M486T	3	8.3E-03
7	112086024	C	A	NS	60654	*Usp47*	16	p.H581N	3	8.3E-03
8	14928847	T	C	NS	83140	*Arhgef10*	3	p.V38A	3	7.9E-03
8	14930203	T	C	NS	5401	*Arhgef10*	4	p.S148P	3	7.9E-03
8	14961286	G	A	SP	83685	*Arhgef10*	16	na	3	7.9E-03
8	105085650	T	A	NS	98420	*Ces3b*	4	p.V177D	3	7.5E-04
8	105088716	C	T	NS	24744	*Ces3b*	8	p.T344I	3	7.5E-04
8	105091569	A	T	NS	98313	*Ces3b*	10	p.D401V	3	7.5E-04
11	69421734	T	C	NS	82086	*Dnah2*	83	p.N4335S	3	1.1E-01
11	69463628	A	G	NS	76582	*Dnah2*	43	p.Y2261H	3	1.1E-01
11	69464975	T	C	NS	76278	*Dnah2*	42	p.D2218G	3	1.1E-01

11	117721060	A	G	NS	10382	*Tnrc6c*	5	p.T175A	3	1.9E-02
11	117721327	G	A	NS	88025	*Tnrc6c*	5	p.V264I	3	1.9E-02
11	117749719	T	A	NS	88041	*Tnrc6c*	15	p.M1445K	3	1.9E-02
11	118040981	C	T	SP	98172	*Dnah17*	na	na	3	1.1E-01
11	118041504	C	T	NS	33095	*Dnah17*	68	p.R3632Q	3	1.1E-01
11	118082870	T	C	NS	98420	*Dnah17*	38	p.Y1937C	3	1.1E-01
12	8001795	T	C	NS	3000	*Apob*	22	p.I1120T	3	1.1E-01
12	8002221	G	A	NS	82723	*Apob*	23	p.V1221M	3	1.1E-01
12	8010844	A	T	NS	13019	*Apob*	26	p.I3109L	3	1.1E-01
12	116059795	T	C	NS	96839	*Zfp386*	3	p.S378P	3	9.8E-04
12	116060481	T	A	NS	88129	*Zfp386*	3	p.N606K	3	9.8E-04
12	116060483	A	C	NS	6654	*Zfp386*	3	p.E607A	3	9.8E-04
12	117880550	A	G	NS	11241	*Dnah11*	80	p.L4327P	3	1.1E-01
12	118007969	A	G	NS	29035	*Dnah11*	54	p.L2951P	3	1.1E-01
12	118111061	T	G	NS	89965	*Dnah11*	23	p.D1352A	3	1.1E-01
13	93083378	A	G	NS	88955	*Cmya5*	4	p.C3188R	3	7.8E-02
13	93090556	T	G	NS	11468	*Cmya5*	2	p.I2675L	3	7.8E-02
13	93098044	T	A	NS	5401	*Cmya5*	2	p.I179F	3	7.8E-02
14	31145819	T	A	NS	83875	*Stab1*	48	p.I1665F	3	3.8E-02
14	31150668	T	A	NS	88262	*Stab1*	32	p.Q1135L	3	3.8E-02
14	31154471	G	A	NS	2383	*Stab1*	25	p.T887I	3	3.8E-02
14	47016301	A	G	NS	83217	*Samd4*	3	p.E74G	3	1.4E-03
14	47016462	T	C	NS	51283	*Samd4*	3	p.Y128H	3	1.4E-03
14	47089105	T	C	NS	76278	*Samd4*	10	p.V565A	3	1.4E-03
15	4899191	A	T	NS	80821	*Mroh2b*	1	p.E2V	3	1.2E-02
15	4904241	T	C	NS	51283	*Mroh2b*	4	p.V91A	3	1.2E-02
15	4915225	A	C	NS	83971	*Mroh2b*	13	p.D436A	3	1.2E-02
15	47650098	C	T	SP	83164	*Csmd3*	na	na	3	8.0E-02
15	47659192	A	T	NS	83689	*Csmd3*	52	p.C2694S	3	8.0E-02
15	47838435	A	T	NS	2383	*Csmd3*	31	p.W1751R	3	8.0E-02
15	58052644	A	T	NS	96868	*Zhx1*	3	p.N735K	3	2.5E-03
15	58052719	A	T	NS	2383	*Zhx1*	3	p.D710E	3	2.5E-03
15	58054047	A	G	NS	13019	*Zhx1*	3	p.S268P	3	2.5E-03
15	66705348	A	G	NS	89285	*Tg*	21	p.T1507A	3	4.4E-02
15	66735223	A	G	NS	22721	*Tg*	29	p.D1822G	3	4.4E-02
15	66764268	T	C	NS	83217	*Tg*	38	p.I2187T	3	4.4E-02
16	32751034	C	G	SG	83140	*Muc4*	2	p.S304X	3	7.0E-02
16	32752353	A	C	NS	98420	*Muc4*	2	p.T744P	3	7.0E-02
16	32753289	T	C	NS	96440	*Muc4*	2	p.S1056P	3	7.0E-02
18	49852300	A	G	NS	90152	*Dmxl1*	7	p.T205A	3	5.3E-02
18	49864168	T	G	NS	29035	*Dmxl1*	11	p.D510E	3	5.3E-02
18	49893679	T	A	NS	11468	*Dmxl1*	24	p.S1951R	3	5.3E-02
19	43966248	T	C	NS	2383	*Cpn1*	6	p.K313R	3	4.1E-04
19	43966305	T	C	NS	60716	*Cpn1*	6	p.D294G	3	4.1E-04
19	43973982	T	C	NS	76278	*Cpn1*	3	p.N176S	3	4.1E-04
19	47897442	T	C	NS	89957	*Itprip*	2	p.T245A	3	7.1E-04
19	47897591	A	T	NS	96868	*Itprip*	2	p.M195K	3	7.1E-04
19	47898054	T	A	NS	82841	*Itprip*	2	p.M41L	3	7.1E-04
1	11140236	A	T	NS	11954	*Prex2*	17	p.I588F	2	7.4E-02

1	11170704	T	C	NS	91570	*Prex2*	25	p.L1012S	2	7.4E-02
1	22475705	T	A	NS	82620	*Rims1*	13	p.H539L	2	6.5E-02
1	22726976	A	T	NS	90152	*Rims1*	2	p.C67S	2	6.5E-02
1	36185863	A	T	NS	88041	*Uggt1*	16	p.D563E	2	7.1E-02
1	36221324	T	A	NS	82620	*Uggt1*	5	p.I137L	2	7.1E-02
1	43051769	T	A	NS	83971	*Tgfbrap1*	12	p.D732V	2	2.7E-02
1	43071541	A	G	NS	2383	*Tgfbrap1*	4	p.I268T	2	2.7E-02
1	45376160	A	C	NS	76989	*Col5a2*	54	p.I1473R	2	6.7E-02
1	45422387	A	T	NS	83875	*Col5a2*	10	p.M246K	2	6.7E-02
1	58056280	C	A	NS	10382	*Aox1*	8	p.P218T	2	5.6E-02
1	58082019	A	T	NS	98491	*Aox1*	25	p.E883V	2	5.6E-02
1	58121005	C	A	NS	11468	*Aox3*	5	p.Q116K	2	5.6E-02
1	58152686	A	G	NS	42058	*Aox3*	14	p.I466V	2	5.6E-02
1	63737880	T	A	NS	10451	*Fastkd2*	6	p.Y392N	2	1.8E-02
1	63748048	T	C	NS	91570	*Fastkd2*	9	p.L547S	2	1.8E-02
1	71599302	A	G	NS	24744	*Fn1*	36	p.Y1842H	2	1.4E-01
1	71600419	T	A	NS	83737	*Fn1*	34	p.T1738S	2	1.4E-01
1	74910539	C	T	NS	29035	*Ccdc108*	22	p.V1220M	2	9.2E-02
1	74931987	C	A	NS	96868	*Ccdc108*	3	p.R57S	2	9.2E-02
1	84370841	C	T	NS	91570	*Dner*	13	p.V713M	2	2.1E-02
1	84534898	T	G	NS	82522	*Dner*	5	p.D316A	2	2.1E-02
1	93320773	A	G	SP	14418	*Pask*	na	na	2	6.0E-02
1	93327376	T	C	NS	83188	*Pask*	7	p.D324G	2	6.0E-02
1	116428850	A	G	NS	82458	*Cntnap5a*	16	p.E810G	2	5.4E-02
1	116455155	C	T	NS	83929	*Cntnap5a*	19	p.T1051I	2	5.4E-02
1	127366425	C	T	NS	6927	*Mgat5*	6	p.S168L	2	2.1E-02
1	127390838	C	T	SG	89957	*Mgat5*	10	p.Q357X	2	2.1E-02
1	128589159	A	C	NS	83882	*Cxcr4*	2	p.F255C	2	5.5E-03
1	128589627	T	C	NS	11468	*Cxcr4*	2	p.D99G	2	5.5E-03
1	130449415	A	T	SP	57258	*Cd55*	na	na	2	6.4E-03
1	130452511	A	T	SG	3000	*Cd55*	6	p.Y243X	2	6.4E-03
1	134987027	A	T	NS	83685	*Lgr6*	18	p.L938Q	2	3.3E-02
1	135072889	T	A	NS	10451	*Lgr6*	3	p.I118F	2	3.3E-02
1	135877676	T	C	NS	83794	*Pkp1*	11	p.N674S	2	2.0E-02
1	135877815	T	C	NS	83971	*Pkp1*	11	p.T628A	2	2.0E-02
1	136281454	T	C	NS	57372	*Camsap2*	13	p.M773V	2	6.6E-02
1	136285962	A	T	NS	96440	*Camsap2*	10	p.N371K	2	6.6E-02
1	138080196	A	G	NS	82723	*Ptprc*	22	p.V729A	2	5.3E-02
1	138082755	A	G	NS	51283	*Ptprc*	20	p.C612R	2	5.3E-02
1	153471745	A	G	NS	11468	*Dhx9*	12	p.S405P	2	5.9E-02
1	153472536	T	C	NS	98491	*Dhx9*	10	p.I311M	2	5.9E-02
1	171216511	A	T	NS	89965	*Nr1i3*	4	p.H134L	2	5.5E-03
1	171217077	T	C	NS	5401	*Nr1i3*	6	p.S194P	2	5.5E-03
1	172210373	T	A	NS	45755	*Casq1*	11	p.D397V	2	6.9E-03
1	172216837	T	G	NS	88041	*Casq1*	3	p.D141A	2	6.9E-03
2	20806213	G	T	NS	82620	*Etl4*	18	p.V1318F	2	1.0E-01
2	20806666	A	T	NS	5401	*Etl4*	18	p.M1469L	2	1.0E-01
2	25083688	A	G	NS	91310	*Entpd8*	6	p.D249G	2	1.0E-02
2	25085084	T	A	NS	13019	*Entpd8*	10	p.F476I	2	1.0E-02

2	25888768	T	G	NS	76989	*Kcnt1*	4	p.I76S	2	5.0E-02
2	25907569	T	A	NS	60654	*Kcnt1*	23	p.V844E	2	5.0E-02
2	31898235	G	A	NS	6654	*Lamc3*	2	p.A136T	2	7.3E-02
2	31920676	G	A	NS	80493	*Lamc3*	14	p.A853T	2	7.3E-02
2	49272874	A	G	NS	60712	*Mbd5*	12	p.T1123A	2	8.3E-02
2	49274741	T	A	NS	89285	*Mbd5*	13	p.N1243K	2	8.3E-02
2	52226552	A	G	NS	24744	*Neb*	82	p.L4137P	2	2.7E-01
2	52325788	T	A	NS	88955	*Neb*	8	p.Q169L	2	2.7E-01
2	54857839	C	T	NS	82458	*Galnt13*	7	p.T244M	2	1.2E-02
2	55112905	T	C	NS	83875	*Galnt13*	13	p.C539R	2	1.2E-02
2	62264042	G	T	NS	6927	*Slc4a10*	11	p.Q446H	2	4.3E-02
2	62304731	A	G	NS	91310	*Slc4a10*	22	p.M1008V	2	4.3E-02
2	66501669	G	A	NS	11477	*Scn9a*	22	p.R1279W	2	NA
2	66533091	T	C	NS	42885	*Scn9a*	17	p.M939V	2	NA
2	66697618	A	T	NS	82522	*Scn7a*	15	p.S843T	2	8.0E-02
2	66703908	T	C	NS	88041	*Scn7a*	12	p.I474M	2	8.0E-02
2	69938252	A	T	NS	5401	*Ubr3*	8	p.I468F	2	9.5E-02
2	70020625	T	C	NS	96868	*Ubr3*	37	p.C1796R	2	9.5E-02
2	72398379	G	A	NS	80493	*Zak*	11	p.R314H	2	2.4E-02
2	72416587	T	C	NS	2164	*Zak*	15	p.F417S	2	2.4E-02
2	73381969	G	T	NS	76526	*Gpr155*	3	p.S103R	2	2.7E-02
2	73382172	A	G	NS	11468	*Gpr155*	3	p.S36P	2	2.7E-02
2	77011612	A	T	NS	11187	*Ccdc141*	24	p.S1492T	2	7.0E-02
2	77014433	T	C	NS	82194	*Ccdc141*	23	p.E1430G	2	7.0E-02
2	86041490	C	A	SG	29035	*Olfr1033*	3	p.Y58X	2	4.2E-03
2	86041852	A	T	NS	82522	*Olfr1033*	3	p.D179V	2	4.2E-03
2	91557676	G	A	SP	96868	*Ckap5*	6	na	2	1.0E-01
2	91576022	T	A	NS	83929	*Ckap5*	18	p.N752K	2	1.0E-01
2	104429946	A	G	NS	88129	*Hipk3*	16	p.I1162T	2	4.7E-02
2	104434435	T	C	NS	53882	*Hipk3*	11	p.I736V	2	4.7E-02
2	119071812	T	A	NS	13019	*Casc5*	8	p.S1331R	2	1.1E-01
2	119086628	T	A	NS	88041	*Casc5*	13	p.V1764E	2	1.1E-01
2	125581775	A	T	NS	42058	*Cep152*	20	p.M902K	2	8.4E-02
2	125594919	G	T	NS	5401	*Cep152*	13	p.T567K	2	8.4E-02
2	126826936	C	A	NS	80493	*Trpm7*	17	p.G687C	2	9.3E-02
2	126851501	T	C	NS	96440	*Trpm7*	4	p.T55A	2	9.3E-02
2	129199827	T	A	NS	76278	*Slc20a1*	2	p.F37I	2	1.8E-02
2	129207616	T	G	NS	11477	*Slc20a1*	7	p.V266G	2	1.8E-02
2	129463543	T	C	NS	88262	*F830045P16 Rik*	4	p.T304A	2	9.7E-03
2	129472641	T	A	NS	88503	*F830045P16 Rik*	3	p.I239F	2	9.7E-03
2	130026791	T	C	NS	82522	*Tgm3*	5	p.V216A	2	1.9E-02
2	130042003	A	C	NS	76526	*Tgm3*	10	p.N527T	2	1.9E-02
2	130671460	T	A	SP	45755	*Itpa*	na	na	2	1.7E-03
2	130671577	C	T	NS	83140	*Itpa*	3	p.P49L	2	1.7E-03
2	132934993	C	T	NS	2164	*Fermt1*	5	p.D192N	2	1.8E-02
2	132936051	T	A	NS	82522	*Fermt1*	4	p.N166I	2	1.8E-02
2	135930006	G	A	NS	11600	*Plcb4*	7	p.V141I	2	4.6E-02

2	135950232	T	A	NS	10382	*Plcb4*	13	p.F292I	2	4.6E-02
2	154227156	A	C	NS	82841	*Bpifb5*	3	p.Q131P	2	9.8E-03
2	154228116	A	T	NS	91310	*Bpifb5*	4	p.Q162L	2	9.8E-03
2	155621351	A	T	NS	96245	*Myh7b*	16	p.Q501L	2	9.9E-02
2	155623228	A	G	NS	83737	*Myh7b*	20	p.N668S	2	9.9E-02
2	156506483	A	T	NS	96868	*Epb4.1l1*	9	p.I336F	2	2.8E-02
2	156533791	T	G	NS	11187	*Epb4.1l1*	18	p.L758R	2	2.8E-02
2	157995409	T	C	NS	82522	*Tti1*	4	p.D917G	2	4.0E-02
2	158008170	G	A	NS	33095	*Tti1*	1	p.T383M	2	4.0E-02
2	158036117	T	A	NS	83010	*Rprd1b*	2	p.H91Q	2	4.6E-03
2	158075012	T	A	NS	82395	*Rprd1b*	7	p.L304Q	2	4.6E-03
2	165420006	C	G	NS	83071	*Slc13a3*	10	p.A436P	2	1.4E-02
2	165445620	A	T	NS	76582	*Slc13a3*	3	p.L138Q	2	1.4E-02
2	168182274	A	T	NS	89957	*Adnp*	4	p.W1034R	2	4.1E-02
2	168184598	T	A	NS	11477	*Adnp*	4	p.N259I	2	4.1E-02
2	178363431	T	C	NS	11468	*Sycp2*	28	p.D881G	2	6.7E-02
2	178401911	A	T	NS	60716	*Sycp2*	5	p.M134K	2	6.7E-02
2	181007874	G	A	SP	83685	*Col20a1*	na	na	2	5.5E-02
2	181015604	T	C	NS	2164	*Col20a1*	33	p.I1239T	2	5.5E-02
2	181351091	A	G	NS	76526	*Rtel1*	23	p.Y648C	2	4.8E-02
2	181355986	A	T	NS	10382	*Rtel1*	34	p.R1176W	2	4.8E-02
3	28048031	T	A	SG	60654	*Pld1*	11	p.C310X	2	3.7E-02
3	28076401	A	T	NS	3000	*Pld1*	15	p.H450L	2	3.7E-02
3	31150319	T	A	NS	10177	*Cldn11*	1	p.V57D	2	1.9E-03
3	31163219	T	C	NS	96440	*Cldn11*	3	p.S179P	2	1.9E-03
3	38949600	T	C	NS	2216	*Fat4*	3	p.S1823P	2	2.5E-01
3	38983056	T	G	NS	98420	*Fat4*	9	p.V3619G	2	2.5E-01
3	53516794	C	T	NS	80821	*Frem2*	24	p.R3074H	2	1.8E-01
3	53547681	C	T	NS	10020	*Frem2*	9	p.G2158E	2	1.8E-01
3	59325883	T	A	NS	11954	*Igsf10*	6	p.T1810S	2	1.4E-01
3	59330916	A	T	NS	88025	*Igsf10*	5	p.F615I	2	1.4E-01
3	63697503	T	C	NS	10020	*Plch1*	23	p.D1660G	2	8.0E-02
3	63784035	G	A	NS	83882	*Plch1*	2	p.T49I	2	8.0E-02
3	72949750	G	T	NS	83140	*Sis*	10	p.Q403K	2	9.0E-02
3	72965643	G	A	NS	91310	*Sis*	2	p.P54L	2	9.0E-02
3	87974803	A	G	NS	76278	*Nes*	3	p.T305A	2	9.3E-02
3	87977807	A	T	NS	83737	*Nes*	4	p.R1124S	2	9.3E-02
3	89221030	A	G	NS	89957	*Thbs3*	11	p.T417A	2	3.2E-02
3	89226419	T	C	NS	83140	*Thbs3*	22	p.S930P	2	3.2E-02
3	92824294	C	A	NS	60693	*Kprp*	2	p.R483L	2	1.7E-02
3	92825401	A	G	NS	60654	*Kprp*	2	p.V114A	2	1.7E-02
3	93470911	T	A	NS	3000	*Tchhl1*	3	p.D307E	2	1.6E-02
3	93471635	C	T	NS	83164	*Tchhl1*	3	p.H549Y	2	1.6E-02
3	99885519	G	T	NS	88262	*Spag17*	1	p.G10W	2	1.3E-01
3	100004747	T	C	NS	2383	*Spag17*	7	p.L311P	2	1.3E-01
3	101439500	T	C	NS	83685	*Igsf3*	7	p.F584L	2	4.7E-02
3	101439746	T	C	NS	88547	*Igsf3*	7	p.S666P	2	4.7E-02
3	108752110	A	G	NS	2216	*Aknad1*	2	p.T147A	2	1.8E-02
3	108774984	T	A	NS	60716	*Aknad1*	8	p.D487E	2	1.8E-02

3	125561508	C	A	NS	60654	*Ndst4*	3	p.T355K	2	2.8E-02
3	125710057	A	G	NS	24744	*Ndst4*	10	p.D650G	2	2.8E-02
4	3904355	A	G	NS	88041	*Plag1*	6	p.S279P	2	1.0E-02
4	3904576	A	T	NS	98491	*Plag1*	6	p.V205E	2	1.0E-02
4	8828316	A	C	NS	83875	*Chd7*	13	p.N1086H	2	1.7E-01
4	8854190	C	T	SG	11082	*Chd7*	29	p.Q1921X	2	1.7E-01
4	16129060	A	T	SG	10562	*Ripk2*	8	p.L330X	2	1.2E-02
4	16155078	A	G	NS	11187	*Ripk2*	3	p.L147P	2	1.2E-02
4	19611757	A	G	NS	11478	*Wwp1*	25	p.L905P	2	3.0E-02
4	19618338	C	A	NS	96247	*Wwp1*	24	p.K868N	2	3.0E-02
4	22487008	A	G	NS	60716	*Pou3f2*	1	p.F375S	2	8.2E-03
4	22487038	A	G	NS	10562	*Pou3f2*	1	p.V365A	2	8.2E-03
4	28938644	G	A	NS	42058	*Epha7*	7	p.A500T	2	3.5E-02
4	28963944	A	G	NS	11187	*Epha7*	17	p.S980G	2	3.5E-02
4	43540616	C	T	NS	83685	*Tln1*	34	p.V1462M	2	1.4E-01
4	43548076	A	G	NS	10562	*Tln1*	18	p.V689A	2	1.4E-01
4	49447771	T	C	NS	6654	*Acnat1*	3	p.Y270C	2	7.3E-03
4	49450650	G	T	NS	13019	*Acnat1*	1	p.P154T	2	7.3E-03
4	58946266	T	A	NS	24744	*Zkscan16*	2	p.F47Y	2	2.0E-02
4	58957625	T	C	NS	82086	*Zkscan16*	6	p.S636P	2	2.0E-02
4	65176264	C	T	NS	11082	*Pappa*	3	p.H509Y	2	7.6E-02
4	65204695	A	T	NS	98491	*Pappa*	7	p.T756S	2	7.6E-02
4	75955248	C	T	NS	82522	*Ptprd*	36	p.V1337M	2	6.8E-02
4	75998536	C	T	NS	88547	*Ptprd*	31	p.V1047I	2	6.8E-02
4	82914754	A	G	NS	11468	*Frem1*	30	p.S1900P	2	1.2E-01
4	82916711	T	C	NS	98420	*Frem1*	29	p.E1844G	2	1.2E-01
4	86774361	C	T	NS	88955	*Dennd4c*	2	p.S36L	2	9.6E-02
4	86786082	A	G	NS	83010	*Dennd4c*	6	p.Y278C	2	9.6E-02
4	88178290	T	C	SP	39748	*Focad*	na	na	2	8.8E-02
4	88403376	T	C	NS	96247	*Focad*	41	p.S1655P	2	8.8E-02
4	108513278	A	T	NS	80821	*Zcchc11*	14	p.Q830H	2	7.7E-02
4	108549321	A	G	NS	33095	*Zcchc11*	27	p.D1357G	2	7.7E-02
4	115601108	T	C	NS	83140	*Cyp4a32*	1	p.L45P	2	1.1E-02
4	115611338	A	T	NS	88955	*Cyp4a32*	8	p.H339L	2	1.1E-02
4	116877793	T	C	NS	6654	*Zswim5*	1	p.Y112H	2	4.7E-02
4	116986873	A	G	NS	83520	*Zswim5*	14	p.Q1036R	2	4.7E-02
4	123465902	C	T	NS	88041	*Macf1*	38	p.S3428N	2	2.7E-01
4	123476142	T	A	NS	83230	*Macf1*	36	p.I1609F	2	2.7E-01
4	138096761	A	G	NS	3000	*Eif4g3*	7	p.R21G	2	7.3E-02
4	138206012	A	G	NS	83230	*Eif4g3*	35	p.E1521G	2	7.3E-02
4	138304883	A	C	NS	83071	*Ddost*	1	p.K2T	2	8.0E-03
4	138311958	T	G	NS	89965	*Ddost*	11	p.M434R	2	8.0E-03
4	141474192	T	C	NS	83689	*Spen*	12	p.T2375A	2	2.1E-01
4	141479234	T	A	NS	6654	*Spen*	12	p.Y694F	2	2.1E-01
4	141796525	T	C	NS	5401	*Casp9*	2	p.S75P	2	8.5E-03
4	141805504	T	G	NS	55922	*Casp9*	4	p.F237C	2	8.5E-03
4	143851812	T	C	NS	22721	*Gm13103*	3	p.I214T	2	9.8E-03
4	143851827	G	A	NS	11187	*Gm13103*	3	p.C219Y	2	9.8E-03
4	148483594	A	T	NS	98491	*Mtor*	21	p.I1053F	2	1.4E-01

4	148549380	T	A	NS	83188	*Mtor*	51	p.N2343K	2	1.4E-01
4	149650647	C	T	NS	76526	*Pik3cd*	24	p.R1045Q	2	3.8E-02
4	149654297	T	C	NS	76278	*Pik3cd*	17	p.Q723R	2	3.8E-02
4	152031440	T	A	NS	76278	*Tas1r1*	4	p.I453F	2	2.6E-02
4	152034647	G	A	NS	55922	*Tas1r1*	2	p.T155I	2	2.6E-02
4	156169312	T	A	SG	83882	*Agrn*	31	p.K1749X	2	1.1E-01
4	156175098	A	T	SP	57258	*Agrn*	na	na	2	1.1E-01
5	21760695	G	A	NS	83929	*Dnajc2*	14	p.H487Y	2	1.5E-02
5	21768554	A	T	NS	91570	*Dnajc2*	9	p.N272K	2	1.5E-02
5	23473531	T	C	NS	80840	*Kmt2e*	7	p.Y203H	2	9.3E-02
5	23485514	T	A	NS	98172	*Kmt2e*	13	p.M509K	2	9.3E-02
5	32316649	G	A	NS	42885	*Plb1*	26	p.V507I	2	6.6E-02
5	32317492	C	A	NS	5401	*Plb1*	29	p.H591N	2	6.6E-02
5	64264336	T	C	NS	11600	*Tbc1d1*	6	p.I357T	2	4.5E-02
5	64279375	T	A	NS	11478	*Tbc1d1*	10	p.D523E	2	4.5E-02
5	66276573	T	C	NS	80840	*Nsun7*	5	p.S189P	2	1.9E-02
5	66289500	A	T	NS	11468	*Nsun7*	10	p.E461V	2	1.9E-02
5	73101557	T	C	NS	83971	*Fryl*	20	p.D628G	2	1.7E-01
5	73125551	A	T	NS	82086	*Fryl*	8	p.L152Q	2	1.7E-01
5	89179786	C	T	NS	2216	*Slc4a4*	16	p.T703I	2	4.1E-02
5	89179810	A	G	NS	91570	*Slc4a4*	16	p.K711R	2	4.1E-02
5	100556535	G	T	NS	22721	*Plac8*	4	p.L99I	2	5.8E-04
5	100556576	T	C	NS	82147	*Plac8*	4	p.Y85C	2	5.8E-04
5	103784319	A	G	NS	83882	*Aff1*	3	p.K276E	2	4.9E-02
5	103815060	C	T	NS	83010	*Aff1*	5	p.P382S	2	4.9E-02
5	112307703	T	A	NS	10382	*Tpst2*	3	p.V36E	2	6.4E-03
5	112308116	T	C	NS	2730	*Tpst2*	3	p.F174L	2	6.4E-03
5	123951216	A	G	NS	10653	*Ccdc62*	7	p.K306E	2	1.9E-02
5	123951228	C	T	NS	80821	*Ccdc62*	7	p.L310F	2	1.9E-02
5	125622539	T	C	NS	57372	*Tmem132b*	2	p.V47A	2	4.0E-02
5	125785991	T	C	NS	98313	*Tmem132b*	8	p.S687P	2	4.0E-02
5	129109635	T	C	NS	80821	*Gpr133*	3	p.I54T	2	2.9E-02
5	129109651	C	A	NS	88129	*Gpr133*	3	p.D59E	2	2.9E-02
5	140635561	A	G	NS	83411	*Ttyh3*	3	p.Y120H	2	1.1E-02
5	140648823	G	A	NS	11478	*Ttyh3*	1	p.A2V	2	1.1E-02
5	147676422	A	T	NS	60712	*Flt1*	8	p.S336R	2	5.6E-02
5	147699817	T	A	NS	60716	*Flt1*	3	p.K119M	2	5.6E-02
5	150038233	T	A	NS	60716	*Rxfp2*	3	p.F73I	2	2.1E-02
5	150051610	G	A	NS	76526	*Rxfp2*	8	p.G214E	2	2.1E-02
5	150722313	A	G	NS	33095	*Pds5b*	4	p.T111A	2	6.4E-02
5	150779226	A	G	NS	88547	*Pds5b*	22	p.T808A	2	6.4E-02
6	3687603	A	T	NS	11468	*Calcr*	16	p.I465N	2	1.1E-02
6	3707599	T	C	NS	6927	*Calcr*	10	p.M234V	2	1.1E-02
6	12379405	A	T	NS	60693	*Thsd7a*	13	p.C1007S	2	7.8E-02
6	12500995	T	A	NS	76989	*Thsd7a*	4	p.D471V	2	7.8E-02
6	22961668	T	A	NS	42058	*Ptprz1*	4	p.I126K	2	1.2E-01
6	23029281	A	G	NS	98172	*Ptprz1*	19	p.D1807G	2	1.2E-01
6	24796067	T	C	NS	5401	*Spam1*	2	p.F6L	2	1.1E-02
6	24796824	T	C	NS	6654	*Spam1*	2	p.L258P	2	1.1E-02

6	28545519	T	A	NS	45755	*Snd1*	10	p.V358E	2	3.0E-02
6	28829804	A	T	NS	11478	*Lrrc4*	1	p.I604N	2	1.7E-02
6	28831364	T	C	NS	83071	*Lrrc4*	1	p.N84S	2	1.7E-02
6	28888083	C	A	NS	89965	*Snd1*	23	p.T876K	2	3.0E-02
6	41032430	A	G	NS	82395	*2210010C04 Rik*	4	p.S157P	2	2.7E-03
6	41033091	T	C	NS	83875	*2210010C04 Rik*	3	p.N103S	2	2.7E-03
6	42673538	A	G	NS	11082	*Fam115a*	8	p.M869T	2	3.0E-02
6	42679172	A	G	NS	76526	*Fam115a*	3	p.V290A	2	3.0E-02
6	43274772	T	C	NS	98172	*Arhgef5*	2	p.I819T	2	7.3E-02
6	43280669	T	C	NS	88025	*Arhgef5*	8	p.L1290P	2	7.3E-02
6	63256935	A	G	NS	14418	*Grid2*	1	p.I27V	2	3.5E-02
6	64094381	T	C	NS	11187	*Grid2*	8	p.V396A	2	3.5E-02
6	71216853	T	A	NS	57931	*Smyd1*	9	p.M397L	2	9.8E-03
6	71262182	T	C	NS	98172	*Smyd1*	1	p.N8S	2	9.8E-03
6	85340715	T	A	NS	96868	*Rab11fip5*	4	p.E1064V	2	5.5E-02
6	85348672	A	G	NS	96440	*Rab11fip5*	2	p.S251P	2	5.5E-02
6	85622422	A	G	NS	88262	*Alms1*	8	p.E1410G	2	1.8E-01
6	85696238	T	A	NS	90152	*Alms1*	18	p.F3031L	2	1.8E-01
6	88586788	T	A	NS	76989	*Kbtbd12*	5	p.H559L	2	1.5E-02
6	88618756	C	T	NS	29035	*Kbtbd12*	2	p.V31I	2	1.5E-02
6	90409351	T	C	NS	91570	*Ccdc37*	13	p.Q428R	2	1.5E-02
6	90413019	A	G	NS	11600	*Ccdc37*	9	p.S250P	2	1.5E-02
6	97160331	A	C	NS	60654	*Tmf1*	13	p.L888R	2	4.0E-02
6	97176228	A	G	NS	11600	*Tmf1*	2	p.S295P	2	4.0E-02
6	115888829	C	T	NS	57931	*Ift122*	11	p.S360L	2	4.6E-02
6	115920373	T	C	NS	10177	*Ift122*	23	p.L911P	2	4.6E-02
6	116695289	C	T	NS	60716	*Tmem72*	5	p.R197H	2	3.3E-03
6	116696858	A	G	NS	83971	*Tmem72*	4	p.S100P	2	3.3E-03
6	118687100	A	T	NS	88025	*Cacna1c*	14	p.M700K	2	1.2E-01
6	118741895	T	C	NS	76387	*Cacna1c*	8	p.N398S	2	1.2E-01
6	119320781	A	G	NS	83875	*Lrtm2*	4	p.S100P	2	5.8E-03
6	119320949	T	C	NS	98172	*Lrtm2*	4	p.T44A	2	5.8E-03
6	120394245	T	A	NS	88955	*Kdm5a*	12	p.V550E	2	8.1E-02
6	120404971	G	A	NS	82086	*Kdm5a*	15	p.V659M	2	8.1E-02
6	122040671	A	G	NS	76582	*Mug2*	12	p.S456G	2	6.4E-02
6	122075274	A	G	NS	76989	*Mug2*	24	p.Q997R	2	6.4E-02
6	124438333	T	A	NS	29035	*Clstn3*	14	p.M728L	2	3.2E-02
6	124457996	C	T	NS	96868	*Clstn3*	7	p.G357D	2	3.2E-02
6	124904543	T	C	NS	60712	*Lag3*	8	p.R489G	2	1.1E-02
6	124908427	T	G	NS	98313	*Lag3*	5	p.H330P	2	1.1E-02
6	125101279	T	C	NS	83794	*Chd4*	5	p.F160S	2	9.7E-02
6	125101969	T	A	NS	11954	*Chd4*	7	p.I289N	2	9.7E-02
6	132957094	A	G	NS	3000	*Tas2r131*	1	p.F251L	2	4.1E-03
6	132957264	A	T	SG	60654	*Tas2r131*	1	p.L194X	2	4.1E-03
6	142658586	T	C	NS	88547	*Abcc9*	16	p.N641S	2	7.1E-02
6	142672612	T	A	NS	96245	*Abcc9*	13	p.I546F	2	7.1E-02
6	149000023	A	T	NS	83217	*Dennd5b*	19	p.C1122S	2	5.2E-02

6	149068427	T	C	NS	14418	*Dennd5b*	3	p.Y176C	2	5.2E-02
7	27877871	T	C	NS	83971	*Zfp607*	5	p.L122P	2	1.8E-02
7	27879333	T	A	NS	82522	*Zfp607*	5	p.N609K	2	1.8E-02
7	29077046	C	T	NS	83929	*Ryr1*	40	p.V2215I	2	2.6E-01
7	29109255	T	C	NS	83457	*Ryr1*	13	p.E464G	2	2.6E-01
7	30775332	A	T	NS	60693	*Dmkn*	13	p.H413L	2	1.1E-02
7	30776115	C	A	NS	82395	*Dmkn*	14	p.Q443K	2	1.1E-02
7	42612599	G	A	NS	88547	*9830147E19 Rik*	4	p.P606S	2	1.6E-02
7	42612837	A	T	NS	10020	*9830147E19 Rik*	4	p.N526K	2	1.6E-02
7	45650928	C	G	NS	83217	*Fut2*	3	p.R140P	2	5.2E-03
7	45651270	A	G	NS	91310	*Fut2*	3	p.I26T	2	5.2E-03
7	65311085	T	C	NS	88025	*Tjp1*	23	p.H1373R	2	8.5E-02
7	65313310	C	A	SG	22721	*Tjp1*	21	p.E1040X	2	8.5E-02
7	66259951	C	T	NS	10562	*Lrrk1*	34	p.G2004S	2	1.0E-01
7	66265494	G	T	NS	83619	*Lrrk1*	31	p.S1615R	2	1.0E-01
7	79097853	T	C	NS	57931	*Acan*	12	p.S791P	2	1.1E-01
7	79099764	T	C	NS	6927	*Acan*	12	p.S1428P	2	1.1E-01
7	79691948	T	A	NS	6654	*Ticrr*	19	p.M1094K	2	9.5E-02
7	79693713	A	G	NS	82620	*Ticrr*	20	p.S1109G	2	9.5E-02
7	80713863	A	G	NS	76824	*Iqgap1*	38	p.F1648S	2	7.9E-02
7	80760889	T	C	NS	51283	*Iqgap1*	7	p.Y192C	2	7.9E-02
7	83973301	T	C	NS	11468	*9930013L23 Rik*	13	p.I557V	2	5.8E-02
7	83973331	T	C	NS	83411	*9930013L23 Rik*	13	p.M547V	2	5.8E-02
7	98067160	A	C	NS	83882	*Myo7a*	33	p.S1471A	2	1.2E-01
7	98092483	T	C	NS	5401	*Myo7a*	13	p.Q493R	2	1.2E-01
7	104893019	A	G	NS	82522	*Olfr666*	1	p.M203T	2	4.3E-03
7	104893325	A	G	NS	83010	*Olfr666*	1	p.V101A	2	4.3E-03
7	107181907	T	A	NS	98491	*Nlrp14*	3	p.W104R	2	3.5E-02
7	107182192	G	A	NS	90152	*Nlrp14*	3	p.V199M	2	3.5E-02
7	110369529	C	A	NS	60654	*Sbf2*	22	p.R888L	2	9.4E-02
7	110447049	G	C	NS	88041	*Sbf2*	9	p.P314A	2	9.4E-02
7	113299364	T	A	NS	82522	*Arntl*	13	p.I333K	2	1.5E-02
7	113304395	T	A	NS	11477	*Arntl*	16	p.M466K	2	1.5E-02
7	118184636	A	T	NS	83689	*Smg1*	22	p.V1009D	2	2.1E-01
7	118212982	A	T	NS	6654	*Smg1*	2	p.S53T	2	2.1E-01
7	127788499	T	G	NS	11954	*Setd1a*	12	p.D997E	2	8.2E-02
7	127799173	T	A	NS	29035	*Setd1a*	18	p.I1641N	2	8.2E-02
7	133930045	C	T	NS	11477	*Adam12*	14	p.C487Y	2	2.9E-02
7	133967900	T	C	NS	2730	*Adam12*	9	p.H282R	2	2.9E-02
7	139089523	T	C	NS	82744	*Dpysl4*	2	p.L18P	2	1.3E-02
7	139096320	T	C	NS	82522	*Dpysl4*	9	p.S322P	2	1.3E-02
7	141620815	T	C	NS	2383	*Ap2a2*	13	p.L525P	2	3.1E-02
7	141627947	A	G	NS	60716	*Ap2a2*	17	p.T753A	2	3.1E-02
8	15081294	A	G	NS	57372	*Myom2*	10	p.M331V	2	6.5E-02
8	15111958	A	T	SP	88129	*Myom2*	na	na	2	6.5E-02

8	15912420	A	G	NS	82086	*Csmd1*	63	p.L3258P	2	2.0E-01
8	16092347	T	A	NS	11600	*Csmd1*	29	p.N1514I	2	2.0E-01
8	41290775	T	C	NS	89285	*Pcm1*	21	p.V1153A	2	1.0E-01
8	41293515	T	A	NS	6927	*Pcm1*	22	p.D1211E	2	1.0E-01
8	44952851	A	C	NS	39748	*Fat1*	1	p.I880L	2	2.4E-01
8	44952852	T	C	NS	60693	*Fat1*	1	p.I880T	2	2.4E-01
8	48235439	C	T	NS	42058	*Tenm3*	25	p.R2355K	2	1.5E-01
8	48276325	T	C	NS	82841	*Tenm3*	21	p.T1533A	2	1.5E-01
8	55872906	G	A	NS	10177	*Adam29*	2	p.S171F	2	2.2E-02
8	55873357	T	C	NS	96440	*Adam29*	2	p.I21V	2	2.2E-02
8	68892757	T	C	NS	96868	*Lpl*	3	p.F138L	2	9.2E-03
8	68896745	A	C	NS	88025	*Lpl*	6	p.N308H	2	9.2E-03
8	84887044	T	C	NS	88503	*Gcdh*	12	p.D427G	2	8.3E-03
8	84893077	C	T	NS	89957	*Gcdh*	4	p.R81H	2	8.3E-03
8	85970927	A	G	NS	83929	*Phkb*	15	p.D455G	2	4.0E-02
8	86016877	A	C	NS	13019	*Phkb*	18	p.I535L	2	4.0E-02
8	87773612	C	T	NS	82147	*Zfp423*	5	p.E1186K	2	5.3E-02
8	87782031	G	A	SG	60716	*Zfp423*	4	p.Q562X	2	5.3E-02
8	90252717	T	C	NS	22721	*Tox3*	6	p.T307A	2	1.3E-02
8	90270360	C	T	NS	82147	*Tox3*	3	p.D92N	2	1.3E-02
8	91102246	G	T	NS	11187	*Rbl2*	14	p.G635C	2	4.3E-02
8	91106796	T	C	NS	45755	*Rbl2*	16	p.L776P	2	4.3E-02
8	105358408	C	A	NS	22721	*Slc9a5*	10	p.L514I	2	2.9E-02
8	105359377	T	A	NS	76582	*Slc9a5*	12	p.V592E	2	2.9E-02
8	105461068	A	G	NS	2164	*Lrrc36*	10	p.T539A	2	2.1E-02
8	105463898	T	A	NS	80840	*Lrrc36*	11	p.V612E	2	2.1E-02
8	106657868	A	G	NS	83971	*Cdh1*	7	p.R323G	2	2.8E-02
8	106665445	A	G	NS	11478	*Cdh1*	14	p.E741G	2	2.8E-02
8	107416245	G	A	NS	82194	*Nob1*	8	p.T268I	2	6.8E-03
8	107424984	C	A	NS	83971	*Nob1*	1	p.L15F	2	6.8E-03
8	110298180	T	C	NS	24744	*Hydin*	3	p.V74A	2	2.6E-01
8	110595458	C	T	NS	10722	*Hydin*	80	p.R4581C	2	2.6E-01
8	110835659	A	T	NS	88547	*Sf3b3*	9	p.S375T	2	4.8E-02
8	110842840	C	A	NS	96868	*Sf3b3*	3	p.S82I	2	4.8E-02
8	110883939	T	C	NS	60716	*Fuk*	22	p.D944G	2	4.0E-02
8	110886577	G	T	NS	57931	*Fuk*	19	p.H829Q	2	4.0E-02
8	120571004	C	T	NS	11600	*Gse1*	9	p.T639I	2	4.9E-02
8	120575134	A	G	NS	98491	*Gse1*	13	p.S982G	2	4.9E-02
8	123373994	C	T	NS	96868	*Tcf25*	1	p.P41L	2	1.8E-02
8	123393197	G	C	NS	82522	*Tcf25*	11	p.R394P	2	1.8E-02
8	128993081	T	A	SP	96440	*Ccdc7*	na	na	2	5.9E-03
8	129061812	A	T	NS	83230	*Ccdc7*	3	p.M12K	2	5.9E-03
9	4330330	A	G	NS	83794	*Kbtbd3*	4	p.T235A	2	1.5E-02
9	4331087	C	T	NS	76824	*Kbtbd3*	4	p.A487V	2	1.5E-02
9	7023334	A	G	NS	82522	*Dync2h1*	70	p.Y3557H	2	2.3E-01
9	7172898	A	G	NS	10562	*Dync2h1*	4	p.F176L	2	2.3E-01
9	15998377	C	T	NS	3000	*Fat3*	9	p.A2110T	2	2.4E-01
9	16006567	T	C	NS	88025	*Fat3*	7	p.D1520G	2	2.4E-01
9	18330818	T	A	NS	11600	*Naalad2*	16	p.T559S	2	2.1E-02

9	18376560	T	C	NS	89957	*Naalad2*	6	p.D220G	2	2.1E-02
9	20772193	C	A	NS	76526	*Col5a3*	64	p.G1561V	2	8.4E-02
9	20801230	G	A	NS	10382	*Col5a3*	14	p.R488C	2	8.4E-02
9	35457424	A	T	NS	88025	*Cdon*	6	p.H318L	2	5.1E-02
9	35478658	T	A	NS	10382	*Cdon*	13	p.N869K	2	5.1E-02
9	42338913	A	G	NS	13019	*Tecta*	18	p.V1861A	2	1.1E-01
9	42373115	G	T	NS	11478	*Tecta*	10	p.D891E	2	1.1E-01
9	52120286	A	T	NS	5401	*Zc3h12c*	4	p.V360E	2	2.9E-02
9	52120378	T	A	NS	11477	*Zc3h12c*	4	p.L329F	2	2.9E-02
9	62796708	G	T	NS	98491	*Fem1b*	2	p.N423K	2	1.5E-02
9	62811164	T	C	NS	57931	*Fem1b*	1	p.T48A	2	1.5E-02
9	64235805	G	A	SG	29035	*Uchl4*	1	p.W189X	2	2.4E-03
9	64235900	A	T	NS	83230	*Uchl4*	1	p.D221V	2	2.4E-03
9	64508751	T	C	NS	10722	*Megf11*	4	p.Y81H	2	4.1E-02
9	64691921	A	T	NS	11082	*Megf11*	17	p.Q737L	2	4.1E-02
9	64924555	T	C	NS	2383	*Slc24a1*	10	p.I1087V	2	4.3E-02
9	64948266	T	A	NS	11477	*Slc24a1*	2	p.H453L	2	4.3E-02
9	69759903	T	C	NS	76989	*Foxb1*	2	p.D115G	2	4.6E-03
9	69759915	A	G	NS	83071	*Foxb1*	2	p.V111A	2	4.6E-03
9	70579361	C	A	NS	11477	*Sltm*	10	p.T436K	2	3.7E-02
9	70586948	C	T	SG	76824	*Sltm*	18	p.R894X	2	3.7E-02
9	72362101	C	T	NS	80840	*Zfp280d*	22	p.T840I	2	3.3E-02
9	72362320	G	A	NS	83737	*Zfp280d*	22	p.R913H	2	3.3E-02
9	72731228	T	A	NS	60712	*Nedd4*	16	p.W466R	2	2.9E-02
9	72739509	A	G	NS	11478	*Nedd4*	23	p.N715D	2	2.9E-02
9	79626992	A	T	NS	83230	*Col12a1*	51	p.H2651Q	2	NA
9	79631641	A	G	NS	96440	*Col12a1*	47	p.F2458L	2	NA
9	95999437	T	C	NS	83164	*Xrn1*	21	p.I788T	2	8.3E-02
9	96051698	A	T	NS	89957	*Xrn1*	41	p.M1607L	2	8.3E-02
9	99576632	A	T	NS	90152	*Dbr1*	2	p.H85L	2	1.2E-02
9	99579443	G	T	SP	89285	*Dbr1*	na	na	2	1.2E-02
9	111349345	A	G	NS	88025	*Trank1*	7	p.D367G	2	1.7E-01
9	111389180	A	T	NS	76278	*Trank1*	19	p.Y1876F	2	1.7E-01
10	5052828	C	A	NS	10020	*Syne1*	43	p.R2263L	2	1.7E-01
10	5117085	A	T	NS	96440	*Syne1*	25	p.V1294E	2	1.7E-01
10	10741602	T	A	NS	80493	*Grm1*	6	p.Y479F	2	4.7E-02
10	11079875	A	T	NS	89285	*Grm1*	2	p.Y222N	2	4.7E-02
10	11164414	T	C	NS	90152	*Shprh*	9	p.Y544H	2	8.0E-02
10	11164592	T	C	NS	83929	*Shprh*	9	p.V603A	2	8.0E-02
10	14128144	A	G	NS	45755	*Hivep2*	4	p.Y162C	2	1.3E-01
10	14132531	T	A	NS	11187	*Hivep2*	4	p.S1624R	2	1.3E-01
10	18498132	A	G	NS	2216	*Nhsl1*	3	p.D104G	2	7.3E-02
10	18516089	T	A	NS	83457	*Nhsl1*	5	p.V197E	2	7.3E-02
10	39805605	A	G	NS	96245	*Rev3l*	7	p.I255V	2	1.8E-01
10	39874219	T	A	NS	10382	*Rev3l*	32	p.F3122I	2	1.8E-01
10	53348693	T	C	NS	80493	*Cep85l*	3	p.T267A	2	2.4E-02
10	53348752	A	G	NS	2164	*Cep85l*	3	p.L247P	2	2.4E-02
10	61614103	T	C	NS	76387	*Npffr1*	2	p.L52P	2	7.8E-03
10	61614178	T	C	NS	10382	*Npffr1*	2	p.V77A	2	7.8E-03

10	76357073	G	A	SG	10722	*Pcnt*	37	p.Q2681X	2	1.6E-01
10	76429217	T	C	NS	22721	*Pcnt*	8	p.N353S	2	1.6E-01
10	84374668	A	G	NS	83010	*Nuak1*	7	p.S519P	2	1.7E-02
10	84380792	A	T	SG	13019	*Nuak1*	5	p.Y219X	2	1.7E-02
10	88400664	T	A	NS	10178	*Gnptab*	2	p.W44R	2	5.0E-02
10	88440309	T	C	NS	83929	*Gnptab*	19	p.S1153P	2	5.0E-02
10	88978802	A	C	NS	82522	*Ano4*	22	p.W675G	2	3.2E-02
10	88995266	T	A	NS	91570	*Ano4*	16	p.K498N	2	3.2E-02
10	93845784	C	T	NS	98172	*Usp44*	3	p.T32I	2	1.9E-02
10	93846545	G	A	NS	5401	*Usp44*	3	p.V286I	2	1.9E-02
10	107771168	T	A	NS	91570	*Otogl*	53	p.D2118V	2	1.3E-01
10	107806754	T	A	NS	83411	*Otogl*	33	p.N1272Y	2	1.3E-01
10	109703351	G	T	NS	24744	*Nav3*	33	p.T2063K	2	1.3E-01
10	109754958	A	T	NS	57372	*Nav3*	19	p.M1544K	2	1.3E-01
10	123002865	T	C	NS	83230	*Mon2*	32	p.K1572E	2	8.3E-02
10	123036045	A	T	NS	89957	*Mon2*	9	p.I358K	2	8.3E-02
10	127331738	T	C	NS	83737	*Gli1*	13	p.S549G	2	4.2E-02
10	127331767	A	G	NS	82086	*Gli1*	13	p.V539A	2	4.2E-02
10	128942934	T	A	NS	83230	*Itga7*	6	p.I306K	2	4.3E-02
10	128943836	A	G	NS	80493	*Itga7*	9	p.D456G	2	4.3E-02
11	5962443	T	C	SP	88129	*Ykt6*	na	na	2	1.7E-03
11	5966040	T	A	NS	96245	*Ykt6*	7	p.M198K	2	1.7E-03
11	12254663	G	T	NS	42885	*Cobl*	12	p.Q680K	2	5.6E-02
11	12267081	T	C	NS	96245	*Cobl*	10	p.E469G	2	5.6E-02
11	29205704	T	A	NS	11468	*Smek2*	11	p.C557S	2	2.5E-02
11	29211624	G	A	NS	83071	*Smek2*	14	p.R666H	2	2.5E-02
11	29553649	G	C	NS	80493	*1700034F02 Rik*	2	p.E22Q	2	1.4E-02
11	29560845	C	A	SG	80840	*1700034F02 Rik*	6	p.Y282X	2	1.4E-02
11	43597466	T	C	NS	83217	*Fabp6*	3	p.E111G	2	7.5E-04
11	43601464	A	T	NS	11241	*Fabp6*	1	p.D16E	2	7.5E-04
11	50873024	T	A	NS	83230	*Zfp454*	6	p.Q527L	2	1.2E-02
11	50873839	C	A	NS	6654	*Zfp454*	6	p.E255D	2	1.2E-02
11	58891502	C	A	SG	24744	*Zfp39*	5	p.E145X	2	2.0E-02
11	58900671	A	T	NS	57372	*Zfp39*	3	p.D63E	2	2.0E-02
11	59090640	T	A	NS	10562	*Obscn*	18	p.S1851C	2	2.6E-01
11	59133029	A	G	NS	83230	*Obscn*	4	p.M605T	2	2.6E-01
11	60779157	A	G	NS	2164	*Smcr8*	1	p.E377G	2	3.1E-02
11	60779587	T	A	NS	6654	*Smcr8*	1	p.S520R	2	3.1E-02
11	67297458	A	G	NS	5401	*Myh8*	24	p.T982A	2	9.8E-02
11	67304394	A	G	NS	11187	*Myh8*	35	p.E1678G	2	9.8E-02
11	68783262	A	G	NS	11600	*Myh10*	16	p.N674S	2	1.0E-01
11	68783426	G	T	NS	90152	*Myh10*	17	p.C701F	2	1.0E-01
11	70617342	C	T	NS	83071	*Chrne*	7	p.G203R	2	1.0E-02
11	70618182	T	C	NS	88129	*Chrne*	5	p.D158G	2	1.0E-02
11	75487163	T	A	SG	57258	*Prpf8*	1	p.Y24X	2	1.3E-01
11	75506451	T	C	NS	88025	*Prpf8*	37	p.S2037P	2	1.3E-01
11	76117805	T	C	NS	6927	*Vps53*	9	p.R230G	2	2.5E-02

11	76163853	T	C	NS	57931	*Vps53*	4	p.D77G	2	2.5E-02
11	76210959	A	G	NS	82522	*Gemin4*	2	p.M992T	2	3.8E-02
11	76211059	A	G	NS	2730	*Gemin4*	2	p.S959P	2	3.8E-02
11	77454398	A	G	NS	14418	*Ssh2*	15	p.T1064A	2	6.2E-02
11	77454405	A	G	NS	57372	*Ssh2*	15	p.E1066G	2	6.2E-02
11	77550971	T	A	NS	82620	*Taok1*	15	p.K535N	2	3.5E-02
11	77578815	T	A	NS	88025	*Taok1*	4	p.I73F	2	3.5E-02
11	78212187	C	T	NS	83457	*Supt6*	31	p.D1407N	2	8.3E-02
11	78229438	T	A	NS	29035	*Supt6*	9	p.I359F	2	8.3E-02
11	78284148	T	C	NS	83882	*2610507B11 Rik*	28	p.I1703T	2	1.2E-01
11	78289883	A	T	NS	80493	*2610507B11 Rik*	39	p.N2202I	2	1.2E-01
11	80243477	T	C	NS	98172	*Rhot1*	11	p.Y299H	2	1.7E-02
11	80253043	T	C	NS	88503	*Rhot1*	17	p.V511A	2	1.7E-02
11	83422059	A	G	NS	83882	*Gas2l2*	6	p.V809A	2	2.7E-02
11	83427400	A	C	NS	83971	*Gas2l2*	2	p.F161C	2	2.7E-02
11	87868677	T	C	NS	2383	*Epx*	10	p.K529E	2	2.0E-02
11	87871344	A	T	SG	83071	*Epx*	7	p.C360X	2	2.0E-02
11	98155404	A	T	NS	10020	*Med1*	17	p.M1522K	2	7.3E-02
11	98156625	T	A	NS	60716	*Med1*	17	p.K1115M	2	7.3E-02
11	106511922	T	TG	FSI	76824	*Tex2*	10	p.P1041fs	2	4.3E-02
11	106567364	A	T	NS	29035	*Tex2*	2	p.D413E	2	4.3E-02
11	113843082	G	A	NS	98491	*Sdk2*	19	p.T845I	2	1.1E-01
11	113885288	T	C	NS	88503	*Sdk2*	5	p.D196G	2	1.1E-01
11	120362479	T	G	NS	42885	*Fscn2*	1	p.S257R	2	9.9E-03
11	120362508	A	G	NS	10562	*Fscn2*	1	p.N267S	2	9.9E-03
12	4701343	C	T	NS	11477	*Itsn2*	31	p.T1284M	2	8.0E-02
12	4712465	A	T	SP	10451	*Itsn2*	38	na	2	8.0E-02
12	13335891	T	C	NS	96868	*Nbas*	20	p.F719L	2	1.3E-01
12	13408196	C	T	NS	98313	*Nbas*	32	p.R1235C	2	1.3E-01
12	38190115	G	A	NS	98420	*Dgkb*	16	p.G464R	2	2.4E-02
12	38190120	T	A	NS	76278	*Dgkb*	16	p.N465K	2	2.4E-02
12	50365637	C	A	NS	11241	*Prkd1*	16	p.A721S	2	3.0E-02
12	50425590	A	T	NS	11478	*Prkd1*	4	p.L180Q	2	3.0E-02
12	51888272	T	C	SP	83929	*Heatr5a*	na	na	2	1.1E-01
12	51889645	C	T	NS	60712	*Heatr5a*	30	p.R1581H	2	1.1E-01
12	53072496	A	T	NS	42058	*Akap6*	11	p.Q1115H	2	1.2E-01
12	53141326	T	C	NS	83737	*Akap6*	13	p.I1841T	2	1.2E-01
12	54916904	A	T	SG	88955	*Baz1a*	18	p.C798X	2	7.1E-02
12	54929601	A	T	NS	83685	*Baz1a*	11	p.M430K	2	7.1E-02
12	69318149	A	G	NS	33095	*Nemf*	26	p.S822P	2	3.9E-02
12	69354717	T	C	NS	83188	*Nemf*	4	p.D96G	2	3.9E-02
12	72481551	T	A	NS	60654	*Lrrc9*	20	p.W876R	2	6.4E-02
12	72486378	T	G	NS	89285	*Lrrc9*	22	p.I1008S	2	6.4E-02
12	73179237	A	G	NS	57372	*Mnat1*	4	p.N117D	2	4.1E-03
12	73272465	T	A	SG	51255	*Mnat1*	8	p.Y287X	2	4.1E-03
12	75391740	T	C	NS	96839	*Rhoj*	3	p.F100S	2	2.0E-03

12	75400177	C	T	NS	90152	*Rhoj*	5	p.A190V	2	2.0E-03
12	78492072	A	G	NS	11477	*Gphn*	7	p.H164R	2	2.2E-02
12	78664559	G	T	NS	83520	*Gphn*	19	p.K638N	2	2.2E-02
12	80339621	C	T	NS	13019	*Dcaf5*	9	p.R577H	2	3.2E-02
12	80339649	A	C	NS	11468	*Dcaf5*	9	p.S568A	2	3.2E-02
12	81917689	T	C	NS	83929	*Pcnx*	6	p.F210S	2	1.3E-01
12	81974410	C	T	NS	29035	*Pcnx*	22	p.T1397I	2	1.3E-01
12	82357325	T	C	NS	10382	*Sipa1l1*	3	p.S531P	2	8.7E-02
12	82450030	A	T	NS	82086	*Sipa1l1*	21	p.I1779L	2	8.7E-02
12	89260402	T	C	NS	10178	*Nrxn3*	6	p.M269T	2	7.2E-02
12	90332016	T	C	NS	5401	*Nrxn3*	20	p.V1441A	2	7.2E-02
12	98222650	A	G	NS	82744	*Galc*	11	p.Y401H	2	1.8E-02
12	98234339	A	G	NS	83619	*Galc*	8	p.W271R	2	1.8E-02
12	104147387	C	T	NS	83737	*Serpina3c*	5	p.G367S	2	7.2E-03
12	104151485	T	G	NS	91570	*Serpina3c*	2	p.D198A	2	7.2E-03
12	110659137	A	G	NS	80821	*Dync1h1*	63	p.E3911G	2	2.4E-01
12	110662923	G	C	NS	13019	*Dync1h1*	70	p.V4254L	2	2.4E-01
12	113544063	G	T	NS	57372	*Adam6a*	1	p.V19F	2	2.1E-02
12	113545101	T	A	NS	82086	*Adam6a*	1	p.C365S	2	2.1E-02
13	9878327	A	T	NS	10178	*Chrm3*	5	p.F224L	2	1.4E-02
13	9878963	C	A	NS	83619	*Chrm3*	5	p.L12F	2	1.4E-02
13	11603732	T	C	NS	53882	*Ryr2*	86	p.T3866A	2	2.5E-01
13	11761406	C	T	NS	76526	*Ryr2*	28	p.G1082R	2	2.5E-01
13	23880453	A	C	NS	91570	*Slc17a1*	9	p.I331L	2	8.9E-03
13	23892542	A	T	NS	2164	*Slc17a1*	12	p.E424V	2	8.9E-03
13	24885627	A	T	SG	90152	*D130043K22 Rik*	17	p.R890X	2	4.0E-02
13	24887916	A	C	NS	42885	*D130043K22 Rik*	18	p.N948H	2	4.0E-02
13	33091347	G	A	NS	57372	*Serpinb1b*	5	p.V152M	2	6.2E-03
13	33091656	A	G	NS	60712	*Serpinb1b*	6	p.D191G	2	6.2E-03
13	49060759	T	C	NS	60716	*Wnk2*	20	p.D1547G	2	1.1E-01
13	49146577	A	G	NS	57258	*Wnk2*	2	p.V219A	2	1.1E-01
13	55639795	T	C	NS	11187	*Ddx46*	3	p.S71P	2	3.7E-02
13	55652099	T	A	NS	83457	*Ddx46*	7	p.V274E	2	3.7E-02
13	59477061	T	C	NS	60716	*Agtpbp1*	19	p.N826S	2	4.9E-02
13	59536282	T	C	NS	83457	*Agtpbp1*	3	p.T42A	2	4.9E-02
13	68620736	C	T	NS	29035	*Adcy2*	25	p.S1091N	2	4.1E-02
13	68732076	A	G	SP	83164	*Adcy2*	na	na	2	4.1E-02
13	74157769	T	A	NS	83619	*Slc9a3*	5	p.S302T	2	2.5E-02
13	74163769	C	T	NS	2164	*Slc9a3*	12	p.T612I	2	2.5E-02
13	76066793	T	C	NS	76582	*Arsk*	6	p.D314G	2	1.2E-02
13	76074863	A	C	NS	10178	*Arsk*	4	p.L205W	2	1.2E-02
13	76140567	A	G	NS	60693	*Ttc37*	29	p.T940A	2	7.2E-02
13	76175330	T	C	NS	11600	*Ttc37*	40	p.S1398P	2	7.2E-02
13	89690534	T	C	NS	11477	*Vcan*	7	p.D1337G	2	1.9E-01
13	89704094	T	C	NS	11187	*Vcan*	7	p.T916A	2	1.9E-01
13	92752365	T	C	NS	98313	*Thbs4*	21	p.Y940C	2	3.3E-02
13	92754437	C	T	NS	29035	*Thbs4*	20	p.V841M	2	3.3E-02

13	103824917	T	C	NS	83875	*Erbb2ip*	24	p.S1294G	2	6.4E-02
13	103845502	A	G	SP	98420	*Erbb2ip*	17	na	2	6.4E-02
13	104297263	T	C	NS	83971	*Adamts6*	3	p.S67P	2	4.2E-02
13	104297477	A	T	NS	10451	*Adamts6*	3	p.Q138L	2	4.2E-02
14	20300606	T	C	NS	6927	*Nudt13*	2	p.Y4H	2	5.3E-03
14	20307741	T	A	NS	42885	*Nudt13*	5	p.I136N	2	5.3E-03
14	21038057	G	A	NS	82744	*Ap3m1*	7	p.T311I	2	7.3E-03
14	21038160	T	C	NS	13019	*Ap3m1*	7	p.K277E	2	7.3E-03
14	24482412	T	A	SG	80821	*Polr3a*	5	p.K205X	2	6.0E-02
14	24482532	T	C	NS	83875	*Polr3a*	5	p.T165A	2	6.0E-02
14	30050249	T	C	NS	10382	*Cacna1d*	42	p.Y1812C	2	1.1E-01
14	30124875	A	G	NS	76582	*Cacna1d*	12	p.F547L	2	1.1E-01
14	32332493	T	A	SG	80840	*Ogdhl*	6	p.Y181X	2	3.7E-02
14	32337845	A	G	NS	11241	*Ogdhl*	11	p.T439A	2	3.7E-02
14	45595537	G	C	NS	83230	*Ddhd1*	15	p.F530L	2	3.0E-02
14	45657675	C	A	NS	24744	*Ddhd1*	1	p.V113F	2	3.0E-02
14	49178115	T	C	NS	88025	*Naa30*	3	p.F283L	2	5.7E-03
14	49187642	T	A	SG	83140	*Naa30*	5	p.Y352X	2	5.7E-03
14	54949892	T	C	NS	88955	*Myh6*	28	p.T1311A	2	9.8E-02
14	54950514	A	G	NS	76989	*Myh6*	26	p.V1161A	2	9.8E-02
14	54982214	A	T	NS	91310	*Myh7*	26	p.I1066N	2	9.8E-02
14	54987349	T	C	NS	88129	*Myh7*	17	p.D587G	2	9.8E-02
14	75316039	G	A	NS	91570	*Zc3h13*	8	p.R302Q	2	8.3E-02
14	75323572	T	C	NS	88041	*Zc3h13*	10	p.V534A	2	8.3E-02
14	79428300	A	G	NS	80821	*Kbtbd7*	1	p.D524G	2	1.8E-02
14	79428513	T	C	NS	82522	*Kbtbd7*	1	p.V595A	2	1.8E-02
14	86810401	T	G	NS	45755	*Diap3*	25	p.E1012A	2	4.6E-02
14	87002913	T	C	NS	88955	*Diap3*	8	p.D245G	2	4.6E-02
14	117435808	A	G	NS	2164	*Gpc6*	3	p.E159G	2	1.3E-02
14	117974998	A	G	NS	90152	*Gpc6*	9	p.E527G	2	1.3E-02
15	12834406	A	G	NS	2216	*Drosha*	4	p.T199A	2	5.9E-02
15	12926209	T	C	NS	42885	*Drosha*	32	p.F1251L	2	5.9E-02
15	30669505	A	G	NS	51255	*Ctnnd2*	8	p.Y420C	2	5.0E-02
15	30806771	T	A	NS	83164	*Ctnnd2*	11	p.L612Q	2	5.0E-02
15	50661091	A	G	NS	10451	*Trps1*	6	p.Y1144H	2	5.3E-02
15	50822221	T	C	NS	83737	*Trps1*	4	p.T849A	2	5.3E-02
15	54863742	C	T	NS	80493	*Enpp2*	17	p.M512I	2	3.0E-02
15	54870264	A	C	NS	76582	*Enpp2*	13	p.D381E	2	3.0E-02
15	63825049	A	T	SG	83457	*Gsdmc2*	12	p.Y424X	2	9.5E-03
15	63835804	C	T	SG	96868	*Gsdmc2*	2	p.W47X	2	9.5E-03
15	76106489	T	C	NS	83010	*Eppk1*	2	p.D2064G	2	2.7E-01
15	76108226	T	C	NS	96440	*Eppk1*	2	p.Y1485C	2	2.7E-01
15	78399732	T	C	SL	83188	*Tst*	2	p.X298W	2	3.9E-03
15	78405731	A	G	NS	76278	*Tst*	1	p.S35P	2	3.9E-03
15	79369690	A	G	NS	89965	*Tmem184b*	5	p.F169L	2	7.2E-03
15	79378585	A	G	NS	82744	*Tmem184b*	2	p.V24A	2	7.2E-03
15	82172845	C	A	NS	60654	*Srebf2*	4	p.N260K	2	4.3E-02
15	82175265	A	T	NS	96245	*Srebf2*	5	p.I335F	2	4.3E-02
15	85120625	T	C	NS	82744	*Smc1b*	7	p.D416G	2	5.0E-02

15	85131901	T	A	SG	2730	*Smc1b*	1	p.K13X	2	5.0E-02
15	88730558	C	T	NS	83689	*Brd1*	2	p.E45K	2	4.7E-02
15	88730597	T	C	NS	96440	*Brd1*	2	p.T32A	2	4.7E-02
15	92677680	A	T	NS	76387	*Pdzrn4*	2	p.E83D	2	3.6E-02
15	92743590	T	C	NS	11477	*Pdzrn4*	4	p.V150A	2	3.6E-02
15	98863972	G	T	NS	82086	*Kmt2d*	11	p.T499K	2	2.7E-01
15	98864972	G	A	NS	96247	*Kmt2d*	8	p.P306S	2	2.7E-01
15	100798220	A	G	NS	90152	*Slc4a8*	14	p.D627G	2	4.0E-02
15	100799733	G	T	NS	60654	*Slc4a8*	15	p.W662L	2	4.0E-02
15	101676647	A	G	NS	33095	*Krt6b*	9	p.F516S	2	1.2E-02
15	101676756	A	G	NS	11082	*Krt6b*	9	p.S480P	2	1.2E-02
16	11104644	A	T	NS	82194	*Txndc11*	5	p.Y235N	2	3.2E-02
16	11128485	A	T	SP	60693	*Txndc11*	na	na	2	3.2E-02
16	17626475	C	T	NS	83520	*Smpd4*	6	p.P131S	2	2.5E-02
16	17629106	A	G	NS	2383	*Smpd4*	9	p.T233A	2	2.5E-02
16	31050630	A	G	SP	82841	*Xxylt1*	na	na	2	6.5E-03
16	31081013	T	C	NS	60716	*Xxylt1*	1	p.E108G	2	6.5E-03
16	31989204	A	G	NS	82620	*Senp5*	2	p.S411P	2	2.1E-02
16	31989939	G	A	NS	83685	*Senp5*	2	p.P166S	2	2.1E-02
16	32273165	C	A	NS	60716	*Smco1*	2	p.N20K	2	2.0E-03
16	32273898	A	G	NS	11468	*Smco1*	3	p.Y129C	2	2.0E-03
16	45581578	A	T	NS	88955	*Slc9c1*	18	p.E776V	2	4.6E-02
16	45599541	G	T	NS	60716	*Slc9c1*	24	p.A1025S	2	4.6E-02
16	64766378	G	A	NS	83010	*4930453N24 Rik*	3	p.H328Y	2	5.2E-03
16	64770802	T	A	NS	83188	*4930453N24 Rik*	1	p.N21I	2	5.2E-03
16	77055175	T	A	NS	76278	*Usp25*	6	p.F193I	2	3.8E-02
16	77071768	T	A	NS	83188	*Usp25*	10	p.D352E	2	3.8E-02
16	90245494	T	A	NS	83071	*Scaf4*	15	p.Q656L	2	4.8E-02
16	90245506	G	A	NS	13019	*Scaf4*	15	p.A652V	2	4.8E-02
17	4995810	A	G	NS	89957	*Arid1b*	1	p.Y239C	2	1.2E-01
17	5040764	C	T	NS	83520	*Arid1b*	2	p.P528L	2	1.2E-01
17	12918163	A	G	NS	29035	*Tcp1*	3	p.T91A	2	1.2E-02
17	12919859	A	G	NS	42885	*Tcp1*	5	p.D141G	2	1.2E-02
17	23580794	C	A	NS	88129	*Zfp13*	4	p.A107S	2	1.0E-02
17	23585491	A	G	NS	83875	*Zfp13*	2	p.S2P	2	1.0E-02
17	24224319	A	G	NS	10177	*Ccnf*	17	p.V638A	2	2.3E-02
17	24249361	G	A	SG	60716	*Ccnf*	2	p.R21X	2	2.3E-02
17	25104614	A	G	NS	88262	*Telo2*	15	p.I613T	2	2.6E-02
17	25115144	T	C	NS	76278	*Telo2*	2	p.E43G	2	2.6E-02
17	25840674	T	C	NS	83619	*Rhot2*	14	p.D392G	2	1.5E-02
17	25842382	T	C	NS	60654	*Rhot2*	6	p.T105A	2	1.5E-02
17	30635430	T	A	NS	2730	*Dnah8*	2	p.V22E	2	2.5E-01
17	30758369	C	T	NS	89965	*Dnah8*	59	p.S2927L	2	2.5E-01
17	33381337	A	G	NS	96440	*Zfp101*	4	p.S482P	2	1.5E-02
17	33382053	A	G	NS	6927	*Zfp101*	4	p.V243A	2	1.5E-02
17	34050434	C	T	SG	11468	*Col11a2*	10	p.R347X	2	7.8E-02
17	34057249	A	G	SP	57258	*Col11a2*	na	na	2	7.8E-02

17	34333356	A	T	NS	60716	*H2-Eb2*	2	p.R58S	2	3.6E-03
17	34333486	G	A	NS	96868	*H2-Eb2*	2	p.A102T	2	3.6E-03
17	34837892	CCCCTCCCCAGGGGGTCCCCGGGCTGG	C	FSD	51255	*Dxo*	3	p.G119fs	2	6.6E-03
17	34838043	A	G	NS	83929	*Dxo*	3	p.T167A	2	6.6E-03
17	46399914	T	G	NS	83217	*Zfp318*	4	p.S854R	2	1.2E-01
17	46412446	T	C	NS	60716	*Zfp318*	10	p.Y1792H	2	1.2E-01
17	56375953	A	G	NS	10653	*Kdm4b*	8	p.T294A	2	4.0E-02
17	56396507	C	T	NS	82086	*Kdm4b*	15	p.T696I	2	4.0E-02
17	66817930	T	C	NS	11478	*Ptprm*	15	p.E783G	2	6.4E-02
17	67095675	T	A	NS	11241	*Ptprm*	3	p.T73S	2	6.4E-02
17	70657501	A	T	NS	83875	*Dlgap1*	3	p.Y113F	2	3.4E-02
17	70787192	A	G	NS	88041	*Dlgap1*	7	p.N526S	2	3.4E-02
17	71394847	G	T	NS	83794	*Smchd1*	25	p.A1050E	2	1.0E-01
17	71426506	A	G	NS	10177	*Smchd1*	16	p.S694P	2	1.0E-01
17	78400689	T	C	NS	96247	*Fez2*	5	p.K277E	2	6.0E-03
17	78417939	T	C	NS	82522	*Fez2*	1	p.S49G	2	6.0E-03
18	13844930	A	G	NS	42058	*Zfp521*	4	p.Y809H	2	5.5E-02
18	13845614	T	G	NS	91570	*Zfp521*	4	p.I581L	2	5.5E-02
18	20451866	C	A	NS	82194	*Dsg4*	6	p.N212K	2	3.7E-02
18	20453066	A	G	NS	2730	*Dsg4*	7	p.K271R	2	3.7E-02
18	20589979	A	G	NS	83140	*Dsg2*	9	p.D354G	2	4.2E-02
18	20590093	A	T	NS	88025	*Dsg2*	9	p.H392L	2	4.2E-02
18	22516409	G	A	NS	98313	*Asxl3*	12	p.C485Y	2	1.2E-01
18	22524317	C	T	NS	11477	*Asxl3*	13	p.P1795S	2	1.2E-01
18	31983320	A	G	NS	11241	*Myo7b*	24	p.V1029A	2	1.1E-01
18	31998034	T	G	NS	60693	*Myo7b*	14	p.Y560S	2	1.1E-01
18	34812382	A	G	NS	83689	*Kdm3b*	10	p.T949A	2	8.6E-02
18	34827490	T	C	NS	76278	*Kdm3b*	16	p.V1376A	2	8.6E-02
18	36968519	C	A	SG	60716	*Pcdha6*	1	p.S255X	2	3.2E-02

18	36969626	T	A	NS	88041	*Pcdha6*	1	p.V624E	2	3.2E-02
18	37265734	T	C	NS	10722	*Pcdhb1*	1	p.V246A	2	2.5E-02
18	37266517	T	C	NS	83164	*Pcdhb1*	1	p.I507T	2	2.5E-02
18	37505896	C	T	NS	83071	*Pcdhb20*	1	p.P492S	2	2.4E-02
18	37506535	T	C	NS	60693	*Pcdhb20*	1	p.S705P	2	2.4E-02
18	74736188	T	C	NS	60654	*Myo5b*	32	p.L1423P	2	9.0E-02
18	74742147	A	C	NS	11478	*Myo5b*	34	p.M1515L	2	9.0E-02
18	77330976	A	T	NS	80493	*Loxhd1*	7	p.Y265F	2	1.1E-01
18	77369158	G	T	NS	10020	*Loxhd1*	18	p.V825L	2	1.1E-01
18	77643121	A	T	NS	83071	*8030462N17 Rik*	4	p.N319K	2	6.7E-03
18	77674470	A	G	NS	11600	*8030462N17 Rik*	2	p.S49P	2	6.7E-03
19	4739905	A	T	NS	83230	*Sptbn2*	19	p.D1307V	2	1.3E-01
19	4748654	G	A	NS	98491	*Sptbn2*	29	p.E2004K	2	1.3E-01
19	7274028	A	G	NS	11478	*Rcor2*	10	p.R302G	2	9.4E-03
19	7274349	A	G	NS	88025	*Rcor2*	11	p.I378V	2	9.4E-03
19	8910491	A	G	NS	3000	*Ganab*	11	p.Y363C	2	3.3E-02
19	8912851	T	C	NS	11954	*Ganab*	18	p.Y715H	2	3.3E-02
19	9017599	T	C	NS	83217	*Ahnak*	5	p.S5416P	2	2.7E-01
19	9017824	A	G	NS	88503	*Ahnak*	5	p.I5491V	2	2.7E-01
19	41877828	A	T	NS	90152	*Rrp12*	17	p.V662E	2	5.3E-02
19	41895986	C	T	NS	10562	*Rrp12*	1	p.C31Y	2	5.3E-02
19	43441968	T	A	SG	82522	*Cnnm1*	1	p.C508X	2	3.2E-02
19	43491533	C	T	NS	60716	*Cnnm1*	8	p.T818I	2	3.2E-02
19	47637718	A	G	NS	96245	*Slk*	16	p.D1100G	2	4.9E-02
19	47637745	T	A	NS	10451	*Slk*	16	p.V1109D	2	4.9E-02
20	20928450	T	A	NS	5401	*Cfp*	5	p.E211V	2	8.9E-03
20	20931221	A	G	NS	83010	*Cfp*	2	p.V49A	2	8.9E-03
20	36611767	T	A	SG	91310	*Akap17b*	7	p.K696X	2	3.3E-02
20	36618661	G	T	NS	82744	*Akap17b*	4	p.Q276K	2	3.3E-02

C=Chromosome; R=Reference allele; A=Alternative allele; E=Exon; AA= Amino Acid; #=Mutation count per gene; NS=Nonsynonymous SNV; SG=Stopgain; SP=Splicing; SL=Stoploss; FSI=Frameshift insertion; FSD=Frameshift deletion

REFERENCES

1. Silverstein, M.D., et al., *Trends in the incidence of deep vein thrombosis and pulmonary embolism: a 25-year population-based study.* Arch Intern Med, 1998. **158**(6): p. 585-93.
2. Stein, P.D., et al., *Pulmonary thromboembolism in American Indians and Alaskan Natives.* Arch Intern Med, 2004. **164**(16): p. 1804-6.
3. White, R.H., H. Zhou, and P.S. Romano, *Incidence of idiopathic deep venous thrombosis and secondary thromboembolism among ethnic groups in California.* Ann Intern Med, 1998. **128**(9): p. 737-40.
4. Beckman, M.G., et al., *Venous thromboembolism: a public health concern.* Am J Prev Med, 2010. **38**(4 Suppl): p. S495-501.
5. Rosendaal, F.R., *Venous thrombosis: a multicausal disease.* Lancet, 1999. **353**(9159): p. 1167-73.
6. Heit, J.A., et al., *Relative impact of risk factors for deep vein thrombosis and pulmonary embolism: a population-based study.* Arch Intern Med, 2002. **162**(11): p. 1245-8.
7. Cushman, M., et al., *Deep vein thrombosis and pulmonary embolism in two cohorts: the longitudinal investigation of thromboembolism etiology.* Am J Med, 2004. **117**(1): p. 19-25.
8. Martinelli, I., V. De Stefano, and P.M. Mannucci, *Inherited risk factors for venous thromboembolism.* Nat Rev Cardiol, 2014. **11**(3): p. 140-56.
9. Heit, J.A., *The epidemiology of venous thromboembolism in the community.* Arterioscler Thromb Vasc Biol, 2008. **28**(3): p. 370-2.
10. Gomes, M.P. and S.R. Deitcher, *Risk of venous thromboembolic disease associated with hormonal contraceptives and hormone replacement therapy: a clinical review.* Arch Intern Med, 2004. **164**(18): p. 1965-76.
11. Battinelli, E.M., A. Marshall, and J.M. Connors, *The role of thrombophilia in pregnancy.* Thrombosis, 2013. **2013**: p. 516420.
12. Souto, J.C., et al., *Genetic susceptibility to thrombosis and its relationship to physiological risk factors: the GAIT study. Genetic Analysis of Idiopathic Thrombophilia.* American Journal of Human Genetics, 2000. **67**(6): p. 1452-1459.
13. Heit, J.A., et al., *Familial segregation of venous thromboembolism.* Journal of thrombosis and haemostasis : JTH, 2004. **2**(5): p. 731-6.
14. Larsen, T.B., et al., *Major genetic susceptibility for venous thromboembolism in men: a study of Danish twins.* Epidemiology, 2003. **14**(3): p. 328-32.
15. Egeberg, O., *Inherited Antithrombin Deficiency Causing Thrombophilia.* Thromb Diath Haemorrh, 1965. **13**: p. 516-30.
16. Lane, D.A., et al., *Molecular genetics of antithrombin deficiency.* Blood Rev, 1996. **10**(2): p. 59-74.
17. Griffin, J.H., et al., *Deficiency of protein C in congenital thrombotic disease.* Journal of Clinical Investigation, 1981. **68**: p. 1370-1373.
18. Comp, P.C., et al., *Familial protein S deficiency is associated with recurrent thrombosis.* J

Clin Invest, 1984. **74**(6): p. 2082-8.
19. Koster, T., et al., *Factor VII and fibrinogen levels as risk factors for venous thrombosis. A case-control study of plasma levels and DNA polymorphisms--the Leiden Thrombophilia Study (LETS).* Thromb Haemost, 1994. **71**(6): p. 719-22.
20. Poort, S.R., et al., *A common genetic variation in the 3'-untranslated region of the prothrombin gene is associated with elevated plasma prothrombin levels and an increase in venous thrombosis.* Blood, 1996. **88**: p. 3698-3703.
21. Koster, T., et al., *Role of clotting factor VIII in effect of von Willebrand factor on occurrence of deep-vein thrombosis.* Lancet, 1995. **345**: p. 152-155.
22. van Hylckama Vlieg, A., et al., *High levels of factor IX increase the risk of venous thrombosis.* Blood, 2000. **95**(12): p. 3678-82.
23. de Visser, M.C., et al., *Factor X levels, polymorphisms in the promoter region of factor X, and the risk of venous thrombosis.* Thromb Haemost, 2001. **85**(6): p. 1011-7.
24. Meijers, J.C., et al., *High levels of coagulation factor XI as a risk factor for venous thrombosis.* The New England journal of medicine, 2000. **342**(10): p. 696-701.
25. Gill, J.C., et al., *The effect of ABO blood group on the diagnosis of von Willebrand disease.* Blood, 1987. **69**(6): p. 1691-5.
26. Germain, M., et al., *Meta-analysis of 65,734 individuals identifies TSPAN15 and SLC44A2 as two susceptibility loci for venous thromboembolism.* Am J Hum Genet, 2015. **96**(4): p. 532-42.
27. Dahlb„ck, B., M. Carlsson, and P.J. Svensson, *Familial thrombophilia due to a previously unrecognized mechanism characterized by poor anticoagulant response to activated protein C: prediction of a cofactor to activated protein C.* Proceedings of the National Academy of Sciences of the United States of America, 1993. **90**: p. 1004-1008.
28. Bertina, R.M., et al., *Mutation in blood coagulation factor V associated with resistance to activated protein C.* Nature, 1994. **369**: p. 64-67.
29. Rees, D.C., M. Cox, and J.B. Clegg, *World distribution of factor V Leiden.* Lancet, 1995. **346**(8983): p. 1133-1134.
30. Koster, T., et al., *Venous thrombosis due to poor anticoagulant response to activated protein C: Leiden Thrombophilia Study* Lancet, 1993. **342**: p. 1503-1506.
31. Roldan, V., et al., *Thrombophilia testing in patients with venous thromboembolism. Findings from the RIETE registry.* Thromb Res, 2009. **124**(2): p. 174-7.
32. Leroyer, C., et al., *Prevalence of 20210 A allele of the prothrombin gene in venous thromboembolism patients.* Thromb Haemost, 1998. **80**(1): p. 49-51.
33. Tregouet, D.A., et al., *Common susceptibility alleles are unlikely to contribute as strongly as the FV and ABO loci to VTE risk: results from a GWAS approach.* Blood, 2009. **113**(21): p. 5298-5303.
34. Germain, M., et al., *Genetics of venous thrombosis: insights from a new genome wide association study.* PLoS One, 2011. **6**(9): p. e25581.
35. Heit, J.A., et al., *A genome-wide association study of venous thromboembolism identifies risk variants in chromosomes 1q24.2 and 9q.* Journal of thrombosis and haemostasis : JTH, 2012. **10**(8): p. 1521-31.
36. Tang, W., et al., *A genome-wide association study for venous thromboembolism: the extended cohorts for heart and aging research in genomic epidemiology (CHARGE) consortium.* Genet Epidemiol, 2013. **37**(5): p. 512-21.
37. Zivelin, A., et al., *A single genetic origin for a common caucasian risk factor for venous*

thrombosis. Blood, 1997. **89**: p. 397-402.
38. Zivelin, A., et al., *A single genetic origin for the common prothrombotic G20210A polymorphism in the prothrombin gene.* Blood, 1998. **92**(4): p. 1119-24.
39. Lutsey, P.L., et al., *Plasma hemostatic factors and endothelial markers in four racial/ethnic groups: the MESA study.* Journal of thrombosis and haemostasis : JTH, 2006. **4**(12): p. 2629-35.
40. Miller, C.H., et al., *Measurement of von Willebrand factor activity: relative effects of ABO blood type and race.* Journal of thrombosis and haemostasis : JTH, 2003. **1**(10): p. 2191-7.
41. Angchaisuksiri, P., *Venous thromboembolism in Asia--an unrecognised and under-treated problem?* Thromb Haemost, 2011. **106**(4): p. 585-90.
42. Rosendaal, F.R., et al., *High risk of thrombosis in patients homozygous for factor V Leiden (activated protein C resistance).* Blood, 1995. **85**(6): p. 1504-1508.
43. Mustafa, S., et al., *Clinical features of thrombophilia in families with gene defects in protein C or protein S combined with factor V Leiden.* Blood Coagul Fibrinolysis, 1998. **9**(1): p. 85-9.
44. Kujovich, J.L., *Factor V Leiden thrombophilia.* Genet Med, 2011. **13**(1): p. 1-16.
45. Emmerich, J., et al., *Combined effect of factor V Leiden and prothrombin 20210A on the risk of venous thromboembolism--pooled analysis of 8 case-control studies including 2310 cases and 3204 controls. Study Group for Pooled-Analysis in Venous Thromboembolism.* Thromb Haemost, 2001. **86**(3): p. 809-16.
46. Cui, J., et al., *Spontaneous thrombosis in mice carrying the factor V Leiden mutation.* Blood, 2000. **96**(13): p. 4222-4226.
47. Eitzman, D.T., et al., *Lethal Perinatal thrombosis in mice resulting from the interaction of tissue factor pathway inhibitor deficiency and factor V Leiden.* Circulation, 2002. **105**: p. 2139-2142.
48. van 't Veer, C., et al., *Increased tissue factor-initiated prothrombin activation as a result of the Arg506 --> Gln mutation in factor VLEIDEN.* Journal of Biological Chemistry, 1997. **272**(33): p. 20721-20729.
49. Veltman, J.A. and H.G. Brunner, *De novo mutations in human genetic disease.* Nat Rev Genet, 2012. **13**(8): p. 565-75.
50. Conrad, D.F., et al., *Variation in genome-wide mutation rates within and between human families.* Nat Genet, 2011. **43**(7): p. 712-4.
51. Kondrashov, A.S., *Direct estimates of human per nucleotide mutation rates at 20 loci causing Mendelian diseases.* Hum Mutat, 2003. **21**(1): p. 12-27.
52. Lynch, M., *Rate, molecular spectrum, and consequences of human mutation.* Proc Natl Acad Sci U S A, 2010. **107**(3): p. 961-8.
53. Kloosterman, W.P., et al., *Characteristics of de novo structural changes in the human genome.* Genome Res, 2015. **25**(6): p. 792-801.
54. Itsara, A., et al., *De novo rates and selection of large copy number variation.* Genome Res, 2010. **20**(11): p. 1469-81.
55. Timms, A.R., et al., *Mutant sequences in the rpsL gene of Escherichia coli B/r: mechanistic implications for spontaneous and ultraviolet light mutagenesis.* Mol Gen Genet, 1992. **232**(1): p. 89-96.
56. Drake, J.W., et al., *Rates of spontaneous mutation.* Genetics, 1998. **148**(4): p. 1667-86.
57. *Mouse Mutant Resource Website*. Available from: http://mousemutant.jax.org/.

58. Davisson, M.T., et al., *A spontaneous mutation in contactin 1 in the mouse.* PLoS One, 2011. **6**(12): p. e29538.
59. DeMambro, V.E., et al., *A novel spontaneous mutation of Irs1 in mice results in hyperinsulinemia, reduced growth, low bone mass and impaired adipogenesis.* J Endocrinol, 2010. **204**(3): p. 241-53.
60. Lorenz-Depiereux, B., et al., *New intragenic deletions in the Phex gene clarify X-linked hypophosphatemia-related abnormalities in mice.* Mamm Genome, 2004. **15**(3): p. 151-61.
61. Russell, W.L. and E.M. Kelly, *Mutation frequencies in male mice and the estimation of genetic hazards of radiation in men.* Proc Natl Acad Sci U S A, 1982. **79**(2): p. 542-4.
62. Russell, L.B., et al., *Chlorambucil effectively induces deletion mutations in mouse germ cells.* Proc Natl Acad Sci U S A, 1989. **86**(10): p. 3704-8.
63. Russell, W.L., et al., *Specific-locus test shows ethylnitrosourea to be the most potent mutagen in the mouse.* Proc Natl Acad Sci U S A, 1979. **76**(11): p. 5818-9.
64. Ding, S., et al., *Efficient transposition of the piggyBac (PB) transposon in mammalian cells and mice.* Cell, 2005. **122**(3): p. 473-83.
65. Luo, G., et al., *Chromosomal transposition of a Tc1/mariner-like element in mouse embryonic stem cells.* Proc Natl Acad Sci U S A, 1998. **95**(18): p. 10769-73.
66. Kile, B.T. and D.J. Hilton, *The art and design of genetic screens: mouse.* Nat Rev Genet, 2005. **6**(7): p. 557-67.
67. Singer, B., *All oxygens in nucleic acids react with carcinogenic ethylating agents.* Nature, 1976. **264**(5584): p. 333-9.
68. *Mutagenetix, UT Southwestern Medical Center*. Available from: https://mutagenetix.utsouthwestern.edu/.
69. Takahasi, K.R., Y. Sakuraba, and Y. Gondo, *Mutational pattern and frequency of induced nucleotide changes in mouse ENU mutagenesis.* BMC Mol Biol, 2007. **8**: p. 52.
70. Justice, M.J., et al., *Mouse ENU mutagenesis.* Human Molecular Genetics, 1999. **8**(10): p. 1955-1963.
71. Andrews, T.D., et al., *Massively parallel sequencing of the mouse exome to accurately identify rare, induced mutations: an immediate source for thousands of new mouse models.* Open Biol, 2012. **2**(5): p. 120061.
72. Bull, K.R., et al., *Unlocking the bottleneck in forward genetics using whole-genome sequencing and identity by descent to isolate causative mutations.* PLoS Genet, 2013. **9**(1): p. e1003219.
73. Ramensky, V., P. Bork, and S. Sunyaev, *Human non-synonymous SNPs: server and survey.* Nucleic Acids Res, 2002. **30**(17): p. 3894-900.
74. Davis, A.P. and M.J. Justice, *An Oak Ridge legacy: the specific locus test and its role in mouse mutagenesis.* Genetics, 1998. **148**(1): p. 7-12.
75. Hitotsumachi, S., D.A. Carpenter, and W.L. Russell, *Dose-repetition increases the mutagenic effectiveness of N-ethyl-N-nitrosourea in mouse spermatogonia.* Proc Natl Acad Sci U S A, 1985. **82**(19): p. 6619-21.
76. Guénet, J.L., et al., *Genetics of the Mouse*. 2015, Springer-Verlag Berlin Heidelberg. p. XVII, 408.
77. Vitaterna, M.H., et al., *Mutagenesis and mapping of a mouse gene, Clock, essential for circadian behavior.* Science, 1994. **264**(5159): p. 719-725.
78. Bode, V.C., et al., *hph-1: a mouse mutant with hereditary hyperphenylalaninemia*

induced by ethylnitrosourea mutagenesis. Genetics, 1988. **118**(2): p. 299-305.
79. Moser, A.R., H.C. Pitot, and W.F. Dove, *A dominant mutation that predisposes to multiple intestinal neoplasia in the mouse.* Science, 1990. **247**(4940): p. 322-4.
80. Su, L.K., et al., *Multiple intestinal neoplasia caused by a mutation in the murine homolog of the APC gene.* Science, 1992. **256**(5057): p. 668-70.
81. Hrabe de Angelis, M.H., et al., *Genome-wide, large-scale production of mutant mice by ENU mutagenesis.* Nat Genet, 2000. **25**(4): p. 444-7.
82. Nolan, P.M., et al., *A systematic, genome-wide, phenotype-driven mutagenesis programme for gene function studies in the mouse.* Nat Genet, 2000. **25**(4): p. 440-3.
83. Gondo, Y., *Trends in large-scale mouse mutagenesis: from genetics to functional genomics.* Nat Rev Genet, 2008. **9**(10): p. 803-10.
84. Arnold, C.N., et al., *ENU-induced phenovariance in mice: inferences from 587 mutations.* BMC Res Notes, 2012. **5**: p. 577.
85. Forsburg, S.L., *The art and design of genetic screens: yeast.* Nat Rev Genet, 2001. **2**(9): p. 659-68.
86. Jorgensen, E.M. and S.E. Mango, *The art and design of genetic screens: caenorhabditis elegans.* Nat Rev Genet, 2002. **3**(5): p. 356-69.
87. St Johnston, D., *The art and design of genetic screens: Drosophila melanogaster.* Nat Rev Genet, 2002. **3**(3): p. 176-88.
88. Carpinelli, M.R., et al., *Suppressor screen in Mpl-/- mice: c-Myb mutation causes supraphysiological production of platelets in the absence of thrombopoietin signaling.* Proceedings of the National Academy of Sciences of the United States of America, 2004. **101**(17): p. 6553-6558.
89. Matera, I., et al., *A sensitized mutagenesis screen identifies Gli3 as a modifier of Sox10 neurocristopathy.* Hum Mol Genet, 2008. **17**(14): p. 2118-31.
90. Buchovecky, C.M., et al., *A suppressor screen in Mecp2 mutant mice implicates cholesterol metabolism in Rett syndrome.* Nat Genet, 2013. **45**(9): p. 1013-20.
91. Tchekneva, E.E., et al., *A sensitized screen of N-ethyl-N-nitrosourea-mutagenized mice identifies dominant mutants predisposed to diabetic nephropathy.* J Am Soc Nephrol, 2007. **18**(1): p. 103-12.
92. Huang, Z.F., et al., *Tissue factor pathway inhibitor gene disruption produces intrauterine lethality in mice.* Blood, 1997. **90**: p. 944-951.
93. Moresco, E.M., X. Li, and B. Beutler, *Going forward with genetics: recent technological advances and forward genetics in mice.* Am J Pathol, 2013. **182**(5): p. 1462-73.
94. King, D.P., et al., *Positional cloning of the mouse circadian clock gene.* Cell, 1997. **89**(4): p. 641-53.
95. Ebersole, T.A., et al., *The quaking gene product necessary in embryogenesis and myelination combines features of RNA binding and signal transduction proteins.* Nat Genet, 1996. **12**(3): p. 260-5.
96. Schumacher, A., C. Faust, and T. Magnuson, *Positional cloning of a global regulator of anterior-posterior patterning in mice.* Nature, 1996. **384**(6610): p. 648.
97. Montagutelli, X., *Effect of the genetic background on the phenotype of mouse mutations.* J Am Soc Nephrol, 2000. **11 Suppl 16**: p. S101-5.
98. Smith, D.R., et al., *Rapid whole-genome mutational profiling using next-generation sequencing technologies.* Genome Res, 2008. **18**(10): p. 1638-42.
99. Zhang, Z., et al., *Massively parallel sequencing identifies the gene Megf8 with ENU-*

induced mutation causing heterotaxy. Proc Natl Acad Sci U S A, 2009. **106**(9): p. 3219-24.
100. Fairfield, H., et al., *Mutation discovery in mice by whole exome sequencing.* Genome Biol, 2011. **12**(9): p. R86.
101. Caruana, G., et al., *Genome-wide ENU mutagenesis in combination with high density SNP analysis and exome sequencing provides rapid identification of novel mouse models of developmental disease.* PLoS One, 2013. **8**(3): p. e55429.
102. Simon, M.M., et al., *High throughput sequencing approaches to mutation discovery in the mouse.* Mamm Genome, 2012. **23**(9-10): p. 499-513.
103. Arnold, C.N., et al., *Rapid identification of a disease allele in mouse through whole genome sequencing and bulk segregation analysis.* Genetics, 2011. **187**(3): p. 633-41.
104. Gallego-Llamas, J., et al., *Variant mapping and mutation discovery in inbred mice using next-generation sequencing.* BMC Genomics, 2015. **16**: p. 913.
105. Scott, C.F., et al., *Alpha-1-antitrypsin-Pittsburgh. A potent inhibitor of human plasma factor XIa, kallikrein, and factor XIIf.* J Clin Invest, 1986. **77**(2): p. 631-4.
106. Vidaud, D., et al., *Met 358 to Arg mutation of alpha 1-antitrypsin associated with protein C deficiency in a patient with mild bleeding tendency.* J Clin Invest, 1992. **89**(5): p. 1537-43.
107. *Online Mendelian Inheritance in Man, OMIM®.* [cited 2015 March 17]; Available from: http://omim.org/.
108. Gibson, W.T., et al., *Mutations in EZH2 cause Weaver syndrome.* Am J Hum Genet, 2012. **90**(1): p. 110-8.
109. Hoischen, A., et al., *De novo mutations of SETBP1 cause Schinzel-Giedion syndrome.* Nat Genet, 2010. **42**(6): p. 483-5.
110. Riviere, J.B., et al., *De novo mutations in the actin genes ACTB and ACTG1 cause Baraitser-Winter syndrome.* Nat Genet, 2012. **44**(4): p. 440-4, S1-2.
111. Tsurusaki, Y., et al., *Mutations affecting components of the SWI/SNF complex cause Coffin-Siris syndrome.* Nat Genet, 2012. **44**(4): p. 376-8.
112. Thaung, C., et al., *Novel ENU-induced eye mutations in the mouse: models for human eye disease.* Hum Mol Genet, 2002. **11**(7): p. 755-67.
113. Li, Y., et al., *Global genetic analysis in mice unveils central role for cilia in congenital heart disease.* Nature, 2015. **521**(7553): p. 520-4.
114. Souto, J.C., et al., *Genetic determinants of hemostasis phenotypes in Spanish families.* Circulation, 2000. **101**(13): p. 1546-1551.
115. Dahlback, B., *The importance of the protein C system in the pathogenesis of venous thrombosis.* Hematology, 2005. **10 Suppl 1**: p. 138-9.
116. Svensson, P.J. and B. Dahlb„ck, *Resistance to activated protein C as a basis for venous thrombosis.* New England Journal of Medicine, 1994. **330**: p. 517-522.
117. Zoller, B., et al., *Identification of the same factor V gene mutation in 47 out of 50 thrombosis-prone families with inherited resistance to activated protein C.* J Clin Invest, 1994. **94**(6): p. 2521-4.
118. Lijfering, W.M., F.R. Rosendaal, and S.C. Cannegieter, *Risk factors for venous thrombosis - current understanding from an epidemiological point of view.* Br J Haematol, 2010. **149**(6): p. 824-33.
119. Westrick, R.J. and D. Ginsburg, *Modifier genes for disorders of thrombosis and hemostasis.* J.Thromb.Haemost., 2009. **7 Suppl 1**: p. 132-135.

120. De Stefano, V., et al., *The risk of recurrent deep venous thrombosis among heterozygous carriers of both factor V Leiden and the G20210A prothrombin mutation.* N Engl J Med, 1999. **341**(11): p. 801-6.
121. Van Boven, H.H., et al., *Factor V Leiden (FV R506Q) in families with inherited antithrombin deficiency.* Thrombosis and Haemostasis, 1996. **75**(3): p. 417-421.
122. Aissi, D., et al., *Genome-wide investigation of DNA methylation marks associated with FV Leiden mutation.* PLoS One, 2014. **9**(9): p. e108087.
123. Weber, J.S., A. Salinger, and M.J. Justice, *Optimal N-ethyl-N-nitrosourea (ENU) doses for inbred mouse strains.* Genesis, 2000. **26**(4): p. 230-3.
124. Justice, M.J., et al., *Effects of ENU dosage on mouse strains.* Mammalian Genome, 2000. **11**(7): p. 484-488.
125. Uchimura, A., et al., *Germline mutation rates and the long-term phenotypic effects of mutation accumulation in wild-type laboratory mice and mutator mice.* Genome Res, 2015. **25**(8): p. 1125-34.
126. Soria, J.M., et al., *The F7 gene and clotting factor VII levels: dissection of a human quantitative trait locus.* Hum Biol, 2005. **77**(5): p. 561-75.
127. Bi, L., et al., *Targeted disruption of the mouse factor VIII gene produces a model of haemophilia A.* Nature Genetics, 1995. **10**: p. 119-121.
128. Lange, K., et al., *Mendel: the Swiss army knife of genetic analysis programs.* Bioinformatics, 2013. **29**(12): p. 1568-70.
129. Lander, E. and L. Kruglyak, *Genetic dissection of complex traits: guidelines for interpreting and reporting linkage results.* Nat Genet, 1995. **11**(3): p. 241-7.
130. Mohlke, K.L., et al., *Mvwf , a dominant modifier of murine von Willebrand factor, results from altered lineage-specific expression of a glycosyltransferase.* Cell, 1999. **96**: p. 111-120.
131. Li, H. and R. Durbin, *Fast and accurate short read alignment with Burrows-Wheeler transform.* Bioinformatics, 2009. **25**(14): p. 1754-60.
132. Garcia-Alcalde, F., et al., *Qualimap: evaluating next-generation sequencing alignment data.* Bioinformatics, 2012. **28**(20): p. 2678-9.
133. DePristo, M.A., et al., *A framework for variation discovery and genotyping using next-generation DNA sequencing data.* Nat Genet, 2011. **43**(5): p. 491-8.
134. Wang, K., M. Li, and H. Hakonarson, *ANNOVAR: functional annotation of genetic variants from high-throughput sequencing data.* Nucleic Acids Res, 2010. **38**(16): p. e164.
135. Beutler, B., X. Du, and Y. Xia, *Precis on forward genetics in mice.* Nat Immunol, 2007. **8**(7): p. 659-64.
136. Kyrle, P.A., et al., *The risk of recurrent venous thromboembolism in men and women.* N Engl J Med, 2004. **350**(25): p. 2558-63.
137. Roach, R.E., et al., *Sex difference in the risk of recurrent venous thrombosis: a detailed analysis in four European cohorts.* J Thromb Haemost, 2015. **13**(10): p. 1815-22.
138. Kleesiek, K., et al., *The 536C -> T transition in the human tissue factor pathway inhibitor (TFPI) gene is statistically associated with a higher risk for venous thrombosis.* Thrombosis & Haemostasis, 1999. **82**(1): p. 1-5.
139. Winckers, K., et al., *Increased tissue factor pathway inhibitor activity is associated with myocardial infarction in young women: results from the RATIO study.* J Thromb Haemost, 2011. **9**(11): p. 2243-50.

140. Yoo, Y.J. and N.R. Mendell, *The power and robustness of maximum LOD score statistics.* Ann Hum Genet, 2008. **72**(Pt 4): p. 566-74.
141. Pollard, T.D. and C.C. Beltzner, *Structure and function of the Arp2/3 complex.* Curr Opin Struct Biol, 2002. **12**(6): p. 768-74.
142. Li, Z., E.S. Kim, and E.L. Bearer, *Arp2/3 complex is required for actin polymerization during platelet shape change.* Blood, 2002. **99**(12): p. 4466-74.
143. Keane, T.M., et al., *Mouse genomic variation and its effect on phenotypes and gene regulation.* Nature, 2011. **477**(7364): p. 289-94.
144. Yalcin, B., et al., *Sequence-based characterization of structural variation in the mouse genome.* Nature, 2011. **477**(7364): p. 326-9.
145. Kong, A., et al., *Rate of de novo mutations and the importance of father's age to disease risk.* Nature, 2012. **488**(7412): p. 471-5.
146. Campbell, C.D. and E.E. Eichler, *Properties and rates of germline mutations in humans.* Trends Genet, 2013. **29**(10): p. 575-84.
147. Taft, R.A., M. Davisson, and M.V. Wiles, *Know thy mouse.* Trends Genet, 2006. **22**(12): p. 649-53.
148. Cullinane, A.R., A.A. Schaffer, and M. Huizing, *The BEACH is hot: a LYST of emerging roles for BEACH-domain containing proteins in human disease.* Traffic, 2013. **14**(7): p. 749-66.
149. Kahr, W.H., et al., *Mutations in NBEAL2, encoding a BEACH protein, cause gray platelet syndrome.* Nat Genet, 2011. **43**(8): p. 738-40.
150. Gunay-Aygun, M., et al., *NBEAL2 is mutated in gray platelet syndrome and is required for biogenesis of platelet alpha-granules.* Nat Genet, 2011. **43**(8): p. 732-4.
151. Albers, C.A., et al., *Exome sequencing identifies NBEAL2 as the causative gene for gray platelet syndrome.* Nat Genet, 2011. **43**(8): p. 735-7.
152. Nurden, A.T. and P. Nurden, *The gray platelet syndrome: clinical spectrum of the disease.* Blood Rev, 2007. **21**(1): p. 21-36.
153. Deppermann, C., et al., *Gray platelet syndrome and defective thrombo-inflammation in Nbeal2-deficient mice.* J Clin Invest, 2013.
154. Kahr, W.H., et al., *Abnormal megakaryocyte development and platelet function in Nbeal2(-/-) mice.* Blood, 2013. **122**(19): p. 3349-58.
155. Guerrero, J.A., et al., *Gray platelet syndrome: proinflammatory megakaryocytes and alpha-granule loss cause myelofibrosis and confer metastasis resistance in mice.* Blood, 2014. **124**(24): p. 3624-35.
156. Raccuglia, G., *Gray platelet syndrome. A variety of qualitative platelet disorder.* Am J Med, 1971. **51**(6): p. 818-28.
157. Tomberg, K. *GitHub repository for WES pipeline*. 2015; Available from: https://github.com/tombergk/NBEAL2/.
158. *Picard tools*. Available from: http://picard.sourceforge.net.
159. Fairfield, H., et al., *Exome sequencing reveals pathogenic mutations in 91 strains of mice with Mendelian disorders.* Genome Res, 2015. **25**(7): p. 948-57.
160. Ewing, B., et al., *Base-calling of automated sequencer traces using phred. I. Accuracy assessment.* Genome Res, 1998. **8**(3): p. 175-85.
161. McCarty, O.J., et al., *von Willebrand factor mediates platelet spreading through glycoprotein Ib and alpha(IIb)beta3 in the presence of botrocetin and ristocetin, respectively.* J Thromb Haemost, 2006. **4**(6): p. 1367-78.

162. *R: A Language and Environment for Statistical Computing*. R Core Team; Available from: http://www.R-project.org/.
163. Brunck, M.E., et al., *Absolute counting of neutrophils in whole blood using flow cytometry.* Cytometry A, 2014. **85**(12): p. 1057-64.
164. Khoriaty, R., et al., *Absence of a red blood cell phenotype in mice with hematopoietic deficiency of SEC23B.* Mol Cell Biol, 2014. **34**(19): p. 3721-34.
165. Schneider, C.A., W.S. Rasband, and K.W. Eliceiri, *NIH Image to ImageJ: 25 years of image analysis.* Nat Methods, 2012. **9**(7): p. 671-5.
166. Isken, O. and L.E. Maquat, *Quality control of eukaryotic mRNA: safeguarding cells from abnormal mRNA function.* Genes Dev, 2007. **21**(15): p. 1833-56.
167. Monteferrario, D., et al., *A dominant-negative GFI1B mutation in the gray platelet syndrome.* The New England journal of medicine, 2014. **370**(3): p. 245-53.
168. Falik-Zaccai, T.C., et al., *A new genetic isolate of gray platelet syndrome (GPS): clinical, cellular, and hematologic characteristics.* Mol Genet Metab, 2001. **74**(3): p. 303-13.
169. De Candia, E., et al., *Defective platelet responsiveness to thrombin and protease-activated receptors agonists in a novel case of gray platelet syndrome: correlation between the platelet defect and the alpha-granule content in the patient and four relatives.* Journal of thrombosis and haemostasis : JTH, 2007. **5**(3): p. 551-9.
170. Westrick, R.J., et al., *A spontaneous Irs1 passenger mutation linked to a gene targeted SerpinB2 Allele.* Proceedings of the National Academy of Sciences of the United States of America, 2010. **107**(39): p. 16904-16909.
171. Lewis, N.D., et al., *Circulating monocytes are reduced by sphingosine-1-phosphate receptor modulators independently of S1P3.* J Immunol, 2013. **190**(7): p. 3533-40.
172. Schlager, G. and M.M. Dickie, *Spontaneous mutations and mutation rates in the house mouse.* Genetics, 1967. **57**(2): p. 319-30.
173. Bannister, L.A., et al., *A dominant, recombination-defective allele of Dmc1 causing male-specific sterility.* PLoS Biol, 2007. **5**(5): p. e105.
174. Strobel, M.C., et al., *Genetic Monitoring of Laboratory Mice and Rats*, in *Laboratory Animal Medicine*, J.G. Fox, Editor. 2015, Elsevier, Academic Press: San Diego, CA.
175. Wansleeben, C., et al., *An ENU-mutagenesis screen in the mouse: identification of novel developmental gene functions.* PLoS One, 2011. **6**(4): p. e19357.
176. Papathanasiou, P., et al., *A recessive screen for genes regulating hematopoietic stem cells.* Blood, 2010. **116**(26): p. 5849-58.
177. Boehnke, M. and L. Ploughman, *SIMLINK: A Program for Estimating the Power of a Proposed Linkage Study by Computer Simulations.* **Version 4.12, April 2, 1997**.
178. Benjamini, Y. and Y. Hochberg, *Controlling the False Discovery Rate - a Practical and Powerful Approach to Multiple Testing.* Journal of the Royal Statistical Society Series B-Methodological, 1995. **57**(1): p. 289-300.
179. Untergasser, A., et al., *Primer3--new capabilities and interfaces.* Nucleic Acids Res, 2012. **40**(15): p. e115.
180. Doench, J.G., et al., *Rational design of highly active sgRNAs for CRISPR-Cas9-mediated gene inactivation.* Nat Biotechnol, 2014. **32**(12): p. 1262-7.
181. Hsu, P.D., et al., *DNA targeting specificity of RNA-guided Cas9 nucleases.* Nat Biotechnol, 2013. **31**(9): p. 827-32.
182. Cong, L., et al., *Multiplex genome engineering using CRISPR/Cas systems.* Science, 2013. **339**(6121): p. 819-23.

183. Pettitt, S.J., et al., *Agouti C57BL/6N embryonic stem cells for mouse genetic resources.* Nat Methods, 2009. **6**(7): p. 493-5.
184. Pease, S., T.L. Saunders, and International Society for Transgenic Technologies., *Advanced protocols for animal transgenesis an ISTT manual*. 2011, Springer: Heidelberg ; New York ;.
185. McBurney, M.W., et al., *Intragenic regions of the murine Pgk-1 locus enhance integration of transfected DNAs into genomes of embryonal carcinoma cells.* Somat Cell Mol Genet, 1994. **20**(6): p. 515-28.
186. Brinkman, E.K., et al., *Easy quantitative assessment of genome editing by sequence trace decomposition.* Nucleic Acids Res, 2014. **42**(22): p. e168.
187. Therneau, T.M. and P.M. Grambsch, *Modeling survival data : extending the Cox model*. Statistics for biology and health. 2000, New York: Springer. xiii, 350 p.
188. White, T.A., et al., *Murine strain differences in hemostasis and thrombosis and tissue factor pathway inhibitor.* Thromb Res, 2010. **125**(1): p. 84-9.
189. Sang, F., et al., *ReDB: A meiotic homologous recombination rate database.* Chinese Science Bulletin, 2010. **55**(27-28): p. 3169-3173.
190. Jensen-Seaman, M.I., et al., *Comparative recombination rates in the rat, mouse, and human genomes.* Genome Res, 2004. **14**(4): p. 528-38.
191. Adzhubei, I.A., et al., *A method and server for predicting damaging missense mutations.* Nat Methods, 2010. **7**(4): p. 248-9.
192. Brinster, R.L., et al., *Factors affecting the efficiency of introducing foreign DNA into mice by microinjecting eggs.* Proc Natl Acad Sci U S A, 1985. **82**(13): p. 4438-42.
193. Doetschman, T., *Influence of genetic background on genetically engineered mouse phenotypes.* Methods Mol Biol, 2009. **530**: p. 423-33.
194. Timmer, J.R., et al., *Tissue morphogenesis and vascular stability require the Frem2 protein, product of the mouse myelencephalic blebs gene.* Proc Natl Acad Sci U S A, 2005. **102**(33): p. 11746-50.
195. Long, A.B., et al., *Apaf1 apoptotic function critically limits Sonic hedgehog signaling during craniofacial development.* Cell Death Differ, 2013. **20**(11): p. 1510-20.
196. Jinek, M., et al., *A programmable dual-RNA-guided DNA endonuclease in adaptive bacterial immunity.* Science, 2012. **337**(6096): p. 816-21.
197. Simon, M.M., et al., *Current strategies for mutation detection in phenotype-driven screens utilising next generation sequencing.* Mamm Genome, 2015. **26**(9-10): p. 486-500.
198. Cleuren, A.C., B.J. van Vlijmen, and P.H. Reitsma, *Transgenic mouse models of venous thrombosis: fulfilling the expectations?* Semin Thromb Hemost, 2007. **33**(6): p. 610-6.
199. Franchini, M. and M. Makris, *Non-O blood group: an important genetic risk factor for venous thromboembolism.* Blood Transfus, 2013. **11**(2): p. 164-5.
200. Wu, C., et al., *Targeted gene sequencing identifies variants in the protein C and endothelial protein C receptor genes in patients with unprovoked venous thromboembolism.* Arterioscler Thromb Vasc Biol, 2013. **33**(11): p. 2674-81.
201. Willis, R. and S.S. Pierangeli, *Pathophysiology of the antiphospholipid antibody syndrome.* Auto Immun Highlights, 2011. **2**(2): p. 35-52.
202. Plow, E.F., K. Allampallam, and A. Redlitz, *The plasma carboxypeptidases and the regulation of the plasminogen system.* Trends Cardiovasc Med, 1997. **7**(3): p. 71-5.
203. Skidgel, R.A. and E.G. Erdos, *Structure and function of human plasma carboxypeptidase*

N, the anaphylatoxin inactivator. Int Immunopharmacol, 2007. **7**(14): p. 1888-99.
204. Sheppard, D., *Epithelial-mesenchymal interactions in fibrosis and repair. Transforming growth factor-beta activation by epithelial cells and fibroblasts.* Ann Am Thorac Soc, 2015. **12 Suppl 1**: p. S21-3.
205. Aoyama, K. and T. Nakaki, *Inhibition of GTRAP3-18 may increase neuroprotective glutathione (GSH) synthesis.* Int J Mol Sci, 2012. **13**(9): p. 12017-35.
206. Khoriaty, R., M.P. Vasievich, and D. Ginsburg, *The COPII pathway and hematologic disease.* Blood, 2012. **120**(1): p. 31-8.
207. Hafner, A., N. Obermajer, and J. Kos, *gamma-1-syntrophin mediates trafficking of gamma-enolase towards the plasma membrane and enhances its neurotrophic activity.* Neurosignals, 2010. **18**(4): p. 246-58.
208. Rieder, M.J., et al., *A human homeotic transformation resulting from mutations in PLCB4 and GNAI3 causes auriculocondylar syndrome.* Am J Hum Genet, 2012. **90**(5): p. 907-14.
209. Hayashi, M., et al., *Fatal thrombosis of antithrombin-deficient mice is rescued differently in the heart and liver by intercrossing with low tissue factor mice.* J Thromb Haemost, 2006. **4**(1): p. 177-85.
210. Jalbert, L.R., et al., *Inactivation of the gene for anticoagulant protein C causes lethal perinatal consumptive coagulopathy in mice.* Journal of Clinical Investigation, 1998. **102**(8): p. 1481-1488.
211. Clark, A.T., et al., *Implementing large-scale ENU mutagenesis screens in North America.* Genetica, 2004. **122**(1): p. 51-64.
212. Ellery, P.E., et al., *A balance between TFPI and thrombin-mediated platelet activation is required for murine embryonic development.* Blood, 2015. **125**(26): p. 4078-84.
213. Chan, J.C., et al., *Factor VII deficiency rescues the intrauterine lethality in mice associated with a tissue factor pathway inhibitor deficit.* J Clin Invest, 1999. **103**(4): p. 475-82.
214. Pedersen, B., et al., *A balance between tissue factor and tissue factor pathway inhibitor is required for embryonic development and hemostasis in adult mice.* Blood, 2005. **105**(7): p. 2777-82.
215. Chan, J.C., et al., *The characterization of mice with a targeted combined deficiency of protein c and factor XI.* Am J Pathol, 2001. **158**(2): p. 469-79.
216. Wang, T., et al., *Genetic screens in human cells using the CRISPR-Cas9 system.* Science, 2014. **343**(6166): p. 80-4.
217. Shalem, O., et al., *Genome-scale CRISPR-Cas9 knockout screening in human cells.* Science, 2014. **343**(6166): p. 84-7.
218. Wang, H., et al., *One-step generation of mice carrying mutations in multiple genes by CRISPR/Cas-mediated genome engineering.* Cell, 2013. **153**(4): p. 910-8.
219. Canver, M.C., et al., *Characterization of genomic deletion efficiency mediated by clustered regularly interspaced palindromic repeats (CRISPR)/Cas9 nuclease system in mammalian cells.* J Biol Chem, 2014. **289**(31): p. 21312-24.
220. Pruim, R.J., et al., *LocusZoom: regional visualization of genome-wide association scan results.* Bioinformatics, 2010. **26**(18): p. 2336-7.